HAL
open science

Experimental study of the HCCI combustion through the use of minor oxidizing chemical species

Jean-Baptiste Masurier

To cite this version:

Jean-Baptiste Masurier. Experimental study of the HCCI combustion through the use of minor oxidizing chemical species. Other. Université d'Orléans, 2016. English. NNT : 2016ORLE2014 . tel-01431037

HAL Id: tel-01431037

https://theses.hal.science/tel-01431037v1

Submitted on 10 Jan 2017

HAL is a multi-disciplinary open access archive for the deposit and dissemination of scientific research documents, whether they are published or not. The documents may come from teaching and research institutions in France or abroad, or from public or private research centers.

L'archive ouverte pluridisciplinaire **HAL**, est destinée au dépôt et à la diffusion de documents scientifiques de niveau recherche, publiés ou non, émanant des établissements d'enseignement et de recherche français ou étrangers, des laboratoires publics ou privés.

UNIVERSITÉ D'ORLÉANS

ÉCOLE DOCTORALE
ENERGIE, MATERIAUX, SCIENCES DE LA TERRE ET DE L'UNIVERS

LABORATOIRE PRISME – Université d'Orléans

ICARE – CNRS

THÈSE présentée par :

Jean-Baptiste MASURIER

soutenue le : **8 Juin 2016**

pour obtenir le grade de : **Docteur de l'Université d'Orléans**

Discipline/ Spécialité : Mécanique et Energétique

Etude expérimentale de la combustion HCCI par l'ajout d'espèces chimiques oxydantes minoritaires

THÈSE dirigée par :

Fabrice FOUCHER	Professeur, PRISME - Université d'Orléans
Guillaume DAYMA	Professeur, ICARE - CNRS

RAPPORTEURS :

António PIRES DA CRUZ	Directeur de Département, IFPEN
Luis LEMOYNE	Professeur, DRIVE - Université de Bourgogne

JURY :

António PIRES DA CRUZ	Directeur de Département, IFPEN
Luis LEMOYNE	Professeur, DRIVE - Université de Bourgogne
Martin TUNÉR	Maître de Conférences, Université de Lund
Robert DIBBLE	Professeur, CCRC - KAUST
Francesco CONTINO	Maître de Conférences, VUB
Fabrice FOUCHER	Professeur, PRISME - Université d'Orléans
Philippe DAGAUT	Directeur de Recherche, ICARE - CNRS

UNIVERSITÉ D'ORLÉANS

ÉCOLE DOCTORALE
ENERGIE, MATERIAUX, SCIENCES DE LA TERRE ET DE L'UNIVERS

LABORATOIRE PRISME – University of Orléans

ICARE – CNRS

THESIS presented by:

Jean-Baptiste MASURIER

defended on: **8 June 2016]**

for the degree of : **PhD from the University of Orléans**

Specialty: Mechanics and Energetics

Experimental study of the HCCI combustion through the use of minor oxidizing chemical species

THESIS supervised by:

Fabrice FOUCHER	Professor, PRISME - University of Orléans
Guillaume DAYMA	Professor, ICARE - CNRS

REVIEWERS:

António PIRES DA CRUZ	Section Head, IFPEN
Luis LEMOYNE	Professor, DRIVE - University of Bourgogne

JURY:

António PIRES DA CRUZ	Section Head, IFPEN
Luis LEMOYNE	Professor, DRIVE - University of Bourgogne
Martin TUNÉR	Associate Professor, Lund University
Robert DIBBLE	Professor, CCRC - KAUST
Francesco CONTINO	Associate Professor, VUB
Fabrice FOUCHER	Professor, PRISME - University of Orléans
Philippe DAGAUT	Research Director, ICARE - CNRS

Remerciements

Ces recherches ont été financées par le Projet Européen ERC 2G-CSafe.

Les travaux qui ont conduits à ces résultats se sont déroulés au sein du Laboratoire Pluridisciplinaire de Recherche en Ingénierie des Systèmes, Mécanique et Energétique (PRISME) de l'Université d'Orléans et de l'Institut de Combustion Aérothermique Réactivité et Environnement (ICARE) du CNRS-INSIS.

Je tiens à remercier en premier lieu Fabrice FOUCHER, Professeur de l'Université d'Orléans et Animateur de l'axe Energie, Combustion, Moteur du Laboratoire PRISME, et Guillaume DAYMA, Professeur de l'Université d'Orléans et Chercheur à ICARE, pour leur encadrement durant ces travaux de recherche. Ils m'ont permis, par leurs conseils et leurs compétences techniques et scientifiques, de développer et accroître mes connaissances dans le domaine de la combustion, respectivement au sein des moteurs à combustion interne et de l'oxydation des carburants.

Je souhaite également exprimer ma profonde gratitude à Philippe DAGAUT, Directeur de Recherche à ICARE et Porteur du Projet Européen ERC 2G-CSafe, pour m'avoir offert l'opportunité d'effectuer cette thèse. Le temps qu'il a consacré à nos réunions de travail ainsi que ses analyses critiques, vis-à-vis de mes interrogations et de mes propositions de recherche au cours de la thèse, ont profondément contribué à l'aboutissement de ces résultats de recherche. De plus, j'ai été honoré qu'il ait accepté de présider mon jury de thèse.

Je tiens enfin à remercier Christine MOUNAÏM-ROUSSELLE, Professeure de l'Université d'Orléans, qui a contribué selon sa disponibilité à quelques uns de mes travaux. Sa rigueur, sa simplicité, son soutien et sa jovialité ont été une aide précieuse.

J'adresse également mes remerciements à António PIRES DA CRUZ, Directeur de Département à l'IFP Energies Nouvelles, et Luis LEMOYNE, Professeur à l'Université de

Bourgogne, pour avoir accepté d'être les rapporteurs de mon mémoire et avoir évalué ces résultats de recherche.

Je remercie aussi vivement Martin TUNÉR, Maître de Conférences à l'Université de Lund (Suède), Robert DIBBLE, Professeur au KAUST (Arabie Saoudite), et Francesco CONTINO, Maître de Conférences à VUB (Belgique), d'avoir accepté de faire le déplacement de leur pays respectif pour compléter mon jury de thèse en tant qu'examinateurs. Leurs questions et commentaires lors de la soutenance joints à ceux des rapporteurs ont fortement apporté au rendu final de ce manuscrit.

Un grand merci également à l'équipe technique du laboratoire PRISME, en particulier de l'axe ECM : Bruno MOREAU, Julien LEMAIRE, Benoît BELLICAUD, Yahia HAIDOUS. Cette thèse n'aurait pas abouti sans leur contribution. Sans eux, il n'y aurait pas d'expériences, donc pas de recherches, donc pas de science et encore moins de thèse. Je leur évoque donc ce merci pour l'apport de connaissance qu'ils ont partagé avec moi, leurs conseils, les échanges que nous avons eu et enfin pour leur collaboration vis-à-vis de mes idées quelques fois loufoques.

Je souhaite enfin adresser mes remerciements aux autres membres du laboratoire (anciens et présents) pour leur soutien de près ou de loin, leur conseil, pour avoir supporté mon caractère de « Normand », leur amitié, pour la bonne ambiance, les moments de rigolade et les différentes activités partagées à la fois au sein du laboratoire mais aussi en dehors : Arnaud, Audrey, Jérémie, Amine, Pierre B, Charles, Haïfa, Antonio, Mehdi, Ricardo, Padipan, Ob, Sokratis, Antoine, Salim, Alexandre, Florian, Ida, Vincent, Kévin, Yann, Sophie, Francesco, Guillaume, Dominique, Sandrine, Annie, Azzedine, Sylvie, Kristan, Muriel, Delphine, Pierre A, Benoît C et toutes les personnes que j'ai pu oublier.

Je terminerai finalement par remercier très chaleureusement ma famille et mes amis qui m'ont fait part de leur soutien, leur encouragement et leur compréhension face à ces années de thèse. Enfin, je dédie ce mémoire à mon père et lui exprime une pérenne gratitude. Bien que son absence soit pesante, l'éducation qu'il m'a prodiguée, les valeurs qu'il m'a transmises, ses conseils passés et le désir de le rendre fier m'ont conféré l'énergie, la volonté et la ténacité pour finaliser chacun des travaux entrepris.

Acknowledgements

The research leading to these results has received funding from the European Research Council under the European Community's Seventh Framework Programme (FP7/2007 – 2013)/ERC grant agreement n° 291049 – 2G – CSafe.

The research works were carried out at the Laboratory PRISME of the University of Orléans and at ICARE, CNRS-INSIS.

Firstly, I would like to thank Fabrice FOUCHER, Professor of the University of Orléans and Animator of the ECM axis at Laboratory PRISME, and Guillaume DAYMA, Professor of the University of Orléans and Researcher at ICARE, for their guidance during these research studies. They allowed me, by their advices and their technical and scientific skills, to develop and grow my knowledge in the field of the combustion, respectively, in the internal combustion engines and the oxidation of fuels.

I also wish to express my deep gratitude to Philippe DAGAUT, Research Director at ICARE and Leader of the European Project ERC 2G-CSafe, for giving me the opportunity to make this thesis. The time he spent at our meetings as well as its critical analysis, concerning my queries and my research proposals, have profoundly contributed to the success of these results. Also, I was honored that he has agreed to chair my thesis committee.

Finally, I would like to thank Christine MOUNAÏM-ROUSSELLE, Professor of the University of Orléans, who contributed according to its availability to some of my work. Her rigor, simplicity, support and cheerfulness were a precious help.

I extend my thanks to António PIRES DA CRUZ, Department Director at IFP Energies Nouvelles, and Luis LEMOYNE, Professor at the University of Bourgogne, for accepting to be the reviewers of my manuscript and evaluating these results of research.

I also warmly thank Martin TUNÉR, Associate Professor at the University of Lund (Sweden), Robert DIBBLE, Professor at KAUST (Saudi Arabia), and Francesco CONTINO, Associate Professor at VUB (Belgium), for accepting to move from their respective country and completing my thesis committee. Their queries and comments at the defense together with those of the reviewers have greatly help me improving the last version of my manuscript.

Many thanks to the technical staff of the ECM axis: Bruno MOREAU, Julien LEMAIRE, Benoît BELLICAUD, Yahia HAIDOUS. This thesis would have not succeeded without their contribution. Without them, there would be no experiment, so no research, so no science and even fewer theses. Therefore, I would like to thank them for sharing their knowledge with me, giving me advice, our exchanges and their collaborations on my ideas sometimes crazy.

I also wish to thank the other members of the laboratory (past and present) for their support in one way or another, their advice, for accepting my character of “Normand”, for their friendship, the good atmosphere, the moments of fun and the different activities shared both inside the laboratory but also outside: Arnaud, Audrey, Jérémie, Amine, Pierre B, Charles, Haïfa, Antonio, Mehdi, Ricardo, Padipan, Ob, Sokratis, Antoine, Salim, Alexandre, Florian, Ida, Vincent, Kévin, Yann, Sophie, Francesco, Guillaume, Dominique, Sandrine, Annie, Azzedine, Sylvie, Kristan, Muriel, Delphine, Pierre A, Benoît C and all the people I have forgotten.

I will finally end by warmly thanking my family and my friends who gave me their support, encouragement and understanding for these years of thesis. Finally, I dedicated this work to my father and expresses him a long-lasting gratitude. Even though its absence is painful, the education he provided me, the values he forwarded to me, his past advices and the desire to make him proud have bring me the energy, the willingness and the tenacity to complete each of the work undertaken.

Table des matières / Table of contents

Publications 15
Abbreviations 17
Introduction 23
1. Contexte 23
1.1. Contexte énergétique 23
1.2. Contexte environnemental 26
2. Objectifs 29
3. Plan du mémoire 31
Introduction 35
1. Context 35
1.1. Energetic context 35
1.2. Environmental context 38
2. Objectives 41
3. Organization of the manuscript 43
Chapitre 1 / Chapter 1 45
1. Internal combustion engines 48
1.1. Conventional combustion engines 48
1.1.1. Spark ignition engines 48
1.1.2. Compression ignition engines 49
1.2. Advances combustion engines 50
1.2.1. Premixed Charge Compression Ignition (PCCI) 51
1.2.2. Reactivity Controlled Compression Ignition (RCCI) 52
1.2.3. Homogeneous Charge Compression Ignition (HCCI) 52
1.2.4. State on advanced combustion engines 52
2. The HCCI combustion process 53
2.1. Principle of the HCCI combustion 53
2.2. Advantages and challenges of the HCCI combustion 56
2.2.1. Advantages 56
2.2.1.1. Low fuel consumption 56
2.2.1.2. High efficiency 56
2.2.1.3. Low levels of NO_x and particulate matters 56

2.2.1.4. Fuel flexibility 56
2.2.2. Challenges 57
2.2.2.1. Combustion timing control 57
2.2.2.2. Operating range 57
2.2.2.3. Unburned hydrocarbons and carbon monoxide emissions 57
2.2.2.4. Level of noise 58
2.2.2.5. Mixture preparation 58
2.2.2.6. Cold start 58
2.3. Kinetics of the HCCI combustion 59
2.3.1. Low-temperature range 59
2.3.2. Negative temperature coefficient range 60
2.3.3. High temperature range 61
3. Control of the HCCI combustion process 62
3.1. Intake temperature 62
3.2. Fuel 63
3.3. Equivalence ratio 64
3.4. Intake pressure 66
3.5. Rotation speed 67
3.6. Geometry of the piston bowl 69
3.7. Compression ratio 70
3.8. Variable valve actuation 71
3.9. Exhaust gas recirculation 72
3.10. Oxidizing chemical species 74
3.10.1. Fuel peroxides 74
3.10.2. Hydrogen peroxide 75
3.10.3. Nitrogen oxides 76
3.10.3.1. Nitric oxide 76
3.10.3.2. Nitrogen dioxide 78
3.10.3.3. Nitrous oxide 79
3.10.4. Ozone 79
4. Conclusion 81
Chapitre 2 / Chapter 2 83
1. Experimental setup 86

1.1. The HCCI engine bench 86
1.2. Controllers and sensors 87
1.3. Fuels selected 89
1.4. Oxidizing chemical species selected 91
1.4.1. Ozone 91
1.4.1.1. Ozone generator 91
1.4.1.2. Ozone analyzer 92
1.4.2. Nitric oxides 93
1.4.3. Seeding of the oxidizing chemical species 94
2. Analysis of the experimental data 95
2.1. Loading of the engine parameters 95
2.2. Loading of the experimental data 95
2.2.1. Loading of the quick file 96
2.2.2. Loading of the slow file 97
2.3. Post-treatment of the experimental data 98
2.3.1. Motoring analysis 99
2.3.2. Combustion analysis 102
2.4. Engine results 106
2.4.1. In-cylinder pressure analysis 106
2.4.2. In-cylinder temperature analysis 108
2.4.3. Heat release rate analysis 109
2.5. Discussion about the post treatment approach 110
3. Computations 112
3.1. The Senkin program 112
3.1.1. System of equations 113
3.1.2. Structure of the program 115
3.2. Kinetics schemes used 116
3.2.1. Fuel oxidation mechanisms 116
3.2.2. Oxidizing chemical species sub-mechanisms 117
3.2.2.1. Ozone sub-mechanism 117
3.2.2.2. Nitric oxides sub-mechanism 117
3.3. Methodology 117
4. Conclusion 119

Chapitre 3 / Chapter 3 121
1. Introduction on Primary Reference Fuels (Article I) 129
2. Combustion of the Primary Reference Fuels 130
3. Experimental results on the effect of ozone 132
3.1. In-cylinder pressure and heat release rates trends 132
3.2. Combustion phasing 133
1.1.1 Cool and main flame phasing 133
3.2.1. CA05 and CA50 139
3.2.2. Cool flame energy 140
3.3. Kinetics results on the effect of ozone 141
3.3.1. Assessment of the kinetic scheme 141
3.3.2. Interaction between ozone and the intake conditions 142
3.3.3. Ignition delays computations 144
3.3.4. Chemical analysis on PRFs 145
3.3.4.1. Pure n-heptane and pure isooctane 145
3.3.4.2. Mixtures of n-heptane and isooctane 150
4. Ozone seeding with intake temperature variation (Article II) 152
4.1. Combustion under unfavorable intake conditions 152
4.2. Combination of intake temperature with ozone 153
4.3. Cool flame occurrence 155
5. Ozone, nitric oxide and nitrogen dioxide seeding (Article III) 157
5.1. Comparison between ozone, nitric oxide and nitrogen dioxide 157
5.1.1. Experimental results 157
5.1.2. Kinetics results 161
5.2. Simultaneous seeding of ozone and nitric oxide 164
5.2.1. Experimental results 164
5.2.2. Kinetics results 168
6. Application case (Article IV) 174
6.1. Ozone calibration 174
6.2. Comparison of the gas supply 176
6.3. Comparison of the injection position 180
6.4. Experimental results 181
6.4.1. Engine outputs 181

6.4.1.1. Combustion phasing 181
6.4.1.2. Indicated mean effective pressure 182
6.4.1.3. Maximum pressure rise rate 183
6.4.2. Pollutants emissions 184
6.4.2.1. Carbon monoxide emissions 184
6.4.2.2. Unburned hydrocarbons emissions 185
6.4.2.3. Nitrogen oxides emissions 186
6.5. Towards a cycle-to-cycle control 187
6.5.1. Cycle-to-cycle approach 188
6.5.2. Dynamic control 190
6.5.2.1. Open-loop control 190
6.5.2.2. Closed-loop control 191
7. Conclusion on Primary Reference Fuels 193
Chapitre 4 / Chapter 4 197
1. Introduction on gaseous fuels (Article V) 202
2. Combustion of gaseous fuels 203
3. Effect of ozone on gaseous fuels 205
3.1. Combustion of methane/propane surrogate 206
3.1.1. Experimental results 206
3.1.1.1. In-cylinder pressure, temperature and heat release rate trends 207
3.1.1.2. Combustion characteristics under intake pressure variation 208
3.1.1.3. Pollutants under intake pressure variation 211
3.1.1.3.1. Carbon monoxide and unburned hydrocarbons 211
3.1.1.3.2. Nitric oxides 211
3.1.1.4. Combustion characteristics under intake temperature variation 212
3.1.1.5. Pollutants under intake temperature variation 214
3.1.1.5.1. Carbon monoxides and unburned hydrocarbons 214
3.1.1.5.2. Nitric oxides 215
3.1.2. Kinetics interpretation 216
3.1.2.1. Assessment of the kinetic scheme 216
3.1.2.2. Ignition delays 216
3.1.2.3. Rates of consumption 222
3.2. Combustion of methane/hydrogen surrogate 224

3.2.1. Experimental results 224
3.2.1.1. In-cylinder pressure, temperature and heat release rate trends 224
3.2.1.2. Combustion characteristics 226
3.2.1.3. Pollutants 228
3.2.1.3.1. Carbon monoxides and unburned hydrocarbons 228
3.2.1.3.2. Nitric oxides 228
3.2.2. Kinetics interpretation 229
3.2.2.1. Ignition delays 229
3.2.2.2. Rates of consumption 231
4. Conclusion on gaseous fuels 236
Chapitre 5 / Chapter 5 237
1. Introduction on alcohol fuels (Article VI) 240
2. Combustion of alcohol fuels 241
3. Effect of ozone 243
3.1. Experimental results 243
3.1.1. In-cylinder pressure and heat release rate traces 243
3.1.2. Engine outputs 250
3.1.2.1. Combustion phasing 250
3.1.2.2. Indicated mean effective pressure 253
3.1.2.3. Combustion duration 254
3.2. Kinetics results 254
3.2.1. Assessment of the kinetic scheme 255
3.2.2. Ignition delays 256
3.2.3. Kinetic analysis 258
4. Conclusion on alcohol fuels 259
Conclusion 261
Conclusion 267
Futures recherches 271
Future research 275
References 277

Publications

Articles de journal / Journal articles

- J-B. Masurier, F. Foucher, G. Dayma, P. Dagaut, *Homogeneous Charge Compression Ignition Combustion of Primary Reference Fuels Influenced by Ozone Addition*, Energy and Fuels, 2013.
- J-B. Masurier, F. Foucher, G. Dayma, P. Dagaut, *Investigation of iso-octane combustion in a homogeneous charge compression ignition engine seeded by ozone, nitric oxide and nitrogen dioxide*, Proceedings of the Combustion Institute, 2014. Presented at the 35th International Symposium on Combustion.
- F. Contino, J-B. Masurier, F. Foucher, T. Lucchini, G. D'Errico, P. Dagaut, *CFD simulations using the TDAC method to model iso-octane combustion for a large range of ozone seeding and temeprature conditions in a single cylinder HCCI engine*, Fuel, 2014.
- J-B. Masurier, F. Foucher, G. Dayma, P. Dagaut, *Ozone Applied to the Homogeneous Charge Compresssion Ignition Engine to Control Alcohol Fuels Combustion*, Applied Energy, 2015. Presented at the 21 ISAF.

Papiers de conférence / Conference papers

- J-B. Masurier, F. Foucher, G. Dayma, C. Mounaïm-Rousselle, P. Dagaut, *Towards HCCI Control by Ozone Seeding,* SAE Paper 2013-24-0049, 2013, doi: 10.4271/2013-24-0049. Presented at the SAE Capri 2013.
- J-B. Masurier, F. Foucher, G. Dayma, P. Dagaut, *Effect of Additives on Combustion Characteristics of a Natural Gas Fueled HCCI Engine*, SAE Technical Paper 2014-01-2662, 2014, doi: 10.4271/2014-01-2662.Presented at the SAE PFL Conference, Birmingham.
- J-B. Masurier, F. Foucher, G. Dayma, C. Mounaïm-Rousselle, P. Dagaut, *Application of an Ozone Generator to Control the Homogeneous Charge Compression Ignition Combustion Process*, SAE Technical Paper 2015-24-2456, 2015, doi : 10.4271/2015-24-2456. Presented at the SAE Capri 2015.
- P. Pinazzi, J-B. Masurier, G. Dayma, P. Dagaut, F. Foucher, *Towards Stoichiometric Combustion in HCCI Engines: Effect of Ozone Seeding and Dilution*, SAE Technical Paper 2015-24-2450, 2015, doi: 10.4271/2015-24-2450. Presented at the SAE Capri 2015.

Posters

- J-B. Masurier, F. Foucher, G. Dayma, C. Mounaïm-Rousselle, P. Dagaut, *Experimental study of the control of HCCI combustion by ozone addition*, ECM 2013.
- J-B. Masurier, P. Pinazzi, S. Sayssouk, F. Foucher, G. Dayma, C ; Caillol, D. Gruel-Nelson, Y. Chamaillard, P. Higelin, C. Mounaïm-Rousselle, P. Dagaut, *Application des Générateurs d'Ozone sur les Nouveaux Modes de Combustion Automobile*, Innovatives Voiture du Futur 2015.

Présentations orales / Oral presentations

- J-B. Masurier, F. Foucher, G. Dayma, P. Dagaut , *Etude du contrôle de la combustion HCCI par l'ajout d'espèces chimiques oxydantes*, Journée François Lacas, Journée des Doctorants en Combustion, PPRIME Poitiers, 2013.
- J-B. Masurier, F. Foucher, G. Dayma, P. Dagaut, *A Study of the HCCI Isooctane Combustion With Ozone Seeding Under Various Intake Temperatures*, 23rd "Journées d'Etudes" of the Belgian Section of the Combustion Institute, Brussels, 2014.

Abbreviations

C_p	Heat capacity at constant pressure
C_v	Heat capacity at constant volume
E_{cf}	Energy released through the cool flame
E_{mf}	Energy released through the main flame
E_t	Total energy released
L_b	Rod length
P_{IVC}	Pressure at the intake valve closure
P_{cyl}	In-cylinder pressure
P_{max}	Maximum in-cylinder pressure
Q_{ht}	Heat transfer heat release
$Q_{crevice}$	Heat release due to crevices
Q_{gross}	Gross heat release
Q_{net}	Net heat release
Q_{wall}	Wall heat release
R_v	Crankshaft radius
$S_{cylinder\ head}$	Cylinder head surface
S_{exch}	Exchange surface
S_{liner}	Liner chamber surface
S_{piston}	Piston surface
T_{IVC}	Temperature at the intake valve closure
T_{cyl}	In-cylinder temperature
T_{max}	Maximum in-cylinder temperature
T_{wall}	Wall temperature
V_{IVC}	Volume at the intake valve closure
V_{cyl}	Displaced volume
V_d	Clearance volume
V_{mp}	Mean piston speed
$\alpha_{P_{max}}$	Maximum pressure phasing
$\alpha_{T_{max}}$	Maximum temperature phasing
θ_{HTHR}	Phasing of the main flame
θ_{LTHR}	Phasing of the cool flame
θ_{offset}	Offset on the crank angle degree
σ_{IMEP}	Standard deviation of the IMEP
CR	Compression ratio
CR_m	Modified compression ratio
$\dot{\omega}$	Molar production

°C	Celsius degree
°CA	Crank Angle
2EHN	2-ethyl-hexyl-nitrate
A/F	Air/Fuel ratio
ABDC	After Bottom Dead Center
ATDC	After Top Dead Center
Atm	Atmosphere (pressure unit)
Bar	Bar (pressure unit)
BDC	Bottom Dead Center
BTDC	Before Top Dead Center
Btu	British Thermal Unit
BuOH	Butanol
C3H8	Propane
C7H16	n-heptane
C8H18	Isooctane
CA05	Crank angle where 5 % of the fuel has burnt
CA10	Crank Angle where 10 % of the fuel has burnt
CA50	Crank angle where 50 % of the fuel has burnt
CA90	Crank angle where 90 % of the fuel has burnt
CAD	Crank Angle Degrees
Cc	Cubic centimeter
CDC	Conventional Diesel Combustion
CFR	Cooperative Research Engine
CH_2O	Formaldehyde
CH3	Methyl radical
CH4	Methane
CI	Compression Ignition
CN	Cetane Number
CO	Carbon monoxide
CO_2	Carbon dioxide
COV	Covariance
CSP	Complete Stoichiometric Products
DBD	Dielectric Barrier Discharge
Dc	Disc
deg	Degrees
DTBP	di-tertiary-butyl-peroxide
EG	End Gases
EGR	Exhaust Gas Recirculation
EIA	U.S. Energy Information Administration

ERC	European Research Council
EtOH	Ethanol
EVC	Exhaust Valve Closure
EVO	Exhaust Valve Open
g/km	Gram per kilometer
g/mol	Gram per mole
Gt	Gigatonnes
h	Convective heat transfer coefficient
H_2	Hydrogen
H_2O	Water
H_2O_2	Hydrogen peroxide
HC	Unburned hydrocarbon
HCCI	Homogeneous Charge Compression Igniton
HO_2	Hydroperoxyl radical
HONO	Nitrous acid
HRR	Heat Release Rate
HTHR	High Temperature Heat Release
HTRA	High Temperature Reaction Appearance
HTRE	High Temperature Reaction End
Hz	Hertz
IEA	International Energy Agency
IGR	Internal Gas Recirculation
IK	Ignition kernel
IMEP	Indicated Mean Effective Pressure
IVC	Intake Valve Closure
IVO	Intake Valve Open
J	Joule
J/°CA	Joule per Crank Angle
J/CAD	Joule per Crank Angle Degrees
J/deg.	Joule per degrees
J/K	Joule per Kelvin
K	Kelvin
kg/m^3	Kilogram per cubic meter
kJ/kg	Kilojoule per kilogram
kV	Kilovolt
LHV	Lower Heat Value
LTC	Low Temperature Combustion
LTHR	Low Temperature Heat Release
LTRA	Low Temperature Reaction Appearance

LTRE	Low Temperature Reaction End
MeOH	Methanol
MFC	Mass Flow Controller
mm	Millimeter
$Mol/cm^3/s$	Mole per cubic centimeter per second
MON	Motor Octane Number
MPa	Mega Pascal
MPRR	Maximum Pressure Rise Rate
N_2O	Nitrous oxide
NA	Naturally Aspirated
NEDC	New European Driving Cycle
NL/h	Liter per hour under normal conditions
NL/min	Liter per minute under normal conditions
NO	Nitric oxide
NO_2	Nitrogen dioxide
NO_x	Nitrogen oxides
NPF	Non-Premixed Flame
NVO	Negative Valve Overlap
O/N	Oxygen to nitrogen ratio
O_2	Oxygen
O_3	Ozone
OECD	Organisation for Economic Cooperation and Development
OH	Hydroxyl radical
OI	Octane Index
ON	Octane Number
OOQOOH	Peroxyhydroperoxyalkyl radical
OPO	Oxygenated hydrocarbon radical
PCCI	Premixed Charge Compression Ignition
P_{in}	Intake Pressure
PLC	Programmable Logic Controller
PM	Particulate matter
ppm	Parts per million
PRF	Primary Reference Fuel
PTF	Premixed Turbulent Flame
QOOH	Hydroperoxyalkyl radical
R	Alkyl radical
RCCI	Reactivity Controlled Compression Ignition
RH	Alkane fuel
RHO/ROH	Alcohol radical

RHOH	Alcohol fuel
RO_2	Alkylperoxyl radical
ROC	Rate of consumption
RON	Research Octane Number
rpm	Revolutions per minute
SC	Supercharged
SI	Spark Ignition
SOI	Start of Ignition
Sq	Square
TDC	Top Dead Center
T_{in}	Intake temperature
TRF	Toluene Reference Fuel
T-S	Temperature – Entropy
UV	Ultraviolet
VCR	Variable Compression Ratio
Vol %	Volume fraction
A	Pre-exponential coefficient
B	Bore
C	Stroke
E	Activation energy
M	Molar mass
Q	Quantity of heat
S	Entropy
V	Instantaneous volume
X	Piston position
X	Molar fraction
Y	Mass fraction
a	JANAF coefficient
e	Internal energy per mass
k	Rate constant
m	Mass
p	Pressure
t	Time
β	Temperature exponent
γ	Ratio of the heat capacities
θ	Crank Angle Degree
λ	Air/Fuel ratio
ν	Specific volume
τ	Combustion phasing

φ	Equivalence ratio
ω	Rotation speed
ϕ	Equivalence ratio
ε	Molar absorptivity
L	Length of the measurement cell
I_0	Reference light intensity
I	Light intensity measured

Introduction

Version française / French version

1. Contexte

1.1. Contexte énergétique

Depuis quelques décennies, la demande énergétique mondiale n'a cessé de croître atteignant en 2010 une consommation d'environ 524 Quadrillion Btu ou encore 553 Exajoules selon les rapports de l'EIA (*U.S. Energy Information Administration*) [1]–[3]. En référence à 1990, cette demande a augmenté d'environ 47 % en 2010 et les prévisions sur les futures décennies envisagent une augmentation de la consommation énergétique mondiale de 2010 à 2040 d'environ 56 % (Figure 1). Ainsi, en 50 ans (de 1990 à 2040), la demande énergétique mondiale aura doublé.

Les principales causes de cette augmentation proviennent de la croissance de la population mondiale (actuellement d'environ 7,3 milliards d'individus en 2015, elle devrait atteindre environ 9,7 milliards en 2050 [4]), du développement industriel et de l'urbanisation. Ainsi, les prévisions sur la demande énergétique envisagent une consommation en énergie quasi-constante pour les pays membres de l'OCDE (*Organisation de Coopération et de Développement Economiques ou en anglais Organisation for Economic Cooperation and Development, OECD*) tandis que les pays non membres, essentiellement la Chine et l'Inde qui sont actuellement en plein essor, seront responsables de la majeure partie de l'augmentation de la consommation énergétique mondiale.

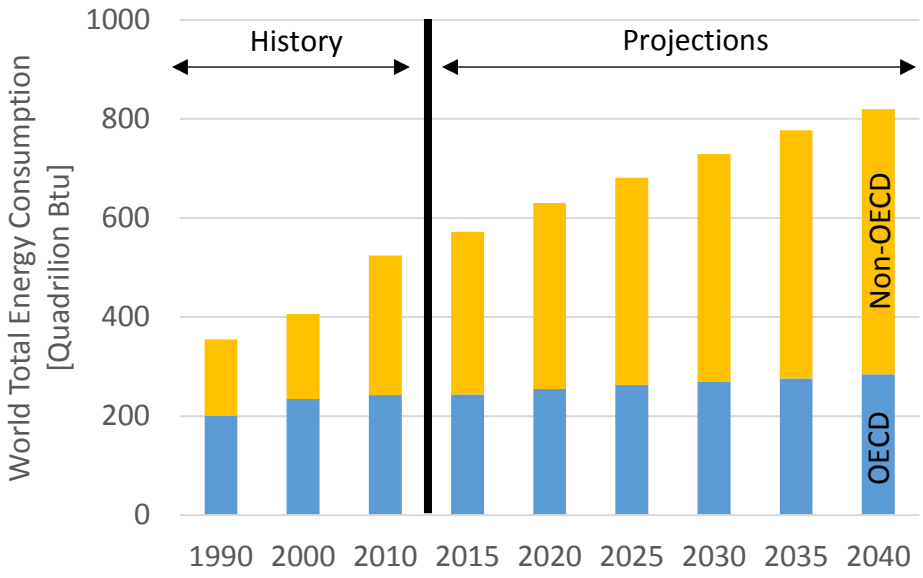

Figure 1. *Historique et projections de la consommation totale en énergie dans le monde de 1990 à 2040 réparti entre les pays membres de l'OCDE et les pays non-membres de l'OCDE [1].*

Cette demande énergétique mondiale est répartie autour de deux grandes familles d'énergie : les énergies renouvelables et les énergies non-renouvelables. Cette première famille est composée de l'énergie solaire, éolienne, hydraulique, géothermique et enfin la biomasse. La seconde famille est quant à elle composée de l'énergie nucléaire et des énergies fossiles, ces dernières étant essentiellement le pétrole, le charbon et le gaz naturel. Les rapports de l'EIA [1]–[3] montrent que la majeure partie de la consommation énergétique mondiale est dépendante des énergies fossiles (Figure 2). En 2013, ces énergies représentaient plus de 80 % de la consommation énergétique mondiale et malgré le besoin énergétique croissant envisagée, ces énergies resteront dominantes en 2040 : respectivement de 28 % pour le pétrole, 27 % pour le charbon et 23 % pour le gaz naturel, soit environ 78 % de l'énergie totale nécessaire. Toutefois, ces ressources sont tarissables et le pétrole qui arrive en tête des énergies consommées est le plus concerné. Selon l'AIE (*Agence Internationale de l'Energie ou en anglais International Energy Agency, IEA*) [5], la production de pétrole provenant des sources actuellement en cours d'exploitation diminue. Ainsi, d'ici à 2035, cette production aura diminué de plus de moitié. Bien qu'il existe d'autres sources permettant de maintenir la demande énergétique de cette ressource, i.e. des sources en cours de développement, des sources encore inexploitées et d'autres sources non-conventionnelles, le pétrole tendra à se raréfier et il est donc impératif que cette ressource énergétique soit économisée.

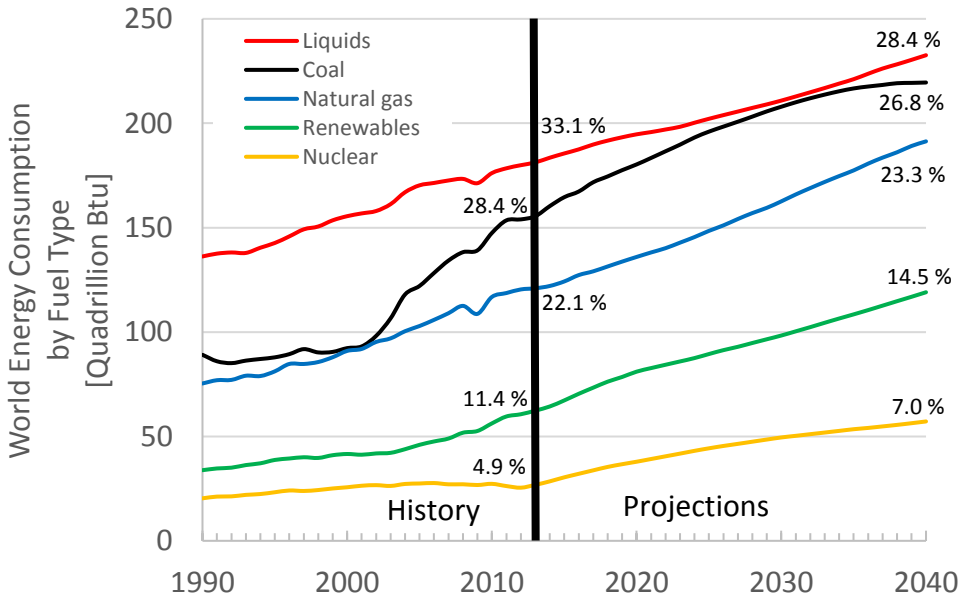

Figure 2. *Historique et prévisions de la consommation des différentes sources d'énergie. Les chiffres en pourcentage représentent la part de l'énergie dépensé pour chaque énergie en référence à l'énergie globale utilisée ou nécessaire respectivement pour 2013 et 2040 [1].*

Le secteur des transports est au cœur de ce contexte énergétique. Il se répartit sous diverses formes (routier, maritime, ferroviaire et aérien) et participent activement au développement économique mondial. A l'échelle mondiale, ce secteur représentait presque 20 % de la consommation énergétique mondiale en 2010 (le reste étant consommé par les

autres secteurs, à savoir, les secteurs résidentiels, commerciaux et industriels) et bien que sa part doive légèrement décroitre dans les scénarios à venir, il devrait atteindre un pourcentage constant d'environ 17 % dès 2025 (Figure 3). La cause de ce maintien est qu'avec la croissance de la population et le développement industriel, le nombre de véhicules devrait fortement augmenter (plus de 1 milliard de véhicules actuellement et le double aux environs de 2040) tout en devenant plus économes. De plus, cette économie d'énergie explique la décroissance de la consommation pour les transports des pays membres de l'OCDE tandis que les pays non-membres et donc en plein essor vont voir leur consommation s'accroitre.

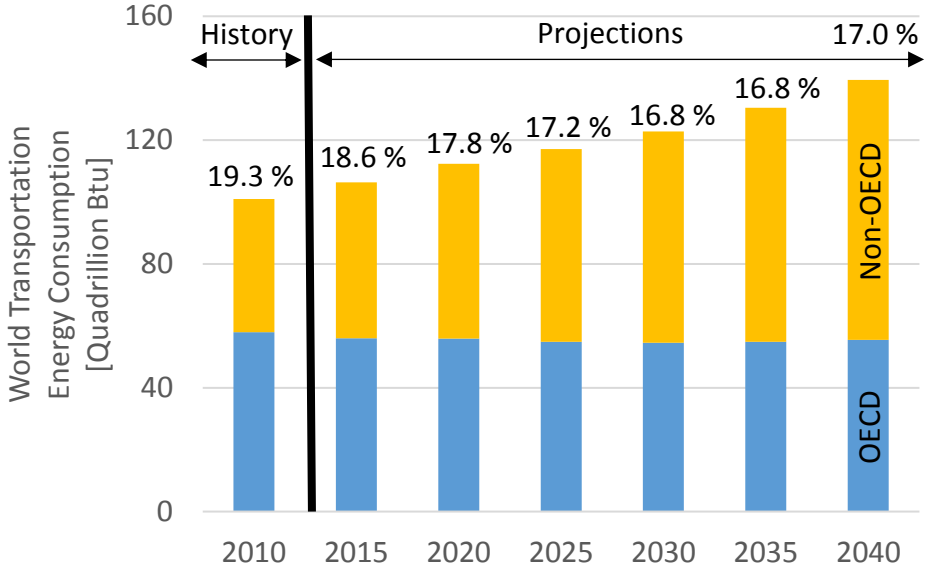

Figure 3. *Historique et prévisions de la consommation en énergie des transports entre 2010 et 2040 réparti entre les pays membres de l'OECD et les pays non membres. Les pourcentages en haut de chaque histogramme représentent la part des transports en référence à la demande énergétique mondiale[1]*

En termes de ressources énergétiques, le secteur des transports est le principal consommateur de pétrole. Les rapports de l'EIA ont estimé que ce secteur consomme plus de la moitié de cette énergie fossile (approximativement 55 %) et cette proportion devrait rester stable d'après les prévisions effectuées. De plus, en observant la répartition de la consommation en énergies primaires au sein de ce secteur, le pétrole représentait plus de 90 % en 2010 et la prévision pour 2040 projette que ce pourcentage aura légèrement diminué au profit d'autres énergies (Figure 4). Ainsi, les énergies renouvelables et le gaz naturel remplaceront progressivement la consommation de pétrole tandis que l'électricité, qui est une énergie secondaire produite à partir de l'ensemble des énergies primaires, ne conservera qu'une faible part de la consommation en énergie des transports. Enfin, le secteur des transports se diversifie sous différentes formes et est principalement dominé par les transports routiers (véhicules légers, utilitaires et poids lourds). Ces derniers

représentent de manière équitable presque 80 % de l'énergie consommée par ce secteur [6]. En conséquence, afin d'aboutir à une économie des ressources fossiles et en particulier du pétrole dans ce contexte énergétique, les transports et plus précisément les transports routiers sont parmi les principaux vecteurs économiques sur lesquels des développements et des améliorations doivent être conduits.

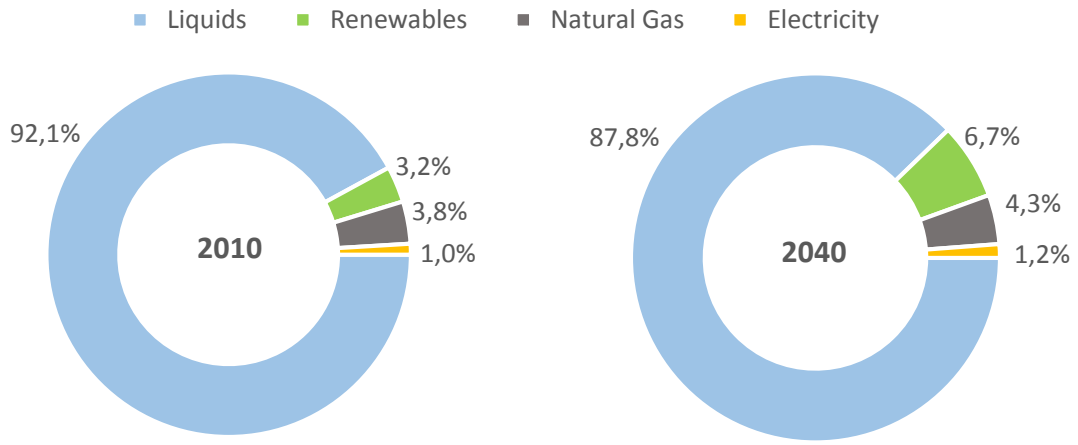

Figure 4. *Consommation en 2010 des différentes sources d'énergie pour le secteur des transports et prévision pour 2040. L'électricité ici est considérée comme une énergie secondaire produite à partir de l'ensemble des ressources énergétiques primaires [1].*

1.2. Contexte environnemental

Outre la problématique énergétique tournant autour de l'économie des ressources primaires, les différents secteurs d'activités ont aussi un impact environnemental. Ils sont majoritairement responsables de l'émission de gaz à effet de serre qui participent au réchauffement climatique. Parmi l'ensemble des gaz à effet de serre produits, le dioxyde de carbone (CO_2) a été désigné comme le principal fautif et est essentiellement produit par l'activité humaine. Ainsi, le bilan établi par l'AIE en 2011 a montré que les émissions globales de CO_2 ont atteint 38 Gigatonnes (Figure 5). La répartition par secteur d'activités fait état que les transports sont responsables de presque le quart de ces émissions et environ 75 % de ces dernières émissions sont émises par les transports routiers tout en étant réparties équitablement entre les véhicules légers et les poids lourds. Ceci s'explique aisément compte tenu de la répartition des différents transports en fonction de leur consommation énergétique. Ainsi, devant ce constat, les transports sont particulièrement ciblés pour réduire leurs émissions de CO_2 et diminuer leurs impacts sur le réchauffement climatique. Différents pays à travers le monde ont donc instauré des objectifs de réduction de leurs émissions de CO_2 pour les futurs véhicules. C'est notamment le cas de l'Union Européen qui a fixé un seuil maximal pour les véhicules légers de moins de 95 g/km de CO2 pour 2021 (Figure 6). Finalement, les émissions de CO_2 des transports sont principalement liées à leur

consommation en pétrole et donc, l'objectif de réduire les émissions de ce gaz à effet de serre est étroitement lié avec l'objectif d'économiser les énergies fossiles.

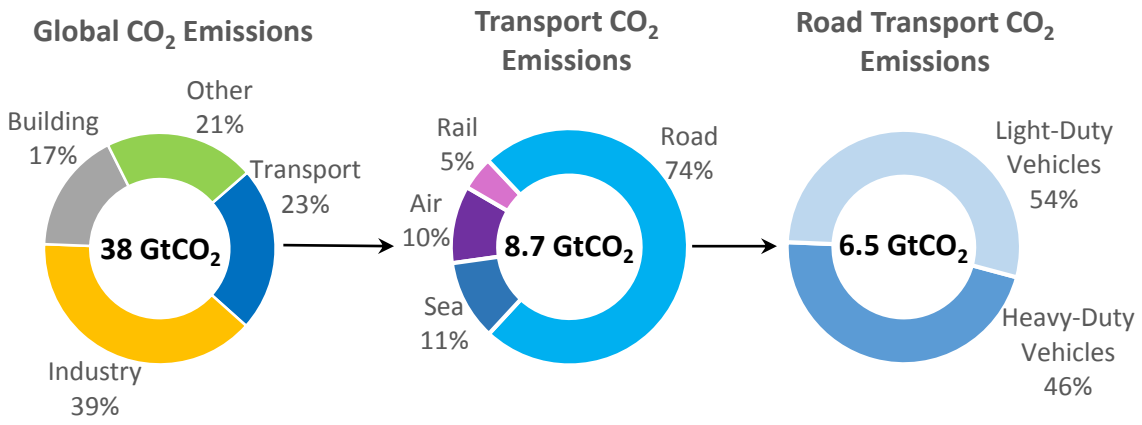

Figure 5. *Répartition par secteur des émissions mondiales de CO_2 en 2010 et la part respectives des transports [5], [7].*

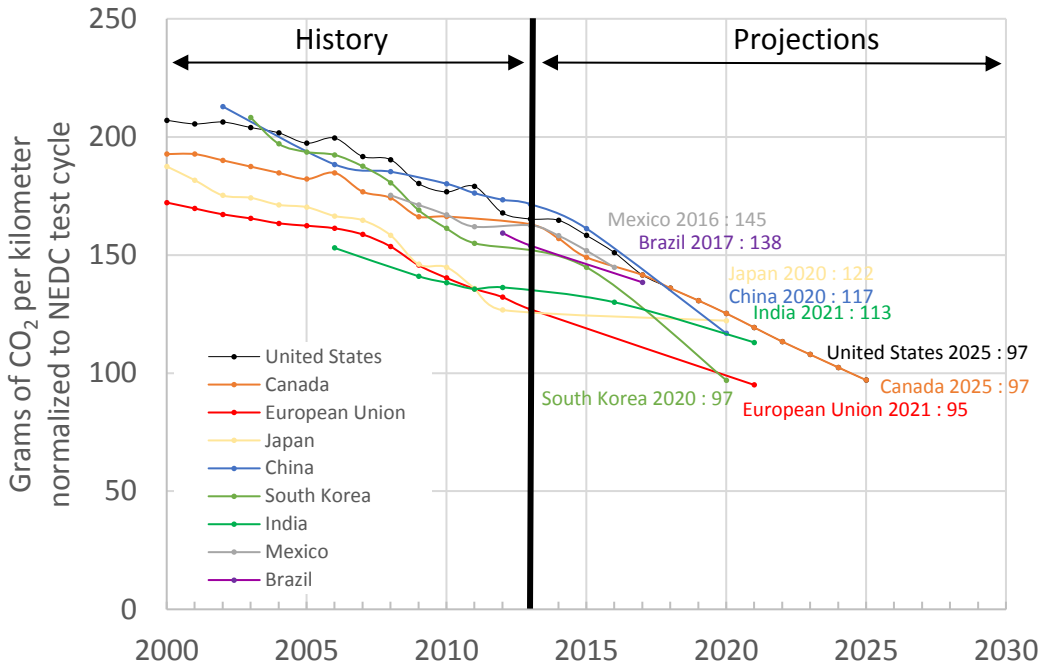

Figure 6. *Projections de la production en CO2 par kilomètre pour les véhicules légers en référence au cycle NEDC [7].*

D'autre part, l'activité humaine est aussi une source d'émissions de polluants (monoxyde de carbone (CO), hydrocarbures imbrulés (HC), oxydes d'azote (NO_x) et particules) dont les effets sont particulièrement néfastes pour la santé et la biodiversité. De plus, les transports participent de manière plus ou moins importante à la pollution atmosphérique, en particulier dans les zones urbaines où les véhicules sont fortement concentrés. Ainsi, afin d'améliorer la qualité de l'air, des restrictions des émissions polluantes ont été mises en place telles que les normes Euro (Figure 7). Ces réglementations

deviennent de plus en plus drastiques et obligent le secteur des transports à effectuer de constantes améliorations.

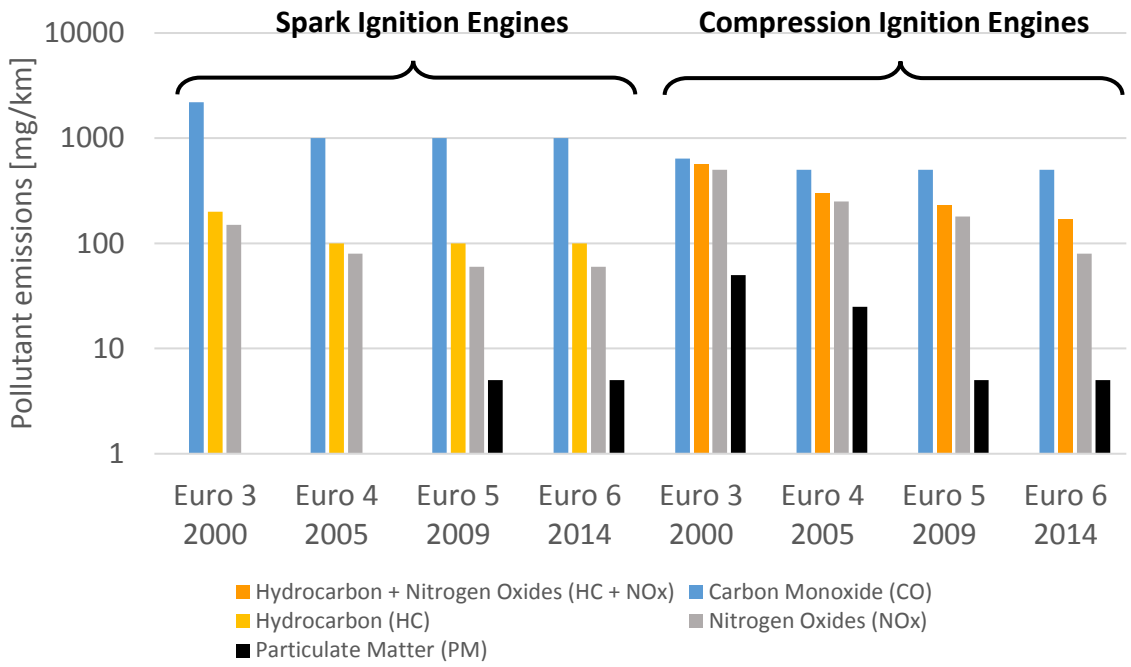

Figure 7. *Evolutions des valeurs limites des émissions polluantes pour les véhicules légers à moteurs à allumage commandé (à gauche) et à moteurs à allumage par compression (à droite) [8]. Remarque : les particules apparaissent pour les moteurs à allumage commandé à partir de la norme Euro 5 avec le développement de l'injection directe stratifiée.*

2. Objectifs

Face à ce contexte énergétique et environnemental, le secteur des transports a donc pour objectifs d'économiser les énergies fossiles utilisées, participant également à réduire les émissions de CO_2 des véhicules, et de participer à l'amélioration de la qualité de l'air. De plus, le secteur doit également continuer d'améliorer les rendements des véhicules.

Actuellement, la propulsion des véhicules est essentiellement réalisée aux moyens des moteurs à combustion interne. Néanmoins, les contraintes énergétiques et environnementales ont permis l'émergence d'autres types de propulsion telle que la propulsion électrique ou encore la propulsion hybride. La première semble être la solution idéale car les véhicules n'émettraient plus aucuns polluants (véhicules zéro émission) mais il faut aussi prendre en considération la production d'électricité. Cette énergie est majoritairement produite à partir des ressources primaires et est elle-même une source importante d'émissions. De plus, ces véhicules sont soumis à deux problèmes majeurs : les réseaux de distribution pour la recharge des batteries ne sont pas suffisamment développés et la densité énergétique des batteries, médiocre en comparaison avec les carburants conventionnels utilisés, pose un problème d'autonomie. L'hybridation, qui consiste à combiner la propulsion au moyen d'un moteur à combustion interne et la propulsion électrique, semble avoir de fortes possibilités d'aboutir à une large utilisation au sein des véhicules mais nécessitera le maintien d'un moteur thermique. Ainsi, le moteur à combustion interne continuera à propulser des véhicules au cours des futures décennies.

Le moteur à combustion interne est essentiellement dominé par deux types de modes de combustion : le moteur à allumage commandé et le moteur à allumage par compression. De nombreuses innovations et améliorations ont été implantées pour chacun d'entre eux afin de répondre au contexte énergétique et environnemental mais face à des réglementations de plus en plus drastiques, de nouveaux modes de combustion ont émergés comme alternatives aux modes de combustion conventionnels. Ces modes de combustion alternatifs, regroupés sous l'acronyme LTC (Low Temperature Combustion), permettent potentiellement de réduire la consommation en carburants des moteurs, et donc leurs émissions de CO_2. Ces moteurs conduisent aussi à des émissions de particules et d'oxydes d'azote (NO_x) très faibles en raison des basses températures de combustion et maintiennent de hauts rendements grâce à l'emploi de fort taux de compression. De plus, leur intérêt est renforcé par leur possibilité d'utiliser un large choix de carburants (conventionnels et alternatifs) dont certains sont actuellement en pleine émergence.

Parmi ces nouveaux modes de combustion, le mode HCCI (Homogeneous Charge Compression Ignition), dont le principe consiste en une combinaison des modes de combustion conventionnels, i.e. la préparation d'un mélange homogène entre l'air et le

carburant comme pour le moteur à allumage commandé puis ce mélange est auto-inflammé comme pour le moteur à allumage par compression, fait l'objet de nombreuses recherches. En effet, il participe activement à la compréhension des phénomènes de combustion homogènes intervenant dans la plupart des nouveaux modes de combustion ainsi qu'à leur développement. Néanmoins, à la différence des moteurs conventionnels, le mode HCCI ne possède pas de dispositifs permettant de contrôler efficacement l'ensemble du processus de combustion. L'initiation de la combustion, entièrement contrôlée par les mécanismes de cinétique chimique, est donc le principal challenge à surmonter. De nombreuses méthodes ont fait l'objet d'investigations et d'applications et les études les plus récentes s'intéressent à l'impact de différentes espèces chimiques oxydantes. Parmi le large panel d'espèces chimiques oxydantes, plusieurs études ont été menées sur l'utilisation de l'ozone et ont démontré que cette molécule a un fort potentiel [9]–[13]. L'ozone est essentiellement formé à l'aide de générateurs à décharges plasma alimentés par un gaz contenant de l'oxygène tel que l'air, ainsi, l'utilisation de tels appareils pourrait susciter un réel intérêt pour de futures applications automobiles intégrant les nouveaux modes de combustion.

Dans le cadre du projet ERC Advanced Grant 2G-CSafe (Combustion of Sustainable Alternative Fuels for Engines used in aeronautics and automotives), un des objectifs est d'étudier l'impact d'espèces chimiques réactives sur le déroulement de la combustion au sein de moteurs tel que le HCCI afin d'apporter de nouvelles stratégies de contrôle de la combustion et éventuellement de nouvelles possibilités technologiques. La présente thèse porte ainsi sur l'effet de l'ensemencement à l'admission d'un moteur HCCI par des espèces chimiques minoritaires oxydantes produites au moyen d'un générateur à décharges plasma et les possibilités applicatives de tels dispositifs au sein d'un véhicule conventionnel. Le travail est majoritairement centré sur la compréhension de l'impact de ces espèces chimiques et s'étend jusqu'à une première approche applicative de ce type de dispositif. Puis, compte tenu de la flexibilité en carburant des nouveaux modes de combustion, une seconde approche s'intéresse à l'effet de l'ozone sur divers carburants alternatifs.

3. Plan du mémoire

La présente thèse traite d'une étude expérimentale couplée à des simulations de cinétique chimique avec pour objectif principal d'étudier l'impact de diverses espèces chimiques oxydantes minoritaires issues des générateurs à décharges plasma sur la combustion HCCI. Les recherches menées considèrent aussi le potentiel applicatif de ces dispositifs ainsi que l'utilisation de différentes familles de carburant. Ces travaux de thèse ont été menés dans le cadre d'un contrat européen et ce manuscrit est basé sur les articles de journaux et papiers de conférence publiés. Il est donc divisé en cinq chapitres distincts intégralement rédigés en anglais. Chaque début de chapitre comporte un résumé en français et en anglais mettant en évidence les principales informations et résultats retenues. Ce mémoire s'organise donc comme ci-après.

Le premier chapitre consiste en une étude bibliographique sur la combustion HCCI. Dans une première partie, un bilan des différents modes de combustion conventionnels sera tout d'abord effectué et introduira les nouveaux modes de combustion dont fait partie le mode HCCI. L'importance des recherches effectuées et en cours sur ce dernier sera mise en avant et permettra de décrire son principe ainsi que ses différentes caractéristiques. Finalement, les avantages et les inconvénients de ce mode de combustion alternatif entièrement gouverné par les mécanismes de cinétique chimique seront exposés pour mettre en évidence les enjeux qui limitent son développement et son application au sein d'un véhicule conventionnel. Parmi les nombreux challenges à surmonter, des méthodes originales ont été proposées afin de contrôler efficacement l'ensemble du processus de combustion. Ce dernier étant fortement influencé par de nombreux paramètres, un état de l'art sur la plupart d'entre eux et leurs impacts respectifs sera présenté.

Le deuxième chapitre fera l'objet d'une description des différents moyens expérimentaux et outils numériques utilisés pour ces travaux de thèse. Le banc moteur utilisé pour les essais expérimentaux HCCI sera entièrement détaillé ainsi que son instrumentation et l'acquisition des données. Ce banc expérimental a permis d'étudier différents types de carburant, un tableau récapitulatif des carburants retenus et de leurs propriétés respectives sera donc dressé. Finalement, dans le cadre de ces recherches, les méthodologies et les dispositifs nécessaires afin d'étudier l'impact des espèces chimiques oxydantes seront également mis en évidence. Suite à cette description, la procédure de post-traitement des données enregistrées mise en place conduisant aux résultats finaux sera décrite. Enfin, ce chapitre se terminera par une description des simulations de cinétique chimique conduites. Le modèle utilisé sera présenté et accompagné des schémas et sous-

schémas cinétiques retenus pour la compréhension de l'impact des différentes espèces chimiques sélectionnées.

Finalement, les chapitres suivants de ce manuscrit seront entièrement consacrés aux résultats obtenus au cours de ces travaux de thèse et valorisés par des publications. Ces chapitres s'organisent donc suivant le fil conducteur décrit ci-après.

La première partie des résultats est consacrée à une large étude sur la combustion des « Primary Reference Fuels (PRFs) », i.e. l'isooctane et le n-heptane ainsi que les mélanges de ces deux carburants. Tout d'abord, les recherches conduites sur la combustion des PRFs sans ensemencement d'espèces chimiques oxydantes seront présentées dans l'objectif d'appréhender les différentes conditions nécessaires à l'auto-inflammation de ces carburants. Suite à ces résultats, l'étude se concentrera sur l'impact de l'ozone sur la combustion des PRFs au moyen d'expériences effectuées à l'aide du banc moteur HCCI ainsi qu'au moyen de simulations numériques. Face aux observations réalisées, un travail expérimental plus approfondi sur l'impact de l'ozone sur la combustion de l'isooctane sera présenté en vue de démontrer le potentiel de l'utilisation de cette molécule chimique oxydante. Finalement, en considérant une probable application d'un générateur à décharges plasma dans un véhicule, d'autres espèces chimiques oxydantes doivent être prises en compte comme le monoxyde d'azote et le dioxyde d'azote, aussi présent dans les gaz résiduels ou la recirculation des gaz d'échappement. Une étude comparative entre ces deux espèces et l'ozone sur la combustion de l'isooctane sera donc également présentée ainsi que l'effet de l'interaction entre l'ozone et le monoxyde d'azote. Enfin, un premier cas d'application en vue de contrôler le processus de la combustion HCCI sera démontré et analysé.

Les deux chapitres de résultats suivants s'intéresseront à la combustion HCCI de carburants alternatifs et une comparaison avec les précédents résultats obtenus sur les PRFs pourra être effectuée. Tout d'abord, les résultats seront focalisés sur les carburants gazeux, en particulier le méthane et des mélanges contenant majoritairement du méthane. Les résultats de ce chapitre suivront le même cheminement que les résultats obtenus avec les PRFs en partant d'une étude de l'auto-inflammation de carburants gazeux purs puis l'impact de l'ozone sera interprété à partir d'essais expérimentaux couplés à des simulations de cinétique chimique. Finalement, le dernier chapitre des résultats se concentrera sur la combustion des carburants de seconde génération et plus précisément sur les carburants de la famille des alcools. L'étude se focalisera sur trois alcools : le méthanol, l'éthanol et le butanol, et s'orientera elle aussi de manière similaire à l'étude conduite sur les PRFs.

Ce mémoire se terminera finalement par un bilan de l'ensemble des expériences et simulations conduites ainsi que sur l'apport des résultats obtenus pour la communauté scientifique et le développement des nouveaux modes de combustion. De plus, compte tenu de l'aspect émergent et innovant de ces recherches, de nombreuses perspectives seront évoquées.

Introduction

Version anglaise / English version

1. Context

1.1. Energetic context

For a few decades, the energy demand continued to rise, reaching in 2010 a consumption of approximately 524 Quadrillion Btu or again 553 Exajoules according to the reports of the U.S. Energy Information Administration (EIA) [1]–[3]. Referring to 1990, this demand grew of approximately 47 % in 2010 and the forecasts for future decades consider a rise of the world total energy consumption from 2010 to 2040 of approximately 56 % (Figure 8). In this way, in 50 years (from 1990 to 2040), the world total energy consumption will double.

The main reasons of this rise come from the growth of the world population (currently around 7.3 billion people in 2015, the demography should reach 9.7 billion in 2050 [4]), the industrial development and the urbanization. Thus, the forecasts estimate an energy consumption almost constant for the OCDE (Organisation for Economic Cooperation and Development) countries while the non-OCDE countries, mainly China and India which grow rapidly, will be responsible of the major part of the increase of the world total energy consumption.

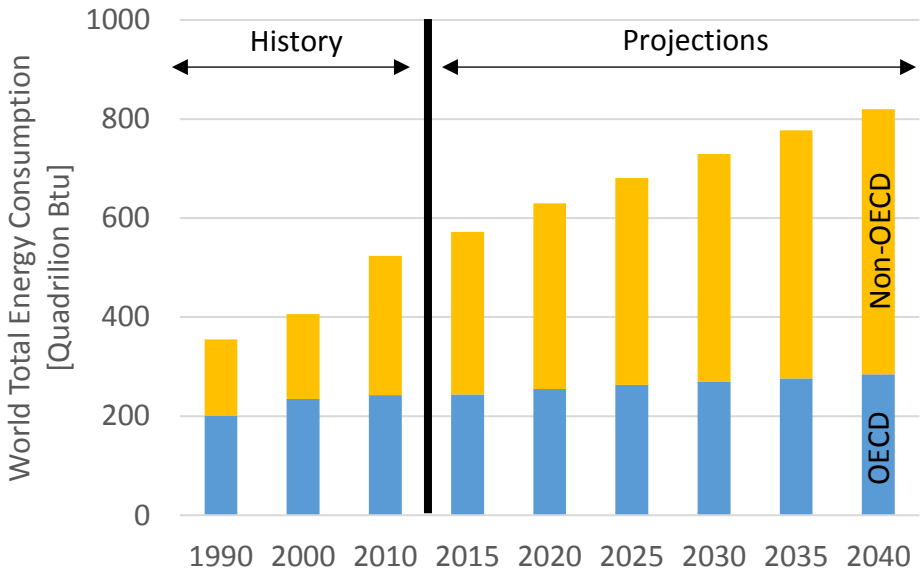

Figure 8. *Past and projected total energy consumption in the world from 1990 to 2040 splitted between OCDE countries and non-OCDE countries [1].*

The world energy demand is spread in two families: the renewables and the non-renewables. This first family involves the solar energy, the wind energy, the hydraulic energy, the geothermal energy and the biomass. The second involves the nuclear energy and

fossil energies, i.e. petroleum, coal and natural gas. The reports of the EIA [1]–[3] show that the main part of the world energy consumption depends on the fossil energies (Figure 9). In 2013, these energies represented more than 80 % of the world energy consumption and despite of the rise of the energy requirement expected, these energies will still dominate in 2040: 28 % for petroleum, 27 % for coal and 23 % for natural gas, respectively, therefore approximately 78 % of the total energy needed. However, these resources deplete and the petroleum, which the major energy consumed, is the most affected. According to the International Energy Agency (IEA) [5], the production of petroleum coming from the sources in operation decreases. Thus, from now to 2035, this production will decrease by more than half. Even through there is other sources allowing to maintain the demand, i.e. sources under development, untapped sources or non-conventional sources, the petroleum will become rare and it is therefore of a main importance to save it.

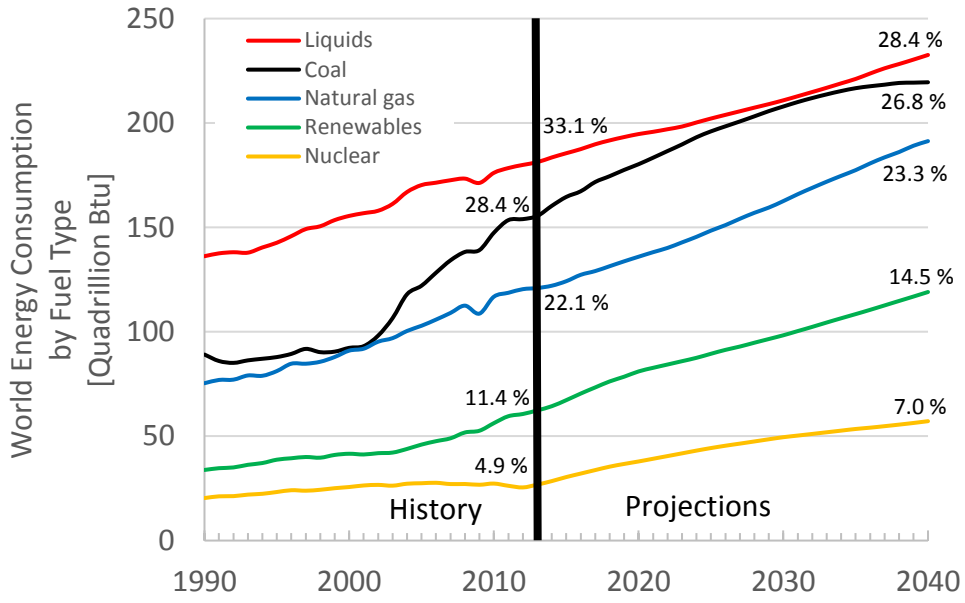

Figure 9. *Past and projected energy consumption by fuel type in the world. Percentages correspond to the ratio of each energy consumption by fuel supply in reference to the global energy consumption used (2013) and needed (2040) [1].*

The transport sector is in the center of this energetic context. It is divided into various types (road, sea, rail and air) and participate actively to the global economic development. Based on a worldwide scale, the transportation represented almost 20 % of the world total energy consumption in 2010 (The rest is consumed by the other sectors, i.e. the residential sector, the industrial sector and the commercial sector) and even though its part must decrease in the forecasts, it should reach a constant percentage of approximately 17 % from 2025 (Figure 10). The main reason of this is that with the growth of the world population and the industrial development, the number of vehicles should strongly increase (around 1 billion now and probably twice as much in 2040) and by becoming more economical. Furthermore, this explains the decline of the consumption of the transports of the OCDE countries while the consumption of non-OCDE countries monotonically increases.

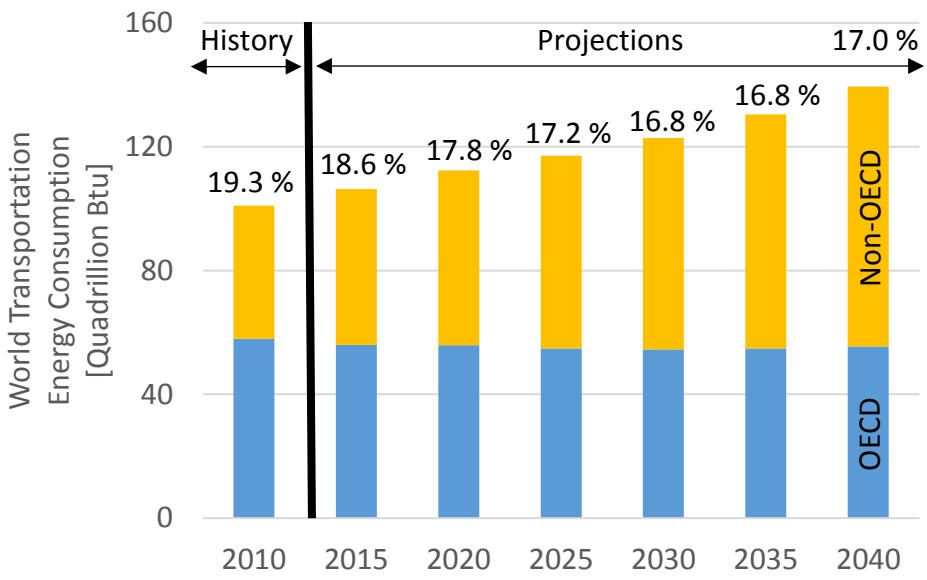

Figure 10. *Past and projected world transportation energy consumption from 2010 to 2040 splitted between OCDE countries and non-OCDE countries. Percentages correspond to the ratio between the transportation energy consumption needed and the total energy consumption [1]*

Regarding to the energetic resources, the transportation is the main consumer of petroleum. The reports of the EIA assessed that this sector consumes more than the half of this fossil energy (around 55 %) and this ratio should remain constant enough according to the forecasts carried out. Moreover, observing the distribution of the consumption in primary energies in this sector, the petroleum corresponded to more than 90 % in 2010 and the forecast for 2040 considers that this ratio will reduce slightly (Figure 11). Thus, the

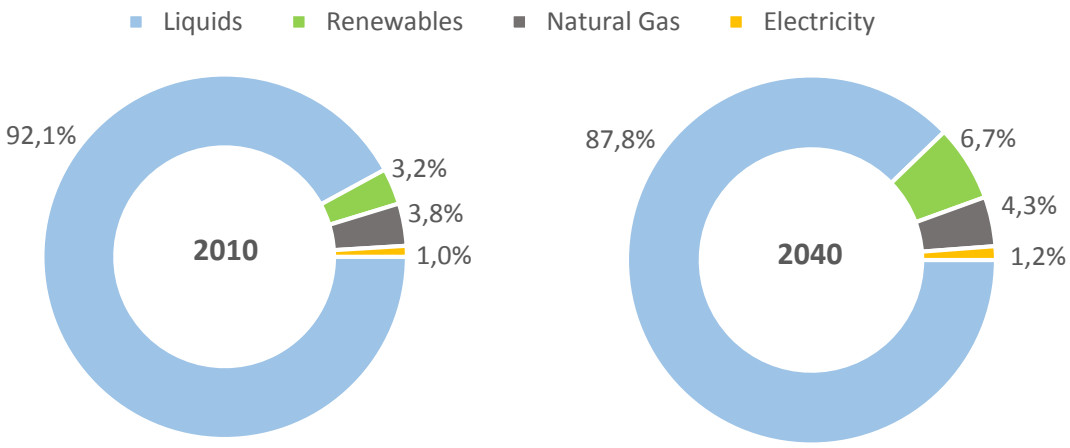

Figure 11. *Consumption of the transportation by fuel type in 2010 and forecasts for 2040. Electricity is considered here as a secondary energy generated from the whole primary energies [1].*

renewables and the natural gas will replace progressively the oil consumption while the electricity, a secondary energy generated from all the primary ones, will keep only a low ratio of the total energy consumed by the transportation. Finally, the sector included several types of vehicles and is mainly dominated by road transports (light-duty vehicles and heavy-duty vehicles) which represent approximately 80 % of the energy consumed by the sector [6]. Consequently, to save the fossil resources and in particular the petroleum in this energetic context, transports and more precisely road transports are among the economic vectors on which developments and improvements must be performed.

1.2. Environmental context

In addition to the energetic context about the saving of the primary resources, the different sectors of activities have also an environmental impact. They are mainly responsible of the greenhouse gas emissions which participate to the global warming. Among all the gases produced, the dioxide of carbon (CO_2) was designated as the relevant guilty and is mainly produced by the human activity. In this way, the overview established by the IEA in 2011 showed that the worldwide emissions of CO_2 reached 38 Gt (Figure 12). The distribution by sectors showed that the transportation is responsible of almost one quarter of these emissions and approximately 75 % of this quarter comes from the road vehicles with a fair distribution between light-duty and heavy-duty vehicles. This is explained easily considering the part in energetic consumption of the different transports. Based on this observation, transports are significantly targeted to reduce their CO_2 emissions and limit their impact on the global warming. Several countries throughout the world set up objectives to reduce the CO_2 emissions of the future vehicles. This is the case of the European Union which fixed a maximum threshold for light-duty vehicles of less than 95 g/km of CO_2 for 2021 (Figure 13). Finally, the CO_2 emissions for transportation are mainly related to the fuel consumption and therefore, the aim of reducing the emissions of this greenhouse gas is tightly related to the aim of saving fossil energies.

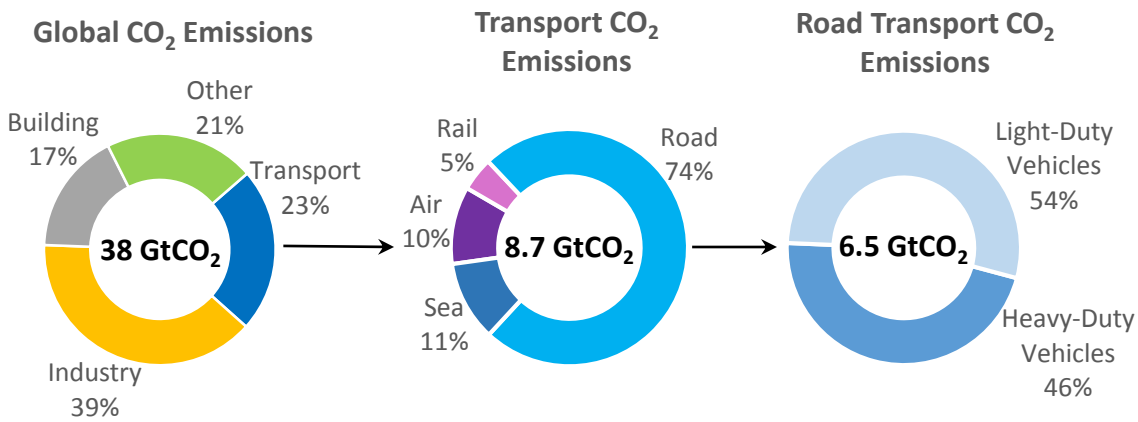

Figure 12. *Parts of the world total CO_2 emissions by sectors in 2010 and parts of the transportation [5], [7].*

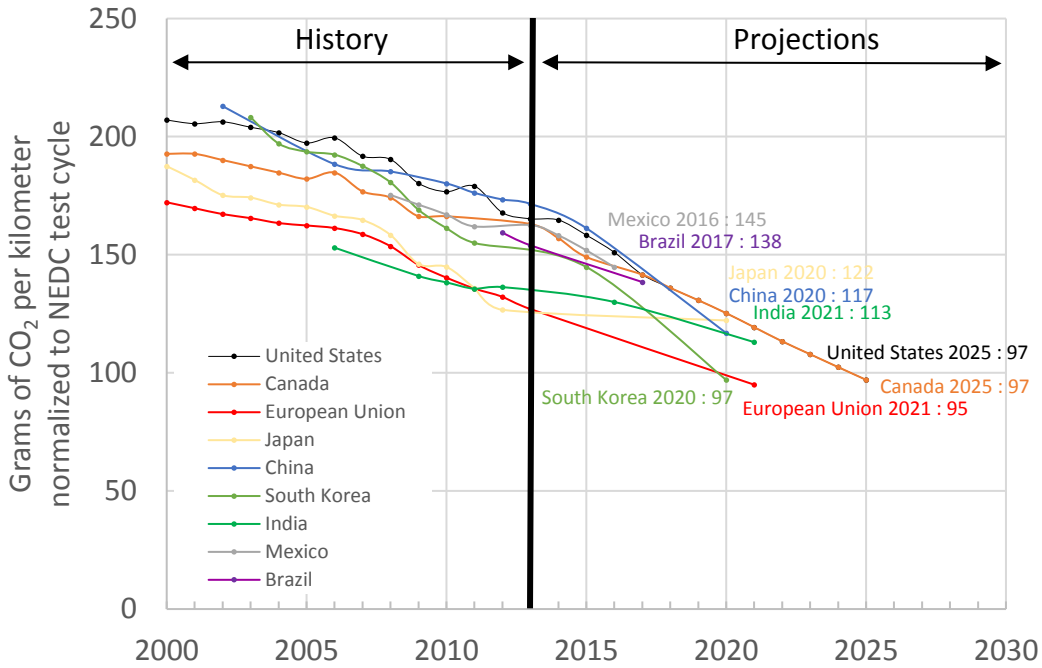

Figure 13. *Forecasts of the CO_2 production per kilometer for light duty vehicles in reference to the NEDC cycle [7].*

On the other hand, the human activity is also a source of pollutant emissions (carbon monoxide (CO), unburned hydrocarbons (HC), nitrogen oxides (NO_X) and particulate matter) whose the effects are particularly harmful for the health and the biodiversity.

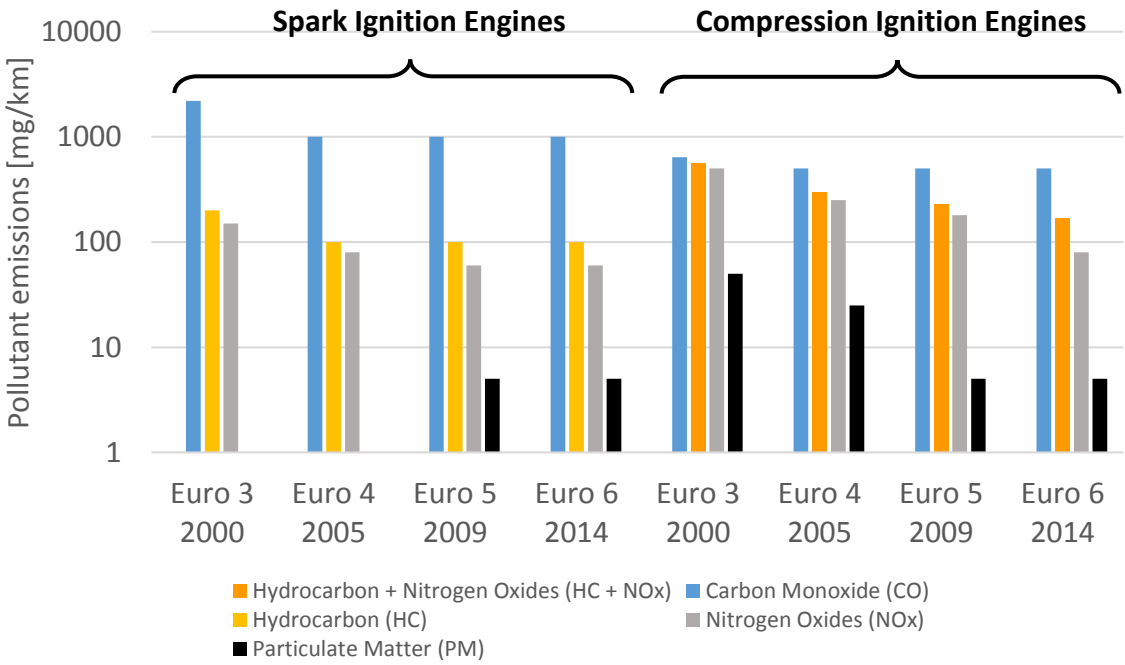

Figure 14. *Evolutions of the pollutant requirements for light duty vehicles with Spark Ignition engines (on the left) and with Compression Ignition engines (on the right) [8]. Note: particles appear for Spark Ignition engines from the Euro 5 pollutant standard with the development of the stratified direct injection.*

Moreover, the transportation participates more or less significantly to the atmospheric pollution, in particular in the urban areas where vehicles are highly concentrated. Thus, in order to improve the air quality, pollutant limitations were established such as the Euro standards (Figure 14). These requirements become increasingly drastic and force the sector to perform improvements continuously.

2. Objectives

Based on this energetic and environmental context, the transports sector has therefore for objectives to save fossil resources used, participating also to the reduction of CO_2 emissions coming from the vehicles, and to enhance the air quality. Moreover, the sector must also continue to improve the efficiencies of the vehicles.

Currently, vehicles propulsion is essentially performed with the help of internal combustion engines. Nevertheless, the energetic and environmental constraints allowed the emergence of other kinds of propulsion such as the electric propulsion or again the hybrid propulsion. The first seems to be the best solution because vehicles do not emit pollutants (zero emission vehicles) but it is necessary to consider the electricity production. This energy is largely produced from primary resources and it is itself a significant source of pollutant emissions. Moreover, these type of vehicles are submitted to two main problems: the distribution networks the battery regeneration are not developed enough and the density of the batteries which is very weak compared to conventional fuels used limits the autonomy. The hybridization, which consists in merging the propulsion coming from an internal combustion engine and the electrical propulsion, seems to have strong possibilities for a wide use into vehicles but maintaining an internal combustion engine is needed. In conclusion, the internal combustion engine still continues to power vehicles in the future decades.

The internal combustion engine is dominated by two kinds of combustion modes: the spark ignition engine and the compression ignition engine. Lots of innovations and improvements were implemented for each of them to answer to the energetic and environmental context. However, in front of the more and more stringent requirements, new combustion modes emerged as alternatives to the conventional ones. Potentially, these advanced combustion modes, gather under the acronym LTC (Low Temperature Combustion), allow to reduce fuel consumption of the engines, and therefore their CO_2 emissions. These engines also allow to achieve low emissions of NO_x and particulate matter due to the low temperatures of combustion and allow to keep high efficiencies thanks to the use of high compression ratios. Finally, their interest is strengthened with the possibility of using a wide range of fuel (conventional and alternative) whose some of them are in full expansion.

Among all the advanced combustion engines, the HCCI (Homogeneous Charge Compression Ignition) mode is of a main interest and many studies focused on. Its principle consists in a combination of the two conventional combustion modes, i.e. the air/fuel mixture is prepared in front of the combustion chamber as in spark ignition engines and this mixture is autoignited with the compression stroke as in compression ignition engines. Therefore, it mainly participates to the understanding of the homogeneous combustion

phenomena observed in all the advanced combustion engines as well as to their development. Moreover, it could be itself implemented into vehicles for real applications. Nevertheless, unlike both conventional combustion modes, HCCI mode does not have system to control efficiently the whole combustion process. The HCCI combustion, which is entirely governed by the kinetics mechanisms, is therefore the main issue to overcome. Plenty of methods were investigated and implemented and the most recent studies focus on the impact of oxidizing chemical species. In particular, several studies were performed on the use of ozone and showed that this molecule has a strong potential [9]–[13]. Ozone is essentially produced with the help of devices generating plasma discharges supplied by a gas containing oxygen such as air. Moreover, these devices tend to become increasingly small. As a result, their use onboard a vehicle could elevate interest for future applications with advanced combustion engines.

Under the ERC Advanced Grant 2G-CSafe (Combustion of Sustainable Alternative Fuels for Engines used in aeronautics and automotives) framework, one of the objectives is to study the impact of oxidizing chemical species on the combustion process into engines such as the HCCI one in order to propose innovative strategies for controlling the combustion and help in the development of new technologies. The aim of the present Thesis is to investigate the impact of seeding the intake of an HCCI engine with minor oxidizing chemical species created by devices generating plasma discharges and to study the potential application of such a device into a real vehicle. This work will mainly focus on the understanding of the impact of these oxidizing chemical species and will extend up to a first application of such a device. Then, considering the fuel flexibility of the advanced combustion engines, a second part will observe the impact of ozone on various alternative fuels.

3. Organization of the manuscript

The present Thesis is about an experimental study on the HCCI combustion coupled to kinetics computations with the aim to investigate the impact of various minor oxidizing chemical species coming from devices generating plasma discharges. Research conducted also considers the potential application of such a device as well as the use of different fuels. This work was performed under a European framework and this memory is based on the journal articles and conference papers published. It is therefore split into five separate chapters entirely written in English. The beginning of each chapter includes an abstract in French and in English to highlight the main discussions and results retained. The manuscript is therefore organized as follows.

The first chapter consists in a review on the HCCI combustion. First, a review on the different conventional combustion modes will be performed and will introduce the advanced combustion modes, in particular, the HCCI combustion. The research conducted and ongoing on this combustion mode will be highlighted and will allow introducing its principle as well as its main features. Finally, advantages and drawbacks of this alternative combustion mode totally governed by kinetics mechanisms will be outlined to show the challenges which limit its development and its implementation into a conventional vehicle. Among the numerous issues to overcome, original methods were proposed to control efficiently the overall combustion process. The HCCI combustion process is strongly influenced by plenty of parameters and a state of the art on most of them and their respective impact will be introduced.

The second chapter consists of a description of the experimental setup and numerical tools used for this work. The engine bench used for the experiments will be described entirely as well as its instrumentation and the data acquisition. This experimental setup allowed studying various kinds of fuel and a table summarizes their main characteristics. Then, for these researches, the methods and the devices needed to investigate the impact of the oxidizing chemical species will be highlighted. Following this, the post-process of the data recorded developed for obtaining the final outputs will be described. Finally, this chapter will end by a description of the kinetics computations performed. The model used will be introduced as well as the main mechanisms and sub-mechanisms retained for understanding the impact of the different oxidizing chemical species selected.

Finally, the next chapters of this memory will focus on the results obtained and the articles published. They are organized according the following main thread.

The first chapter of the results consists in a wide study on the combustion of Primary Reference Fuels (PRFs), i.e. isooctane and n-heptane as well as mixtures of these two fuels. First, the research conducted on the combustion of PRFs without any seeding with

the aim to determine the conditions needed to autoignite the fuels selected. Following these results, the study will focus on the effect of ozone on the combustion of the PRFs through experiments performed on the engine bench and computations. Based on these prior observations, a deeper experimental investigation on the impact of ozone on the HCCI combustion for isooctane as fuel will be presented to highlight the potential of this oxidizing chemical species. Then, considering a potential application of the device generating plasma discharges onboard a vehicle, others oxidizing chemical species must be taken into account such as nitric oxide and nitrogen dioxide, also found into residuals or exhaust gas recirculation. A comparison between both species and ozone on the isooctane combustion will be also introduced as well as the interaction between ozone and nitric oxide. Finally, a first application case for controlling dynamically the HCCI combustion process has been implemented and analyzed.

The two following chapters of results will consider the HCCI combustion of alternative fuels and a comparison with previous results obtained with PRFs could be carried out. First, the results will focus on gaseous fuels, in particular methane and blend with high fractions of methane. A similar analysis of the outputs obtained for these fuels than for PRFs will be conducted, i.e. a study on the autoignition of each fuel without any seeding and a study of the ozone effect through experiments and computations. Then, the last chapter of results will focus on the combustion of second-generation fuels and more precisely on alcohol fuels. Three fuels were selected: methanol, ethanol and n-butanol and a similar approach than that already carries out for PRFs will be performed.

This manuscript will end by a summary of all the experiments and computations performed as well as the contribution brings to the scientific community and to the development of advanced combustion engines. Moreover, according to the innovative and emerging aspect of these research, lots of prospects will be discussed.

Chapitre 1 / Chapter 1

Etat de l’art sur la combustion HCCI

Review on the HCCI combustion

Résumé

Le premier chapitre de ce mémoire est consacré à une étude bibliographique sur la combustion HCCI (Homogeneous Charge Compression Ignition). Cette étude débute par une introduction des différents moteurs conventionnels, à savoir le moteur à allumage commandé et le moteur à allumage par compression. Les principes de ces deux modes de combustion sont énoncés et permettent d'introduire les modes de combustion alternatifs. Compte tenu du grand nombre de nouveaux modes existants, seul les plus pertinents et répandus pour répondre au contexte énergétique et environnemental du secteur des transports ont été présentés.

La combustion HCCI étant un contexte d'étude obligatoire pour la compréhension des phénomènes d'auto-inflammation dans les moteurs, elle a été l'objet d'une attention particulière. Son principe de combustion a été comparé à ceux des modes de combustion conventionnels puis ses avantages et inconvénients ont été mis en évidence. Toutefois, il existe un frein au développement applicatif de la combustion HCCI. La totalité du processus de combustion est gouvernée par les mécanismes d'auto-inflammation qui peuvent être décrit à l'aide de la cinétique chimique et doit être contrôlé. En conséquence, le principal challenge à surmonter est donc de trouver des techniques pour contrôler efficacement le processus de la combustion HCCI sur un large domaine d'opérations du moteur, en termes de charge et de vitesse de rotation.

L'étude bibliographique s'est donc porté par la suite sur le contrôle du processus de la combustion HCCI au moyen de différents paramètres. Chacun d'entre eux a ses propres avantages et inconvénients pour aboutir à un contrôle dynamique et efficace. En conséquence, le potentiel développement d'un moteur HCCI dans les années à venir emploiera certainement plusieurs d'entre eux pour atteindre un phasage idéal sur un large domaine d'utilisation. Parmi ces nombreux paramètres, l'impact de l'ajout d'espèces chimiques à fort potentiel oxydant a fait l'objet de récentes études et celui de l'ozone est particulièrement intéressant puisque de très faibles concentrations, de l'ordre du ppm, permettent d'avancer considérablement le phasage de la combustion [9], [11]–[13]. Sa production étant basée sur une technologie qui tend à se miniaturiser, une potentielle application de ces dispositifs pourrait donc être développée pour l'automobile.

Cette étude préliminaire permet ainsi d'introduire les deux objectifs principaux de ces travaux de thèse :

- Premièrement, évaluer le potentiel applicatif des générateurs d'ozone pour contrôler la combustion HCCI.
- Deuxièmement, étudier l'influence de l'ozone sur des carburants conventionnels et alternatifs.

Abstract

The first chapter of this manuscript focuses on a review on the HCCI (Homogeneous Charge Compression Ignition) combustion. This study starts with an introduction of both conventional engines: the spark ignition engine and the compression ignition engine. Their respective principle was outlined and this allowed introducing the advanced combustion engines. As there are lots of new combustion modes, only the most relevant and widespread to address the energetic and environmental context of the sector of transports were presented.

The HCCI combustion is of a considerable importance for understanding the autoignition phenomena occurring into engines and was of a particular attention. Its principle was compared to both conventional combustion modes and its advantages and drawbacks were highlighted. Nevertheless, there are limits in the application of the HCCI combustion. The whole combustion process is governed by the mechanisms of auto-ignition which are described with the help of kinetics and must be controlled. Consequently, the main challenge to overcome is therefore to find techniques for controlling efficiently the overall HCCI combustion process on a wide range of operations, in term of charge and speed.

The bibliography was therefore focused on the control of the HCCI combustion with the help of different means. Each of them has its own advantages and drawbacks to achieve an efficient and dynamic control. As a result, the potential development of a HCCI engine for the future years will use certainly several of them to achieve an ideal phasing on a wide operating range. Among these parameters, the addition of chemical species with a strong oxidizing potential was the topic of recent studies and that of ozone is particularly interesting since very low concentrations, a few ppm, allow to advance significantly the combustion phasing [9], [11]–[13]. Its production is based on a technology which becomes increasingly small and therefore, a potential application of these devices could be developed for automotive.

This prior study allows introducing the two main objectives of this Thesis:

- First, assess the potential application of ozone generators to control the HCCI combustion.
- Second, study the influence of ozone on conventional and alternative fuels.

1. Internal combustion engines

Internal combustion engines are dominated by two conventional combustion modes better known as Spark Ignition (SI) and Compression Ignition (CI). As presented in the general introduction, engines are responsible for approximately 25% of the total world CO_2 emissions, mainly consume fossil fuels and impact air quality due to the production of pollutant emissions. Consequently, both conventional engines have to reduce their fuel consumption which allows to save fuel and also to decrease CO_2 emissions as well as limit the other pollutant emissions. Several solutions were achieved to meet these requirements through the use of new technologies but these objectives became increasingly stringent. New research areas on the internal combustion engine were investigated to overcome these issues and led to alternative engines also called advanced combustion engines. The first part of this chapter introduces the conventional combustion engines as well as the advanced combustion engines. Among the many advanced combustion engines developed, three of them, the most observed in the literature and the most promising for the future, will be described.

1.1. Conventional combustion engines

Spark ignition (SI) and compression ignition (CI) engines are both conventional combustion engines used in vehicles. Their respective combustion process is described hereafter as well as their effect on the efficiency and on pollutants.

1.1.1. Spark ignition engines

Spark ignition engines mainly use gasoline as fuel. This one is mixed with the air upstream of the combustion chamber by using a port fuel injection. The air/fuel mixture which must be as homogeneous as possible is then aspired by the engine during the intake stroke and finally compressed. The combustion does not occur by itself and an external energy input is needed. A spark plug ignites the air/fuel mixture just before the end of the compression stroke and a premixed turbulent flame therefore expands from the plug towards the walls. Finally, combustion in spark ignition engines leads to carbon monoxide (CO) and unburned hydrocarbons (HC) formation due to the inhomogeneity of equivalence ratio as well as due to parts of the air/fuel mixture trapped into areas where no combustion exists. In parallel, the high temperature in the flame propagation leads to the formation of nitric oxides (NO_X). The equivalence ratio of the air/fuel mixture is therefore fixed closed to the stoichiometry due to the tradeoff on pollutants formation (Figure 15) and to post-treat it efficiently with three-way catalyst in order to meet pollutant requirements. Such equivalence ratio may lead to knock and to avoid these undesired auto-ignitions which may damage the engine, the compression ratio is voluntary weak (around 10). Due to the weak compression ratio and the low heat capacities ratio of the air/fuel mixture, the efficiency of

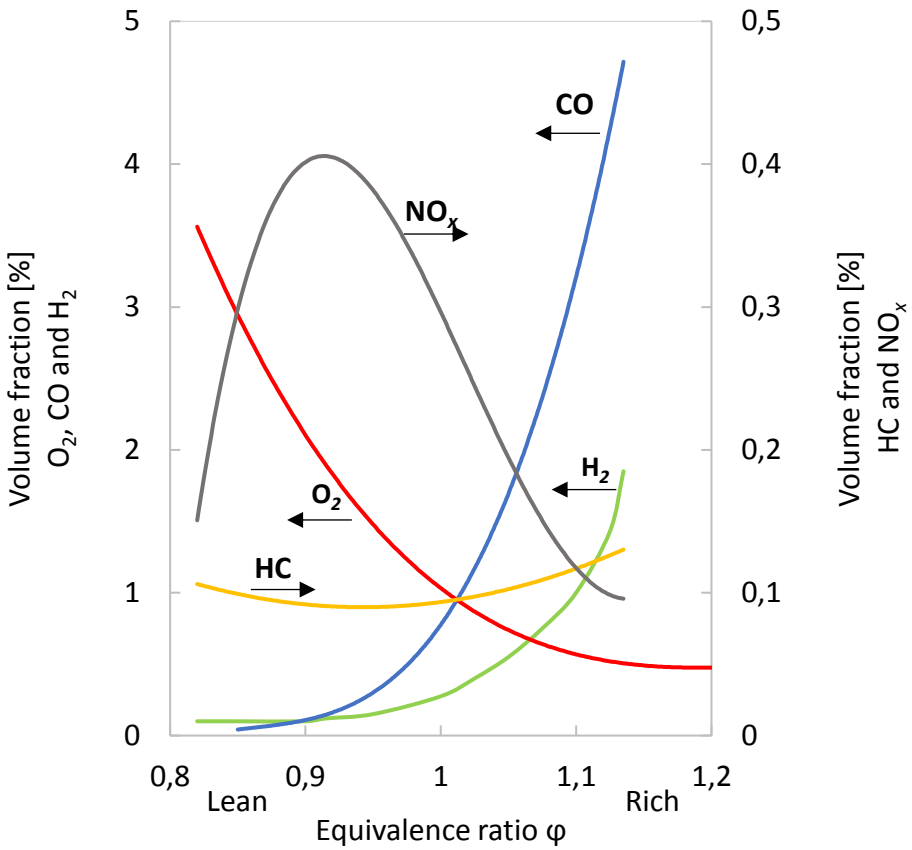

Figure 15. *Typical emissions from SI engines as a function of the equivalence ratio* [14].

spark ignition engines is therefore limited. Moreover, the amount of air for the mixture is managed by a throttle which makes pumping losses and also limits the efficiency.

1.1.2. Compression ignition engines

Compression ignition engines use diesel as fuel. Unlike spark ignition engines, only the air is aspired by the engine and the fuel is injected through an injector directly inside the combustion chamber before the end of the compression stroke. Fuel mixes with the air due to the internal aerodynamic and the injection pressure. Then, when air/fuel is well mixed and the internal conditions are reached, a spontaneous combustion also called auto-ignition occurs and a diffusion flame stabilizes around the spray. As there are no pumping losses and the compression ratio is high (around 16), compression ignition engines may reach high efficiencies. Moreover, the global equivalence ratio is lean, approximately of 0.7 in average, and also contributes to the high efficiency. Nevertheless, due to the direct injection, some rich areas located in the spray lead to the formation of soot while the diffusion flame reaches high temperatures and produces nitric oxides (NO_x). Compression ignition engines are therefore equipped with a particulate filter and NO_x trap or Selective Catalytic Reduction (SCR) devices allowing to reduce both undesired pollutants.

1.2. Advances combustion engines

Although the internal combustion engines are dominated by the two conventional combustion modes previously described, the objectives of reducing fuel consumption, CO_2 emissions and pollutant emissions lead to advanced combustion modes [15], [16] as alternative engines. A multitude of new concepts were developed and designed under various acronyms observed in the literature:

- ARC (Active Radical Combustion)
- ATAC (Active Thermo Atmosphere Combustion)
- CAI (Controlled Auto Ignition)
- CIHC (Compression Ignited Homogeneous Charge)
- Dual Fuel
- HCCI (Homogeneous Charge Compression Ignition)
- MK (Modulated Kinetics)
- PCCI (Premixed Charge Compression Ignition)
- PFS (Partial Fuel Stratification)
- PPC (Partially Premixed Combustion)
- PPCI (Partially Premixed Compression Ignition)
- PREDIC (Premixed Diesel Combustion)
- RCCI (Reactivity Controlled Compression Ignition)
- SACI (Spark Assisted Compression Ignition)
- SCCI (Stratified Charge Compression Ignition)
- TS (Toyota Soken Combustion)
- UNIBUS (Uniform Bulky combustion System)
- …

This list is non-exhaustive and each one is slightly different from the other. Classifications according to several parameters such as the engine basis (similar to CI or SI), 2 or 4 strokes or again the type of mixture (totally homogeneous or totally heterogeneous) may be conducted [17] but all these advanced combustion mode may be gathered under “Low Temperature Combustion” (LTC) engines. In comparison with both conventional combustion engines, LTC modes may be considered as hybrids of spark ignition and compression ignition engines. For all these advanced combustion engines, the aim is to prepare an air/fuel mixture as homogeneous as possible and then, this mixture is auto-ignited during the compression stroke. Due to the homogeneity of the air/fuel mixture, the formation of particulate matter is avoided. Moreover, the mixture in such combustion mode is often lean or diluted and leads to earlier combustion and low in-cylinder temperatures which result in low NO_x emissions (Figure 16). However, other pollutants, i.e. CO and HC, are strongly produced and LTC engines will need efficient post-treatment systems to drastically reduce it. Finally, LTC engines have often high compression ratio and no pumping losses.

They can therefore achieve high efficiencies and researchers have a great interest on these advanced combustion engines.

All these advanced combustion engines cannot be entirely detailed and only three of them are going to be presented below. They are among the most commonly encountered in the literature (Figure 16) and the most promising to replace both conventional SI and CI engines: the PCCI (Premixed Charge Compression Ignition), the RCCI (Reactivity Controlled Compression Ignition) and the HCCI (Homogeneous Charge Compression Ignition). They are all LTC modes and they are presented hereafter according to their mixture formation.

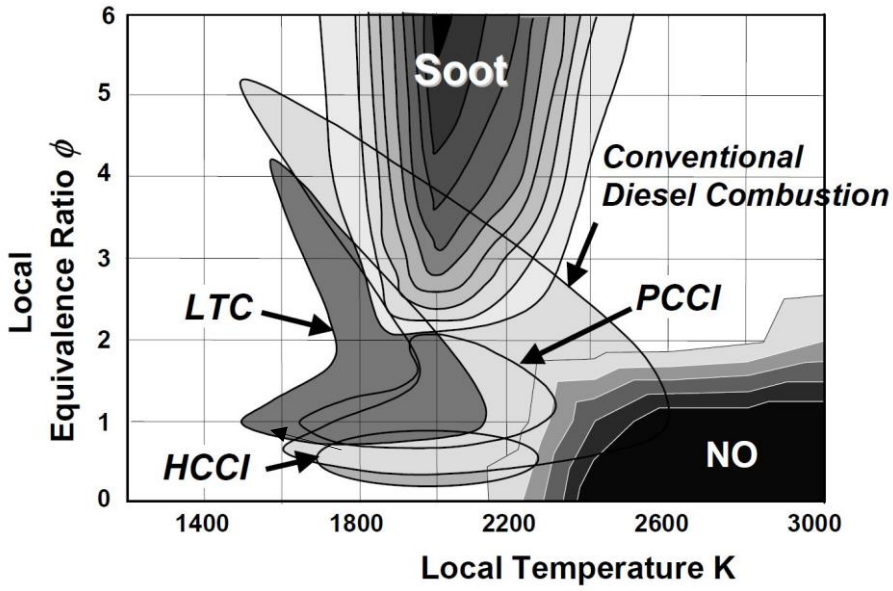

Figure 16. *Equivalence ratio - Local temperature diagram from Kitamura et al.* [18] *and the location of Conventional Diesel Combustion and some of the most advanced combustion modes encountered into the literature* [19].

1.2.1. Premixed Charge Compression Ignition (PCCI)

PCCI combustion mode is very close to the combustion occurring in CI engines [20]. The fuel is directly injected inside the combustion chamber during either the admission or the compression stroke using an injector. The injection is therefore carried out earlier than in conventional CI. This process allows promoting the air/fuel mixture which has enough time to tend towards a homogeneous mixture and lead to lower particulate matter and NO_x emissions. Moreover, such approach enables to maintain a high efficiency on the engine and cycle-to-cycle may be achieved by controlling the fuel quantity and its early injection. Finally, according to this principle, a wide interest is focused on the use of lower reactivity (high octane) fuel whose volatility and high octane number may let enough time to achieve a perfectly homogeneous air/fuel mixture.

1.2.2. Reactivity Controlled Compression Ignition (RCCI)

RCCI is a recent combustion concept applied to the internal combustion engine [21], [22]. It consists of controlling the reactivity of the air/fuel mixture inside the combustion chamber by separately injecting two different fuels with their own reactivity. A lower reactivity fuel is injected using a port fuel injection while a higher reactivity fuel, which is the pilot of the combustion, is early injected through an injector. The total reactivity (which can be assimilated to a cetane number or an octane number) is therefore modulated by adjusting the amounts of each fuel injected depending on the engine work conditions. Finally, this strategy demonstrated that cycle-to-cycle control, optimal engine outputs and low emissions of particulate matter and NO_x may be achieved by managing the ratio between the two fuels applied and their injection time.

1.2.3. Homogeneous Charge Compression Ignition (HCCI)

Unlike the two previous combustion modes, the air/fuel mixture in HCCI engines is fully premixed [23]–[25]. Most of the time, the mixture is prepared upstream of the combustion chamber as in SI engines, then the mixture is compressed and finally auto-ignites as in CI engines. In theory, HCCI combustion takes place in the overall volume at the same time but in reality, the combustion occurs in several hot spots due to temperature and equivalence ratio stratification. Finally, such strategy allows avoiding particulate matter formation as well as NOx emissions or at least maintaining it near zero. However, HCCI combustion is violent and therefore, cycle-to-cycle approaches are limited to lower engine speeds and reduce its operating range.

1.2.4. State on advanced combustion engines

Among all the advanced combustion modes which emerged, the three concept described above are the most promising modes for replacing both conventional engines. Compare to the two others, HCCI combustion mode will have probably more difficulties than PCCI and RCCI modes to be integrated due to its limited operating range. Nevertheless, some applications could be possible with the emergence of hybridization for instance or in combination with these other combustion modes. On the other hand, there is some common characteristics between these three combustion modes. In particular, the air/fuel mixture is fully premixed for HCCI and both PCCI and RCCI have a part of their mixture quite homogeneous. As a consequence, HCCI investigations are essential for increasing the knowledge on homogeneous auto-ignitions occurring in these advanced combustion modes and are also intermediate studies for their future development. Moreover, HCCI combustion may help in the understanding of knocking as well as pollutants formation. For the rest of this investigation, the researches will be focused on the HCCI combustion. Further details of this combustion mode will be given. Note that the observation made for HCCI could be extend to all the advanced combustion modes demonstrating a part of homogeneous combustion.

2. The HCCI combustion process

The homogeneous charge compression ignition is one of the most investigating advanced combustion mode. In this part, its principle and its main characteristics will be fully described. Advantages will be highlighted and the main challenges to overcome before a potential application will be argued. As this combustion mode is entirely governed by kinetics, the combustion process will be described according to this kind of approach.

2.1. Principle of the HCCI combustion

The HCCI combustion is defined as a combination of the spark ignition combustion and the compression ignition combustion [23]–[25]. The aim of such mode is to take the advantages of conventional engines without their drawbacks. Most of the time, the air/fuel mixture is prepared upstream the combustion chamber, often in the intake like in SI engines, to be the most homogeneous as possible. Then, this mixture is auto-ignited inside the combustion chamber during the compression stroke like in CI engines. Moreover, the HCCI combustion mode has a high thermodynamic interest. Such engines operate without throttling losses, with high compression ratio, with a globally lean mixture and fast combustion. Therefore, HCCI engines achieve high efficiencies quite similar to those of CI engines. Although it appears very attractive, controlling this kind of combustion is not obvious. SI and CI engines respectively use spark plug whose the timing is managed and an injector which controls the injection timing. For HCCI engine, none of them is available. The heat release rate is therefore not controlled either by the rate of fuel injected or by the flame propagation but according to chemical kinetics which is depending on the conditions of temperature and pressure within the combustion chamber as well as the air/fuel mixture. HCCI combustion therefore occurs throughout the combustion chamber when self-ignition conditions are achieved and results in high heat release rates and high pressure rise rates. This leads to ringing which may damage the engine and as a consequence, it is necessary to limit such phenomenon, the power output of the engine is also limited. Globally, the HCCI combustion well occurs in the overall combustion chamber but according to optical diagnostics, this combustion takes place in several hot sites randomly distributed. This is mainly due to fuel and temperature stratification. Moreover, as the mixture is lean and with a high reactivity, flame propagation does not have enough time for taking place and consequently, the HCCI combustion process is well entirely governed by chemical kinetics. Figure 17 shows a scheme of the combustion for both conventional engines and the HCCI engine.

According to emissions, particulate matter emissions are drastically reduced and research zero due to the homogeneity of the air/fuel mixture and its lean equivalence ratio. Moreover, the in-cylinder temperatures are quite uniform during the combustion the HCCI combustion and do not exceed the critical temperature correspond to the formation of NO_x.

These emissions are therefore very low or near zero. However, for carbon monoxide and unburned hydrocarbon emissions, high levels may be observed due to the presence of the air/fuel mixture into the crevices of the combustion chamber with the homogeneity. Moreover, the low in-cylinder temperatures limit the conversion of these emissions into the main combustion products (CO_2 and H_2O).

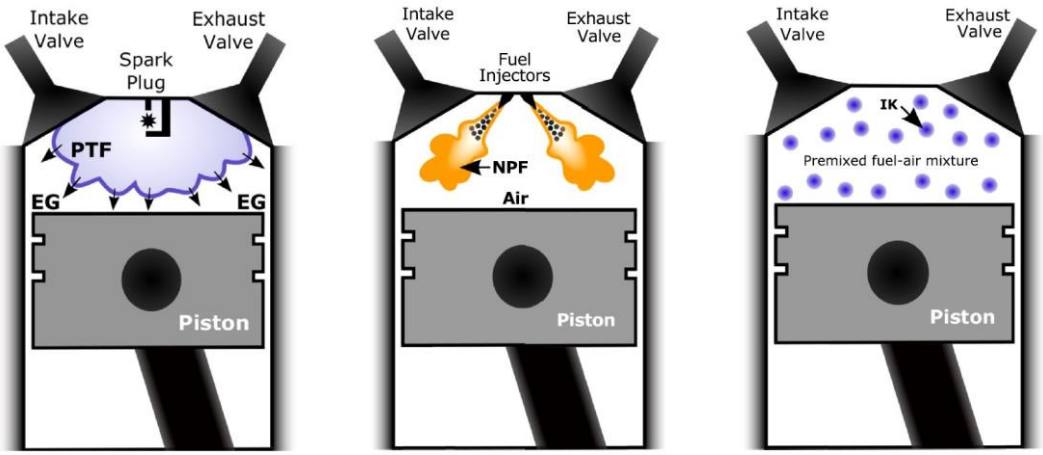

Figure 17. *Scheme of both conventional engines combustion compared to the HCCI combustion. From the left to the right: Spark Ignition, Compression Ignition and Homogeneous Charge Compression Ignition* [26]. *(PTF: Premixed Turbulent Flame; EG: End Gases; NPF: Non-Premixed Flame; IK: Ignition Kernels)*

Finally, unlike SI and CI which use respectively gasoline and diesel like fuel, HCCI is fuel flexibility provided that the air/fuel mixture preparation has been met (i.e. a high volatility of the fuel) and the engine leads to the auto-ignition of the fuel (i.e. an appropriate compression ratio). As the combustion process is governed by chemical kinetics, HCCI may either be fueled by gasoline or diesel or any kind of fuels as fuel blends or even alternative fuels. Combustion will occur as soon as the auto-ignition conditions will be reached. For this reason, this combustion mode was widely investigated. Globally, the heat release rate during conventional combustion process is in one stage. For HCCI, the combustion may display two stages on heat release rates depending on the fuel. This is mainly related to the reactivity of the fuel used and due to its octane number. The higher the reactivity is (low octane number), the most significant the first stage of the heat release rate is. Figure 18 showed the heat release rates trace for two different fuels, PRF80 and isooctane. The first stage corresponds to the low temperature regime where the fuel is partially oxidized, due to its reactivity, under lower temperatures than those of its main fuel oxidation. This part of the heat release rate is important in the sense that this results in a low increase of the temperature within the combustion chamber which is valuable for achieving the main combustion. The second stage therefore corresponds to the main combustion or high temperature regime and finally, the area between both combustion stages is associated to the negative temperature coefficient (NTC) regime. NTC is related to a decrease of the reactivity of the system while the in-cylinder temperature increases with the compression

stroke. Further details about these combustion stages are given above in the kinetics description of the HCCI combustion. Finally, all the features of the HCCI combustion process and comparisons with conventional engines are summarized in Table 1.

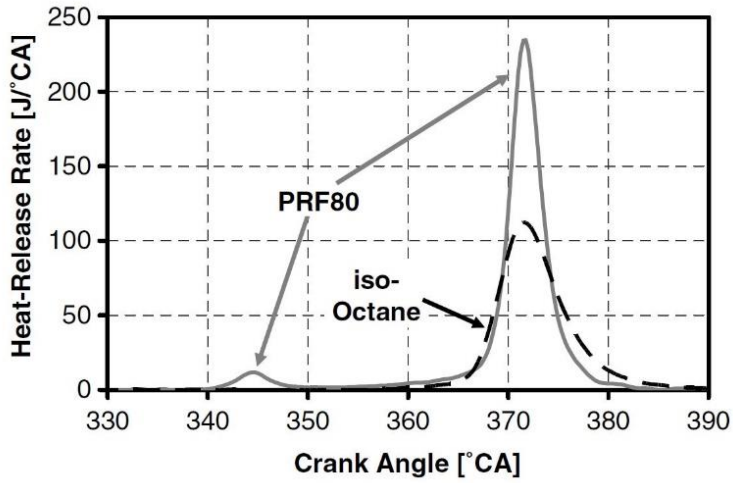

Figure 18. *Heat release rate traces for isooctane and PRF80 (80% isooctane and 20% n-heptane)* [27]. *Isooctane combustion is in single stage while PRF80 is in two stages. The first stage between 340 and 350 °CA corresponds to the low temperature regime or cool flame. The area from 350 to 360 °CA is related to the negative temperature coefficient (NTC) regime and after 360, the peaks corresponds to the main combustion.*

Table 1. *Main HCCI characteristics and comparison with spark ignition and compression ignition* [23], [25].

Engines	Spark Ignition	Compression Ignition	HCCI
fuel	gasoline	diesel	flexible
equivalence ratio (φ)	near the stoichiometry (1 – 1.1)	wide range (0.3 – 1)	very lean (0.3)
air/fuel mixture	premixed	non-premixed	premixed
ignition	spark ignited	compression ignited	compression ignited
combustion form	premixed	premixed and diffusion	autoignition
fuel burning rate limitation	flame propagation speed	fuel vaporization and mixing rate	multipoint or spontaneous hot sites
combustion stage	one stage	two stages	one or two stages depending of the fuel
flame front	yes	yes and no	without
combustion temperatures	high	partially high	relatively low
efficiency	moderated	high	high
pollutant emissions	higher HC, CO and NO_x	higher HC, CO, particulates and NO_x	very higher HC and CO lower NO_x and particulates.

2.2. Advantages and challenges of the HCCI combustion

According to the principle of the HCCI combustion previously described, the advantages and the drawbacks of this combustion mode may be established [24], [25], [28]. The benefits are firstly presented above and then, the challenges mainly related to the combustion process are highlighted.

2.2.1. Advantages

2.2.1.1. Low fuel consumption

HCCI combustion is based on the use of very lean air/fuel mixture, such engine may potentially minimize their fuel consumption when the combustion efficiency is high enough. This gives to HCCI engines a first advantage which is strengthened by the fact that perspectives for the automotive field needs to reduce the fuel consumption in the aim to save fossil resources and limit CO_2 emissions.

2.2.1.2. High efficiency

HCCI engines mainly use lean air/fuel mixture and high compression ratio to reach the auto-ignition conditions. This participates to the achievement of a high efficiency. The efficiency is also improved by the fact that there are no throttle losses in front of the intake. Furthermore, as the combustion of the lean mixture is very fast and the in-cylinder temperatures reach reasonable values, HCCI engine may therefore achieve very high efficiency.

2.2.1.3. Low levels of NO_x and particulate matters

NO_x and particulate matters are mainly produced due to excessive temperature and rich area within the combustion chamber. For HCCI engine, the homogeneity of the lean air/fuel mixture allows to avoid particulate matters formation. Moreover, in-cylinder temperature is quite uniform and does not exceed the critical temperature corresponding to the NO_x formation. Consequently, levels of both particulate matters and NO_x are very low, even near zero, in such combustion mode.

2.2.1.4. Fuel flexibility

The occurrence of the combustion for HCCI engine is based on the chemical kinetics which depends on the conditions inside the combustion chamber, i.e. pressure and temperature evolutions as well as the air/fuel mixture. According to this, HCCI is not dedicated to a single fuel and may therefore be supplied by a wide range of fuels. This flexibility provides it a very interesting advantage as conventional fuels, which mainly come from fossil resources, will be progressively replaced by alternative ones.

2.2.2. Challenges

Although HCCI combustion looks ideal for replacing conventional combustion modes, there are several issues which limit its use for practical applications. Therefore, before such engines are suitable for integration into vehicles and a commercial development, several challenges must be addressed.

2.2.2.1. Combustion timing control

Controlling the HCCI combustion process is the most important challenge to overcome. To obtain the full benefits of such combustion, the combustion must occur near the top dead center over a wide range of working conditions, i.e. in term of speed and load. Unlike conventional engines, there is not a direct method for controlling the HCCI combustion process. Instead the combustion timing is entirely governed by kinetics. The auto-ignition therefore depends on the physical and chemical properties of the air/fuel mixture as well as the thermodynamic conditions history into the combustion chamber. As a consequence, the combustion process may be managed indirectly by a lot of parameters with more or less sensitivity as for example: intake temperature, intake pressure, fuel properties, equivalence ratio, exhaust gas recirculation or mixture composition, engine speed, heat transfer or other parameters.

2.2.2.2. Operating range

As important as the control of the combustion phasing, HCCI engines operate in a narrow window and must extend their operating range. Unlike conventional engines, HCCI is limited to medium operating range and needs to cover low and high loads. Under low loads, there is a lack of energy for allowing the auto-ignition. In-cylinder temperatures are too weak to convert emissions and HCCI engines achieve less efficiency in particular near idle operations. Moreover, this is a main drawback according to emissions requirements. In the opposite, at high loads, the heat release rate is very intense due to the fast combustion occurring. This provides a rapid increase of the pressure rate which may damage the engine. Moreover, unacceptable levels of NO_x emissions can be formed due to elevated temperatures. Strategies have to be developed to overcome this issue.

2.2.2.3. Unburned hydrocarbons and carbon monoxide emissions

During the compression stroke, a part of the air/fuel mixture is trapped into the crevices of the combustion chamber and is not consumed during the combustion. This results in high levels of HC and CO emissions and decreases the combustion efficiency. Moreover, this drawback is more important under low loads and near idles due to the low temperatures within the combustion chamber. It is therefore essential to develop emissions control devices to limit levels of HC and CO as well as increase the temperatures during the expansion stroke to enable the conversion of these emissions into combustion products.

However, too elevated temperatures may result in NO_x formation. There is a tradeoff to find in order to keep the benefit of HCCI combustion.

2.2.2.4. Level of noise

With the homogeneous air/fuel mixture, the combustion occurs throughout the combustion chamber. Such a combustion leads to high heat release rates with short combustion durations and is finally responsible of a high pressure rise rate. Rapid rise of the in-cylinder pressure is related to intense ringing or noise and may therefore damage the engine. Moreover, in case of high equivalence ratios or when the engine works under high loads, the level of noise becomes too strong and is totally unacceptable for the engine. Therefore, it is crucial to avoid, or at least limit, too rapid and high combustion.

2.2.2.5. Mixture preparation

Preparation of the air/fuel mixture is also an important challenge in HCCI engines. The aim is to improve the fuel vaporization and mixing which lead to a charge the most homogeneous as possible. A main parameter is therefore the fuel and its properties, in particular its evaporating temperature and its volatility. Moreover, inhomogeneity may lead to auto-ignition alteration as well as unfavorable particulate matter (rich area) and NO_x formation (very high temperatures). On the other hand, the homogeneous mixture unfortunately results in wall impingement causing oil dilution and HC formation which in turn decrease the combustion efficiency. Finally, the mixture preparation is challenging as the aim is to easily auto-ignite it and avoid unacceptable levels of pollutants.

2.2.2.6. Cold start

Auto-ignition may easily be altered by temperatures. During cold start, the initial temperatures are very weak to make combustion possible and this results in misfires. Moreover, this is all the more important that there is no preheating of the charge into the intake manifold and there are significant heat transfers to the walls. This challenge is as important as the objective of achieve an ideal combustion at low loads.

All the challenges previously described are mainly focused on the auto-ignition of the air/fuel mixture and the pollutants formation. Obviously, there are other challenges to address before integrating HCCI engines in a real vehicle such as, the engine control (feedbacks and close loop control), the response of transient cycle which has to be as fast as possible, the cylinder to cylinder interaction or others. However, the control of the combustion phasing is the main challenge to overcome for HCCI engines and is central to the present work. The effect of various parameters will be therefore fully analyzed on the combustion phasing in the next part.

2.3. Kinetics of the HCCI combustion

Usually, the combustion process is described according to a unique reaction where the reagents are consumed to give products of combustion. Typically, in the case of a stoichiometric reaction, the reagents are the fuel and the oxygen contained in the air, while the products are mainly carbon dioxide and water. However, a combustion process is more complex and involves numerous chemical species and reactions. Furthermore, the amount of species and reactions increases with the complexity of the fuel composition.

HCCI combustion is totally governed by chemical kinetics and its combustion process may be described by a kinetics approach. In the present part, the main reactions involved during this kind of combustion are going to be highlighted. In particular, the reactions which lead to each heat release part, i.e. the low temperature regime, the NTC and the high temperature regime. These different regimes occur in various temperature ranges depending of the fuel properties. Generally, they are respectively estimated in the following range: below 800 K, 800 to 1000 K and above 1000 K. The reactions involved presented hereafter are those established for alkane fuels, more precisely primary reference fuels (n-heptane and isooctane) and are based on the works of *Curran et al.* [29], [30] and *Dagaut et al.* [31], [32].

2.3.1. Low-temperature range

The low temperature regime starts by an initiation reaction for temperatures below 800 K. It mainly involves a H-atom abstraction from the fuel considered (RH) through a bimolecular reaction with an oxygen molecule (O_2). This leads to the formation of a hydroperoxyl radical (HO_2) and an alkyl radical (R).

$$RH + O_2 \rightarrow R + HO_2 \qquad \text{R-1}$$

The alkyl radical then reacts with another molecular oxygen to produce an alkylperoxyl radical (RO_2). It contributes to the beginning of a chain branching which may release a part of the energy contained into the fuel.

$$R + O_2 \rightarrow RO_2 \qquad \text{R-2}$$

The alkylperoxyl radical finally isomerizes into hydroperoxyalkyl radical ($QOOH$), i.e. that an H atom is transferred from a carbon atom to the O_2.

$$RO_2 \rightarrow QOOH \qquad \text{R-3}$$

Depending on its structure and its size, the $QOOH$ radical is consumed through four distinct propagation reactions leading to the production of stable species (olefin, carbonyl or

cyclic ether) and hydroperoxyl (HO_2), hydroxyl (OH) or peroxyhydroperoxyalkyl ($OOQOOH$) radicals.

$$QOOH \rightarrow olefin + HO_2 \quad \text{R-4}$$

$$QOOH \rightarrow olefin + carbonyl + OH \quad \text{R-5}$$

$$QOOH \rightarrow cyclic\ ether + OH \quad \text{R-6}$$

$$QOOH + O_2 \rightarrow OOQOOH \quad \text{R-7}$$

This last propagation reaction is similar to the reaction R-2 and is responsible of the cool flame chain branching reactions. The $OOQOOH$ species isomerizes and finally releases three radicals, an oxygenated hydrocarbon radical (OPO) and in particular two hydroxyl radicals (OH).

$$OOQOOH \rightarrow HOOPOOH \rightarrow OPO + 2\,OH \quad \text{R-8}$$

OH is then responsible for the fuel consumption through H-abstractions reactions R-9 where X is a radical (mainly OH and HO_2) and XH a stable species (H_2O and H_2O_2) under this temperature range. This leads to an increase of the overall reactivity determining for the auto-ignition of the main temperature regime.

$$RH + X \rightarrow R + XH \quad \text{R-9}$$

2.3.2. Negative temperature coefficient range

The low temperature regime is followed by a negative temperature coefficient (NTC) regime. During the NTC, the chemical reactivity decreases while the temperature continues to rise due to the compression. The reaction rates of the cool flame are altered due to the temperature and the system is governed by linear chain reactions. In particular, the propagation reaction R-4 dominates reaction R-7 to form olefins and HO_2 radicals.

Moreover, the reaction pathway that led to the production of $QOOH$ from alkyl radicals is modified (R-2 and R-3). There is therefore less $QOOH$ species produced and the chain branching which leads to a heat release is broken. Instead of the recombination which leads to the formation of $RO_2$the reaction with an alkyl radical and molecular oxygen produces an olefin and a HO_2radical.

$$R + O_2 \rightarrow olefin + HO_2 \quad \text{R-10}$$

Finally, the NTC regime is dominated by a significant production of HO_2 radicals while OH radicals are entirely consumed by the fuel through reaction R-9. Consequently, the formation of OH is stopped while HO_2 radicals, which are less reactive than OH radicals and do not lead to exothermic reactions, mainly react together and with the fuel (R-9) to form hydrogen peroxide (H_2O_2). Under these temperatures, H_2O_2 is a stable species and limit strongly the reactivity of the system.

$$HO_2 + HO_2 \rightarrow H_2O_2 + O_2 \qquad \text{R-11}$$

2.3.3. High temperature range

The high temperature regime is initiated by the increase of the temperature due to the compression and a new modification of the reaction rates. The hydrogen peroxide is broken down into two hydroxyl radicals which lead to a strong rise of the global reactivity of the system.

$$H_2O_2 + M \rightarrow OH + OH + M \qquad \text{R-12}$$

This last reaction shows the impact of both previous regimes on the main combustion stage. The NTC regime is responsible of the high production of H_2O_2 from the HO_2 radicals and the low temperature regime allows to achieve earlier the H_2O_2 decomposition and therefore the main combustion due to a slight increase of the temperature.

The OH radicals produce through the previous chain branching reaction oxidize the fuel and lead to the production of other OH radicals according to the pathway composed of the reactions R-9, R-10, R-11 and R-12. With the formation of OH and the chain branching which takes place, the reactivity and the temperature of the system exponentially grow. Finally, as soon as the temperature is important enough, a high amount of OH radicals is formed from the reactions R-13, R-14 and R-15 while the fuel and the other species decompose into smaller species.

$$H + O_2 \rightarrow O + OH \qquad \text{R-13}$$

$$O + H_2 \rightarrow H + OH \qquad \text{R-14}$$

$$O + H_2O \rightarrow OH + OH \qquad \text{R-15}$$

Finally, all the fuel mainly reacts with OH radicals through reaction R-9 and as soon as it is totally consumed, OH radicals participates to the production of final species.

3. Control of the HCCI combustion process

Controlling the HCCI combustion process with efficiency over a wide range of load and speed is the main issue to overcome before a widespread application of such an engine. Unlike the conventional SI and CI engines, there is no direct control of the HCCI combustion which is entirely dominated by kinetics. Instead, there are lots of parameters that may affect the ignition timing of the homogeneous air/fuel mixture and help to achieve an efficient control of the overall combustion process. The present part aims to introduce the impact of all these parameters.

3.1. Intake temperature

As introduced previously, the HCCI combustion is entirely governed by kinetic mechanisms. Obviously, the temperature is a key parameter for controlling the reaction rates and the ignition timing of the combustion. Therefore, several studies were performed on the impact of the intake temperature.

Dubreuil et al. [33] carried out experiments on the combustion of three surrogates and ranged the intake temperature from 40 °C to 120 °C. Figure 19 displays its results on heat release rates and ignition delays of both flames. As expected, the increase of this parameter led to an early combustion occurrence and also to an improvement of the combustion. In fact, the temperature allowing the first oxidation of the fuel is reached earlier in the cycle and explains the linear advance observed on the cool flame phasing.

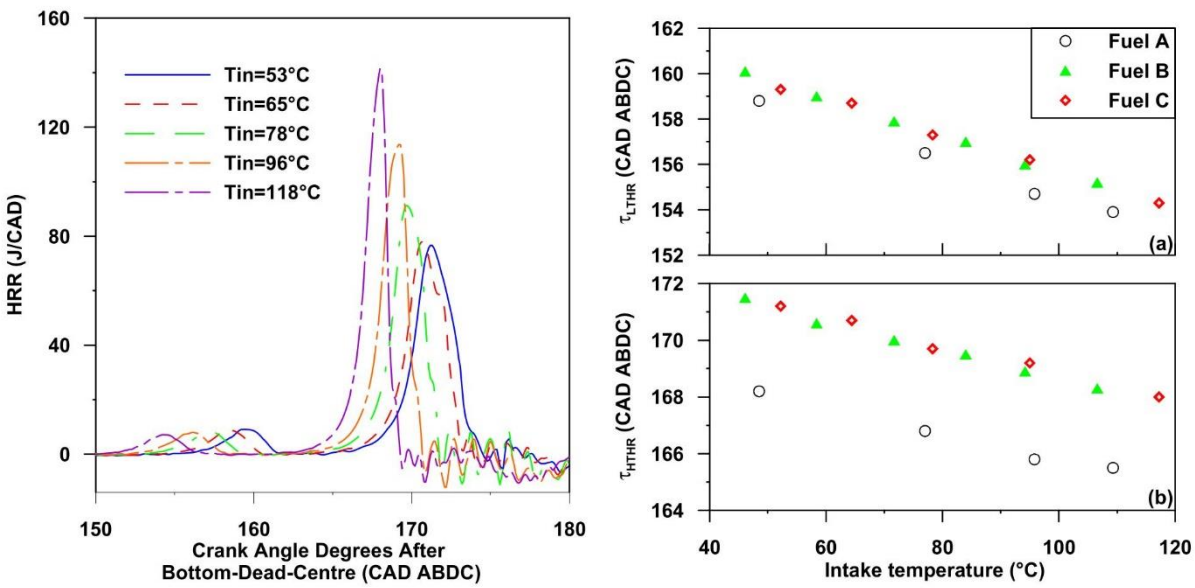

Figure 19. *Effect of the intake temperature on heat release rate for TRF24 as fuel (on the left) and effect of the intake temperature on combustion timing (on the right). Results on the top correspond to the cool flame and those on the bottom to the main flame. Fuels A, B and C represent n-heptane, PRF25 and TRF24, respectively* [33].

Moreover, the cool flame brings a weak rise on the in-cylinder temperature and therefore, an advance of the main flame may also be observed. Finally, as the combustion starts earlier, a fast consumption of the fuel takes place, increases the whole reactivity and leads to higher heat release rates.

Lu et al. [34] also investigated for three different PRFs the impact of the intake temperature but on a smaller range. He observed also an advance of the combustion timing but fuels present different sensitivities to this thermodynamic parameter due to the heat capacity of the air/fuel mixture. Finally, many authors reached the same conclusion with other fuels [35]–[41]. Additionally, even if the intake temperature is of a significant importance, further experiments investigates the thermal stratification inside the combustion chamber [42]–[44]. Results showed that there are some inhomogeneities inside the combustion chamber due to heat transfers, the motion of the mixture and the motion of the piston. The combustion occurs therefore into several hot spots. Finally, controlling the combustion timing with efficiency by ranging the intake temperature was investigated by *Haraldsson et al.* [45]. He proposed to warm up one part of the intake air into a second pipe with the help of the temperature of the exhaust gases and manage the intake temperature with two throttles.

3.2. Fuel

The second most obvious parameter which can influenced the autoignition is the fuel and it is of a main importance. HCCI engines offer fuel flexibility and may therefore use a wide range of fuels. Many studies were performed on the impact of the fuel on the HCCI combustion process and nowadays, it still remains a main topic. The aim is to find a fuel whose the properties allow combustion on a wide operating range for the engine. As a result, fuel must have autoignition indexes as low as possible to easily burn and a high volatility to rapidly achieve a homogeneous mixture [46].

Lots of fuels were investigated in the literature [10], [47], [48]. Results included studies on pure fuels such as Primary Reference Fuels (PRFs) [37], [49]; n-heptane, isooctane and mixtures of both fuels; gaseous fuels [50],[41]; natural gas and/or hydrogen; alcohol fuels [51], [52] or even other alternative fuels [13], [53], [54]. In general, the results showed that autoignition of pure fuels mainly depends on their own chemistry and their respective properties of RON (Research Octane Number), MON (Motor Octane Number), ON (Octane Number); i.e. the average between the RON and the MON; and CN (Cetane Number), which is inversely proportional to RON and MON. For instance, many experiments were performed with PRFs and showed that lower the ON of the fuel is, easier its autoignition is and inversely [37], [49] (Figure 20). Unfortunately, all the experiments conducted with pure fuels indicated that only a few part of the engine operations may be covered. As a result, studies were carried out with mixture of fuels. Most of the time, these surrogates included only a few pure fuels to keep the possibility of coupling the results with computations [55]–[57].

Mixtures of liquid fuels were investigated [58], [59] as well as blends of liquids and gas [60], [61]. Other authors also investigated the impact of ignition improvers [37], [62], [63]. Finally, techniques were developed to control the ON of the fuel inducted inside the combustion chamber, i.e. the mixture reactivity, and cover a wide part of the operating range [21], [22], [64].

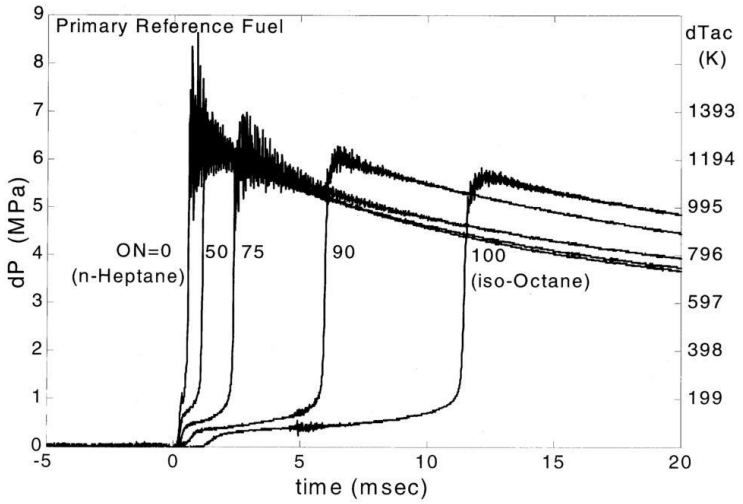

Figure 20. *HCCI characteristics of PRFs for an equivalence ratio of 0.4, an intake pressure of 1 bar, an intake temperature of 318 K and a compression ratio of 16* [37].

Moreover, most of the studies for fuels used in HCCI engines are mainly based on their own properties previously cited. Nevertheless, all these indices were established for SI and CI engines, respectively, and many authors think that a special index for HCCI combustion is needed [10], [48], [65]–[68]. In this way, several studies has been carried out and proposed new indices. *Kalghatgi* [46] was the first to introduce an index for HCCI engines. He called it OI (Octane Index) and based it on RON, MON and the experimental conditions of the engine. *Shibata and Urushihara* [69] proposed another one based on the MON and the composition of the fuel. Finally, recently, *Truedsson et al.* [70] suggested a HCCI number based on the compression ratio needed.

3.3. Equivalence ratio

The equivalence ratio mainly consists of raising the energy supplied into the combustion chamber to achieve more power and torque. Lots of studies considered the use of a wide range of equivalence ratio to reach a wide operating range on HCCI engines but only a few articles analyzed the impact of this parameter on the combustion timing.

Lü et al. [49] analyzed the ignition delays through experiments with several PRFs. He ranged the equivalence ratio from 0.17 to 0.37 and the results obtained are presented in Figure 21 for both cool flame ignitions and main flame ignitions. As observed, the two ignition timings advance with the increase of the equivalence ratio. Similar outcomes were observed for n-heptane as fuel by *Zhang et al.* [40] and for PRF90 as fuel by *Tanaka et al.*

[37]. This is mainly due to the raise of the energy supplied into the combustion chamber which increases the chemical reactivity. However, other phenomena have to be considered.

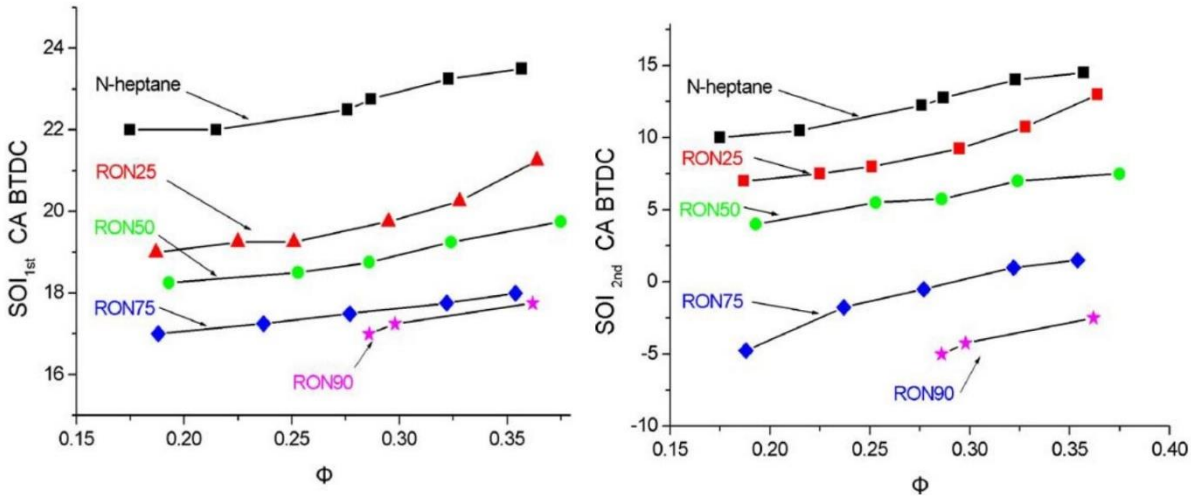

Figure 21. *Ignition timing of both cool flames (on the left) and main flames (on the right) for several PRFs as a function of the equivalence ratio* [49].

Machrafi et al. [35] examined the impact of the equivalence ratio and widely discussed on. Increase the equivalence ratio provides more fuel into the combustion chamber and therefore leads to a higher reactivity and a higher energy to release. On the other hand, the fuel has also its own heat capacity, lower than that of the air, and decreases the temperature history reached into the combustion chamber during the compression stroke. As a result, when the equivalence ratio varies, the combustion timing competes with the reactivity of the air/fuel mixture and its heat capacity. Therefore, a lean mixture will have a greater temperature history following the compression heating than a rich mixture but a high equivalence ratio will have a higher reactivity. Figure 22 provides the results obtained by *Machrafi et al.* on the ignition delays of n-heptane for both experiments and computations performed. It may be observed that both ignition delays decrease with the increase of the first equivalence ratios. Therefore, the reactivity dominates the compression heating. Then, the ignition delays of the first combustion stage slightly increase (approximately at an equivalence ratio of 0.35). This means that the occurrence of the combustion is delayed but the main ignition always advances. Nevertheless, its ignition delay is less pronounced. From this, the compression heating starts to overcome the reactivity of the air/fuel mixture. Finally, the results were extended with computations and showed clearly the delay on the cool flame as well as that on the main flame. Moreover, it may also observe that the negative temperature coefficient decreases and when the equivalence ratio is enough high, both ignition delays converge and the combustion should occur into a single stage.

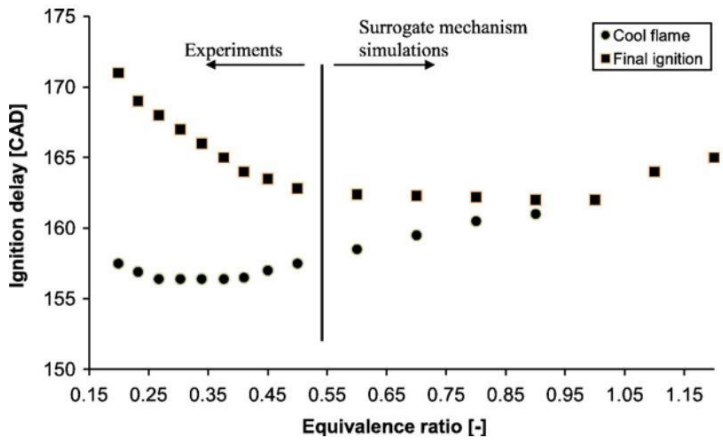

Figure 22. *Ignition delays for n-heptane as fuel as a function of the equivalence ratio at a compression ratio of 10 and an intake temperature of 70 °C. Results for equivalence ratios up to 0.55 correspond to experimental results and upper than 0.55 come from computations* [35].

3.4. Intake pressure

The intake pressure is one solution to dramatically increase the indicated mean effective pressure of HCCI engines and extend their operating range [71]–[75]. This parameter is closely linked to the temperature and it is obvious that increasing the intake pressure leads to an advance of the combustion timing since higher temperatures within the combustion chamber are reached during the compression stroke. *Liu et al.* [76] studied the impact of supercharging the intake of an HCCI engine for four different fuels and showed that the peak pressure increases and combustion is advanced (Figure 23). However, an increase of the in-cylinder temperature history due to the highest mass inducted inside the

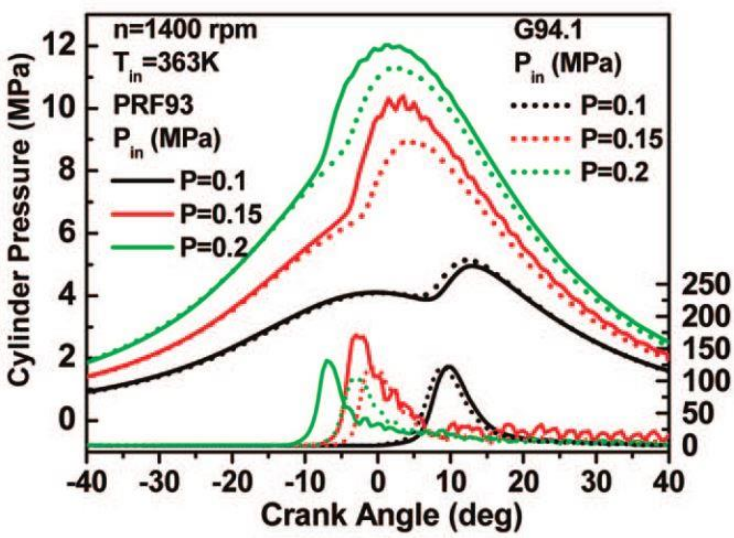

Figure 23. *Impact of the intake pressure on in-cylinder pressure and heat release rate traces for PRF93 and a gasoline* [76].

combustion chamber is not the only one effect of the intake pressure. The intake pressure also leads to a raise of the collision frequency between chemical species and therefore, to an increase of the overall reaction rates. Similar results were observed by *Silke et al.* [77] for simulations with PRF80 as fuel.

3.5. Rotation speed

The HCCI combustion must cover a wide range of rotation speed before a widespread implementation of such an engine. It was observed experimentally that this parameter affects the combustion timing of the HCCI combustion. *Lü et al.* [34] investigated the effect of the rotation frequency on PRF75 ignition delays from 1500 rpm to 2200 rpm. He showed that increase the rotation speed delays slightly both cool flame ignition and main flame ignition (Figure 24) and argued that both trends are due to a reduction of the compression time.

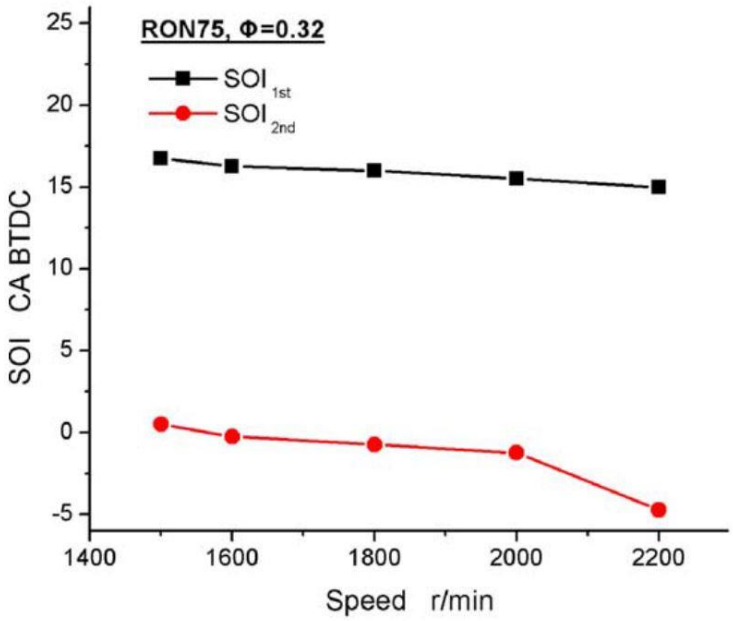

Figure 24. *Effect of the rotation speed on both cool flame ignition and main flame ignition for RON75 as fuel and an equivalence ratio of 0.32* [34].

A more visible delay was observed by *Aroonsrisopon et al.* [78] on the combustion of PRF70 for a rotation speed ranging from 600 rpm to 2000 rpm (Figure 25). He showed clearly that the combustion timing moves later, significantly on the main combustion timing, and that the magnitude of both flames decrease.

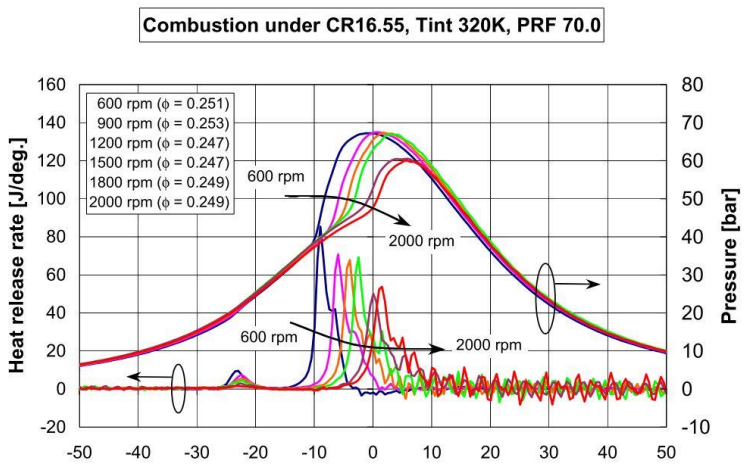

Figure 25. *In-cylinder pressure and heat release rate traces as a function of the rotation speed for PRF70 as fuel and an equivalence around 0.25* [78].

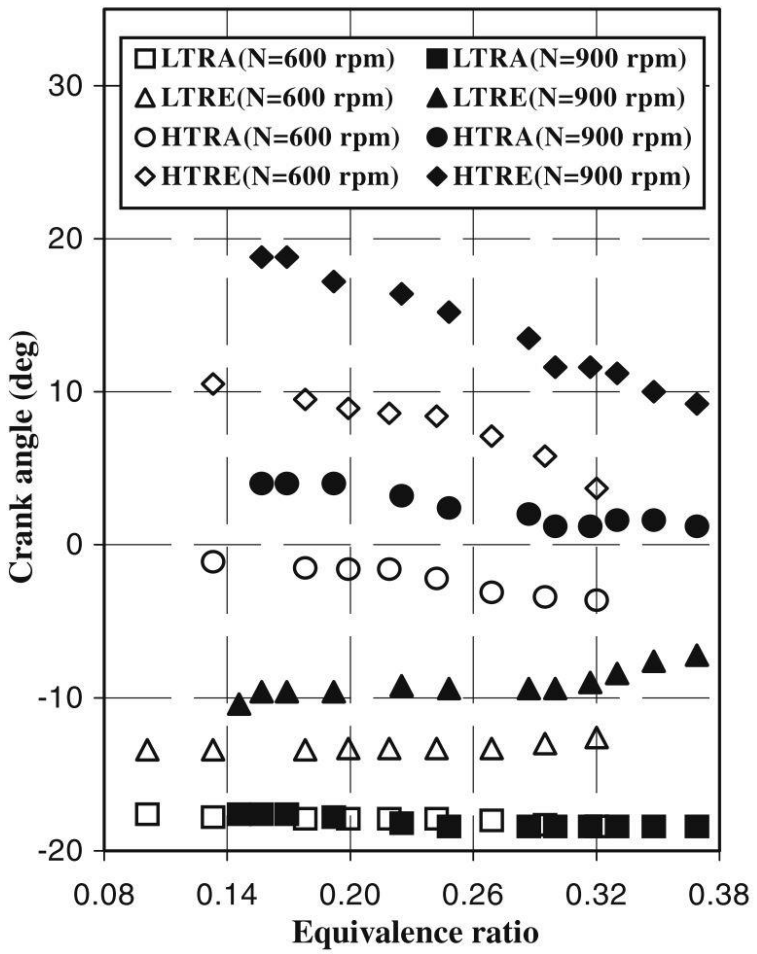

Figure 26. *Effect of the engine speed and the equivalence ratio on the ignitions and the ends of both cool and main combustion stages for iso-butane as fuel* [79]. *LTRA corresponds to the Low Temperature Reaction Appearance, LTRE to the Low Temperature Reaction End, HTRA to the High Temperature Reaction Appearance and HTRE to the High Temperature Reaction End.*

Finally, *Ebrahim et al.* [79] displayed similar results than both previous authors for iso-butane as fuel by comparing two rotation speeds. Figure 26 presents its results on ignitions and ends of the two combustion stages. He observed that combustion occurs around the same timing for both rotation speeds but the other ends and ignitions are delayed with the increase of the rotation frequency and a fixed equivalence ratio. Moreover, he also observed that the magnitude of the cool flame decreases but the in-cylinder temperature at the end of the first combustion stage is the same.

In fact, the effect of the rotation speed may be explained easily. The HCCI combustion is entirely governed by kinetics which is time based and mainly depends on the temperature history. In the case of a fuel with two combustion stages, increase the rotation speed increases the time necessary to achieve the autoignition and increases the thermal exchange towards the walls. The occurrence of the first combustion is therefore delayed. Then, the fuel consumption is limited and this combustion stage is longer. Finally, due to the weak increase of temperature during the first stage and the increase of the autoignition delay, the main combustion stage starts later and finally, the whole combustion is longer.

3.6. Geometry of the piston bowl

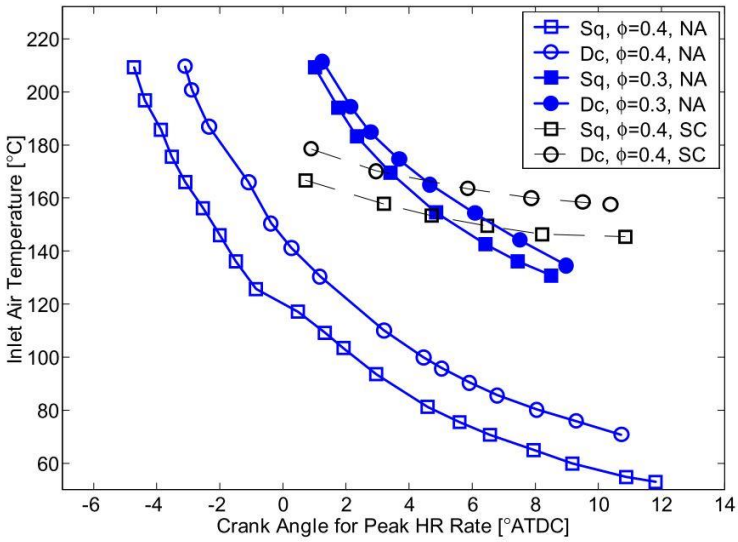

Figure 27. *Intake air temperature versus combustion timing for two different piston geometries (Square: Sq and Disc: Dc). NA corresponds to Naturally Aspirated and SC to Supercharged* [80].

Unlike other parameters, the effect of geometry of the piston bowl on the combustion timing was poorly investigated. The main reason results in the fact that it is impossible to change cycle-to-cycle the shape of the piston of an engine as the geometry of the piston is a fixed parameter of the engine. Instead, the studies focused on the geometry of the piston bowl in order to improve the efficiencies of the engine and reduce the pollutants [80]–[86]. However, the geometry may slightly influence the overall HCCI combustion process. *Christensen et al.* [80] studied the effect of combustion chamber

geometry on HCCI operation through two different pistons with the same compression ratio. The first was a flat disc meaning that combustion will occur in the overall cylinder. The second was a piston with square bowl and combustion will be located mainly inside the bowl. Figure 27 presents its results. With the square piston, a lower intake temperature is required to reach the same combustion phasing compared to the disc piston. According to the author, this is due to a higher turbulence with the square shape and because this piston is warmer during operations. Moreover, this is also responsible of longer combustion durations. Therefore, the piston shape and the combustion chamber will affect the HCCI combustion process.

3.7. Compression ratio

The compression ratio (CR) may also help controlling the HCCI combustion timing. This is possible by using variable compression ratio (VCR) engines [50], [87]–[90]. The variation of this parameter affects the thermodynamic conditions inside the combustion chamber, in particular, increasing the compression ratio allows to achieve high in-cylinder temperatures. On the other hand, increasing the compression ratio means for a same engine that the clearance volume becomes smaller and this leads to a high concentration of all the species at the end of the compression stroke. As a result, this two effects improve the overall reactivity inside the combustion chamber and earlier autoignitions are reached.

Machrafi et al. [35] examined the influence of the compression ratio on two fuels whose their respective heat release rate present two-stage combustions: n-heptane (PRF0) and PRF40. He observed that increasing the compression ratio affects both cool flame and main flame ignition delays (Figure 28). With a higher value of the compression ratio,

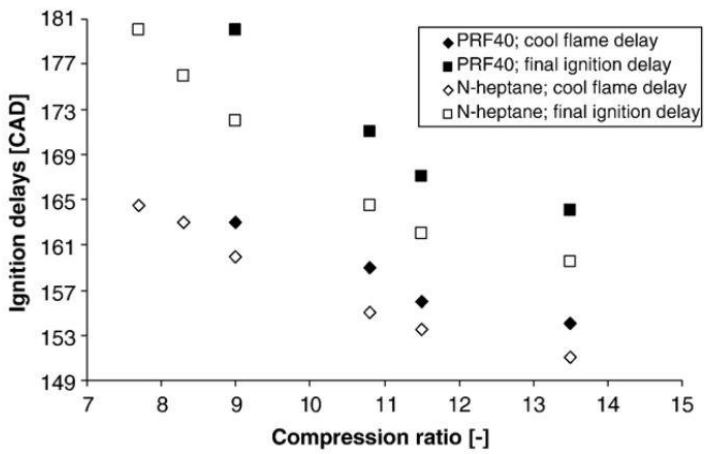

Figure 28. *Influence of the compression ratio on the cool flame and main ignition delays of n-heptane and PRF40 for an intake temperature of 70 °C and an equivalence ratio of 0.33* [35].

the in-cylinder temperature leading to autoignition is reached earlier and the cool flame ignition delays decrease. This first stage combustion allows a slight increase of the in-cylinder temperature and, combined with the temperature rise due to the compression stroke, an earlier main ignition delay is also achieved.

Olsson et al. [91] studied the impact of the compression ratio on the combustion of natural gas with addition of hydrogen. Obviously, he observed that increase the compression ratio of their engine leads to an advance of the autoignition. Furthermore, he also showed that due to the highest in-cylinder temperatures reached, the intake temperature can decrease while the compression ratio increases to keep constant the combustion timing. Similarly, by varying the amount of hydrogen, he showed that the reactivity of the fuel may reduce and the combustion phasing may be maintained by adjusting the compression ratio. Similar results were observed by *Christensen et al.* [89] with fuels whose the octane number ranged from 0 to 100. Conclusions showed that, with the intake temperature, the compression ratio is one of the strongest parameters affecting the combustion timing and therefore, adjusting quickly and correctly both parameters may lead to the control of the combustion at any condition. Finally, *Hyvonen et al.* [90] performed experiments on a multi-cylinder VCR engine and showed that a wide range of speed and load may be covered. Moreover, this operating range was extended by using supercharger [73].

3.8. Variable valve actuation

The HCCI combustion process is determined by the initial conditions at the intake valve closure (IVC). In this way, variable valve timing has been studied as a mean of control. With the technology, it is possible to change either the opening period of the intake valves or that of the exhaust valves or again those of both valves. Depending on the strategy, the variable valve timing always provides a delay of the combustion process but with different effects. In fact, controlling the HCCI combustion timing with variable valve actuation may be carried out according two main different methods. The first consists of closing early the exhaust valve and delaying the IVO. This strategy is mainly called negative valve overlap (NVO). In this case, residuals are trapped into the combustion chamber and compressed during the end of the exhaust stroke. The second consists of opening both intake and exhaust valves to draw down together fresh mixture and hot residuals during the induction stroke.

Liu et al. [92] examined the impact of varying the exhaust valve closure (EVC) and the intake valve closure. With a fixed mass of fuel inducted, an earlier closure of the exhaust valve traps more residuals and less fresh air is inducted resulting therefore into a dilution. Even if the temperature is high at the IVC due to the residuals, the dilution and the heat capacity of the bulk mass lead to a delay of the combustion timing. In the case of delaying the IVC, the effective displacement of the piston is lower and therefore the effective compression ratio is reduced. This results into lower in-cylinder temperatures which increase

the ignition delays. Similar results were observed by *Strandh et al.* [93] by controlling rapidly the closure of the intake valve and by *Yeom et al.* [94] by delaying the intake valve opening (IVO) which in turn reduce the volumetric efficiency. Finally, *Milovanovic et al.* [95] investigated the impact of each open and closure and concluded that EVC leads to the strongest impact on the combustion timing, then IVO and both others, EVO and IVC, have minor influences.

3.9. Exhaust gas recirculation

In recent years, the implementation of exhaust gas recirculation (EGR) was widespread on CI engines to meet NO_x requirements. This strategy was also applied to HCCI combustion but not to reduce pollutant emissions but rather to control the combustion timing. Lots of authors [33], [34], [96] studied the impact of this strategy and they showed that EGR mainly leads to a delay of the combustion (cool and main flame phasing) due to air dilution and due to the heat capacity of CO_2 and H_2O as observed in Figure 29. Air dilution limits the overall reaction and heat capacities limit the in-cylinder temperatures. As a result, fuel with high reactivity may supply HCCI engine with EGR to achieve effective combustion timing.

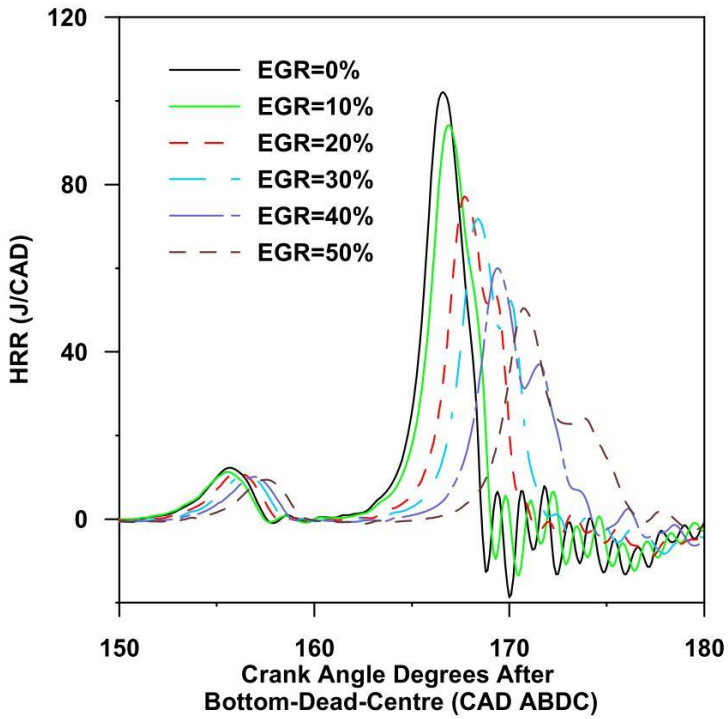

Figure 29. *Effect of the EGR on the heat release rate traces for n-heptane as fuel* [33].

There are several strategies to put into practice EGR. As observed previously, variable valve timing allows to trap some exhaust gases, i.e. residuals, into the combustion chamber. This is also called internal exhaust gas recirculation (iEGR). With this strategy, a thermal management at the IVC may be achieved. The second strategy consists of re-inject the exhaust gases into the intake either directly or with a cooling [97]–[100]. It is therefore

possible to control the HCCI engine over a wide operating range. The IGR helps to prevent misfiring due to thermal effects while EGR allows extending the combustion to the high loads mainly due to the dilution. However, a homogeneous mixture with these gases is required [101], [102].

According to all the results presented in the literature, EGR shows a thermal effect, an air dilution and a heat capacity [103]. However, the HCCI combustion is entirely governed by kinetics meaning that chemical effects must be considered. The impact of the main components was therefore investigated separately by *Sjöberg et al.* [104], [105] on various fuels. Ignition delays represented by CA10 are presented in Figure 30 for two fuels: isooctane and PRF80. The first presents one-stage combustion and the second two-stages. He showed that with only nitrogen, the cylinder temperatures are higher. The combustion must be advanced. Nevertheless, nitrogen leads to a delay of the combustion and highlights the oxygen dilution. Moreover, fuels with two-stage combustion are very sensitive to the dilution with nitrogen compare to fuels with only one-stage. This is due to a lack of oxygen which reduce the overall combustion rate and the heat released during the low temperature regime. In the case of CO_2, the combustion timing is mainly delayed due to the heat capacity of this molecule. Note that its presents the highest heat capacity. Isooctane is very significant because there is no low temperature regime which may help with a slight increase of the temperature and because its reactivity is lower than that of two-stage combustion fuel. H_2O also leads to a delay of the combustion [106] but with less impact compared to the CO_2. This is mainly due to its heat capacity which is the second most important among the main components of the EGR. However, for two-stage combustion fuels, the presence of H_2O showed an improvement of the reaction rates in front of the main ignition. Finally, *Sjöberg and al.* also analyzed the real EGR by comparing with a synthetic one composed of the main components and showed that trace species influence the combustion.

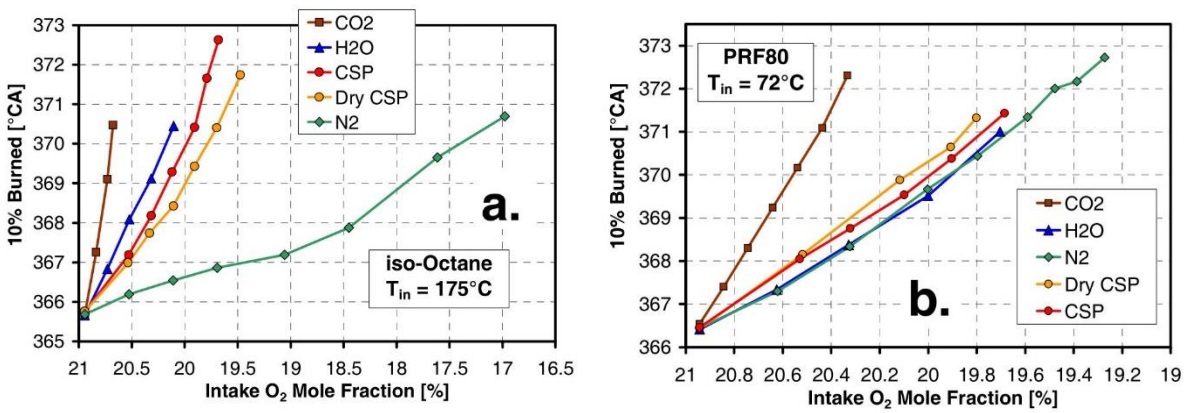

Figure 30. *Effect of the main components of the EGR on CA10 for isooctane (on the left) and PRF80 (on the right) as fuel. CSP corresponds to the Complete Stoichiometric Products and is therefore composed of CO_2, H_2O and N_2. Dry CSP corresponds to CSP without H_2O* [104].

The main trace species observed in the exhaust gases due to incomplete HCCI combustion are carbon monoxide (CO), unburned hydrocarbons (HC) and oxygenated components such as formaldehyde (CH_2O) [107]. The impact of CO has been carried out for higher concentrations than those normally produced by the combustion. *Dubreuil et al.* [33] and *Machrafi et al.* [108] showed that CO seeded into the intake of the engine does not modify the combustion phasing but they assume that CO may speed up the combustion. However, according to *Sato et al.* [109], CO delays the combustion of methane but high concentrations are needed to reduce significantly the combustion timing. This is mainly due to the high temperature, around 1500 K, necessary to oxidize CO [110] while fuels may oxidize with lower temperatures. The impact of HC was also studied by *Dubreuil et al.* [33]. Instead of injecting HC compounds, volume fractions of CH_4 were used and results showed that small additions of these species do not affect the combustion timing. This low influence depends on the reactivity of the fuel compared to that of the HC, most of the time, HC are less reactive. For the last species, CH_2O was investigated by *Machrafi et al.* [108] on PRF40 and results showed a weak delay of the HCCI combustion due to the consumption of very reactive radicals (OH) for less reactive ones (HO_2). However, in the case of isooctane [10] and methane [111] as fuel, CH_2O promotes the HCCI combustion. As a result, CH_2O is mainly an inhibitor for fuels with two-stage combustion and a promoter for others. Finally, HCCI combustion is mainly studied because it allows low NO_x. However, high temperatures inside the combustion chamber and lean equivalence ratio may generate some NO_x which may also alter the combustion timing. It was observed that these species are rather combustion promoters [108], [112] and their impact will be treated into the following part.

3.10. Oxidizing chemical species

In addition to the influence of the previous parameters on the HCCI combustion, some authors proposed modifying the initial composition of the mixture inside the combustion chamber by injecting minor concentrations of very reactive additives which can alter the combustion by a promoting effect. The impact of many species were assessed and the only ones leading to a significant advance of the combustion were retained [10]. Moreover, these species have to be sufficiently stable and must be used on board a vehicle. Some of them, among the most powerful, are presented here.

3.10.1. Fuel peroxides

The use of fuel peroxides to improve the HCCI combustion is quite similar to the addition of combustion improvers such as 2-ethyl-hexyl-nitrate (2EHN) or di-tertiary-butyl-peroxide (DTBP) [37]. Both components showed that they might strongly advance the combustion timing. According to *Aceves et al.* [10], components which present peroxide structure are the strongest species leading to an advance of the combustion timing. In recent works, *Schönborn et al.* investigated new approaches to alter the fuel molecular structure into fuel peroxides [113]–[115]. He used two different chemical treatments. The

first consists of using ozone, a powerful oxidizing chemical species. This species is injected into a tank containing the fuel and oxidized it through peroxides. The second is quite similar and consists of applying UV-irradiation to also produce peroxide species. These species decomposes earlier into the cycle and may produce active radicals which strongly improve the combustion and finally, the combustion timing may be controlled by adjusting the proportion of pure fuel to that of the modified fuel (Figure 31).

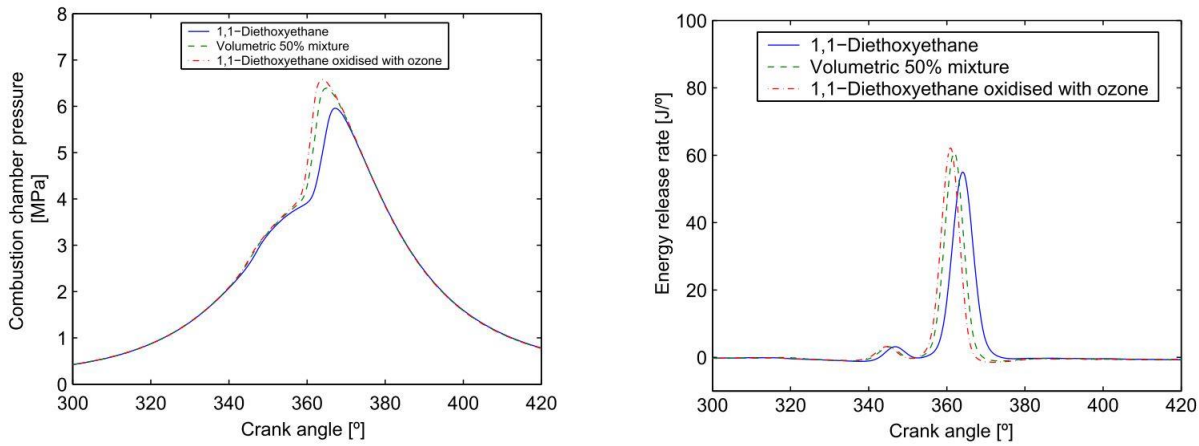

Figure 31. *Impact of varying the proportion of pure fuel and modified fuel into an HCCI engine* [113].

3.10.2. Hydrogen peroxide

Hydrogen peroxide (H_2O_2) was also identified as a promoter of combustion (Figure 32). This was demonstrated on methane autoignition by *Golovitchev et al.* [116] and by *Morsy et al.* [111]. Both authors are in agreement on the fact that the promoting effect of hydrogen peroxide comes from its decomposition into two hydroxyl radicals (R-12).

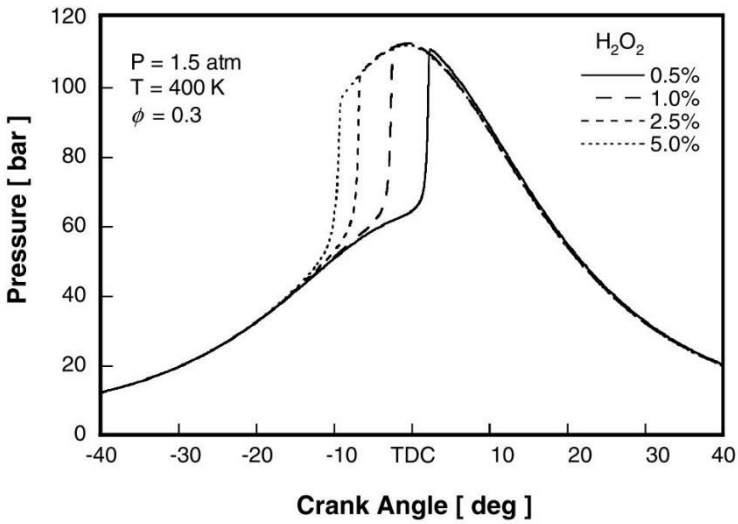

Figure 32. *Impact of hydrogen peroxide additions on methane combustion* [116].

As methane is highly difficult to autoignite, the decomposition of the hydrogen peroxide helps to decrease the temperature needed to start the combustion due to the high reactivity of hydroxyl radicals. Nevertheless, this decomposition mainly occurs during temperatures closed to 1000 K. Therefore, it is expected that on other fuels, in particular fuels with two-stage combustion, addition of hydrogen peroxide will promote only the main combustion stage as low temperature reactions take place at temperatures lower than 1000 K [10].

3.10.3. Nitrogen oxides

Instead of previous additives, nitrogen oxides were strongly studied and most of them indicated an oxidizing potential [33], [112], [117]. Therefore, they can help to improve and advance the HCCI combustion. Among the wide variety of nitrogen oxides, only the most encountered in engine applications were reviewed.

3.10.3.1. Nitric oxide

Nitric oxide (NO) was significantly investigated because it is mainly observed into the exhaust gases and its impact on the combustion is well figure out now [118]–[120]. Previous study showed that its presence into the residuals may lead to a run-away of the HCCI combustion [112], advancing the combustion timing, and further investigations highlight its oxidizing potential. *Dubreuil et al.* studied the impact of NO for several fuels [121]. Results are introduced in Figure 33. It was observed that NO, up to 100 ppm, promotes the HCCI combustion by advancing cool and main flame phasing. Then, higher concentrations lead to a delay of the cool flame phasing while the main flame advances monotonically and seems to reach a constant value. This results in a decrease of the NTC regime and a lower heat released during the low temperature heat release. Similar results on ignition delays were obtained by *Machrafi et al.* [108], [122] for PRF40 as fuel, except that the transition occurs at 45 ppm. Finally, the impact has been explained through kinetics. The exhibiting effect for low NO concentrations is provided by reactions R-16 and R-17. Both reactions compete together but the first one dominates and allows the consumption of hydroperoxyl radical ($HO_2^{\bullet}$) producing hydroxyl radical (OH), a more reactive radical, and leading to an increase of the reactivity.

$$NO + HO_2 \rightarrow NO_2 + OH \qquad \text{R-16}$$

$$NO + RO_2 \rightarrow NO_2 + RO \qquad \text{R-17}$$

When the NO concentration increase, inhibiting reactions become more and more important and lead to chain-terminating reactions (R-18 and R-19) with the production of nitrous acid ($HONO$) which is stable under the low temperature regime.

$$NO + OH + M \rightarrow HONO + M \qquad \text{R-18}$$

$$ROOH + NO \rightarrow RO + HONO \qquad \text{R-19}$$

For higher temperatures, i.e. under the intermediate and high temperature regime, reaction R-18 reverses leading to OH radicals. Moreover, the reaction R-16 still dominates the overall NO consumption also leading to a high reactivity of the system and providing the advance observed on the main combustion phasing.

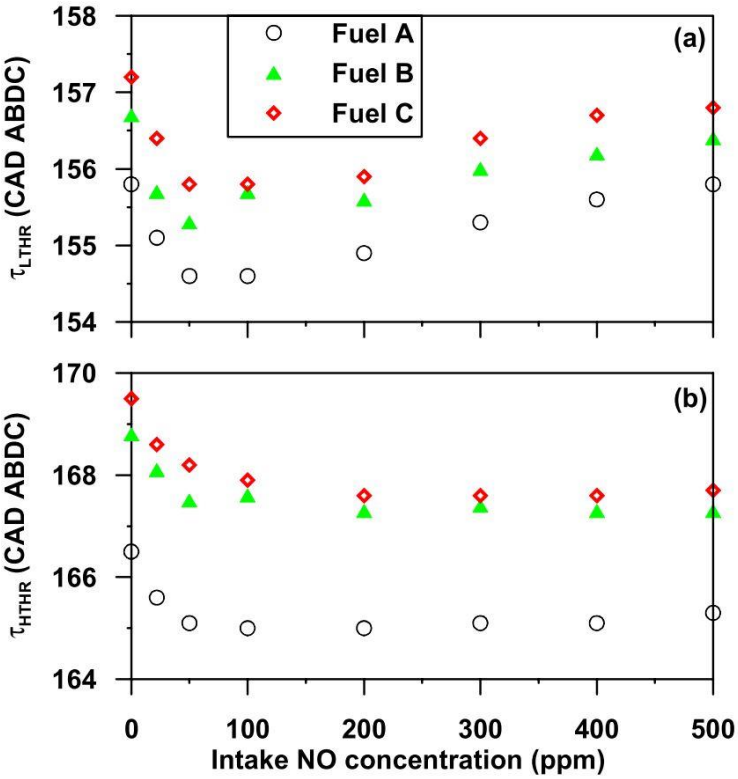

Figure 33. *Impact of NO on ignition timings for the cool flame (on the top) and for the main flame (on the bottom)* [33]*. For three fuels: Fuel A: n-heptane, Fuel B: PRF25 75% n-heptane and 25% isooctane; Fuel C: TRF24 80% n-heptane and 20% toluene.*

In the case of isooctane as fuel, the absence of cool flame avoids the inhibiting reactions with NO and the combustion is entirely improved due to the conversion of less reactive radicals for strong reactive radicals through the reaction R-16. Hence, *Contino et al.* [123] showed that injecting 500 ppmv of NO may advance the CA50 of approximately 15 CAD. Similar results were also observed for methane as fuel [124]. Finally, in the case of TRFs as fuel, the cool flame is less delayed than for PRFs and therefore, the ignition timing may still decrease depending on the intake temperature. This is due to $HONO$ species which are chain-terminating for PRFs while they are chain-branching for TRFs due to the presence of toluene [117], [125].

3.10.3.2. Nitrogen dioxide

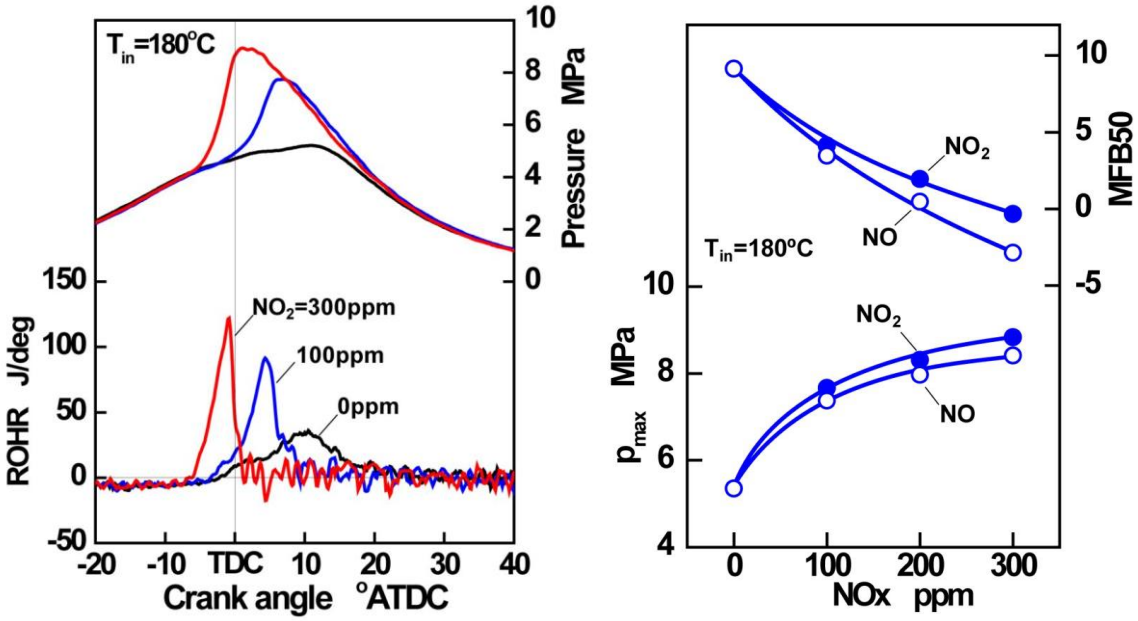

Figure 34. *Effect of nitrogen dioxide on the in-cylinder pressure and heat release rate traces for natural gas as fuel (on the left). Comparison of NO and NO_2 effect on the maximum pressure and on the CA50 (on the right)* [124].

Nitrogen dioxide (NO_2) was also investigated as the other NO_x component found into the exhaust gases. It was observed that NO_2 provides a similar effect than NO on the combustion [124], [126], [127] (Figure **34**). This is mainly due to the cyclic production and consumption of NO and NO_2 [119]. The main reaction involving NO_2 produces NO and inversely. Under intermediate temperatures, the enhancement of the combustion is provided by reactions R-20, R-21, R-22 and R-16 which lead to the production of OH radicals.

$$NO_2 + HO_2 \rightarrow HONO + O_2 \qquad \text{R-20}$$

$$NO_2 + CH_3O \rightarrow HONO + CH_2O \qquad \text{R-21}$$

$$HONO + M \rightarrow NO + OH + M \qquad \text{R-22}$$

At higher temperatures, the combustion is still improved by the cyclic system of reaction involving consumption and production of NO and NO_2 which leads to the formation of OH radicals. However, the system of reactions with NO_2 is replaced by another system which consists of reactions R-23, R-24 and R-16.

$$NO_2 + H \rightarrow NO + OH \qquad \text{R-23}$$

$$NO_2 + CH_3 \rightarrow NO + CH_3O \qquad \text{R-24}$$

3.10.3.3. Nitrous oxide

Recently, the impact of nitrous oxide (N_2O) on the ignition delays has been carried out for methane as fuel [128]–[130] and becomes of a main interest. All the authors indicated that this species allows promoting the autoignition by reducing the ignition delays. The advance of the ignition timing is due to reactions R-25 and R-26, the first being the main responsible and the most reactive but both reactions lead to the formation of the main radicals allowing a rapid fuel consumption, i.e. O-atoms and OH radicals.

$$N_2O + M \rightarrow N_2 + O + M \qquad \text{R-25}$$

$$N_2O + H \rightarrow N_2 + OH \qquad \text{R-26}$$

3.10.4. Ozone

Ozone (O_3) was largely studied on flame velocity [131]–[137] and indicated that ozone may strongly increase the combustion reactivity or initiate the combustion under lower temperatures than those necessary normally [138]. Ozone is therefore an excellent promoter of combustion and is among the most powerful for potential HCCI application by *Aceves et al.* [10]. Instead of *Schönborn et al.* who used ozone to alter the molecular structure of the fuel [113], [114], some studies were performed by seeding directly the intake of an HCCI engine with this oxidizing chemical species. *Tachibana et al.* [139] studied the impact of ozone on fuels with different cetane number (CN) into a Cooperative Fuel Research (CFR) engine. He observed that ozone allows increasing the CN, meaning that the fuel may auto-ignite more easily and finally lead to a reduction of the ignition delays. Moreover, easily the fuel auto-ignite without ozone, higher the impact of ozone is. Therefore, the compression ratio of the engine can also be reduced with the use of ozone. Reduction of the ignition delays were also observed by *Mangus et al.* [140] with a Diesel engine with a mechanical injection system from low to middle loads. By comparison with a common rail injection, results showed that ozone has a stronger impact with a mechanical injection due to lots of heterogeneity of the air/fuel mixture within the combustion chamber while common rail injection which is largely premixed rapidly reaches the diffusion flame. *Foucher et al.* [9] seeded the intake of an HCCI engine with ozone for n-heptane as fuel. Its results showed that ozone advance the combustion phasing of both cool and main flame with the same trends (Figure 35), i.e. a strong decrease of the combustion phasing under low concentrations and then, the impact is less pronounced. Similar results were observed for other authors with other fuels [11]–[13]. Through kinetics interpretations, it was showed that ozone improves the combustion due to an earlier production of OH radicals through a direct oxidation of the fuel (R-27) from species coming from the breakdown of ozone (R-28). Finally, managing the ozone concentration at the intake of the engine may easily control the HCCI combustion timing.

$$RH + O \rightarrow R + OH \qquad \text{R-27}$$

$$O_3 + M \rightarrow O + O_2 + M \qquad \text{R-28}$$

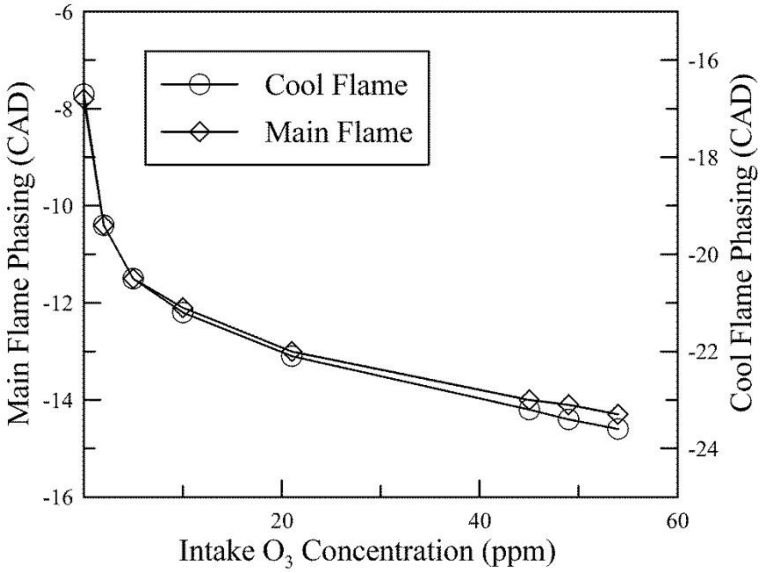

Figure 35. *Cool and main flame phasing as a function of the ozone concentration seeded in the intake of an HCCI engine [9].*

4. Conclusion

This first chapter focused on a review on the HCCI combustion. The two conventional engines, i.e. Spark Ignition and Compression Ignition engines were introduced and defined according to their own principles. With the more and more stringent requirements on these two engines, many advanced combustion modes were investigated and are very promising since they allow keeping high efficiencies and low NO_x and particulate matter emissions. PCCI, RCCI and HCCI are considered as the most interesting modes for automotive applications and were described. The respective principle of PCCI, RCCI and HCCI showed that all these combustion modes present homogeneous auto-ignitions and figure out perfectly the autoignition is needed for a widespread development of advanced combustion modes.

Consequently, this study further investigated the HCCI combustion. HCCI was compared to both conventional combustion modes and prior investigations showed that the whole combustion process is dominated by kinetics instead of an element such as a spark plug or an injector. Therefore, the HCCI combustion was also defined according to a kinetic interpretation and the main reactions dominating the different combustion phases. Additionally, the advantages and drawbacks were introduced and finally, a widespread development of an HCCI engine will be considered once the main challenge for such an engine will be overcome, i.e. once an efficient control of the entire combustion process over a wide operating range (in term of loads and speeds) could be implemented.

A literature review revealed that many parameters may help controlling the HCCI combustion. Each of them have its own pros and cons and a future HCCI engine will probably use several of them for efficiently controlling the HCCI combustion. Among all the parameters introduced, a recent interest was made on oxidizing chemical species, in particular, that of ozone (O_3) which is among the most powerful oxidizing species. Indeed, few ppm of ozone indicated that the combustion timing may be significantly advanced. Moreover, its production is based on the use of ozone generator whose the size tends to becoming increasingly small and means that a potential application may be developed on a vehicle.

From this prior investigation on HCCI combustion, two objectives were drawn:

- First, assess the potential of applying an ozone generator for controlling the HCCI combustion process. Basically, ozone generators produce ozone from pure oxygen but considering an implementation on-board a vehicle, use air will be more suitable. Unfortunately, supply the ozone generator with air could produce other reactive species such as nitrogen oxides which may alter the combustion. Moreover, ozone mainly breaks down due to the temperature, the influence of temperature must therefore be also considered.

- Second, conventional engines are associated to a unique fuel while HCCI engines are flexible, depending on the conditions of pressure, temperature, equivalence ratio and dilution. A wide range of fuel may be used and therefore, the influence of ozone on the combustion of various fuels selected have to be performed and compared.

Chapitre 2 / Chapter 2

Dispositif expérimental et moyens numériques

Experimental setup and numerical tools

Résumé

Le second chapitre de ce manuscrit décrit le dispositif expérimental ainsi que les outils numériques utilisés. Les études conduites ont été réalisées au moyen d'un banc d'essai moteur et la première partie de ce chapitre décrit l'ensemble de l'installation expérimentale. Le moteur utilisé est un moteur monocylindre dont l'admission a été modifiée afin de permettre un fonctionnement HCCI, c'est-à-dire avec un mélange air/carburant le plus homogène possible. De plus, l'intégralité des paramètres de fonctionnement sont pilotables. Compte tenu des objectifs, un générateur d'ozone commercial a été installé et est décrit ainsi que le matériel associé tel que l'analyseur d'ozone.

L'acquisition des résultats se fait au moyen du banc expérimental qui enregistre le signal de pression cylindre. Ces essais sont ensuite traités suivant un programme d'analyse développé au cours de ces travaux de thèse. La méthodologie consiste en une étude thermodynamique basée sur une analyse de la pression cylindre et des différentes conditions d'essais. L'ensemble des calculs effectués est décrit et finalement, l'ensemble des paramètres qui seront analysés dans les chapitres de résultats sont définis.

La combustion HCCI étant entièrement gouvernée par la cinétique chimique, des simulations sont effectuées en complément des essais expérimentaux à l'aide de Chemkin II et de l'exécutable Senkin. Le modèle sélectionné est décrit ainsi que les mécanismes et sous-mécanismes retenus. Enfin, la méthodologie mise en place pour effectuer ces simulations est finalement définie.

Abstract

This second chapter of this Thesis describes the experimental setup as well as the numerical tools used. The investigations conducted were carried out with the help of an engine bench and the first part of this chapter introduces the whole experimental setup. The engine used is a single cylinder engine whose the intake has been adapted to enable HCCI operations, i.e. with an air/fuel mixture as homogeneous as possible. Moreover, all the working parameters are controllable. According to our objectives, a commercial ozone generator has been set up and is described as well as the associated devices such as the ozone analyzer.

The acquisition of the results is performed by the use of the experimental bench which records the in-cylinder pressure signal. The experiments are then post-treated with the help of a program developed during the Thesis. The methodology consists of a thermodynamic study based on an analysis of the in-cylinder pressure signal and the test conditions. All the calculations performed are introduced and finally, all the parameters which will be analyzed in the chapters presenting the results are defined.

The HCCI combustion is entirely governed by kinetics, computations are carried out to complete the experiments with the help of Chemkin II and the Senkin executable code. The model selected is described as well as the mechanisms and sub-mechanisms chosen. Finally, the methodology considered to perform these computations is defined.

1. Experimental setup

1.1. The HCCI engine bench

The engine used for the experiments is a four cylinders four stroke Diesel engine PSA DW10. It was converted into a single-cylinder engine. Three cylinders were deactivated and the combustion takes only place inside the fourth cylinder. Main parameters of the engine are listed in Table 2. As the engine cannot be itself in a continuous rotation, it was directly coupled to an electric motor which allows to maintain a constant rotation speed.

Table 2. *Main characteristics of the single-cylinder HCCI engine.*

Bore [mm]	85
Stroke [mm]	88
Rod length [mm]	145
Displaced volume [cc]	499
Geometric compression ratio [-]	16:1
Number of valves per cylinder [-]	4
Intake valve opening [CAD]	351
Intake valve closure [CAD]	-157
Exhaust valve opening [CAD]	140
Exhaust valve closure [CAD]	366
Coolant temperature [°C]	~ 95
Oil temperature [°C]	~ 95

Operating under homogeneous conditions, the intake of the engine was modified. A plenum was set up in front of the intake pipe and enables to mix all the compounds of the charge. The inducted charge for an engine is mainly the air and the fuel but for experimental researches, pure components such as nitrogen, oxygen, EGR components or other specific components may be added. The quality of the homogeneity was examined in previous experiments carried out in the lab on an optical engine by *Dubreuil et al.* [33]. Results showed that the charge may be consider homogeneous with such a device and there is only inhomogeneity in temperature inside the combustion chamber. For the preparation of the mixture, all the components are separately injected before their entrance inside the plenum. Gases, as for instance the air, are all directly introduced inside the main pipe of the experimental setup. This pipe is long enough and enable the homogeneity of all the gases injected. Liquids, mainly fuels, are stored inside a pressurized tank. For the admission inside the combustion chamber, the fuel has to be in the form of gases. It is therefore initially

blended with a short part of the total air which is used as a carrier gas. Then, this first blend passes into an evaporator and is finally introduced in the main pipe just upstream the plenum. The Figure 36 shows a scheme of the experimental setup.

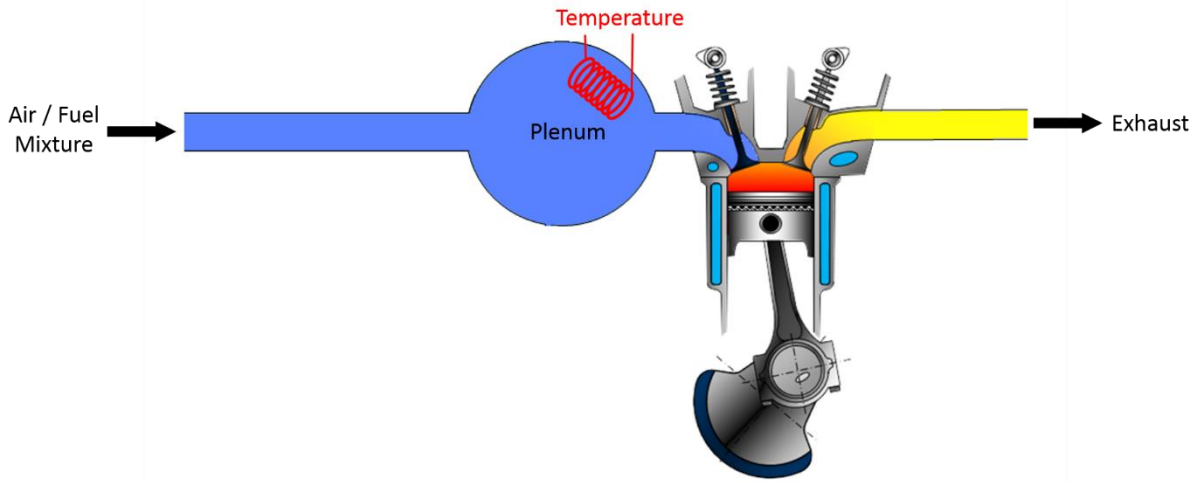

Figure 36. *Scheme of the experimental setup in its normal configuration.*

1.2. Controllers and sensors

Managing the overall experimental setup, controllers and sensors were set. They allow controlling all the parameters during experiments, more specifically, the intake pressure, the intake temperature, the equivalence ratio, the composition of the charge and the rotation speed.

The rotation speed is managed using an electric motor referred as Brushless Servo Motor IEC 60034-1. As mentioned before, the use of the electric motor allows maintaining a constant rotation speed. The setpoint of the rotation speed may be changed from an idling speed (~500 rpm) to a maximum speed of 2000 rpm (value fixed to avoid violent combustion with high knock) while the engine is running and with a constant acceleration (dN/dt = constant) fixed before to start experiments.

For the composition of the charge, each component is managed by using a mass flow controller (MFC). Gases are controlled by means of Brooks gas MFCs. These devices present an accuracy of ± 0.7% on the measure and ± 0.2% on the full scale. For liquids, Bronkhorst Coriolis liquid MFCs are employed and present an accuracy of only ± 0.2% on the measure. Before to start experiments, the gas or liquid controlled by each MFCs have to be defined as well as the fractions of oxidant and the fractions of fuel. Then, the final fractions on each MFC are recalculated from the equivalence ratio tuned. More precisely, this calculation is based on the oxygen ratio, the amount of fuel is determined from the equivalence ratio which is defined as the ratio between the fuel fraction and the oxygen

fraction measured in reference to the same ratio in the stoichiometric case (whether $X_{fuel} = \varphi \times X_{O_2} \times \left(X_{fuel}/X_{O_2}\right)_{st}$). Finally, the flow on each MFC is automatically adjusted in agreement with the fraction and the equivalence ratio defined with the aim to reach the intake pressure setpoint. A Keller PAA-33X/80794 absolute pressure sensor measures this last parameter with an accuracy of 0.1% on its measuring range. In conclusion, the present approach is for a pressure regulation inside the plenum or again, for controlling the pressure at the intake of the engine. Another approach is available to substitute the control of the intake pressure and consists in managing independently the flow of each MFC by setting a constant value on each of them. Therefore, the flows are fixed and in consequence, the intake pressure is measured but not controlled. Finally, it is important to state that both approaches may be combined. It is possible to control some MFCs with a constant flow and adjust the other to achieve the intake pressure setpoint and the composition of the charge. This combination will be particularly useful as part of the experiments performed during the present work.

The intake temperature, the last parameter to tune, is controlled using several heating resistance. The first heater is located inside the main pipe in front of the plenum and upstream the fuel injection. As the temperature around the resistance can be very high, this strategy enables to avoid ignition of the air/fuel mixture as there is no fuel near this heating element and the gases inside the main pipe may be warm up to regulated temperatures near 240 °C. The second heating resistance is a heater band positioned all around the plenum. The aim of this element is not to warm up the air/fuel mixture but to limit heat losses and maintain a high temperature of the charge before it is admitted inside the combustion chamber. Most of the time, this heater band regulates a temperature similar to that of the main heater. The last element influencing the intake temperature is the evaporator. It is not use to control the temperature at the entrance of the engine but to ensure that liquids, mainly fuels, will be well evaporated. However, as it warms up a part of the flow up to 200 °C, it can slightly affect the intake temperature. Finally, the intake temperature is a parameter measured when all the regulated temperature of all previous element are well stabilized. Two K thermocouples, one in each pipe of the engine intake, are used to determine the intake temperature. Each of them presents an accuracy of ± 2K and the final intake temperature retained is the average of both measures.

All the parameters previously discussed; i.e. the intake conditions, the equivalence ratio, the flow rates and the engine speed; are measured and recorded inside one file called “Slow Acquisition File”. This file contains the average based on 40 measurements for each parameter of the experimental setup. Then, these data will be used for a thermodynamic analysis of the results described in the next part. Moreover, additional data on the exhaust of the engine are also recorded inside this file. It consists of the exhaust pressure, the exhaust temperature as well as pollutant emissions. The exhaust pressure is also measured

with a Keller absolute pressure sensor, the same kind than that for the intake pressure. The exhaust temperature is given from a K thermocouple similar to those used for the intake temperature. Finally, emissions are examined using a HORIBA gas analyzer bay referred as MEXA-7100HEGR. It collects a sample with a constant flow in the plenum located downstream of the engine. A backpressure valve was set up to maintain a constant pressure and avoid any perturbation on the exhaust of the engine. Then, the sample is separately injected in the four different analyzers which quantified the following species: carbon monoxide (CO), carbon dioxide (CO_2), nitric oxide (NO), nitrogen oxides (NO_x), oxygen (O_2) and unburned hydrocarbons (HC).

For the experimental results, the analyses are based on the evolutions of the in-cylinder pressure. A Kistler 6043A piezo-electric relative pressure sensor measures this pressure with an accuracy of ± 2%. Measurements are carried out every 0.1 crank angle degree through the use of an optical encoder positioned on the crankshaft of the engine. Therefore, 7200 points are recorded per cycle and each cycle starts at -180 CAD. In parallel to the measurements of the in-cylinder pressure, pressure evolutions inside the manifolds, i.e. intake and exhaust, are also measured with the same discretization. The intake pressure is measured by a Kistler 4075A piezo-resistive absolute pressure sensor positioned on one of the intake pipe. This sensor presents an accuracy of ± 0.3% of the full scale. The exhaust pressure is also measured by the same kind of sensor except that an additional cooling adapter has been mounted to remain inside the operating range of the pressure sensor. Finally, all these pressures traces are recorded inside another file named “Quick Acquisition File” which contains the data of 100 cycles.

1.3. Fuels selected

HCCI engines may use a wide range of fuels. More details were given in the first chapter of the manuscript. The present experimental is suitable for testing different fuels and according to the objectives, several fuels were selected among three fuel families, i.e. Primary Reference Fuels (PRF), gaseous fuels and alcohol fuels. PRFs were chosen because they are representative of conventional fuels already employed, n-heptane for diesel and isooctane for gasoline. Moreover, they were widely studied as references for fuel investigations. For the two other families, they are less employed than conventional fuels. Nevertheless, regarding the forecasts, gaseous and alcohol fuels will grow in importance and were therefore included in the present work. All the fuels selected are listed in Table 3 with their respective properties.

Table 3. *Properties of the fuels.*

Fuel	State	C	H	O	H/C ratio	O/C ratio	Lower Heat Value[1] [kJ/kg]	Density[1] [kg/m^3]	Molar mass[1] [g/mol]	Air Fuel Ratio	RON	MON	ON[2]	CN[3]
n-heptane	Liquid	7	16	0	2.286	-	44566	684	100.205	15.11	0	0	0	54.6
*iso*octane	Liquid	8	18	0	2.25	-	44310	690	114	15.06	100	100	100	12.6
PRF20	Liquid	7.2	16.4	0	2.278	-	44514.8	685.2	102.8	15.10	20	20	20	46.2
PRF40	Liquid	7.4	16.8	0	2.27	-	44463.6	686.4	105.6	15.09	40	40	40	37.8
PRF60	Liquid	7.6	17.2	0	2.263	-	44412.4	687.6	108.4	15.08	60	60	60	29.4
PRF80	Liquid	7.8	17.6	0	2.256	-	44361.2	688.8	111.2	15.07	80	80	80	21
Methane	Gas	1	4	0	4	-	50009	0.656	16	17.17	120	120	120	4.2
Propane	Gas	3	8	0	2.667	-	46357	0.5070	44.10	15.57	110	97	103.5	8.4
Hydrogen	Gas	0	2	0	-	-	120971	0.0852	2.016	34.05	>130	-	-	-
Methanol	Liquid	1	4	1	4	1	19937	791.8	32	6.44	109	89	99	8.82
Ethanol	Liquid	2	6	1	3	0.5	28865	789	46	8.96	109	90	99.5	8.82
n-Butanol	Liquid	4	10	1	2.5	0.25	33075	810	74	11.13	98	85	91.5	13.44

1. Lower Heat Value, Density and Molar Weight come from *Guibet* [187]

2. Octane Number is defined as the average of the Research Octane Number and Motor Octane Number, whether $ON = (RON + MON)/2$

3. Cetane Number is defined from a linear relationship with the Research Octane Number, whether: $CN = 54.6 - 0.42 \times RON$ [46]

1.4. Oxidizing chemical species selected

The aim of the present work is to investigate the seeding effect of some oxidizing chemical species at the intake of the engine on the HCCI combustion of the fuels previously presented. According to the context introduces at the beginning of the manuscript, three different species were retained: ozone, nitric oxide and nitrogen dioxide. This part presents the devices used to seed the intake of the engine and the methodology to estimate the concentration of these oxidizing chemical species.

1.4.1. Ozone

Ozone is an unstable molecule whose the half-life time is particularly short. Therefore, this species needs an on-site production or on board in the case of a vehicle. Devices used to create it are usually ozone generators and that employs for these researches is described hereafter. Additionally, it is important quantifying the concentration of ozone. An ozone analyzer was therefore used to estimating the amount of ozone produced and is also describes.

1.4.1.1. Ozone generator

The ozone generator used all along this work is a commercial device referred as COM-AD-01 from the society ANSEROS. It works on the principle of a dielectric barrier discharge which produces ozone between two electrodes separated by a dielectric material and powered by a high voltage signal. A scheme of the generator is presented in Figure 37.

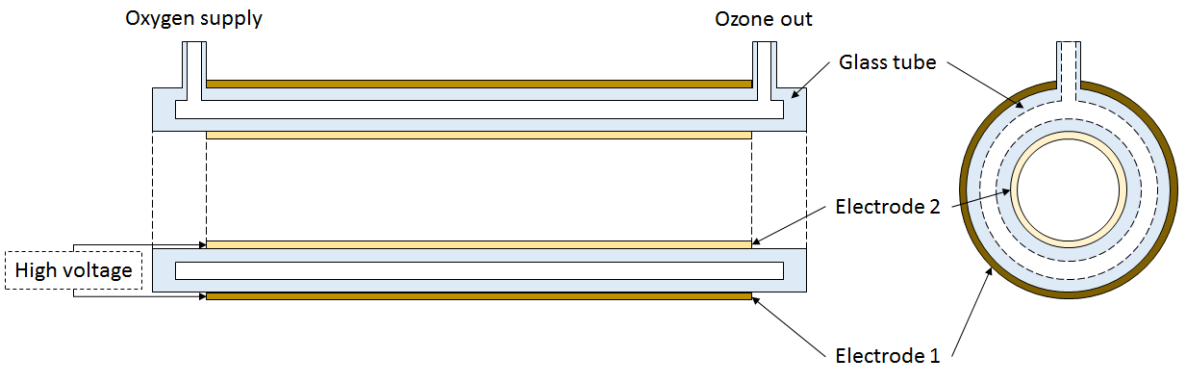

Figure 37. *Scheme of the ozone generator.*

According to the scheme, ozone is produced inside a cylindrical volume of glass usually supplied by pure oxygen. This allows preventing any nitrogen oxidation. Two electrodes surround the glass: one inside the cylinder and the other one outside. By separating the electrodes to the volume of ozone production with glass, the output flow contains only oxygen with ozone and this enables to avoid the production of pollutants or undesired species. Electrodes are powered by high voltages (~ 10 kV) which allow to produce pulsed discharges inside the cylindrical volume containing oxygen. The amount of ozone is

therefore controlled by tuning the pulse frequency of the discharge which is managed by a potentiometer varying from 0 to 100% (the real frequency applied is therefore unknown). The other way for controlling the ozone produced is to manage the flow crossing the cylindrical volume. This enables controlling the residence time and higher it is, higher is the ozone concentration at the output. According to the manual of users, the flow has not to exceed 250 NL/h (~ 4.2 NL/min). A mass flow controller was therefore set up to control perfectly the inflow and was limited to the maximum flow authorized by the generator. Generally, for all this work, the flow is maintained constant and only the pulse frequency is modified. The ozone produced by this device is finally injected via a separated way than those already introduced in the engine bench part. This is due to the unstable properties of this molecule and the location of this injection will be further described later.

Finally, previous description of the ozone generator is for a general use which consists of tuning the potentiometer manually. Improvements were therefore performed to allow a remote control. As the function of the potentiometer is to tune a low voltage enabling to manage the pulse frequency, a voltage source controlled by the PLC (Programmable Logic Controller) was linked in parallel to the potentiometer. The voltage delivered by the PLC was adjusted to be the same than one initially delivered by the manual control. This voltage source delivers therefore a value as a function of the percentage asked by the operator. Finally, the ozone production is now controlled independently either manually or by a remote control.

1.4.1.2. Ozone analyzer

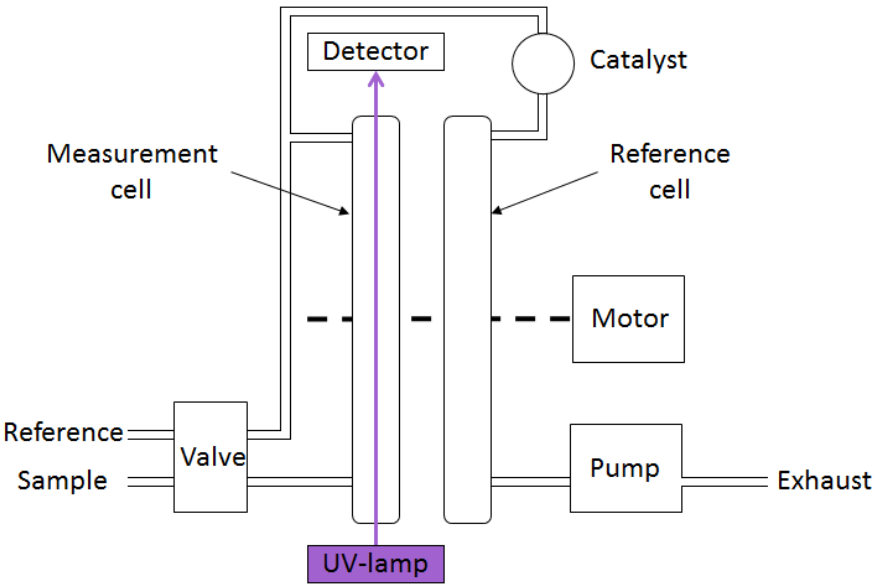

***Figure 38**. Scheme of the ozone analyzer used.*

The ozone generator previously described produces ozone based on a capacity given in percentage but there is no value of the ozone generated. An ozone analyzer is

therefore used to measuring the concentrations which seed the intake of the engine. The device used is also a commercial one coming from the society ANSEROS. It is referred as an Ozomat MP analyzer. The determination of the ozone concentration is based on the absorption of UV radiation by ozone and it has been set to measure concentrations up to 200 ppm. Concentrations are then recorded with other data in the slow acquisition file. A scheme of the measurement system is presented in Figure 38.

$$[O_3] = -\frac{1}{\varepsilon L}\log\frac{I}{I_0} \quad (1)$$

As the measure is based on the UV absorption, the device is fitted of one UV lamp. The UV light swept the measurement cell where a constant flow of the sample passes through and the light intensity is determined by a detector. Then, the ozone concentration is estimated from a Beer-Lambert law (Equation 1) where I is the light intensity measured, L is the length of the measurement cell, ε is the molar absorptivity; which depends on the wavelength, the temperature and the chemical entity; and finally I_0 is the reference light intensity. Parameters L and ε are internal settings defined by ANSEROS while I_0 must be determined before a series of measures. This last parameter is established by using a reference cell. This volume has the same characteristics than the measurement cell and may be positioned in the UV light field with the help of a motor. When the device is under its calibration step, the valve replaces the flow crossing the reference cell by ambient air instead of the sample. Finally, before to pass through the reference cell, the flow, either the sample or the ambient air, crosses a catalyst ($2\ O_3$ + catalyst → $3\ O_2$). This allows avoiding ozone concentration for determining the reference light intensity and to ensure no ozone in the exhaust. Moreover, as the sample flow passes through the measurement cell and then the reference cell, this methodology enables avoiding wrong measurements due to pollutants. Finally, as for the ozone generator, the location of this materiel on the experimental bench will be further described after.

1.4.2. Nitric oxides

Unlike ozone, nitric oxide and nitrogen dioxide are both stable chemical species. They do not need any device to generate it and may be stored inside gas bottles. For experiments, both molecules were separately available inside such materiel, diluted with nitrogen to avoid any reaction and presented concentrations of 5000 ppm. Gas is injected directly inside the main pipe of the experimental setup by using mass flow controller and after being relaxed. Finally, the amount of these oxidizing chemical species seeded at the intake of the engine is entirely controlled and quantified knowing the volume fraction on this mass flow controller and the total flow.

1.4.3. Seeding of the oxidizing chemical species

For this investigation, all the oxidizing chemical species selected were seeded in front of the intake of the engine. The configuration of these injections is presented by the scheme in Figure 4. Nitrogen oxides were injected inside the main pipe of the experimental setup and there is enough time to ensure the homogeneity with these chemical species. Ozone is injected directly inside the plenum and the homogeneity was checked using the ozone analyzer. This analyzer was positioned close to the intake of the engine to enable a sample near the intake valves of the engine (Figure 39). Samples were achieved on the two intake pipes of the engine by sweeping the ozone concentrations injected and the measurements showed the same results. The ozone seeding was therefore validated. Moreover, the position of the ozone analyzer allows determining the concentrations added during experiments. Finally, as ozone is produced from pure oxygen and as nitrogen oxides are diluted with nitrogen, flows of oxygen and nitrogen were added in the main pipe to keep an O/N ratio similar to that of the air and to ensure an air/fuel mixture with only the seeding of the oxidizing chemical species selected.

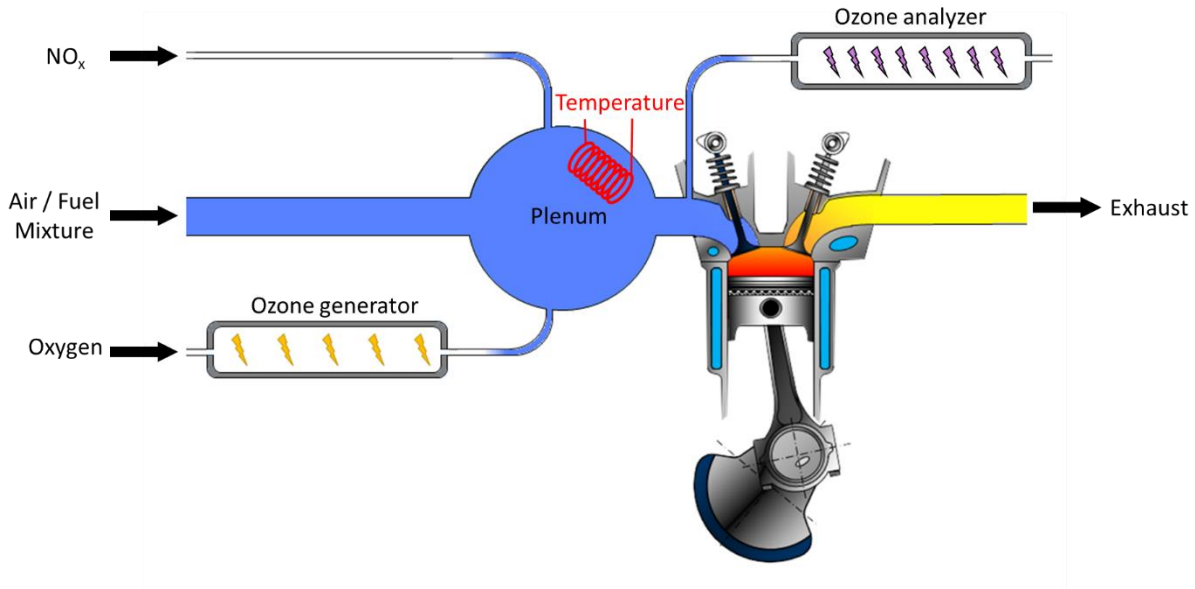

Figure 39. *Scheme of the experimental setup with the injection locations of both ozone and nitrogen oxides and the position for the sample of the ozone analyzer.*

2. Analysis of the experimental data

The previous part introduced the experimental setup as well as fuels and additional devices used for the present work. Measurements performed were recorded under two files simply called “slow acquisition file” and “quick acquisition file”. The “quick acquisition file” contains the pressure data recorded every 0.1 CAD for 100 cycles while the “slow acquisition file” contains the average values of every sensor mounted on the experimental setup. Then, these data must be post-treated and analyzed. Several approaches may be found in the literature [141]–[144] depending of several parameters such as the engine, the type of combustion or others. Based on the different post-treatments observed, the present part describes the post-treatment methodology developed and implemented for analyzing the acquired data and obtaining the engine outputs.

2.1. Loading of the engine parameters

Initially, the engine used must be configured in the post-treatment program. Features of the engine given by Table 2 are therefore input and the program calculates the other engine parameters needed for the analysis of the data recorded.

The first parameter determined from the features of the engine is the displaced volume (V_{cyl}). It is defined in Equation 2 as a function of the stroke (C) and the bore (B). In parallel, the crankshaft radius (R_v) may be calculated and correspond to the half of the stroke (Equation 3). Then, the geometric clearance volume may be determined from the displaced volume and knowing the compression ratio (CR) (Equation 4). Three last parameters have to be found out. It is the rod length (L_b), a modified compression ratio (CR_m) and an offset for the crank angle degree (θ_{offset}). Their use will be defined in the following parts.

$$V_{cyl} = C \times B^2 \frac{\pi}{4} \tag{2}$$

$$R_v = \frac{C}{2} \tag{3}$$

$$V_d = \frac{V_{cyl}}{\tau_c - 1} \tag{4}$$

2.2. Loading of the experimental data

Experimental data are recorded in two files: the quick acquisition file and the slow acquisition file. The first contains the data of the pressures acquired every 0.1 crank angle

degree while the second contains the average data of the other parameters. Details about both files are given hereafter.

2.2.1. Loading of the quick file

As describe previously in the experimental setup, the quick acquisition file contains the data records from the pressure sensors, i.e. the intake pressure, the in-cylinder pressure and the exhaust pressure. Data were acquired for 100 cycles every 0.1 crank angle degree and for each sensor. This is a good tradeoff for achieving an excellent statistical analysis and avoid too much data [143]. Intake and exhaust pressure sensors are both absolute pressure sensors while in-cylinder pressure sensor is a relative one. Therefore, the in-cylinder pressure must be reset under absolute conditions by using either the intake pressure or the exhaust pressure. In the present case, the reset is performed from the intake pressure evolution according to the Equation 5 because this pressure is more stable than the exhaust one (Figure 40).

$$P_{cyl} = P_{cyl\,gross} + \int_{CAD_{low}}^{CAD_{high}} P_{manifold} - \int_{CAD_{low}}^{CAD_{high}} P_{cyl\,gross} \qquad (5)$$

To achieve a good reset of the in-cylinder pressure, it is necessary to select a range between CAD_{low} and CAD_{high} where the intake pressure is assumed equal to the pressure inside the combustion chamber. The area chosen starts to 530 CAD and finishes to 540 CAD, whether around the bottom dead center and before the intake valve closing.

Then, the 100 cycles of the in-cylinder pressure are all filtered. The overall analysis may be led by an average of the 100 cycles but a filtering approach allows if necessary providing statistical analysis of the results determined from the pressure traces. Moreover, both approaches do not change a lot the final results. It is therefore most interesting conducting an analysis by keeping the 100 cycles. In the present post-treatment analysis, the filter used consists of a low pass “Butterworth” filter whose the cutting frequency was fixed at 3000 Hz. The frequency selected allows limiting the information loss on the in-cylinder pressure signal (less than 1%) and to well fit the in-cylinder pressure trace for the following assessment.

In parallel to the loading of the pressure evolutions, the crank angle degree (θ) must be rebuilt with the same accurate than the optical encoder allowing the data record. This device has been positioned manually on the crankshaft and starts the acquisition from the top dead center (-180 CAD). The crank angle degree is therefore defined from -180 to 540 by step of 0.1 CAD. However, it may be a lag with the position of the optical encoder, an offset is therefore added to the definition of the crank angle degree. The determination of this offset is introduced in the part 2.3.1.

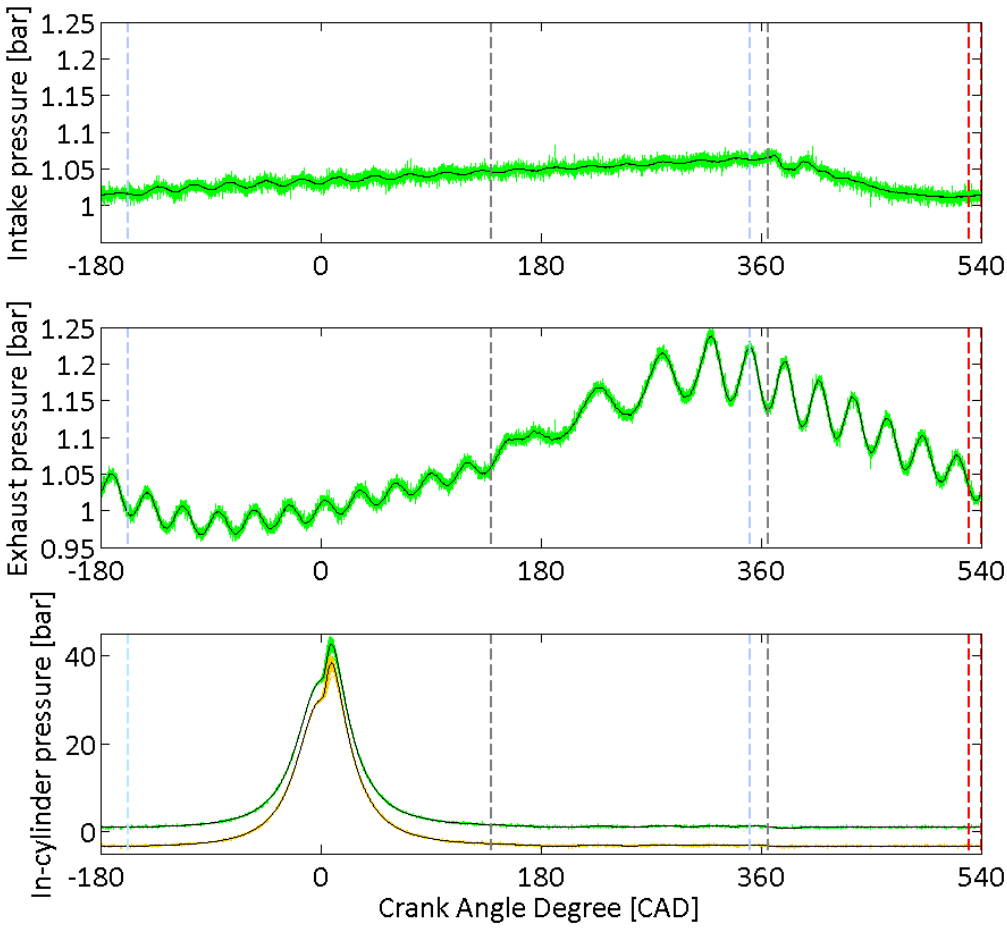

Figure 40. *Intake pressure (on the top), exhaust pressure (on the middle) and in-cylinder pressure (on the bottom) traces as a function of the crank angle degree. Black traces are the average for each pressure trace and color ones represent the 100 cycles recorded. Orange curves correspond to the gross in-cylinder pressure and the green curves to the in-cylinder pressure after its readjustment. Vertical lines correspond to the opening and closure of the intake (blue) and exhaust (grey) valves. Red lines correspond to the area defined for the readjustment.*

2.2.2. Loading of the slow file

The slow acquisition file contains the average of each sensor mounted on the experimental setup. Averages are based on forty measures for each parameter. For the thermodynamic analysis of the engine outputs, several parameters must be uploaded. First of all, the intake thermodynamic conditions, i.e. the intake pressure (P_{in}) and the intake temperature (T_{in}), are necessary for determining the in-cylinder temperature. This calculation is defined in the next part. Then, the flows of the different reactants must be loaded. From them, the fractions of each reactant (X_i) may be calculated and allow estimating the equivalence ratio (φ) according to Equation 6 as well as establishing the

combustion equation. The combustion equation enables finally evaluating the products of combustion and their respective fractions (X_j). Moreover, pollutants measurements may be uploaded when they are available and the equivalence ratio previously calculated can be compared with one obtained from a pollutants analysis. Finally, a last parameter must be load from the slow acquisition file, it is the rotation speed (ω) whose use will be described below.

$$\varphi = \frac{\left(\frac{X_{fuel}}{X_{O_2}}\right)_{real}}{\left(\frac{X_{fuel}}{X_{O_2}}\right)_{st}} \tag{6}$$

2.3. Post-treatment of the experimental data

From now on, all the parameters needed to achieve the analysis of the experimental data were uploaded and the thermodynamic analysis may be run. The aim is to obtain the evolutions of some thermodynamic parameter during the combustion process in order to assess by some of its features. As the moment, only the in-cylinder pressure trace is available and for conduct such analysis, it is of prime importance to know the instantaneous volume as well as the in-cylinder temperature. The approach for achieving these results is described hereafter.

The instantaneous volume of the combustion chamber must be rebuilt from the geometry of the engine. As the volume changes with the piston motion, the calculation of the volume must be expressed as a function of the piston position (X) which depends on the crank angle (θ) and is defined in Equation 7. R_v and L_b are respectively the crankshaft radius and the rod length provided with the definition of the engine (part 2.1). Finally, the instantaneous volume (V) is expressed by the slider-crank equation (Equation 8) [141].

$$X = R_v \times \cos\left(\theta \times \frac{\pi}{180}\right) + \sqrt{L_b^2 - \left(R_v \times \sin\left(\theta \times \frac{\pi}{180}\right)\right)^2} \tag{7}$$

$$V = \frac{\pi \times B^2 \times (L_b + R_v - X)}{4} + V_d \tag{8}$$

Then, the in-cylinder temperature may be calculated from the in-cylinder pressure and the instantaneous volume of the combustion chamber. At the start of the admission of the homogeneous air/fuel mixture, it is possible to consider a perfect gas. Therefore, the ideal gas law may be applied to the combustion chamber (Equation 9). The unknown parameter in this equation is nR. It is supposed a constant and it has to be determined. This equation is also valid at the beginning of the compression stroke or more precisely at the

intake valve closing. nR can therefore be expressed as in Equation 10 and by replacing the term in Equation 9, the in-cylinder temperature may be finally rewritten as in Equation 11. For the analysis, the initial volume V_{IVC} is taken at the crank angle degree of the intake valve closing (Table 2) according to Equations 7 and 8. For the initial thermodynamic conditions, i.e. P_{IVC} and T_{IVC}, these parameters are respectively taken as the pressure and the temperature at the intake, i.e. P_{in} and T_{in}, uploaded from the slow file acquisition.

$$P_{cyl}V = nRT_{cyl} \tag{9}$$

$$nR = \frac{P_{IVC}V_{IVC}}{T_{IVC}} \tag{10}$$

$$T_{cyl} = \frac{P_{cyl}VT_{IVC}}{P_{IVC}V_{IVC}} \tag{11}$$

For the rest of the post-treatment, the analysis is separated into two parts: a motoring analysis and a combustion analysis. Both of them are separately described below.

2.3.1. Motoring analysis

The motoring analysis used in the present post-treatment program was developed to adjust some parameters and therefore, improve the final results. Parameters, which need to be corrected, are the position of the top dead center, or rather the crank angle (θ), and the compression ratio (CR). The first alters the phasing of the volume with the in-cylinder pressure trace while the second alters the calculation of the volume. A wrong phasing of the crank angle is due to the optical encoder. This element mounted on the experimental setup has been positioned to start the record from the bottom dead center but its position can be shifted due to its manual positioning. An offset (θ_{offset}) on the crank angle definition has been therefore integrated to correct the phasing. A wrong compression ratio is due to a wrong determination of the clearance volume which is used to calculate the instantaneous volume. For the present engine, this volume has been estimated by determining the volume of the piston bowl but the real clearance volume must consider the small volume between the piston and the cylinder head. Therefore, a new compression ratio (CR_m) has been integrated for the analysis and replaced the geometric compression ratio defined with the engine characteristics.

The determination of both parameters is based on a thermodynamic analysis of an experimental motoring. The methodology was proposed by *Tazerout et al.* [145], [146] and consists of examining the temperature-entropy (T-S) diagram of the data record. Ideally, this diagram must look like a symmetrical evolution at the maximum in-cylinder temperature on the compression and expansion strokes. If not, it is interpreted with no thermodynamic

sense and this means that either the top dead center position or the compression ratio or both parameters are not well calibrated. Calibrations needed are identified as a function of the shape of the T-S diagram (Figure 41 and Figure 42).

The in-cylinder temperature is already calculated and it is necessary to estimate the entropy (S). This thermodynamic characteristic is determined according to Equations 12 and 13 from θ_{min} to θ_{max}. Values of these two crank angles are respectively taken as -30 and + 30 to cover the parts of the compression and expansion strokes where the in-cylinder temperature is the highest. For calculating the entropy, the heat capacity at constant pressure (C_p) and the molar mass (M) of the mixture are needed. C_p is defined as the sum of the product of the molar fraction of each component of the mixture by their respective heat capacity (C_{p_i}) (Equation 14) and where each C_{p_i} is obtained from the in-cylinder temperature and the JANAF coefficients ($a_{i,k}$) found in the table of *Burcat* [147] (Equation 15). Finally, the molar mass (M) is defined like a constant because no reactions are considered during a motoring and is expressed as the sum of the products of the molar fractions of each chemical species by their respective molar mass (Equation 16).

$$\frac{dS}{d\theta} = \frac{C_p}{M} \times \frac{1}{T_{cyl}} \times \frac{dT_{cyl}}{d\theta} - \frac{R}{M} \times \frac{1}{P_{cyl}} \times \frac{dP_{cyl}}{d\theta} \tag{12}$$

$$S(\theta) = \int_{\theta_{min}}^{\theta_{max}} \frac{dS}{d\theta} \tag{13}$$

$$C_p(\theta) = \sum_i X_i \times C_{p_i}(\theta) \tag{14}$$

$$C_{p_i}(\theta) = R \times \sum_{k=1}^{5} a_{i,k} \times T_{cyl}(\theta)^{k-1} \tag{15}$$

$$M = \sum_i X_i \times M_i \tag{16}$$

Once the entropy is calculated, the T-S diagram may be plotted and the adjustment on the crank angle (θ_{offset}) as well as the new compression ratio (CR_m) have to be determined. According to the shape observed, it is necessary to modify progressively one by one either the compression ratio or the offset on the crank angle up to obtain the symmetry explained above. Final results normally observed for a motoring analysis are represented by

Figure 41 and Figure 42. Both graphics show the effect of a wrong compression ratio and the effect of a wrong top dead center position, respectively. From this, θ_{offset} and τ_{cm} are integrated in the program, θ_{offset} is added to the crank angle previously defined while τ_{cm} replaced the geometric one (τ_c) entered with the engine parameters, and will be used for combustion analyses. Ideally, one motoring cycle has to be record and analyze before each series of experiments in order to improve the final results.

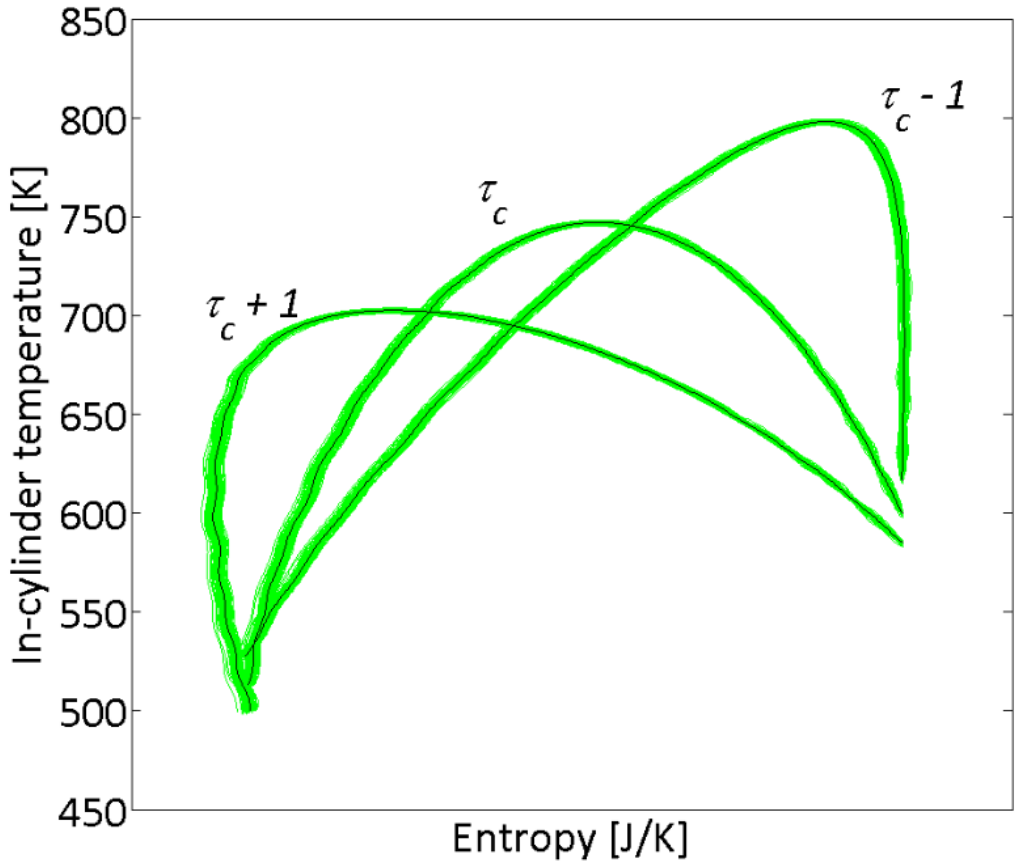

Figure 41. *Temperature-Entropy diagram under various compression ratios. A wrong compression ratio shifts the shape of the diagram either towards the left or towards the right. This results in no thermodynamic senses while a good compression ratio allows obtaining the symmetry desired.*

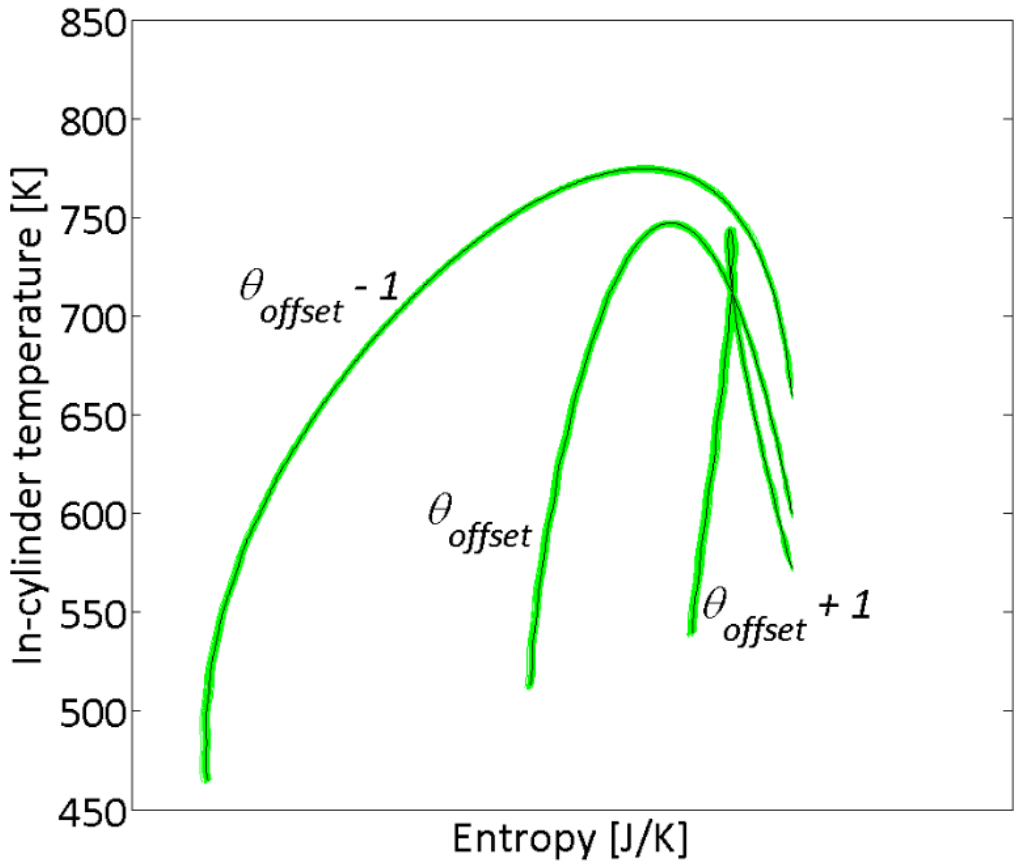

Figure 42. *Temperature-Entropy diagram under various offset on the crank angle. A wrong offset creates an expansion of the diagram or a loop. Both results have no thermodynamic sense. A good offset results in the symmetry desired.*

2.3.2. Combustion analysis

The second part of the post-treatment analysis consists of an analysis of the experiments with combustion. This part is used to provide the engine results due to the combustion. The analysis is focused on previous parameters, mainly the in-cylinder pressure and the in-cylinder temperature evolutions, as well as on the energy released by the combustion. The energy released is expressed by the gross heat release rate from *Heywood* (Equation 17) [141].

$$\frac{dQ_{gross}}{d\theta} = \frac{dQ_{net}}{d\theta} + \frac{dQ_{ht}}{d\theta} + \frac{dQ_{crevice}}{d\theta} \qquad (17)$$

The gross heat release rate is expressed as the sum of three different terms which are the net heat release rate, the heat transfer heat release rate and the heat release due to the crevice effects, respectively. Most of the time, the last is sufficiently small compared to

the two other and therefore, it is assumed negligible. The net heat release rate represents the energy release due to the combustion. According to the 1st law of thermodynamics and considering an ideal gas, it may be expressed as a function of the in-cylinder pressure and the instantaneous volume (Equation 18).

$$\frac{dQ_{net}}{d\theta} = \frac{\gamma}{\gamma - 1} P_{cyl} \frac{dV}{d\theta} + \frac{1}{\gamma - 1} V \frac{dP_{cyl}}{d\theta} \tag{18}$$

$$\gamma = \frac{C_p}{C_v} \tag{19}$$

$$C_p - C_v = R \tag{20}$$

The only unknown in this expression is γ which corresponds to the ratio of the heat capacity at constant pressure (C_p) with the heat capacity at constant volume (C_v) (Equation 19). Moreover, for an ideal gas, both heat capacities are linked by the Mayer's relation (Equation 20) and finally, γ can be expressed as a function of the heat capacity at constant pressure. As defined previously, the heat capacity at constant pressure corresponds to the sum of the products of the molar fraction of each species by their respective heat capacity at constant pressure and this last parameter is calculated from the in-cylinder temperature and the JANAF coefficients found in the table of *Burcat* [147]. However, instead of a motoring cycle, the reactant species, mainly the fuel and the air, are consumed during the combustion to form combustion products. Therefore, the mixture inside the combustion chamber evolves gradually and this must be considering for γ calculation. Consequently, two γ were introduced in the post-treatment. The first represents the fresh gases (γ_r) while the second corresponds to the burnt gases (γ_p). They are calculated from Equations 21 to 23 and from 24 to 26, respectively.

$$\gamma_r(\theta) = \frac{C_{p_r}(\theta)}{C_{p_r}(\theta) - R} \tag{21}$$

$$C_{p_r}(\theta) = \sum_i X_i \times C_{p_{r\,i}}(\theta) \tag{22}$$

$$C_{p_{r\,i}}(\theta) = R \times \sum_{k=1}^{5} a_{i,k} \times T_{cyl}(\theta)^{k-1} \tag{23}$$

$$\gamma_p(\theta) = \frac{C_{p_p}(\theta)}{C_{p_p}(\theta) - R} \tag{24}$$

$$C_{p_p}(\theta) = \sum_j X_j \times C_{p_{p\,j}}(\theta) \tag{25}$$

$$C_{p_{p\,j}}(\theta) = R \times \sum_{k=1}^{5} a_{j,k} \times T_{cyl}(\theta)^{k-1} \tag{26}$$

Finally, to obtain the evolution of γ during the combustion, it is necessary to know the fuel consumption which needs a first calculation of the heat release rate. Consequently, for the moment, γ is defined equal to γ_r before the top dead center and equal to γ_p after and will be recalculated as soon as the fuel consumption is estimated. Another definition of this parameter will be given later.

The second part of the gross heat release rate corresponds to the heat transfers to the walls. It is therefore expressed as an energy transfers by convection (Equation 27) where h is the convective heat transfer coefficient, S_{exch} the instantaneous exchange surface, T_{cyl} the in-cylinder temperature previously calculated, T_{wall} the wall temperature and finally ω the rotation speed. The rotation speed is taken from the data uploaded in the slow acquisition file and the wall temperature is assumed to be the same than the temperature of the coolant temperature, whether ~ 95 °C.

$$\frac{dQ_{wall}}{d\theta} = h(\theta) \times S_{exch} \times \left(T_{cyl} - T_{wall}\right) \times \frac{60}{\omega \times 360} \tag{27}$$

The instantaneous exchange surface is considered as the sum of the exchange surfaces formed by the piston S_{piston}, the cylinder head $S_{cylinder\ head}$ and the chamber S_{liner} (Equation 28). Both first surfaces are constant and expressed as a function of the bore (Equation 29). The last one changes with the motion of the piston and is expressed here from the instantaneous volume (Equation 30).

$$S_{exch} = S_{piston} + S_{cylinder\ head} + S_{liner} \tag{28}$$

$$S_{piston} = S_{cylinder\ head} = \frac{\pi \times B^2}{4} \tag{29}$$

$$S_{liner} = \frac{4 \times V}{B} \tag{30}$$

Finally, the last parameter to determine to obtain the heat transfers to the wall is the convective heat transfer coefficient. It is based on correlations found in the literature which mainly depend on the kind of engine and the combustion mode. The relationship selected is that of Hohenberg whose previous results showed that it is well adapted for the cases of HCCI combustion (*Soyhan et al.*) [148]. Its expression is given by Equation 31 which depends on the instantaneous volume, the in-cylinder pressure, the in-cylinder temperature and the mean piston speed (V_{mp}). This last parameter is function of the stroke and the rotation speed (Equation 32). Moreover, this relationship of Hohenberg needs two constants $C1$ and $C2$. Both values are specific to the engine used and have to be determined[1]. Their estimations are based on the fact that, under a motoring case, the gross heat release rate must be zero or rather, the heat transferred must compensate the net heat release rate. Constants are therefore adjusted from their default values up to the trace of the gross heat release rate fits zero (blue trace in Figure 43).

$$h(\theta) = C1 \times V^{-0.06} \times P_{cyl}^{0.8} \times T_{cyl}^{-0.4} \times \left(V_{mp} + C2\right)^{0.8} \tag{31}$$

$$V_{mp} = 2 \times C \times \frac{\omega}{60} \tag{32}$$

From now, the gross heat release rate for experiments carried out with combustion may be calculated. According to previous descriptions, the heat capacity ratio was assumed to be equal to the heat capacity ratio of fresh gases before the top dead center and the heat capacity ratio of the burnt gases after. However, the fuel is not totally consumed at the top dead center but progressively. A new definition of γ must be integrated from the fuel consumption to obtain the final gross heat release rate. A first gross heat release rate is therefore estimated by considering the previous hypothesis. Then, Equation 33 determines the gross energy released and a new heat capacity ratio may be calculated from Equation 34. Finally, the calculations of the net and gross heat release rate are reiterated up to the CA10, CA50 and CA90 (i.e. the crank angle where 10, 50 and 90 % of the total energy released has been consumed) changed from less than 0.1, whether the accuracy of the optical encoder and the final gross energy released is obtained (Figure 43).

$$Q_{gross}(\theta) = \int_{\theta_{min}}^{\theta_{max}} \frac{dQ_{gross}}{d\theta} \tag{33}$$

[1] Usually, both constants of the relationship are by default $C1 = 130$ and $C2 = 1.4$.

$$\gamma = \left(1 - \frac{Q_{gross}(\theta)}{Q_{gross_{max}}}\right) \times \gamma_r(\theta) + \frac{Q_{gross}(\theta)}{Q_{gross_{max}}} \times \gamma_p(\theta) \tag{34}$$

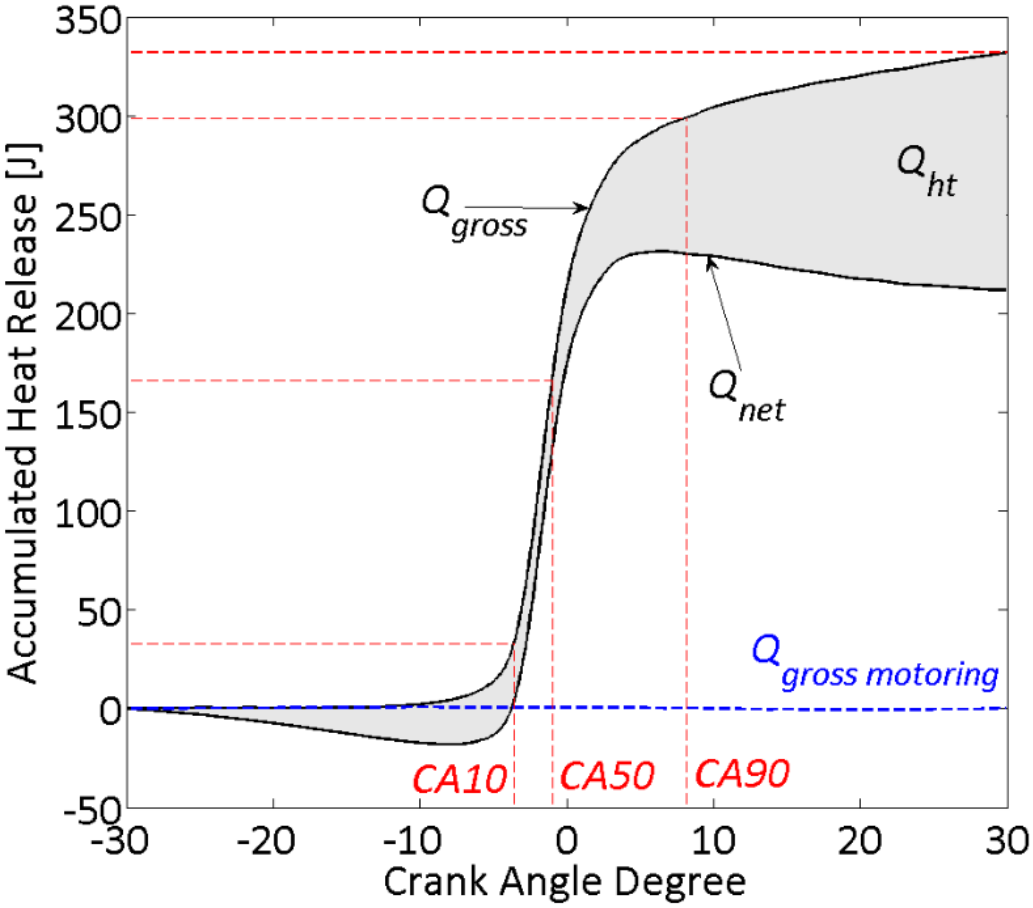

Figure 43. *Example of an accumulated heat release as a function of the crank angle degree. Each curve corresponds to an average of the heat release. The blue one represents the gross heat release in the case of a motoring. For a combustion case, the gross heat release has been broken down into the net heat release and the heat tranfers to the wall (grey area). CA10, CA50 and CA90 are respectively defined as the crank angle where 10, 50 and 90 % of the total energy released has been consummed.*

2.4. Engine results

Once the post-treatment achieved, all the curves obtained are globally analyzed and from them, engine results may be determined. Their respective determination is described hereafter.

2.4.1. In-cylinder pressure analysis

The in-cylinder pressure is the first parameter obtained as it directly comes from the sensor set up on the engine. An example of the evolution of this thermodynamic

parameter may be observed in Figure 44. The engine results are determined by analyzing the average of the 100 cycles recorded and are the maximum pressure coupled with its location in the cycle. Moreover, the in-cylinder pressure trace may be derived in order to estimate the highest pressure gradient. This last parameter will be used to discuss about the combustion noise. A too higher value of the pressure gradient results in heavy noise and leads to knock which can damage the engine.

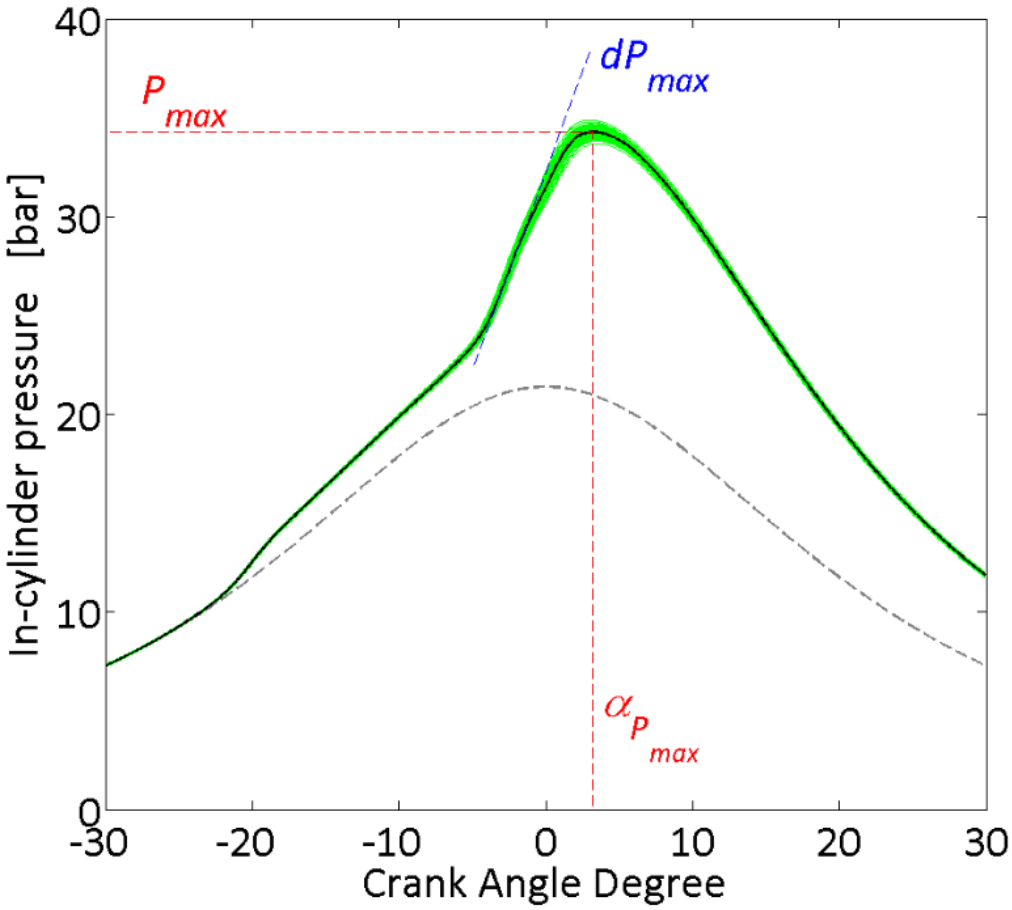

Figure 44. *Example of an in-cylinder pressure trace as a function of the crank angle. Dotted line corresponds the motoring trace of the pressure in average inside the combustion chamber. Green area represents the 100 cycles recorded while the black line is the average of the same 100 cycles. From the average trace, the maximum in-cylinder pressure (P_{max}) is determined as well as its phasing ($\alpha_{P_{max}}$) and finally the maximum pressure gradient (dP_{max}) determines from the derivative of the in-cylinder pressure trace.*

Finally, the in-cylinder pressure trace may be used with the instantaneous volume to determine the net indicated mean effective pressure (IMEP) which allows to estimate the work output of the engine. This parameter is established from one cycle by using the Equation 35. Therefore, there is 100 values of IMEP and it is possible to provide statistical analysis of this parameter. Its standard deviation may be estimated and by making the ratio

with the average of IMEP, it is possible to obtain the covariance of the IMEP (Equation 36). This statistical parameter is particularly useful to provide information on the combustion stability, cycle-to-cycle fluctuations or again misfires.

$$IMEP = \frac{\int_{\theta} P_{cyl}(\theta)\frac{dV}{d\theta}}{V_{cyl}} \tag{35}$$

$$COV(IMEP) = \frac{\sigma_{IMEP}}{\overline{IMEP}} \times 100 \tag{36}$$

2.4.2. *In-cylinder temperature analysis*

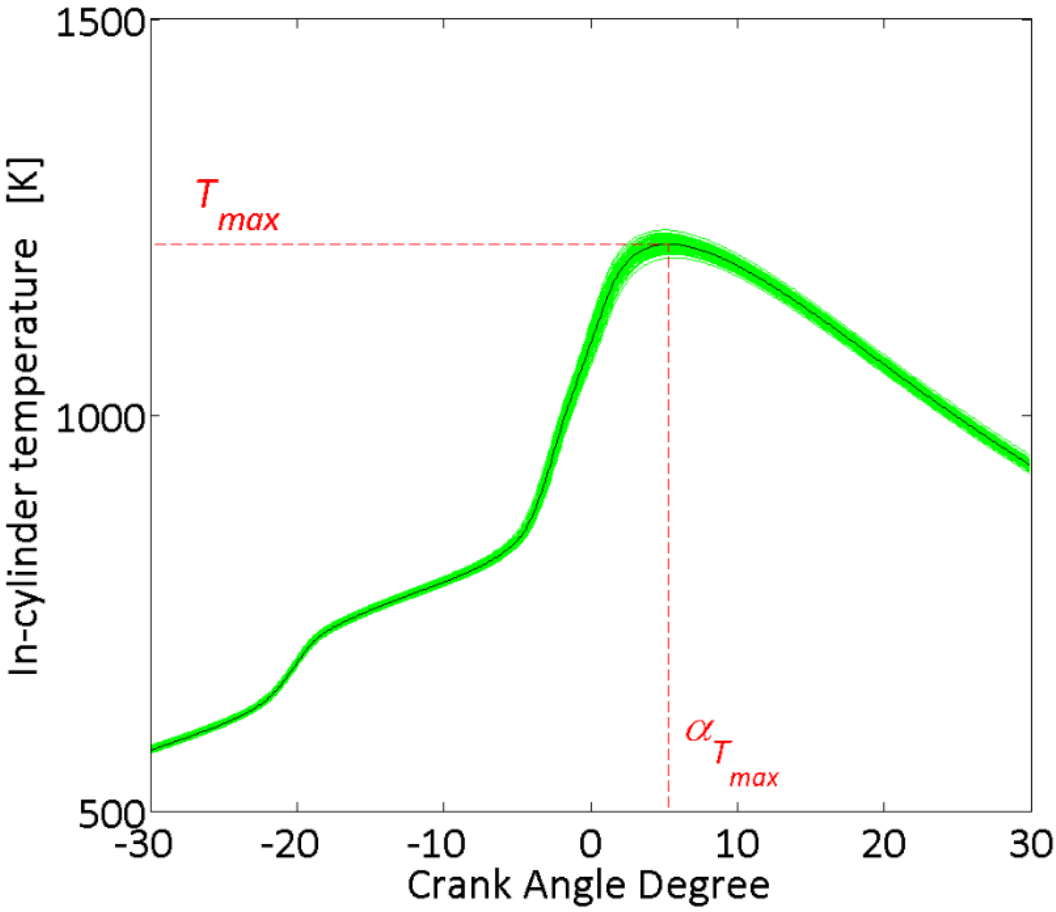

Figure 45. *Example of an in-cylinder temperature trace as a function of the crank angle. Green area corresponds to the 100 cycles recorded while the black line corresponds to the average of the same 100 cycles. The maximum temperature (T_{max}) inside the combustion is determined from this average as well as its phasing ($\alpha_{T_{max}}$).*

The in-cylinder temperature evolution is the second main parameter analyses here. Figure 45 shows an example of in-cylinder temperature history. From the average

temperature of the 100 cycles recorded, the maximum temperature as well as its phasing can be determined. Such trends provide information on the bulk temperature but it is not totally representative of the temperatures in the overall combustion chamber. It may have some hot spots where the temperature is higher than the maximum temperature determined and cold spots as near the walls. However, such outputs could be correlated with heat transfer and pollutants measurements when they are available.

2.4.3. Heat release rate analysis

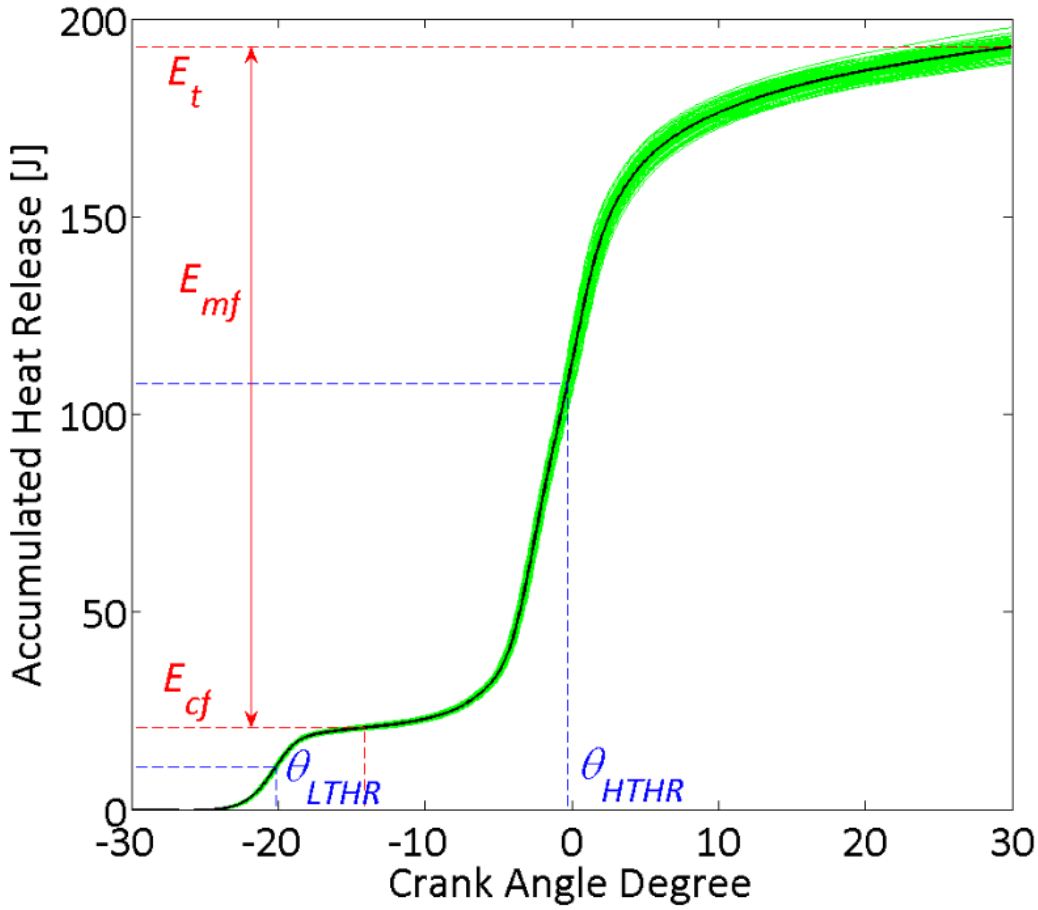

Figure 46. *Example of an accumulated heat release as a function of the crank angle for a case with a cool flame. Green area corresponds to the 100 cycles recorded and the black line to the average of the same 100 cycles. The energy released by the cool flame is determined as the energy released from the start of the combustion up to the lower energy released between the two peaks of combustion observed on the heat release rate trace. The energy released by the main flame therefore corresponds to the difference between the total energy released and the energy released by the cool flame. Finally, phasing of each flame respectively corresponds to the crank angle where the half of the energy of each flame has been released.*

The heat release rates are the final results analyzed. Quality of the combustion may be observed either from the gross heat release rate previously estimated or from the accumulated heat release. Examples of the accumulated heat release are shown in Figure 43 and Figure **46**. Globally, these curves are used to determine the combustion phasing mainly represented by CA10, CA50 and CA90. The CA10 corresponds to the beginning of the combustion while the CA90 corresponds to the end. The combustion duration is therefore determined as the difference of both parameters (Equation 37). Finally, the CA50 represents the crank angle where 50% of the combustion occurred. All these parameters are obtained here from the accumulated heat release and are defined as the crank angle where 10, 50 and 90 % of the total energy released has been consumed, respectively (Figure 43).

$$combustion\ duration = CA90 - \mathrm{CA10} \tag{37}$$

The previous analysis is applied to all the results obtained but in the case of HCCI combustion, the heat release rate may involve cool flame as observed in Figure **46**. For such curves, further analysis is conducted and consists of determining the phasing of each flame as well as their respective energy released. The energy produced by the cool flame corresponds to the accumulated heat release from the occurring of the combustion up to the minimal energy released between the peaks of the flame on the heat release rate trace. The energy provided by the main flame is therefore the difference between the total energy released and the cool flame energy. Finally, both flame phasing are determined as the crank angle where 50 % of the energy of each flame has been released.

2.5. Discussion about the post treatment approach

It is possible to bring some improvements on the post-treatment used. For instance, before to make any calculations, the in-cylinder pressure trace is filtered with the same kind of filter on the overall cycle. It could be better to apply another kind of filter which enables to strongly reduce the noise without information losses such as a filter per part on the cycle.

Another improvement possible is about the methodology to calculate the in-cylinder temperature. For the moment, it involves the intake measurements as initial conditions. However, the initial temperature to consider is the internal temperature just before the closure of the intake valve [149], [150]. The in-cylinder temperature within the combustion chamber at the bottom dead center may be higher or lower than the intake temperature due to heat transfer and due to the presence of burned gases. On the other hand, this methodology may also be replaced by considering the mass admitted (fresh gases) and the mass of residuals (burnt gases) inside the combustion chamber instead of using the initial conditions [151]–[153]. This is therefore another way which could be easily take place as the flows of each components of the charge, the intake conditions and the exhaust conditions are known

Then, the gross heat release rate is decomposed in two parts: the net one and the heat transfer one. The first is mostly dependent on the previous parameters calculated while the second involves the use of a correlation. Instead of the Hohenberg correlation, another ones may be replaced it such as Woschni correlation mainly used in the literature [141]. Moreover, the heat transfer also needs to know the wall temperature, which is here taken as the coolant temperature, but it can be higher and different depending on the surface considered.

Finally, the post-treatment approach here employed needs to tune some parameters through motoring experimental data and to select intake conditions before to run analysis of the combustion data. It may be very interesting to perform a parametric investigation by involving an error on tuned parameters to observe the errors on final results. Moreover, such investigation may also lead to incertitude analysis which is not really used on engine experiments due to the lot of calculations carried out. This is among the perspectives of developing a robust post-treatment analysis for combustion experiments performed on internal combustion engines

3. Computations

The best computations for simulating the HCCI combustion will be CFD computations with a variable volume divided into lots of areas for considering all the complexity of a combustion chamber (temperature stratification, aerodynamics, heat exchange). Such a computation costs time for running calculations and configuring the model in agreement with experimental results. The main goal here is to interpret the results obtained in a sound scientific way. A simpler model has therefore been selected for giving kinetics analyses in parallel to the experiments performed by using the Chemkin II package. This program allows solving complex kinetics problems and it is used here to further analyze the effect of the chemical oxidizing species investigated on the oxidations of the fuel selected. In particular, the program selected to lead these analyses is the Senkin program [154]. The present part will bring details about this program as well as the model chosen to provide the kinetics analyses in agreement with the experiments conducted. Finally, the fuel oxidation scheme will be given as well as the sub-mechanisms used to compute the effect of the chemical oxidizing species.

3.1. The Senkin program

Senkin is a Fortran program which enables to compute in zero-dimension complex kinetics problems of homogeneous reacting gas mixture in closed systems. It is particularly adapted to solve problems which needs detailed kinetics schemes. Moreover, it also allows performing sensitivity analysis of the kinetics scheme. Among the wide kinds of kinetics applications existing, the Senkin program may compute six different problems that are function of the conditions chosen:

- Adiabatic system with constant pressure
- Adiabatic system with constant volume
- Adiabatic system with the volume a specified function of time
- Pressure and temperature constant
- Volume and temperature constant
- Pressure and temperature are function of the time

For computing the HCCI combustion taking place in the engine, the best model should be the third where the volume is variable. However, such a model does not consider all the complexity of an engine problem as the aerodynamic or the heat transfer or even the temperature stratification. Moreover, the objective with the present computations is to provide kinetics analysis of the effect of the oxidizing chemical species. In order to isolate the analysis to only kinetics and as, in theory, the HCCI combustion occurs very quickly in the overall combustion chamber, the second model was selected. Further details of the Senkin program are given hereafter.

3.1.1. System of equations

The present part describes the equations considered to solve the problem of an adiabatic system with constant volume. The model is a closed homogeneous reactor which means that there is no leakages and the mass is assumed to be constant. This can be summed up as:

$$m = \sum_{1}^{K} m_k \quad \text{and} \quad \frac{dm}{dt} = 0 \tag{38}$$

where m_k is the mass of the kth species and K the total of species in the scheme selected.

Observing individually the species, the variation of their mass as a function of the time is:

$$\frac{dm_k}{dt} = V \times \dot{\omega}_k \times M_k \tag{39}$$

where V is the volume, $\dot{\omega}_k$ the molar production of the kth species and M_k the molecular weight of the kth species.

However, as the mass is assumed to be constant, Equation 39 may be rewritten in terms of the mass fractions:

$$\frac{dY_k}{dt} = v \times \dot{\omega}_k \times M_k \tag{40}$$

where $Y_k = \frac{m_k}{m}$ is the mass fraction of the kth species and $v = \frac{V}{m}$ is the specific volume.

To solve the problem, the energy equation is necessary because the temperature is an unknown parameter. From the first law of thermodynamics, it is assumed that:

$$\frac{de}{dt} = \frac{dQ}{dt} - p\frac{dv}{dt} \tag{41}$$

where e is the internal energy per mass, Q the quantity of heat and p is the pressure.

The model selected is assumed to be adiabatic and with a constant volume. Therefore, the terms of the quantity of heat and the variation of volume are respectively zero and Equation 41 becomes:

$$\frac{de}{dt} = 0 \tag{42}$$

Considering an ideal mixture of gases, the internal energy may be expressed as the sum of the internal energy of each species multiplied by their respective mass fraction (Equation 43).

$$e = \sum_{1}^{K} e_k \times Y_k \tag{43}$$

This expression can be derivate and the energy equation becomes:

$$\sum_{1}^{K} Y_k \frac{de_k}{dt} + \sum_{1}^{K} e_k \frac{dY_k}{dt} = 0 \tag{44}$$

Assuming a calorific perfect mixture of gases, the derivative of the internal energy per species may be write:

$$\frac{de_k}{dt} = C_{v_k} \frac{dT}{dt} \tag{45}$$

where C_{v_k} is the specific heat capacity at constant volume of the kth species and T is the temperature.

Moreover, the mean specific heat capacity at constant volume is defined as follow:

$$C_v = \sum_{1}^{K} C_{v_k} \times Y_k \tag{46}$$

Finally, by injecting Equations 40, 45 and 46 in Equation 44 and by rearranging, the final energy equation becomes:

$$C_v \frac{dT}{dt} + v \sum_{1}^{K} e_k \times \dot{\omega}_k \times M_k \tag{47}$$

To solve the problem, the last parameter needed is the chemical production rate. It is expressed as the sum of the rate of progress variables for all reactions (I) involving the kth species:

$$\dot{\omega}_k = \sum_{1}^{I} \nu_{k,i} \times q_i \tag{48}$$

where

$$\nu_{k,i} = \nu''_{k,i} - \nu'_{k,i} \tag{49}$$

and

$$q_i = k_{f_i} \times \prod_{1}^{K} [X_k]^{\nu'_{k,i}} - k_{r_i} \times \prod_{1}^{K} [X_k]^{\nu''_{k,i}} \tag{50}$$

with $\nu'_{k,i}$ and $\nu''_{k,i}$ respectively the reactants and products stoichiometric coefficients of the ith reaction, X_k the molar fraction determined from the mass fraction ($X_k = {}^{\rho \times Y_k}/_{W_k}$) and k_{f_i} and k_{r_i} respectively the forward and the reverse rate constants of the ith reactions. These rate constants are calculated using the following Arrhenius relationship:

$$k = A \times T^{\beta} \times \exp\left(\frac{-E}{RT}\right) \tag{51}$$

where A is the pre-exponential coefficient, β the temperature exponent and E the activation energy. All these parameters are tabulated in kinetics scheme with their respective reaction.

3.1.2. Structure of the program

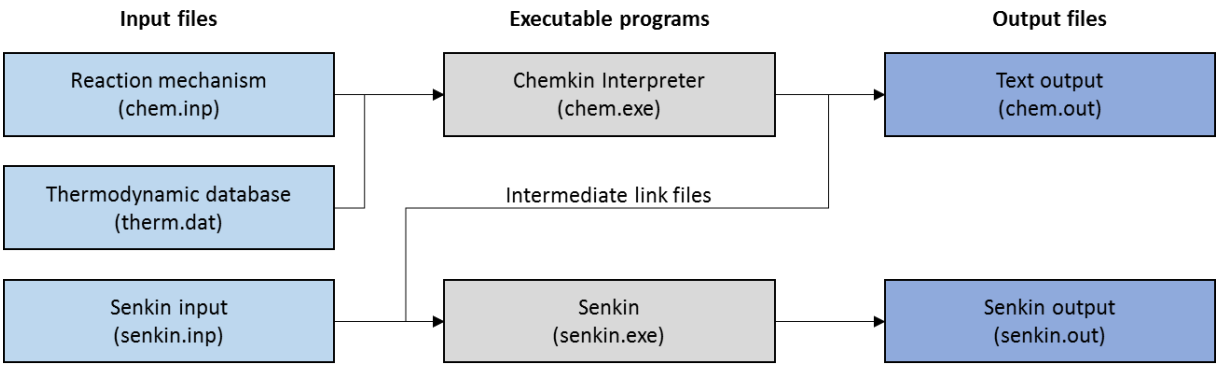

Figure 47. *Structure of the Senkin program.*

The present part describes the structure of the Senkin program from the input files to the output results. This is summarized in Figure 47. First of all, the input files must be made of the reaction mechanism and the thermodynamic database. The first file contains all the species declared as well as all the reactions considered with their respective coefficients for the Arrhenius relationship. The second contains the thermodynamic coefficients used to calculate the thermodynamic data. Both files are interpreted by a Chemkin code which reads, reorganizes and memorizes these input data. It finally provides an output file containing the kinetics scheme rearranged which will be used for the analysis of the final results. In parallel, it also provides intermediate files necessary for the Senkin program. The Senkin program may then solve the problem knowing the initial conditions stored into the

Senkin input file. All the results are computed as a function of the time, more precisely, the thermodynamic parameters such as the pressure and the temperature as well as the concentrations of the species. They are finally tabulated in an output file whose the reading enables the kinetics analysis.

3.2. Kinetics schemes used

To complete with the experimental results, different kinetics schemes were run with the Senkin program according to the fuels selected and the oxidizing chemical species studied. The present part put forward the features of the schemes retained to compute the oxidation of the fuel, the sub-mechanisms to analyze the effect of the oxidizing species and finally the methodology applied.

3.2.1. Fuel oxidation mechanisms

In the present work, three different families of fuels have been selected and represent a dozen of fuels. To perform kinetics analysis in agreement with the experiments, three different detailed schemes, one for each fuel family, were selected. Table 4 provides the main features of these schemes.

Table 4. *Features of the kinetics schemes selected.*

Fuels	Species	Reactions	Reference
n-heptane/isooctane	1033	4238	*Curran et al.* [30]
H2/CO/C1-C4	111	784	*Wang et al.* [155]
MeOH/EtOH/BuOH	431	2336	*Sarathy et al.* [156]

Analyses on the oxidation of the PRFs, i.e. n-heptane, isooctane and blends of both fuels, are carried out from the detailed mechanism proposed by Curran et al. [30] for the oxidation of isooctane. This kinetics scheme is based on the oxidation of n-heptane [29] and therefore allows to compute the oxidation of all the PRFs. Moreover, it was validated on a wide type of applications as well as a wide range of conditions.

For the oxidation of the gaseous fuels, i.e. hydrogen, methane and propane, the detailed chemical kinetics mechanism proposed by Wang et al. [155] has been used. The scheme is based on several mechanisms and was updated. It finally allows considering a wide variety of combustion applications supplying by hydrogen, carbon monoxide and hydrocarbons from C1 to C4.

Finally, investigation on the oxidation of alcohol fuels is an ongoing topic of intense research [157]. Recently, numerous studies on these fuels were conducted, in particular for fuels composed of four carbons or less. The kinetics mechanism retained for the present investigation is the scheme proposed by *Sarathy et al.* on the four isomers of the butanol

[156]. It was built on previous schemes with alcohol fuels containing less than four carbons in their structure and validated on several types of combustion devices. It can therefore be used to examine the oxidation of fuels such as methanol, ethanol and n-butanol as in the present work.

3.2.2. Oxidizing chemical species sub-mechanisms

According to the objective of studying the impact of oxidizing chemical species on the oxidation of the fuels previously enumerated, sub-mechanisms involving these species were selected to supplement the three schemes described above. There are two sub-mechanisms, one for investigate the effect of ozone and one for studying the effect of nitric oxides, and they are further described hereafter.

3.2.2.1. Ozone sub-mechanism

The ozone sub-mechanism selected in the present work is that proposed by *Halter et al.* [132]. It consists of 17 reactions that involve ozone consumption and production reactions mainly coming from the atmospheric studies. In the publication, the scheme has been only validated on laminar burning velocity and provides similar results than those already reported in the literature. Note that reactions often considered in the literature are similar and were applied on various combustion systems. Moreover, this sub-mechanism has been recently used in the case of the combustion of n-heptane by *Foucher et al.* [9] to explain the influence of ozone.

3.2.2.2. Nitric oxides sub-mechanism

The other sub-mechanism used in the present work is a nitric oxides sub-mechanism. It was proposed by *Dagaut and Dayma* [158]. The results obtained in a jet stirred reactor were satisfactory but the mechanism needed further validations. Finally, it was recently combined by *Contino et al.* [123] with the kinetics scheme of PRFs previously described to investigate the effect of nitric oxide in the case of engine modeling. Final results showed that modeling results well fitted with experimental results and helped to explain the influence of nitric oxide on isooctane oxidation. This sub-mechanism may also be used under various combustion systems.

3.3. Methodology

The present part describes the methodology used to observe the impact of the oxidizing chemical species on the oxidation of the fuels selected. From the previous kinetics mechanisms and sub-mechanisms presented, new schemes were built. They consist of combining one or both sub-mechanisms with the fuel mechanisms. For the present work, four new schemes were prepared and are summed up in Table 5.

Table 5. *Features of the new kinetics schemes built for the present investigation.*

Names	Species	Reactions	Reference
PRFs O3	1037	4255	[30], [132]
PRFs O3 NO NO2	1062	4506	[30], [132], [158]
Gas O3	115	784	[132], [155]
Alcohols O3	435	2353	[132], [156]

Before to run simulations with these new mechanisms, it is necessary to validate them. It was chosen here to carry out two kinds of computations. The first by using a mechanism without any sub-mechanism implemented and the second with the sub-mechanism. For both computations, all the initial conditions are kept constant. The validation will be based on ignition delays and by analyzing the main reaction pathways. These validations will be showed in the results of the present investigation.

Finally, once the mechanism validated, computations with oxidizing chemical species will be launched according to the model retained in the Senkin program. Initial conditions will be set in agreement with experiments and results will provide supplementary analyses with the comments on experimental results. The analyses of these simulations will be mainly focused on ignition delays and on reaction pathways of the fuel oxidation.

4. Conclusion

The present chapter 2 introduced the experimental setup and the numerical tools used all along this work. The first part of the second chapter was about the engine bench which was widely described. In particular, the properties of the engine, the methodology and the devices used to prepare a mixture at the intake of the engine the most homogeneous as possible have been introduced. Then, the sensors mounted and the control of each part of the experimental setup were described up to the record of the experimental data. The fuels considered for this investigation were also introduced in this part as well as the oxidizing chemical species selected. Finally, the methodologies to produce these oxidizing chemical species, when it is necessary, control it and seed it were described.

The second part considers the analysis of the experimental data recorded. The post-treatment applied and developed all along this work was fully described step by step from the gross data to the final results. The approach is based on a common approach widely observed in the literature which consists of analyzing the in-cylinder pressure recorded. From the in-cylinder pressure traces, evolutions of the thermodynamic parameters inside the combustion chamber may be calculated according to the relationships given to finally provide engine outputs.

Finally, the last part of the chapter 2 exposed the computation approach implemented into this work. Simulations were based on the use of the Senkin program which is linked with Chemkin II software. In this program, the model selected was the constant volume. The structure of the program and the calculations solved in this particular case were described. Finally, the schemes and sub-mechanisms retained to further analyze experimental results were introduced as well as the procedure to build the new ones. The new schemes need validation which will be showed in the next chapters and will be finally used to describe the impact of the different oxidizing chemical species selected.

Chapitre 3 / Chapter 3

Résultats sur la combustion des « Primary Reference Fuels »

Results on the combustion of Primary Reference Fuels

Résumé

Ce chapitre regroupe l'ensemble des résultats obtenus dans le cadre de la combustion des « Primary Reference Fuels » (PRFs). Il s'organise en partant d'un intérêt scientifique jusqu'à l'aboutissement d'une réelle application et a été établi en fonction des différents travaux publiés. Le plan de ce chapitre est donc le suivant (Figure 48) :

- Article I : J-B. Masurier, F. Foucher, G. Dayma, P. Dagaut, *Homogeneous Charge Compression Ignition Combustion of Primary Reference Fuels Influenced by Ozone Addition*, Energy and Fuels, 2013.
- Article II : J-B. Masurier, F. Foucher, G. Dayma, C. Mounaïm-Rousselle, P. Dagaut, *Towards HCCI Control by Ozone Seeding,* SAE Paper 2013-24-0049, 2013.
- Article III : J-B. Masurier, F. Foucher, G. Dayma, P. Dagaut, *Investigation of iso-octane combustion in a homogeneous charge compression ignition engine seeded by ozone, nitric oxide and nitrogen dioxide*, Proceedings of the Combustion Institute, 2014.
- Article IV : J-B. Masurier, F. Foucher, G. Dayma, C. Mounaïm-Rousselle, P. Dagaut, *Application of an Ozone Generator to Control the Homogeneous Charge Compression Ignition Combustion Process*, SAE Technical Paper 2015-24-2456, 2015.

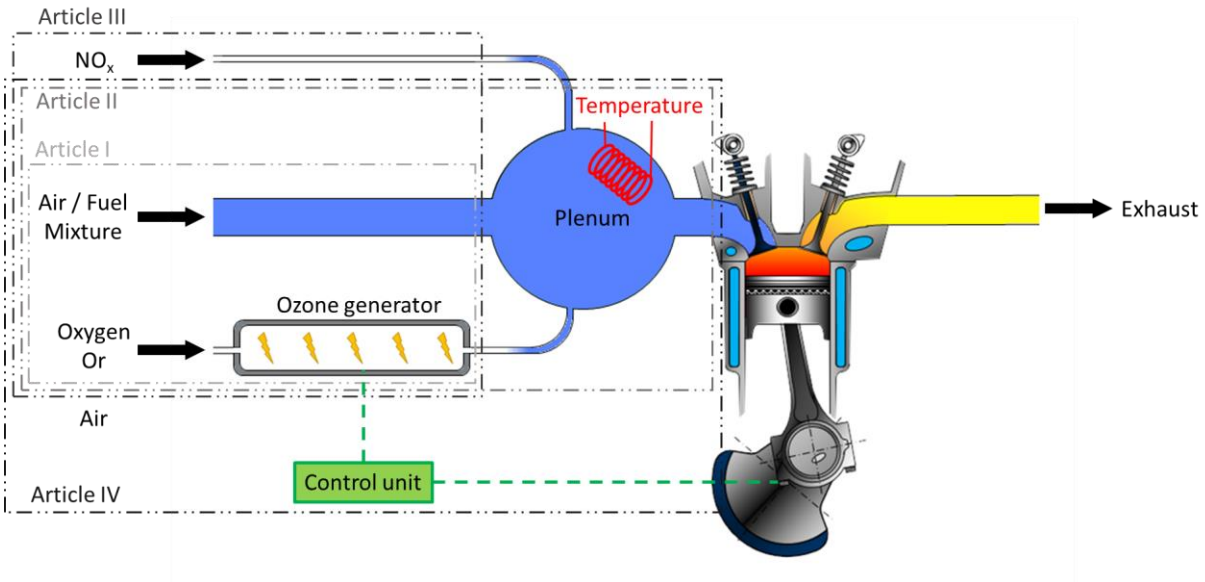

Figure 48. *Schéma résumant l'organisation de chapitre en s'appuyant sur les résultats publiés.*

A partir de précédents résultats provenant de la littérature et décrits dans le chapitre bibliographique de ce manuscrit, la première étape de ces travaux de recherche a été d'étudier l'impact de l'ozone sur les carburants de référence aussi dénommés « Primary

Reference Fuels ». Au moyen d'une étude préliminaire où les domaines de combustion idéals du n-heptane, de l'isooctane et de mélanges préalablement choisis de ces deux carburants ont été déterminés, l'impact de l'ozone a été démontré (Article I). Les résultats regroupent des essais expérimentaux sur banc moteur et ont été couplés à des simulations de cinétique chimique. Il a ainsi été mis en évidence, grâce à son effet promoteur, que l'ozone améliore très rapidement la combustion moyennant de faibles concentrations tout en permettant d'avancer le phasage de la combustion. Cet effet intervient très tôt dans le processus de combustion puisque les résultats ont montré que l'ozone altère le début de la combustion (CA05) ainsi que le phasage de la flamme froide. De plus, les études de cinétique chimique conduites sur les délais d'autoinflammation et les chemins de réactions ont permis de mettre en exergue que l'ozone est en réalité un promoteur indirect de la combustion HCCI. L'effet promoteur provient de l'atome d'oxygène issu de la décomposition de l'ozone qui oxyde directement le carburant bien plus rapidement que par les voies habituelles et donne finalement lieu à une avance de l'autoinflammation. En fonction des carburants retenus, il a été observé que l'ozone procure un effet similaire sur le phasage de la combustion du n-heptane et des mélanges PRFs sélectionnés. Cela est principalement dû au n-heptane présent en différentes proportions selon les mélanges et qui réagit facilement avec l'ozone. Dans le cas de l'isooctane, celui-ci a montré qu'il était plus sensible à cette espèce chimique oxydante. L'impact significatif est principalement dû à la température d'admission réglée qui était bien supérieure à celle des essais avec les autres carburants et est responsable d'une accélération de la décomposition de l'ozone.

A la suite de ces premiers résultats, des essais supplémentaires ont été menés sur la combustion de l'isooctane (Article II). La température d'admission nécessaire à son autoinflammation étant relativement élevée comparée à celles rencontrées dans un moteur à combustion interne conventionnel (démarrage à froid et lors du fonctionnement normal du moteur), des essais ont été effectués en diminuant la température d'admission et en utilisant l'effet promoteur de l'ozone pour maintenir la combustion. Les résultats ont démontré que l'ozone permet clairement de maintenir la combustion de l'isooctane sous des conditions où celle-ci ne se produit pas habituellement. De plus, la température d'admission diminuant, l'ozone se décompose moins rapidement et le phasage de la combustion est moins sensible. En conséquence, l'ozone est une espèce chimique qui permet de contrôler le déroulement de la combustion HCCI sous différentes conditions moteur et un réel cas d'application pourrait être développé. Finalement, ces résultats ont aussi révélé l'existence d'une flamme froide lors de la combustion HCCI de l'isooctane et ainsi justifient que cette molécule oxydante réagit dès le début de l'oxydation du carburant.

Considérant que l'ozone est un atout majeur pour le contrôle de la combustion HCCI et étant donné que les dispositifs permettant sa production tendent à devenir de plus en plus petits, l'hypothèse d'une intégration véhicule a donc été posée. Idéalement, un tel

dispositif devrait fonctionner avec de l'air mais il en résulte qu'en plus d'une production d'ozone, des espèces azotées tel que les oxydes d'azote (NO_x) peuvent être formées et les précédentes études ont montré qu'il existe une forte interaction entre l'ozone et les NO_x. De plus, ces dernières peuvent aussi être présentes dans les résiduels de combustion au sein de la chambre de combustion (IGR) ou encore dans les produits de combustion réinjectés (EGR). Il a donc été indispensable d'évaluer l'impact des NO_x et de l'ozone sur la combustion HCCI. Une étude comparative entre l'ozone, le monoxyde d'azote et le dioxyde d'azote a donc été effectuée avec l'isooctane (Article III). Les résultats ont montré que ces trois espèces chimiques oxydantes accélèrent la combustion en raison de leur effet promoteur. De plus, l'ozone est responsable de la meilleure amélioration de la combustion tandis que le dioxyde d'azote fournit une avance bien moins importante. L'impact de chaque espèce a été démontré au moyen de la cinétique chimique. L'ozone permet d'agir directement sur l'oxydation du carburant tandis que les oxydes d'azote nécessitent la formation des premiers radicaux résultant de l'oxydation normale de l'isooctane avant de promouvoir la combustion. Finalement, le monoxyde d'azote est l'oxyde d'azote le plus présent dans les gaz d'échappement et peut se retrouver dans des proportions minoritaires dans les résiduels de la chambre de combustion ou avec l'utilisation de l'EGR. Par ailleurs, il pourrait aussi être formé préalablement dans les générateurs d'ozone dans certains cas de fonctionnement. L'interaction de cette espèce chimique avec l'ozone a donc été étudiée lorsque ces deux molécules oxydantes sont simultanément injectées avec le mélange air/carburant. Il a ainsi été mis en évidence que ces deux espèces réagissent ensemble pour former du dioxyde d'azote. Bien que ce type d'ensemencement permette de continuer à avancer le phasage de la combustion, leur impact reste toutefois modéré comparé aux résultats obtenus lorsqu'elles sont injectées séparément. De plus, il a été démontré expérimentalement et à l'aide une analyse de cinétique chimique que la réaction entre l'ozone et le monoxyde d'azote intervient bien avant que ces deux espèces soient introduites dans la chambre de combustion du moteur.

Enfin, l'ensemble de ces résultats a été complété par la mise en place d'un contrôle dynamique de la combustion HCCI au moyen d'un générateur d'ozone afin de démontrer le potentiel applicatif de ces dispositifs (Article IV). Des essais préalables avec le générateur ont montré qu'en réalité le générateur produisait uniquement de l'ozone et ce dans des proportions suffisantes pour permettre le contrôle. Cependant, le générateur d'ozone utilisé lors cette étude est adaptée à une production d'ozone seul tandis que des cas non favorables pourrait éventuellement être rencontré lors de réelles applications automobiles. Un complément d'essais par rapport à l'ensemble des résultats déjà établis a démontré que l'ajout d'ozone à l'admission du moteur permet de contrôler les paramètres du moteur ainsi que les polluants. Enfin, deux types de contrôle ont été appliqués : un contrôle basé sur une cartographie préalablement dressée et un contrôle en boucle fermée. Le premier a montré un temps de réponse relativement court mais avec un manque de précision tandis que le

second a montré l'inverse. Finalement, les voies d'amélioration pour tendre vers une application réelle ont été identifiées.

Abstract

The chapter 3 contains all the results obtained on the combustion of Primary Reference Fuels (PRFs). It is organized from a scientific interest up to an application case and it is based on the different results published. Therefore, the chapter follows the order of the articles below (Figure 49):

- Article I: J-B. Masurier, F. Foucher, G. Dayma, P. Dagaut, *Homogeneous Charge Compression Ignition Combustion of Primary Reference Fuels Influenced by Ozone Addition*, Energy and Fuels, 2013.
- Article II: J-B. Masurier, F. Foucher, G. Dayma, C. Mounaïm-Rousselle, P. Dagaut, *Towards HCCI Control by Ozone Seeding,* SAE Paper 2013-24-0049, 2013.
- Article III: J-B. Masurier, F. Foucher, G. Dayma, P. Dagaut, *Investigation of iso-octane combustion in a homogeneous charge compression ignition engine seeded by ozone, nitric oxide and nitrogen dioxide*, Proceedings of the Combustion Institute, 2014.
- Article IV: J-B. Masurier, F. Foucher, G. Dayma, C. Mounaïm-Rousselle, P. Dagaut, *Application of an Ozone Generator to Control the Homogeneous Charge Compression Ignition Combustion Process*, SAE Technical Paper 2015-24-2456, 2015.

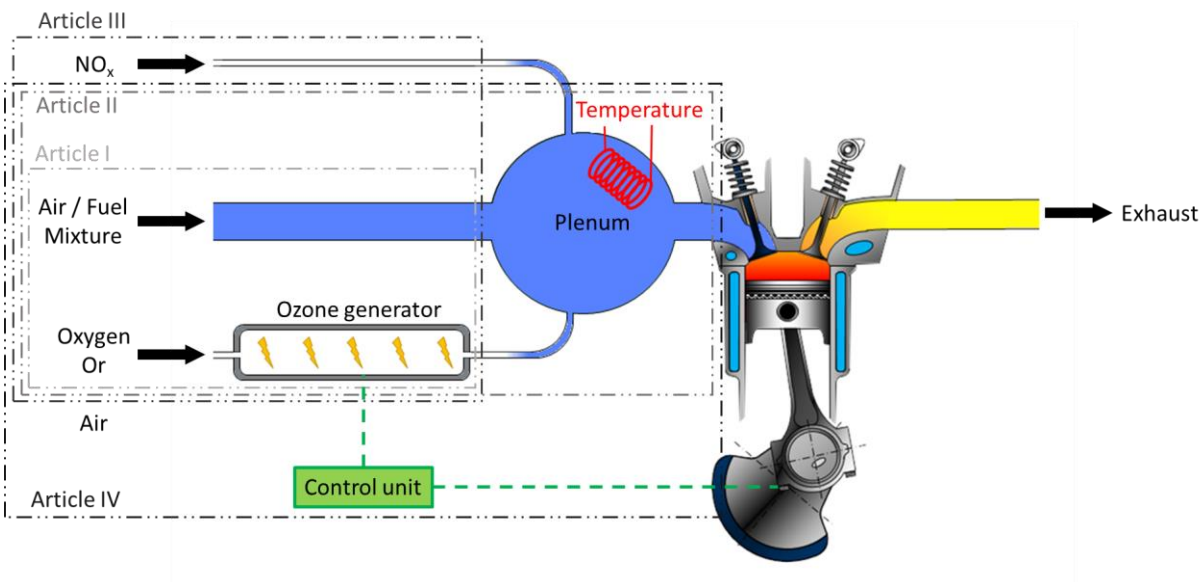

Figure 49. *Graphical abstract on the plan of the chapter 3 from the published results.*

From previous results found in the literature and described in the first chapter of this memory, the first step of these researches was to study the impact of ozone on PRFs. Based on a prior investigation where the optimum combustion areas for n-heptane,

isooctane and blends of both fuels selected were determined, the impact of ozone has been showed (Article 1). Outputs gather experiments on engine bench coupled to computations of kinetics. It was highlighted, due to its promoting effect, that ozone improves very rapidly the combustion with low concentrations while the combustion phasing advances. This effect occurs very early in the combustion process since the results showed that ozone alters the beginning of the combustion as well as the cool flame phasing. Moreover, kinetics studies conducted on ignition delays and reaction pathways allow highlighting that ozone is in reality an indirect promoter of the HCCI combustion. The promoting effect is provided by the O-atom coming from the ozone break down which oxidizes directly the fuel faster than by the normal pathways and finally leads to an advance of the autoignition. According to the fuels selected, it was observed that ozone leads to a similar effect on the phasing of n-heptane and PRFs selected. The similar impact is mainly due to the presence in different ratios of n-heptane into the blends selected which reacts easily with ozone. In the case of pure isooctane, results showed that this fuel was more sensitive to ozone. The significant impact is mainly due to the intake temperature set which was upper than that for experiments with the other fuels and speed up the ozone break down.

Following these first results, further experiments were performed on isooctane combustion (Article II). The intake temperature needed to achieve its autoignition is very high compared to those encountered into conventional internal combustion engine (cold start and during the normal operations of the engine), experiments were therefore carried out by reducing the intake temperature and by using the promoting effect of ozone to maintain the combustion. Outputs showed that ozone allows clearly achieving combustion of isooctane under intake conditions where the combustion does not occur usually. Moreover, as the intake temperature decreases, ozone breaks down less rapidly and the phasing of the combustion is less sensitive. Consequently, ozone is an oxidizing chemical species which allows controlling the HCCI combustion process under a wide range of engine conditions. Moreover, a real application could be developed. Finally, these results also showed the occurrence of the isooctane cool flame and justified that ozone modifies the beginning of the oxidation of isooctane.

Considering that ozone is major asset for controlling the HCCI combustion and as ozone generators become increasingly small, the assumption of implementing such a device into a vehicle has been made. Ideally, such a device should work with air but additionally to the production of ozone, NO_x could be generated and previous investigations highlighted that there is a strong interaction between ozone and NO_x. Moreover, NO_x can also be found into residuals of the engine or again into the exhaust products with the use of EGR. It is therefore essential to assess the impact of NOx and ozone on the HCCI combustion. Consequently, a comparison between ozone, nitric oxide and nitrogen dioxide has been performed for isooctane as fuel (Article III). Results showed that the three oxidizing chemical species speed up the combustion due to their respective promoting effect. Moreover, ozone

is responsible of the best improvement of the combustion while nitrogen dioxide provides a less significant advance. Additionally, the impact of each species has been displayed with kinetics. Ozone allows oxidizing directly the fuel while the NO_x need the presence of the first radicals coming from the normal oxidation of isooctane before promoting the combustion. Finally, nitric oxide (NO) is the NO_x the most encountered into the combustion products and can be found into minor concentrations into hot residuals or with the use of EGR. On the other hand, it could be produce preliminarily into ozone generators in case of malfunctions. The interaction between NO and ozone was therefore studied when both oxidizing molecules are injected simultaneously with the air/fuel mixture. It was highlighted that both species react together resulting in the production of nitrogen dioxide ($NO + O3 \rightarrow NO2 + O2$). Even if this seeding allows to continue to advance the combustion phasing, their impact remains quite moderated compare to the results observed when they seed separately the intake of the engine. Moreover, it was showed through experiments and computations that the reaction between ozone and nitric oxide takes place in front of the entrance of both species into the combustion chamber of the engine.

Finally, all these results were completed by the implementation of a dynamic control of the HCCI combustion with the use of an ozone generator in order to show the potential of these devices (Article IV). Prior experiments with the generator showed that this device generates only ozone and with suitable concentrations to achieve the control. However, the ozone generator used for this study is adapted to only an ozone production while it could not be the case with real automotive applications. Referring to all the results obtained, extra experiments were performed and showed that ozone added in the intake of the engine enables to control all the engine parameters as well as pollutants. Two kinds of control were then applied: 1) based on “look up table” built in advance and 2) a closed-loop control. The first displayed a response time very short but with a lack of accuracy while the second showed the inverse. Finally, the ways of improvement for achieving a real application were identified.

1. Introduction on Primary Reference Fuels (Article I)

Primary Reference Fuels (PRFs) were first investigated. This fuel family brings together n-heptane and isooctane as well as blends of both fuels. PRFs are widely used as representative fuels of conventional fuels such as gasoline or diesel and were employed into numerous studies because PRFs are easy to apply for researches [34], [37], [46]. A set of six PRFs was selected to start these investigations. It includes pure n-heptane (PRF0) and pure isooctane (PRF100) and four surrogates from the mixture of both fuels, more precisely PRF20, PRF40, PRF60 and PRF80 where the number corresponds to the volume fraction of isooctane and the complement to 100 corresponds to the volume fraction of n-heptane. Moreover, according to the definition of PRFs, this number also represents RON and MON indexes and therefore the octane number (ON) of the fuel. More properties of these fuels are available in the table of the chapter 2.

2. Combustion of the Primary Reference Fuels

First experiments start with combustion of PRFs without seeding of any oxidizing chemical species. The aim was to establish the conditions needed for the engine to achieve the autoignition of each PRFs selected and determine their respective "optimal" combustion area. This area for HCCI combustion is limited by two phenomena: misfires and knocking. It is therefore defined here as the region where there is combustion and where the CA50, i.e. the crank angle for which 50% of the total energy has been released, is located between 1 and 5 CAD (Crank Angle Degree).

Experiments to determine these "optimal" combustion area were performed, for each fuel, by varying the intake pressure under different intake temperatures. The other parameters, i.e. the rotation speed and the equivalence ratio, were maintained constant at 1500 rpm and 0.3, respectively. The CA50 was determined for each experiment and only the data points with a CA50 ranging from 1 to 5 CAD were kept to plot the ideal combustion

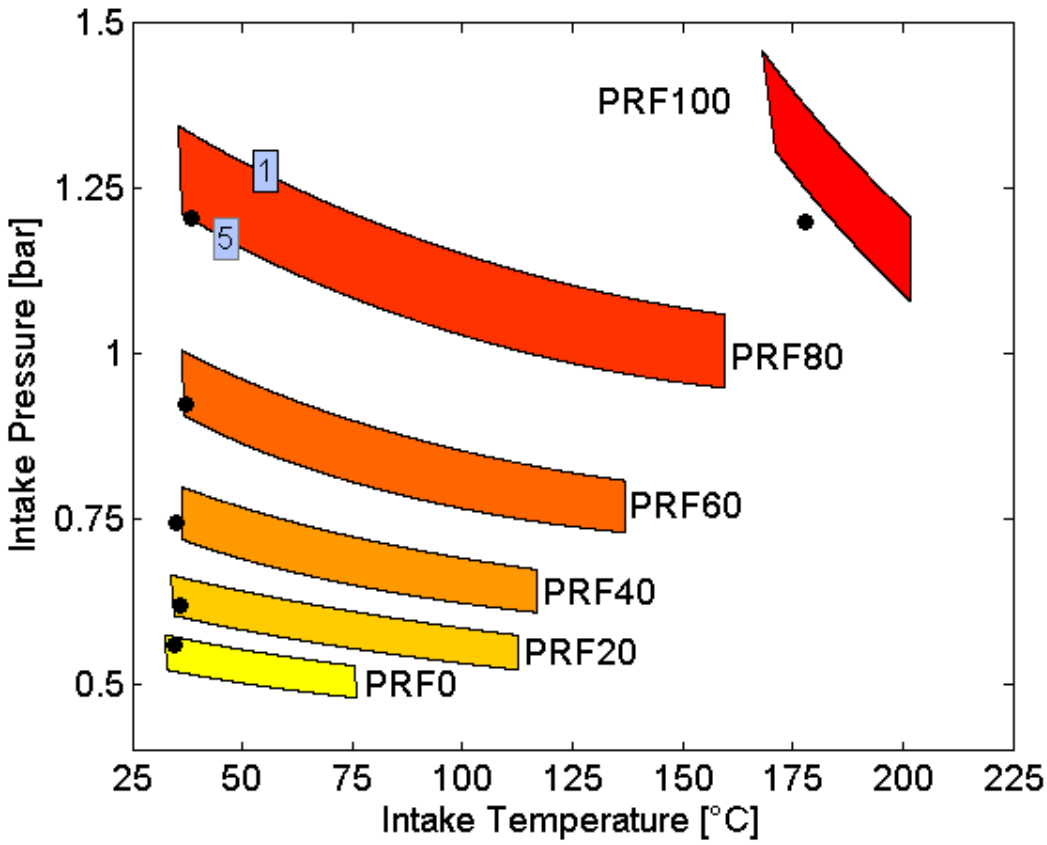

Figure 50. *Optimal combustion areas for each PRFs selected as a function of the intake pressure and the intake temperature of the engine for an equivalence ratio of 0.3 and a rotation speed of 1500 rpm. 1 and 5 correspond to the iso-CA50 limits. Black points correspond to the conditions selected to examine the effect of ozone.*

region of each fuel. The final results obtained for each PRFs selected are presented into the intake pressure – intake temperature diagram in Figure 50. For each fuel, the upper limit corresponds to an iso-CA50 of 1 CAD, then, there is risk of knocking beyond this limit, while the lower limit represents an iso-CA50 of 5 CAD and below, there is risk of misfires.

Results show that n-heptane (PRF0) burns with the lowest intake conditions on the engine while isooctane (PRF100) is the most difficult to autoignite. For intermediate PRFs, their combustion correlates with their respective ON. Therefore, lower is the ON, easily the autoignition occurs and needs low intake pressure and temperature. Reversely, higher is the ON, difficult the autoignition is and high thermodynamic intake conditions are necessary. Moreover, it may be observed that each blend of isooctane and n-heptane burn at ambient temperature but the intake pressure must be increasingly high depending on the ON. This comes from the presence of n-heptane into the surrogates and was already observed in previous researches [37], [46].

3. Experimental results on the effect of ozone

As ozone is the main species produced from dielectric barrier discharge generator, it was the first species studied. From the previous results on the combustion of PRFs without seeding of any oxidizing chemical species, experiments were defined to examine the effect of ozone. Starting points were fixed at the lowest intake temperature and intake pressure, therefore under the most difficult conditions for autoignite. These initial conditions are summarized into Table 6 and may visualized as black point in Figure 50. Other conditions, i.e. engine speed and equivalence ratio, were respectively kept at 1500 rpm and 0.3 as previously without ozone seeding.

Table 6. *Intake conditions of pressure and temperature selected to investigate the effect of ozone on the combustion of PRFs.*

Fuel	Intake pressure [bar]	Intake temperature [°C]
PRF0	0.52	33
PRF20	0.62	34
PRF40	0.74	34
PRF60	0.92	37
PRF80	1.20	38
PRF100	1.20	180

Experiments were performed for each PRFs under these conditions by only varying the ozone concentrations seeding at the intake. In general, concentrations range from 0 to 50 ppm of ozone for all PRFs except for pure isooctane. For isooctane as fuel, injection of ozone did not exceed 10 ppm. The results obtained are presented hereafter.

3.1. In-cylinder pressure and heat release rates trends

In-cylinder pressure and heat release rate traces were first analyzed. Results are shown in Figure 51 for PRF0 and PRF100 with different ozone concentrations seeded in the intake. Black curves correspond to the average of the 100 cycles recorded and colored areas represent the lower and upper limits over the same 100 cycles.

Generally, it may be observed that ozone seeding leads to an increase of both in-cylinder pressure and heat release rate meaning that the HCCI combustion is improved. Such a conclusion may also be made with the indicated mean effective pressure (IMEP) which increases with the ozone seeding. Moreover, the combustion process is advanced with the increase of the ozone concentration. Maximum pressure and maximum heat release rate locations move towards the top dead center. For PRF0, in the absence of ozone, the in-cylinder pressure shows a slight maximum due to the low thermodynamic intake conditions which make combustion difficult. With small amounts of ozone, the maximum pressure strongly increases and finally, further additions of this oxidizing chemical species continue to

increase the maximum pressure but the impact is less pronounced. Regarding heat release rate trends for PRF0, it may be observed that combustion occurs in two-stages. Both flames advance with the increase of ozone. Similarly to the in-cylinder pressure trace, the maximum heat release rate is very low without ozone, quickly increases with the first ozone seeding and continues with further additions but with a weaker growth. For PRF100, the in-cylinder pressure is strongly improved with very low ozone concentrations (less than 10 ppm) and lead to a similar maximum pressure rise than PRF0 with approximately 50 ppm. Similar effects may be concluded for its heat release rate traces except that compared to PRF0, results show only one combustion stage. Finally, for the other PRFs not presented here, the results of in-cylinder pressure and heat release rate traces show similar evolutions than those observed for PRF0.

Regarding variations of the 100 cycles for both trends either for PRF0 or PRF100 (colored areas), it may be observed that increasing the ozone concentration leads to a better stabilization of the cycle-to-cycle combustion and was confirmed according to the covariance of IMEP. Results on the covariance are lower than 2% for all fuels. From results presented in Figure 51, it may concluded that the bulk temperature inside the combustion chamber is higher, meaning that fuel is consumed earlier and faster, avoiding misfires and therefore the occurrence of a better stabilization. Finally, all these results are in agreement with previous results found into the literature [9], [11]–[13].

3.2. Combustion phasing

The main objective is to investigate the effect of ozone on the HCCI combustion process. According to engine outputs, the best parameters to observe are flame phasing, CA05 and CA50. Flame phasing are defined as the crank angle at which 50% of the total energy of each flame has been released while CA05 and CA50 corresponds respectively to the crank angles where 5% and 50% of the total energy has been released. In the case of PRF100, CA50 is equivalent to the main flame phasing as no cool flame is detected. The results for these parameters are presented for each fuel in Figure 52 and Figure 53 respectively for the shift of flame phasing and CA50 in reference to their respective initial value without ozone. Results on CA05 are available in Article I.

1.1.1 Cool and main flame phasing

The results on flame phasing clearly show that ozone seeding lead to earlier fuel combustion. Generally, for all of the PRFs selected except PRF100, the main flame phasing is more impacted by the ozone than the cool flame phasing as observed in Figure 52.

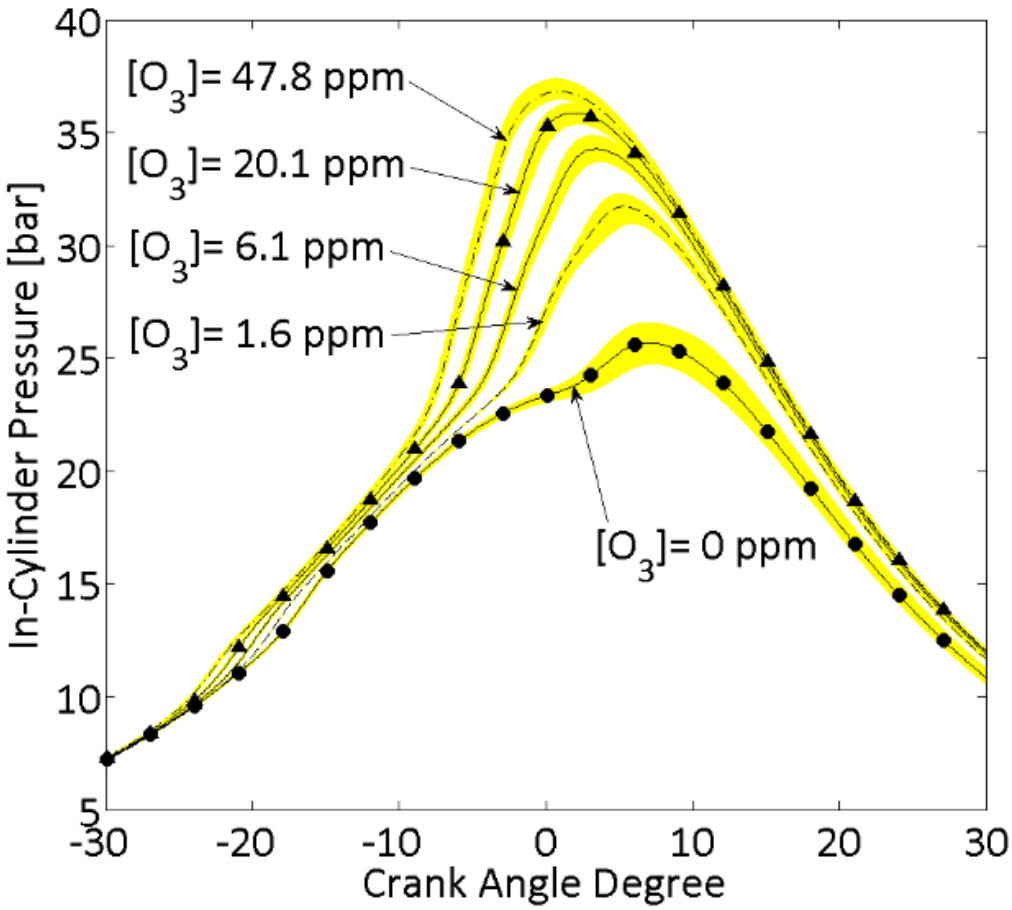

Figure 51. A. *In-cylinder pressure evolutions as a function of the ozone concentration injected in the intake of the engine for n-heptane/PRF0 as fuel.*

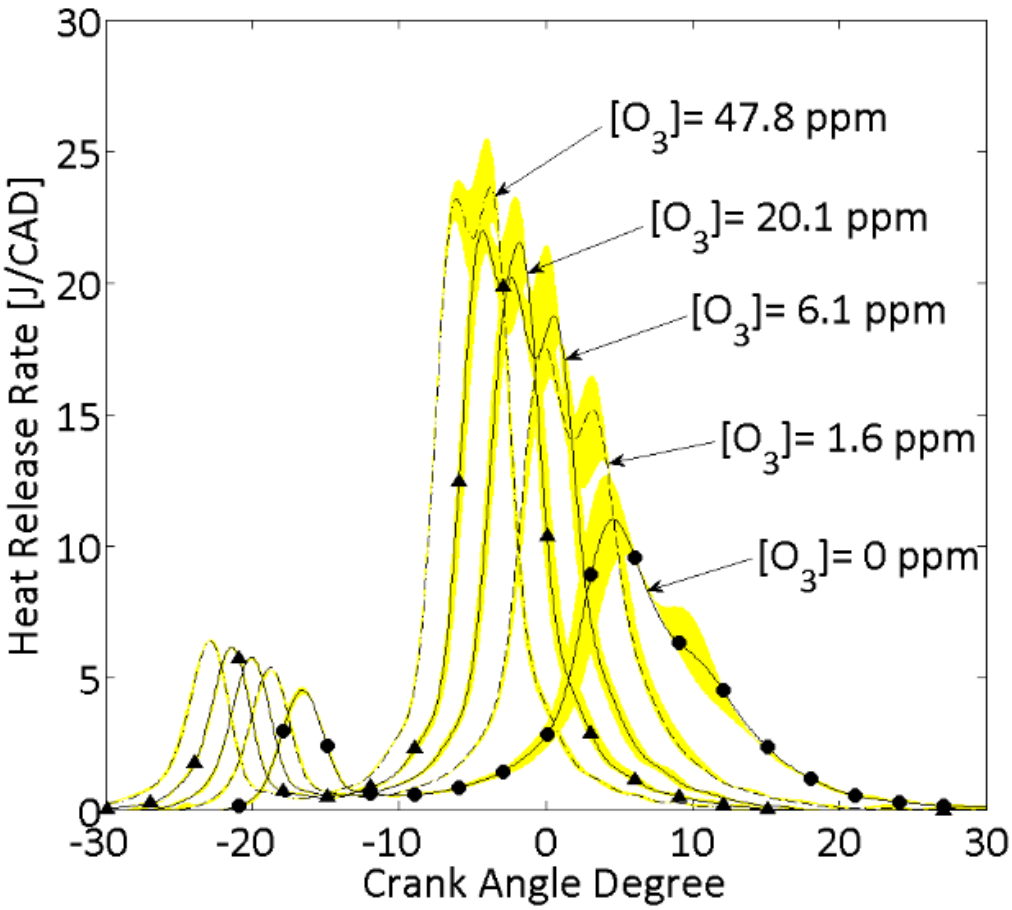

Figure 51. B. *Heat release rate evolutions as a function of the ozone concentration injected in the intake of the engine for n-heptane/PRF0 as fuel.*

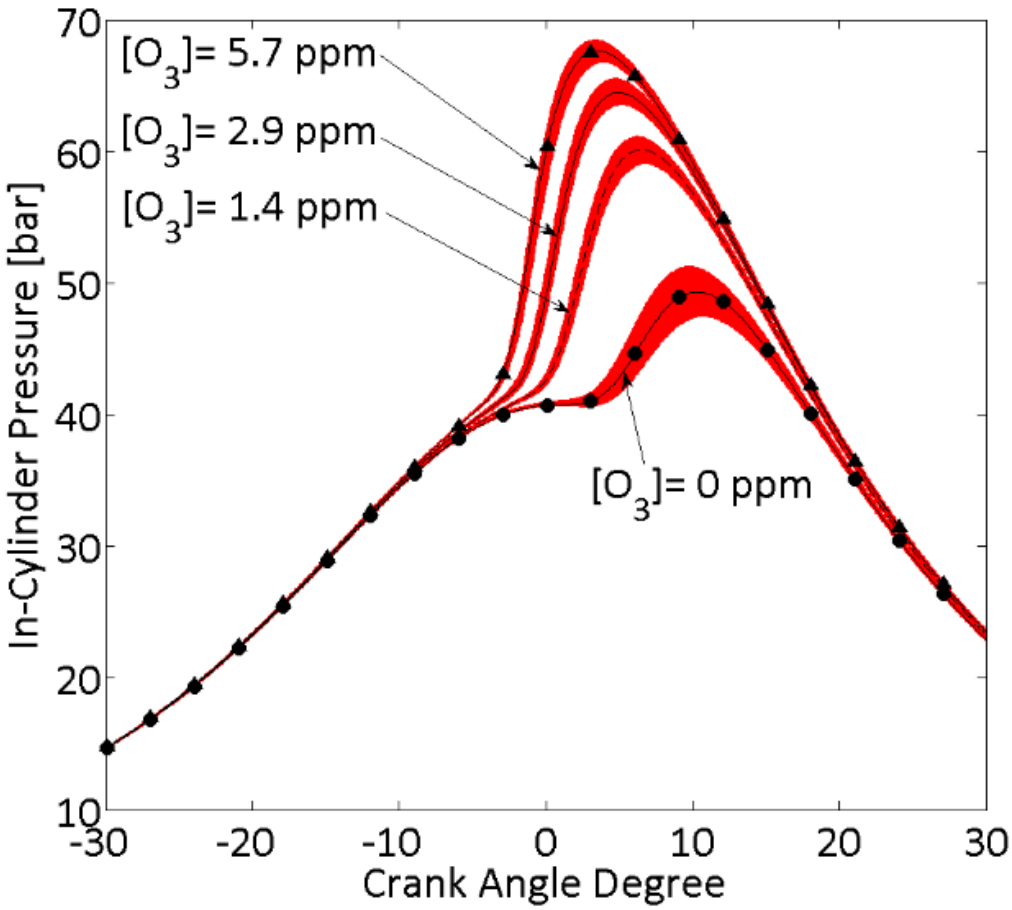

Figure 51. C. *In-cylinder pressure evolutions as a function of the ozone concentration injected in the intake of the engine for isooctane/PRF100 as fuel.*

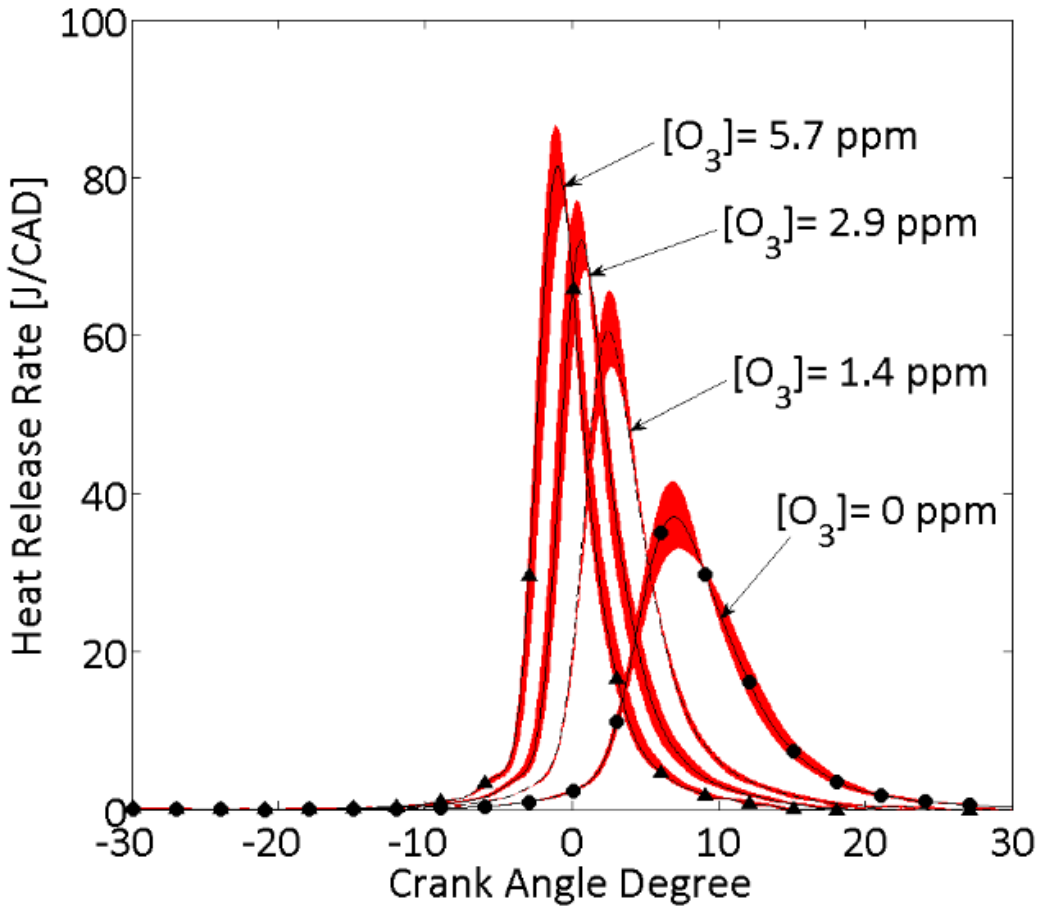

Figure 51. D. *Heat release rate evolutions as a function of the ozone concentration injected in the intake of the engine for isooctane/PRF100 as fuel.*

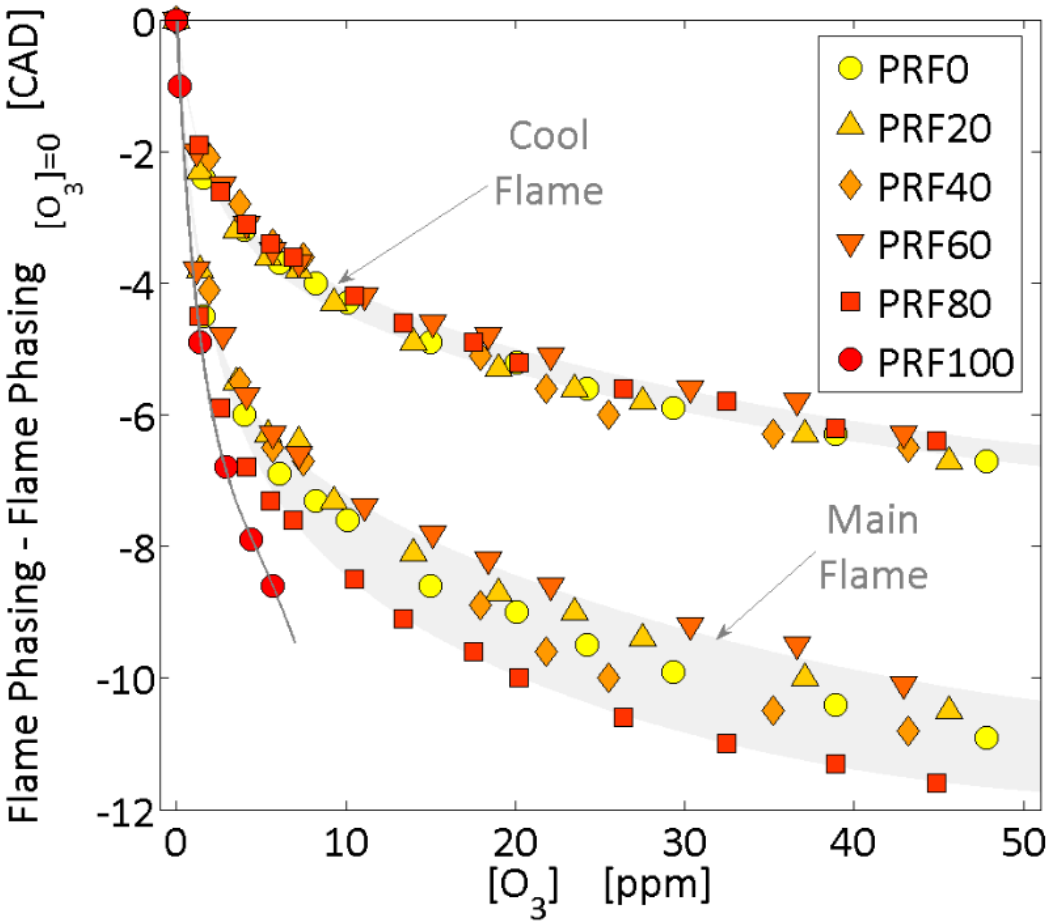

Figure 52. *Shift of the low temperature heat release (LTHR) and high temperature heat release (HTHR) as a function of the ozone concentration at the intake of the engine for each PRF in reference to the initial combustion phasing of each one without ozone.*

Foucher et al. [9] observed that both flames follow the same trends. Results are well reproduced for the cool flame and the impact on the main flame may be explained by the intake conditions selected. As intake pressure and temperature were fixed for combustions near misfires without ozone additions, the reference flame phasing are much delayed, in particular for the main flame phasing. Observing the trends of both flame phasing, it may conclude that the ozone seeding advances exponentially the phasing of the HCCI combustion. The ozone effect is mainly pronounced from 0 to 20 ppm and for higher concentrations, flame phasing advances slightly. Moreover, considering that these parameters present standard deviations of 0.1 and 0.25 CAD, respectively for the cool flame and the main flame, it may conclude that all of the PRFs (from PRF0 to PRF80) follow the same trends and that ozone acts similarly on their combustion process. The similar effect observed is attributed to the presence of n-heptane into each surrogate fuel. Finally, it may also be observed that for ozone concentrations higher than 20 ppm, both flame phasing advances linearly and follow parallel slopes.

For PRF100, the combustion does not present cool flame. Therefore, the ozone acts directly on its main flame phasing and abruptly advances its combustion. Compare to all the other PRFs investigated, the ozone effect is more pronounced and less than 10 ppm were seeded in the intake to avoid damages on the engine. Indeed, the earlier combustions led to an important growth of the pressure which results into high maximum pressure rise rate and excessive levels of noise. However, experiments for pure isooctane were performed for higher intake temperature than for all the other PRFs and as ozone is strongly impacted by the temperature [159]–[161], an early decomposition of this oxidizing chemical species explained the advance observed for PRF100.

3.2.1. CA05 and CA50

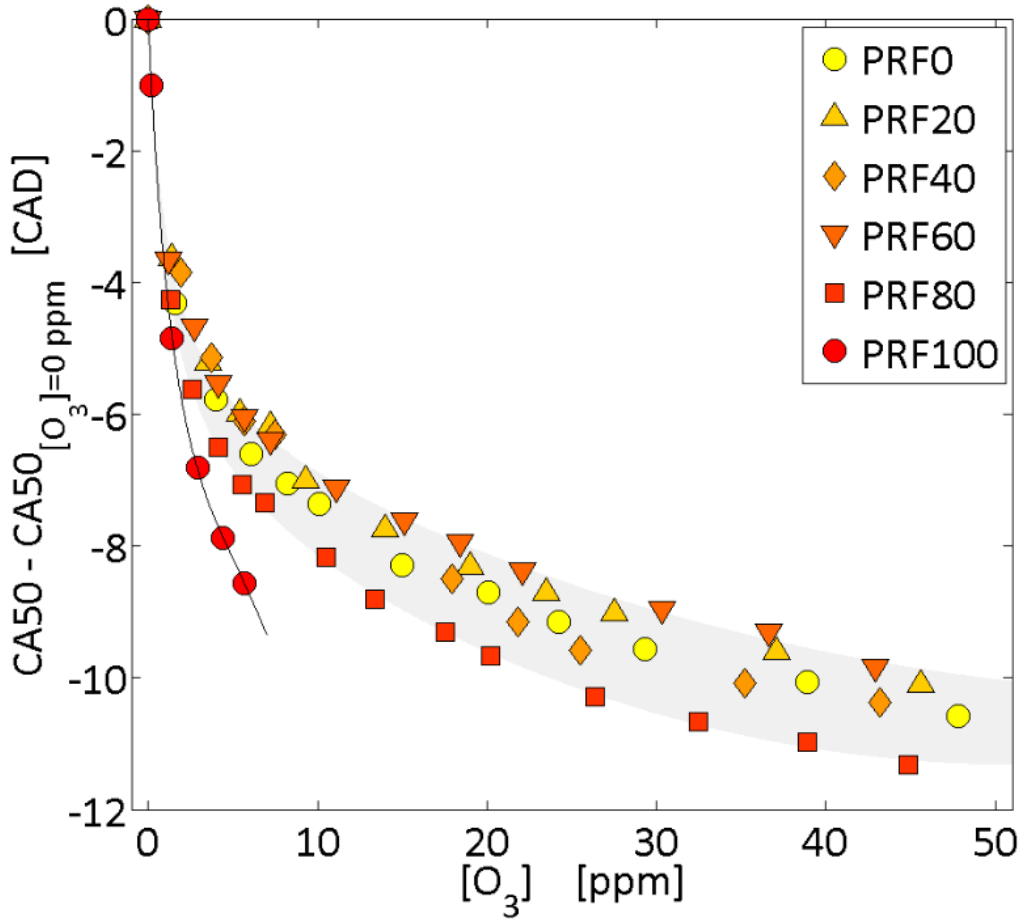

Figure 53. *Shift of the CA50 as a function of the ozone concentration for each fuel in reference to the CA50 of each one without any ozone seeding in the intake.*

Ozone is considered as one of the most powerful oxidizing chemical species and it was observed that it might alter the beginning of the combustion. The shift of CA05 (Article I) and the shift of CA50 (Figure 53) in reference to their respective initial value for each fuel were therefore examined. For the CA05, it may conclude that ozone modified the beginning

of the fuel oxidation. Furthermore, observing both parameters, fuels which present a cool flame chemistry are less impacted by ozone than fuel without. Isooctane needs very low ozone concentrations (less than 10 ppm) to strongly advance its combustion process while other PRFs need much more than 10 ppm to achieve similar advances of their CA05 and CA50. However, as PRF100 does not easily autoignite, a high intake temperature is necessary [37]. Such a temperature improves ozone decomposition and as ozone enables earlier combustion, a stronger advance observed may be observed on CA50 [159], [160].

3.2.2. Cool flame energy

As ozone mainly acts on the start of the combustion, its effect on the energy released by the low temperature heat release was studied. More precisely, the ratio between the cool flame energy and the total energy admitted was investigated. Figure 54 introduces the evolutions of this ratio for each fuel selected which has a cool flame occurrence, i.e. from PRF0 to PRF80, as a function of the shift of the cool flame phasing and

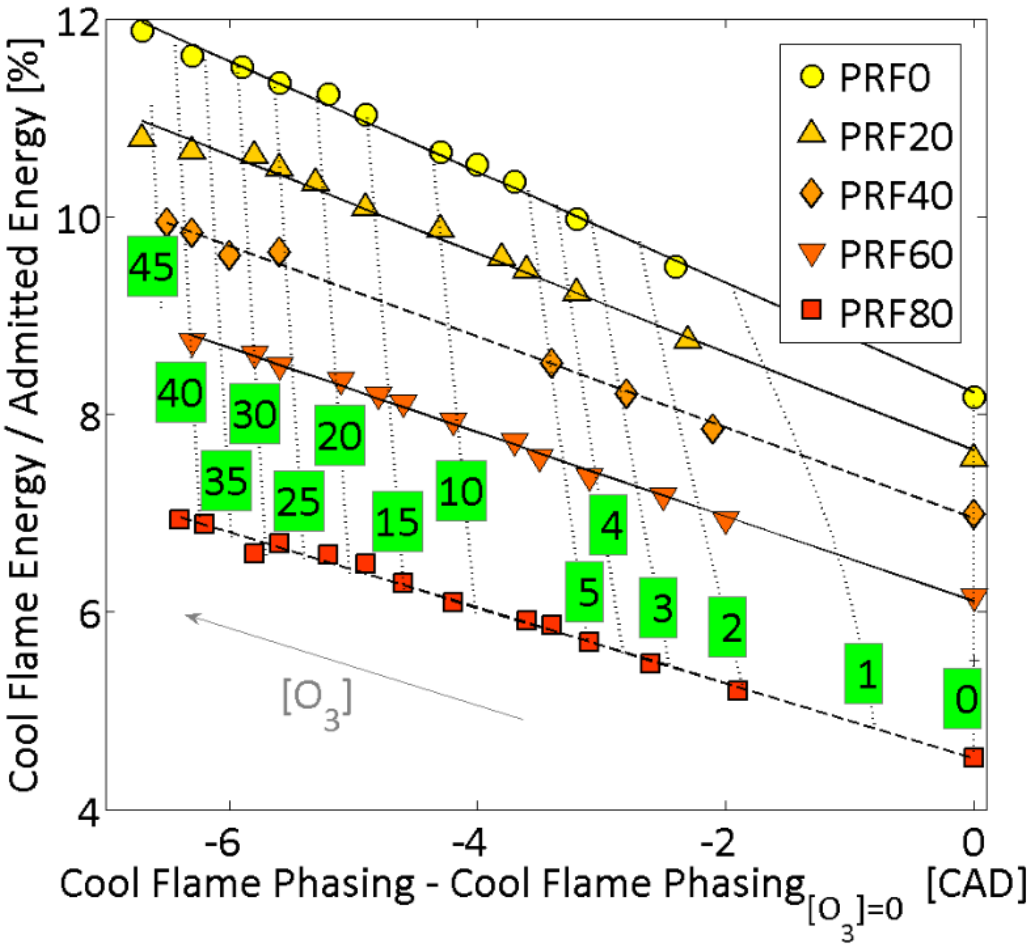

Figure 54. *Ratio between the cool flame energy released and the total energy released as a function of the cool flame shift and the ozone seeding into the intake.*

the ozone concentration. As shown previously, the increase of the ozone seeded into the intake of the engine leads to an advance of the combustion phasing with a linear increase of the ratio of energy released by the cool flame. The first ozone additions strongly rise the cool flame energy and seeding the intake with further ppm continue to increase the cool flame energy released but the impact is less pronounced. Therefore, these results showed that ozone leads to a combustion which occurs earlier, i.e. under lower bulk temperatures, and release more energy which involve a higher temperature growth. The increase in temperature influences the main combustion and allows finally advancing it (Figure 52 and Figure 53).

By comparing fuels, it may be observed that they all present linear trends and parallel between them. Moreover, the impact on the cool flame can be related to the presence of n-heptane into each surrogate fuels and their respective octane number. PRF0, which corresponds to pure n-heptane, shows the highest cool flame energy released and PRF80 the lowest. The maximum energy released by the cool flame therefore decreases with the increase of the octane number. Finally, according to previous results on pure n-heptane and isooctane, the first showed two-stage heat release while the second presented only one stage. Consequently, higher the volume fraction of n-heptane is, higher the energy released by the cool flame of a PRF surrogate is.

3.3. Kinetics results on the effect of ozone

Additionally to the experimental results previously introduced, computations with the help of the Chemkin package, in particular the constant volume model, and the kinetic scheme described in Chapter 2 were run. The aim is to further study the impact of ozone on the oxidation of PRFs.

3.3.1. Assessment of the kinetic scheme

Initially, the kinetic scheme used to compute ozone simulations consists of a combination of a main scheme which contains n-heptane and isooctane oxidation reactions [29], [30] with a submechanism which contains ozone decomposition [132]. This mechanism has never been used and has to be validated. The n-heptane – isooctane scheme was already validated for various combustion devices under a wide range of conditions. For validate the ozone – PRFs mechanism, ignition delays computations were performed by using the mechanism with and without the presence of the ozone submechanism. These simulations were run for pure n-heptane and isooctane under conditions observed during experiments. The equivalence ratio was therefore fixed at 0.3, for two different pressures (20 and 40 bar according to the cylinder pressure traces in Figure 55) and computations were carried out under a wide temperature range, from approximately 600 K to 1350 K. Ignition delays are presented in Figure 7. Results without the presence of the ozone submechanism match with

the results with this submechanism. It may therefore conclude that ozone submechanism does not affect the computed ignition delays.

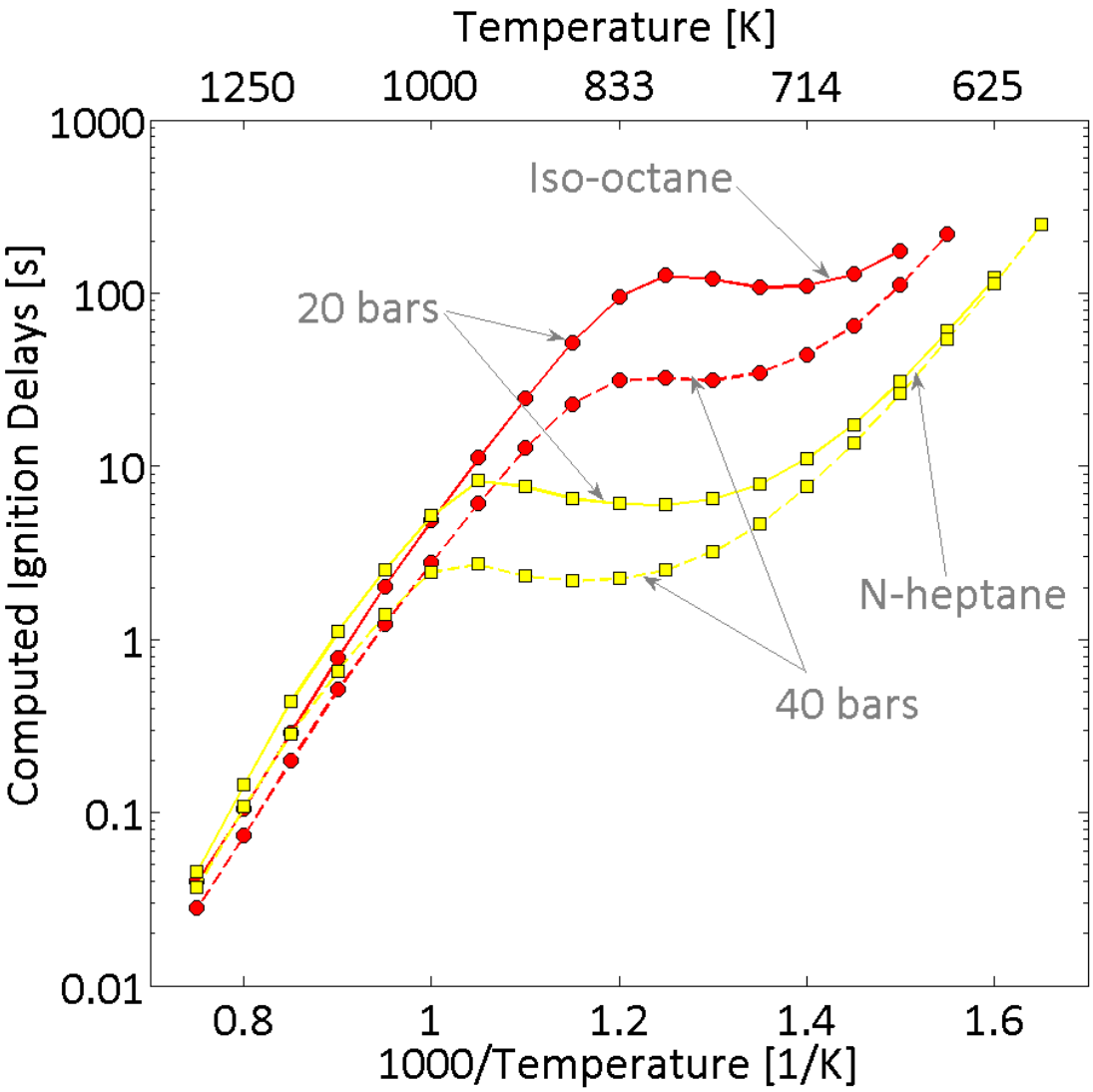

Figure 55. *Computed ignition delays as a function of the inverse temperature for an equivalence ratio of 0.3, two initial pressure (20 bar in filled symbols and 40 bar in open symbols) and two fuels (squares for n-heptane and circles for isooctane). Symbols correspond to computed ignition delays results with the ozone submechanism and lines represent results without.*

3.3.2. Interaction between ozone and the intake conditions

According to the design of experiments used for investigate the effect of ozone on the PRFs selected, thermodynamic intake conditions were fixed for each fuel. The aim is to study the impact of the intake pressure and the intake temperature on the ozone decomposition during the compression stroke. Exceptionally, these simulations were performed by using an internal combustion engine model. Characteristics of the engine for the model were chosen identical to those of the experimental engine (see Chapter 2) and computations were carried out for a motoring, i.e. a pure compression. The initial mixture consists of pure air seeded

with 10 ppm of ozone and the input conditions were fixed according to the experimental intake conditions. Two series of computations were therefore run to separately study the intake pressure and the intake temperature. For studying the intake pressure, simulations were performed for values from 0.6 to 1.4 bar and by tuning the intake temperature at 30 °C. Inversely, for investigating the intake temperature, initial conditions of temperatures were ranged from 30 °C to 200 °C while the initial pressure was fixed at 1 bar.

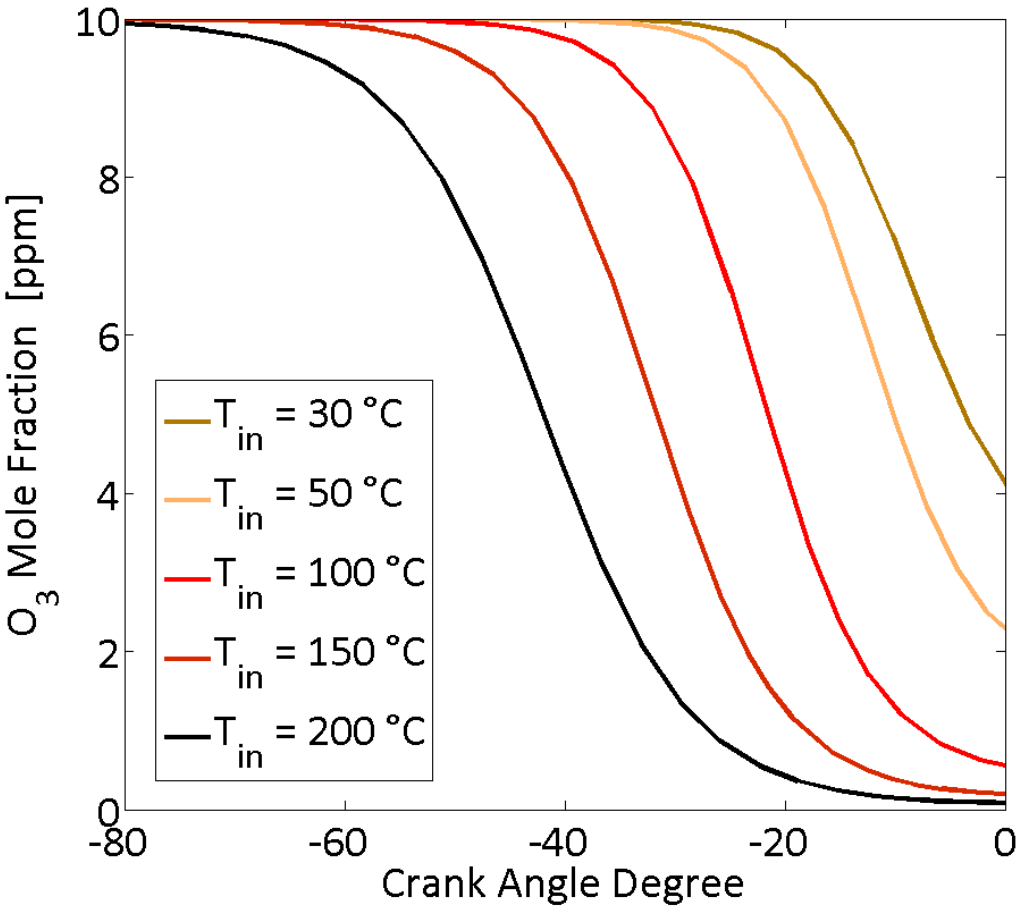

Figure 56. *Computed ozone mole fraction during the compression stroke of an engine as a function of the crank angle degree under temperatures from 30 °C to 200 °C at a constant pressure of 1 bar.*

Results showed that the intake pressure has a very slight effect on ozone decomposition. The impact of this thermodynamic parameter may be therefore neglected and the computed results easily explained the similar experimental results on cool and main flame observed for all of the PRFs selected except for the PRF100. According to Figure 56, it may see that the intake temperature has an important effect on the ozone decomposition. By increasing this parameter, ozone breaks down earlier [159], [160] and therefore, the oxidation of the fuel starts earlier. This prior oxidation explains why PRF100 which needs high intake temperature to auto-ignite is more influenced by ozone seeding.

3.3.3. *Ignition delays computations*

Ignition delays computations were run to further analyze the impact of ozone on the combustion of PRFs. These simulations were carried out for pure n-heptane and pure isooctane by using the constant volume model described in Chapter 2 and by setting an equivalence ratio of 0.3. Initial pressures were selected at 25 bar and 50 bar, respectively for PRF0 and PRF100. These conditions correspond to the pressure observed before the start of the main combustion for each fuel and enable us to ensure combustion. Finally, computations were performed under a wide temperature range, from approximately 600 K to 1350 K, and for four different ozone concentrations, i.e. 0, 1, 10 and 45 ppm. Figure 57 shows the ignition delays obtained as a function of the inverse temperature. From these results, it may clearly observe that ozone modified the ignition delays up to a temperature of

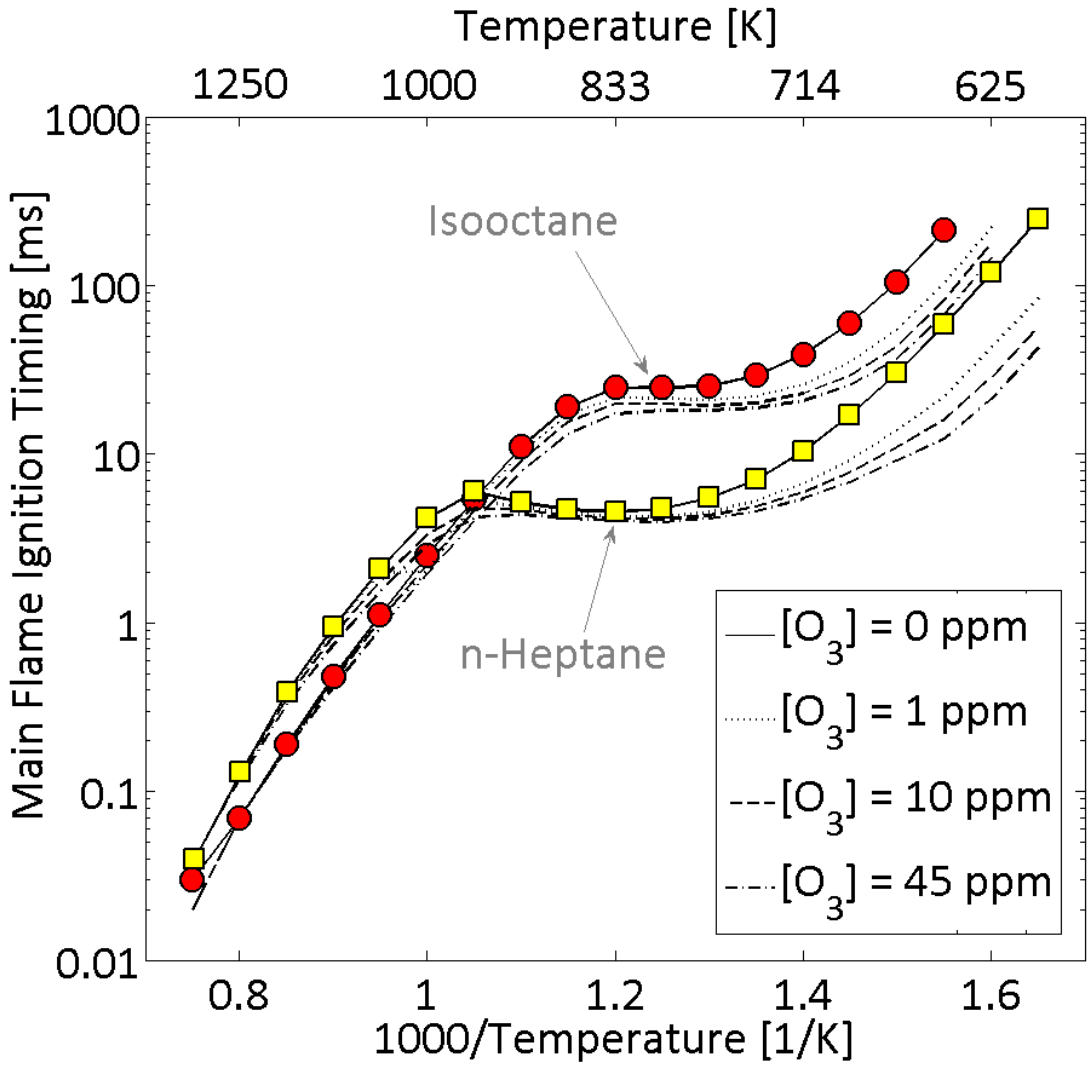

Figure 57. *Computed main flame ignition timing as a function of the inverse temperature for various ozone concentrations. "□" symbols and curves under this result correspond to PRF0 as fuel, and "○" symbols and curves under this result correspond to PRF100 as fuel.*

1000 K. In the case of PRF0, ozone mainly acts on the low temperature regime and less on the negative temperature coefficient and the main temperature regime, as already observed by *Foucher et al.* [9]. For PRF100 as fuel, the overall combustion process is also influenced but with a more significant impact on the overall temperatures. These results are therefore in agreement with the experimental observations. Moreover, it may also see that a low ozone concentration lead to an important advance of the computed ignition delays and further additions continue to decrease the ignition delay but with a lower impact.

3.3.4. Chemical analysis on PRFs

3.3.4.1. Pure n-heptane and pure isooctane

Additionally to the computed ignition delays, chemical pathway analyses were conducted by considering pure n-heptane and pure isooctane. The description of the oxidation of n-heptane has already been established by *Foucher et al.* [9]. Accordingly, only the main reactions involved on the isooctane oxidation are analyzed. Computations were run in agreement with the experiments conducted. Initial conditions were therefore fixed at 800 K for the temperature, 50 bar for the pressure and 0.3 for the equivalence ratio. To conclude on the ozone impact, simulations were carried out with and without the presence of this oxidizing chemical species. Results obtained are presented in Figure 58 for the mole fractions of the main radicals and for the main oxidation reactions of the isooctane for the case without ozone and with 10 ppm.

Without ozone, the isooctane oxidation starts by an initiation reaction involving the oxygen molecule (O_2) to form a hydroperoxyl radical (HO_2) and an alkyl isooctane radical (R). Then, R is rapidly oxidizes and leads to the formation of hydroxyl radicals (OH) according to the reaction pathways of alkane fully described in the literature [30], [31]. Finally, the fuel becomes mainly consumed by reactions with OH and HO_2 radicals. With ozone inside the initial mixture, fuel oxidation shows a different pathway. Instead of a first reaction with oxygen molecule, fuel is initially consumes through a reaction with O-atom. The O-atom mainly comes from the ozone decomposition (R-29). The earlier initiation reaction then results into the production of an OH radical which in turn accelerates the consumption of the fuel and finally leads to a rapid combustion through reactions involving the fuel with either O-atom or OH radical.

$$O_3 + M \rightarrow O_2 + O + M \qquad \text{R-29}$$

In the case of n-heptane, its fuel oxidation demonstrates identical pathways with and without ozone [9]. The oxidation of alkanes may therefore be summarized as follow. Figure 59 highlights the initial reactions involving alkane fuel oxidation in both cases, i.e. with and without ozone seeding. Without ozone seeding, fuel (RH) oxidation is initiated by

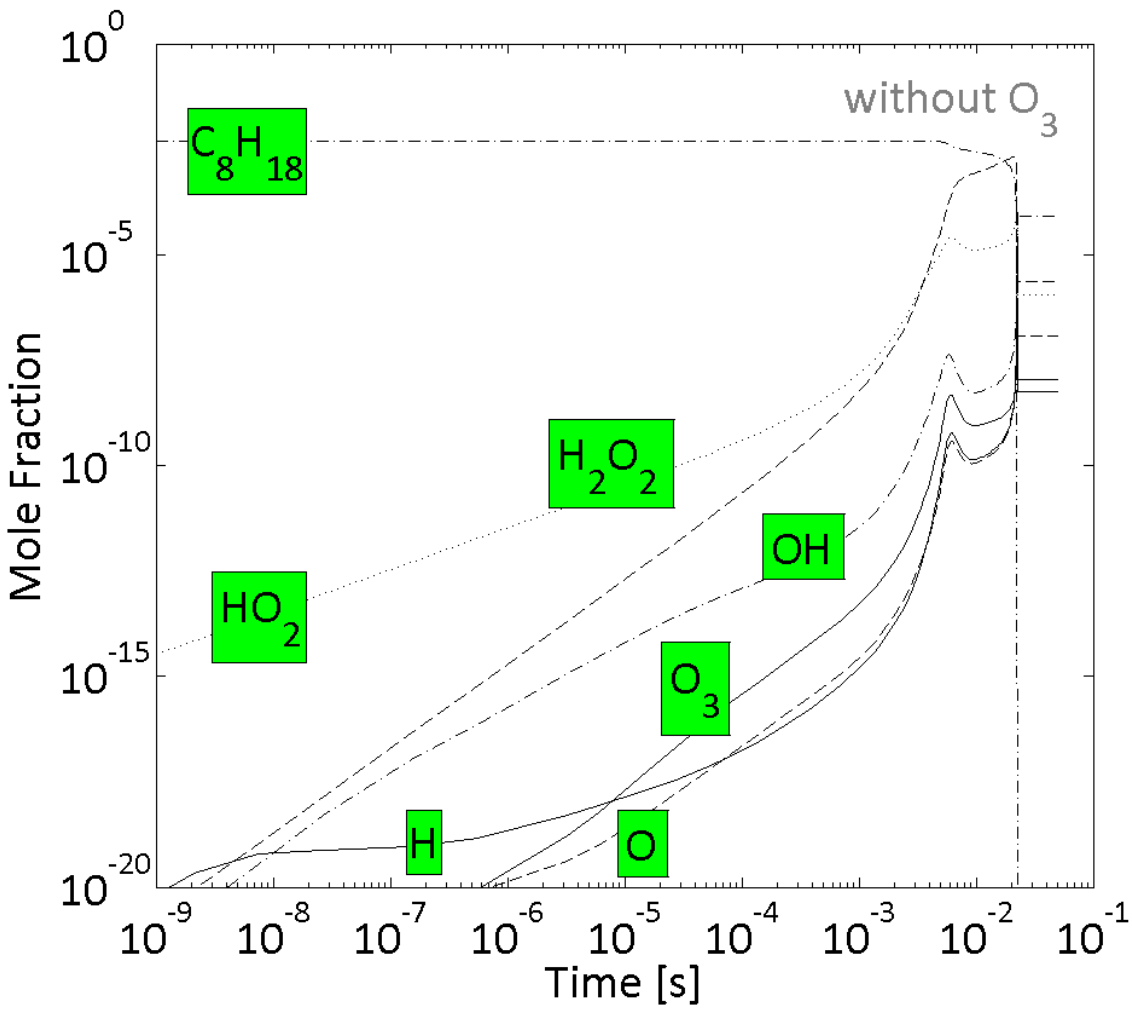

Figure 58. A. *Mole fractions of the main radicals and the fuel for isooctane (PRF100) at an initial temperature of 800 K, initial pressure of 50 bar, an equivalence ratio of 0.3 and without ozone.*

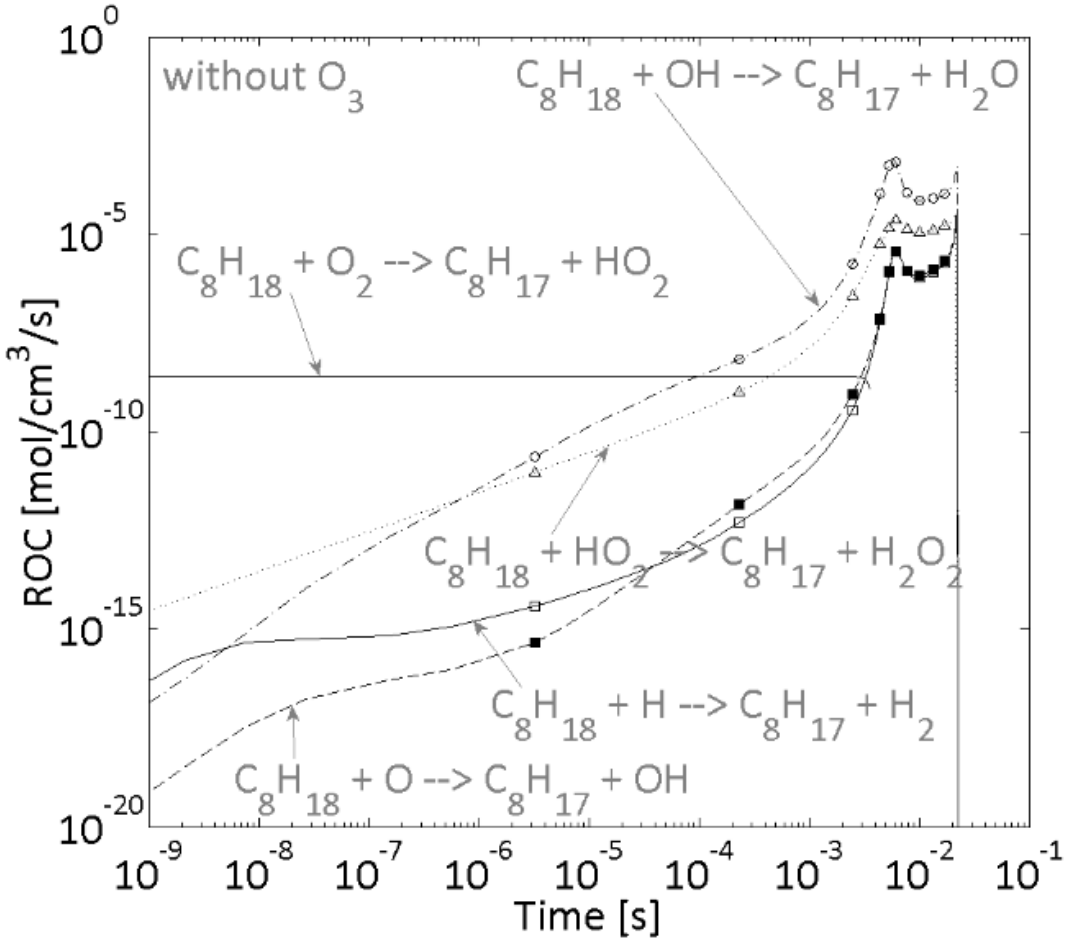

Figure 58. B. *Reaction pathway analysis from rates of consumption for isooctane (PRF100) at an initial temperature of 800 K, initial pressure of 50 bar, an equivalence ratio of 0.3 and without ozone.*

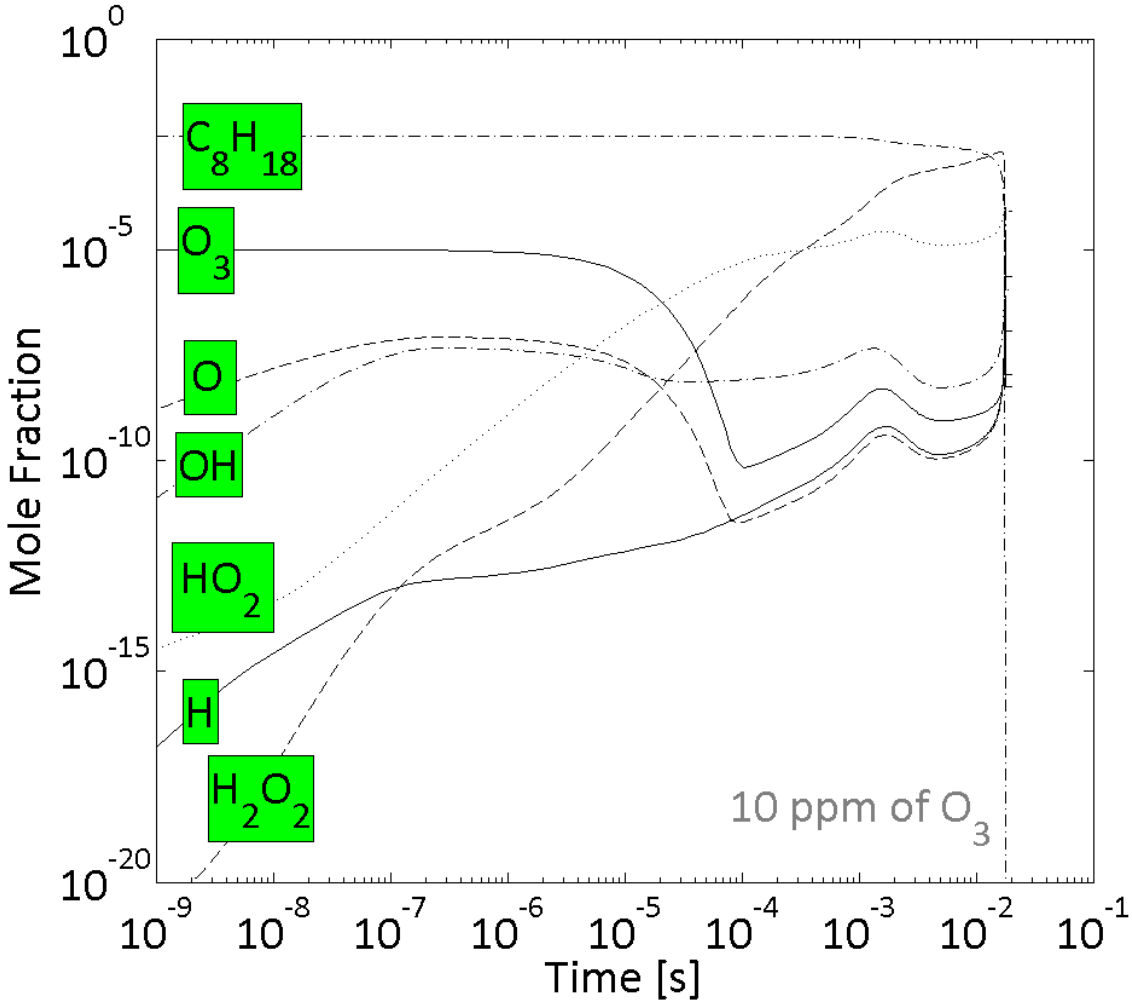

Figure 58. C. *Mole fractions of the main radicals and the fuel for isooctane (PRF100) at an initial temperature of 800 K, initial pressure of 50 bar, an equivalence ratio of 0.3 and with 10 ppm of ozone.*

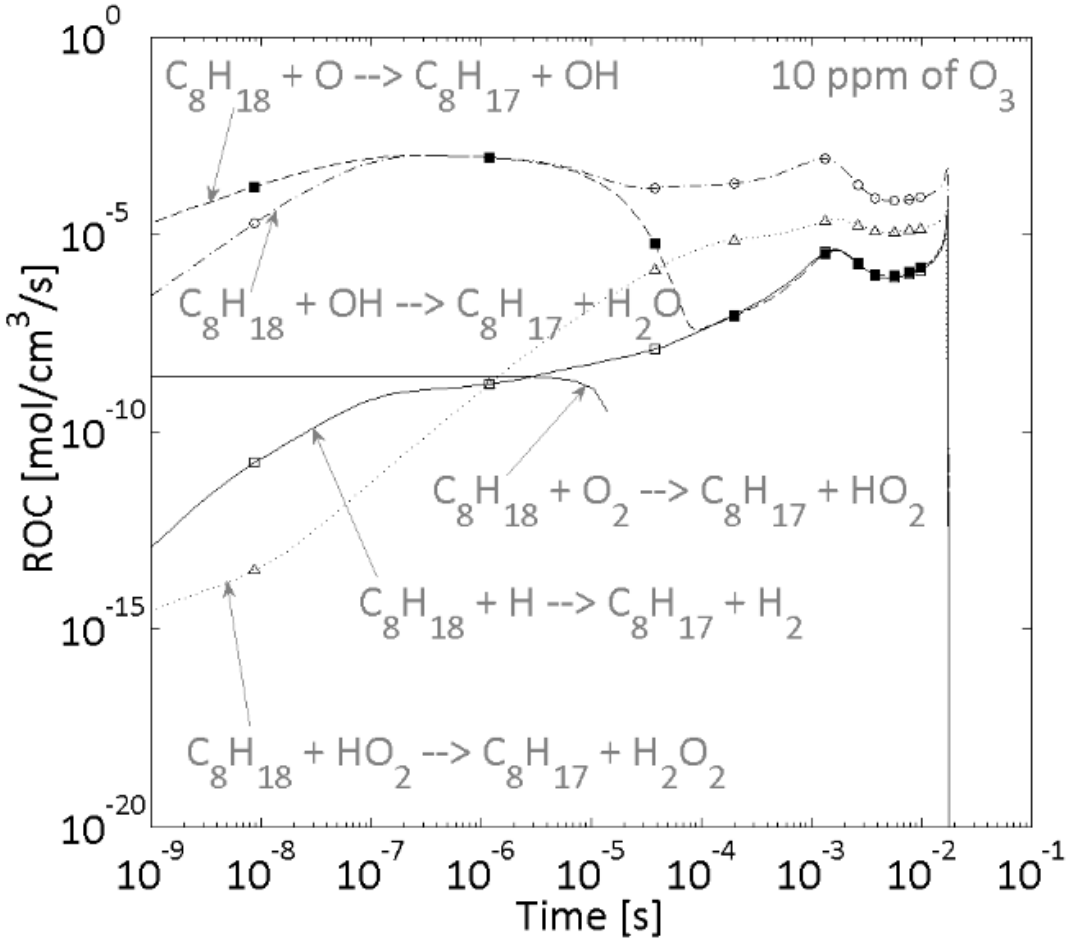

Figure 58. D. *Reaction pathway analysis from rates of consumption for isooctane (PRF100) at an initial temperature of 800 K, initial pressure of 50 bar, an equivalence ratio of 0.3 and with 10 ppm of ozone.*

oxygen molecule (O_2) which leads to the formation of a hydroperoxyl radical (HO_2) and an alkyl fuel radical (R). Then, the alkyl radical is mainly consumed through low temperature reactions up to form hydroxyl radical (OH) and finally, fuel is consumed by reaction with HO_2 radical and mainly with OHradical, this last reaction leading to the combustion. In presence of ozone, the fuel initially reacts with an O-atom coming from the ozone decomposition. The presence of O-atom leads to the production of an alkyl radical and a OH radical which in turn rapidly consumes the fuel to lead to the occurrence of the combustion. As a result, OH radicals are produced sooner in the presence of ozone and therefore, explain the strong advance observed during the experimental result.

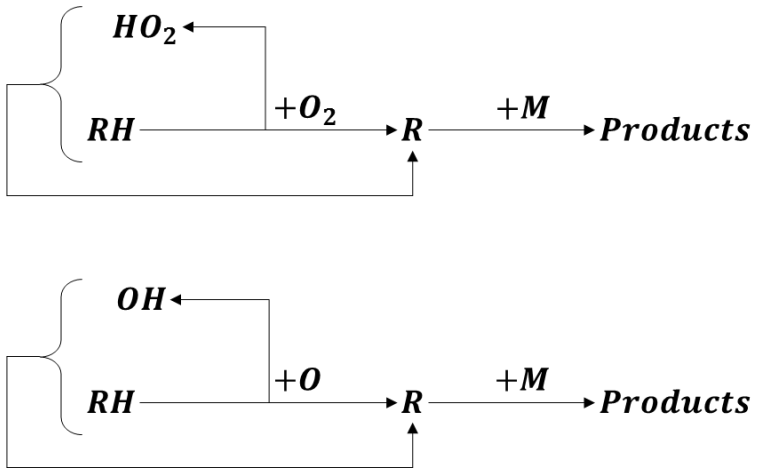

Figure 59. *Initial reactions involving alkane fuel oxidation in the case without ozone seeding (top) and with ozone seeding (bottom).*

3.3.4.2. Mixtures of n-heptane and isooctane

Computations in the case of mixture of n-heptane and isooctane were also considered. The case selected was that of the PRF40, i.e. a surrogate composes of 40 % of isooctane in volume and the rest of n-heptane (60 %), and results obtained were presented in Article I. Simulations were run similarly than for pure isooctane except for the initial pressure which was set up at 25 bar, a pressure near the in-cylinder pressure just before the autoignition of the fuel. As observed previously, the same reactions pathways for both fuels are highlighted with ozone seeding. Moreover, n-heptane shows higher rate of consumption than isooctane due to its volume fraction and both fuels are oxidized together according to the characteristic time. However, n-heptane should be autoignite first but this is not clearly visible on these results. Extra simulations for pure n-heptane and isooctane were therefore performed by considering the same initial parameters. Results showed that n-heptane autoignites earlier and inversely, the isooctane autoignites later. As a result, n-heptane oxidation in PRF40 is delayed while isooctane oxidation is considerably shortened. In the case of n-heptane, the delay is explained by the fact that its volume fraction is weaker and that the presence of isooctane consumes a part of the radicals produced which oxidize it. For isooctane, the advance of its oxidation may be explained by the presence of radicals

released from n-heptane oxidation and due to a slight increase of the temperature with n-heptane consumption [32].

4. Ozone seeding with intake temperature variation (Article II)

Previous experimental results considered the impact of ozone on the HCCI combustion of six PRFs. Among them, PRF100 showed that its combustion phasing is the most influenced compared to other fuels tested. The strong advance observed was attributed to the high intake temperature used which speed up its break down [159]. Additionally, the intake temperature of conventional engines does not reach very high temperatures and sometimes, the value of this thermodynamic parameter may be very weak (cold start) [141], [162]. There are therefore several interests of assessing the impact of ozone under intake temperature variation. Finally, as ozone is known as one of the most powerful oxidizing chemical species and as it may enable to control the combustion phasing, according to CA50 results previously observed, further researches were carried out with isooctane as fuel to demonstrate the potential of ozone. They consist of experiments performed under unfavorable conditions for isooctane as fuel and the main objective is to study the ozone effect when the intake temperature is lower than the minimum temperature required. These experiments were carried out under similar conditions than those selected for PRFs investigation, i.e. a rotation speed of 1500 rpm and an equivalence ratio of 0.3.

4.1. Combustion under unfavorable intake conditions

Starting from previous results on isooctane combustion without ozone seeding, an “optimal” combustion area has been established by varying the intake conditions of the engine. The aim here is to investigate the intake conditions needed to conserve this ideal region when a fixed ozone concentration is injected. Experiments were therefore performed for three different ozone concentrations (0, 10 and 40 ppm) by changing the intake pressure and the intake temperature in order to obtain CA50s located between 1 and 5 crank angle degrees. Results are presented in Figure 60. As previously presented, the lower limit of each combustion region corresponds to a CA50 of 5 CAD and the upper limit to a CA50 of 1 CAD. Without ozone, the ideal combustion takes place for pressures in the range of 1 to 1.6 bar and temperatures in the range of 150 to 210 °C. With ozone, this region moves towards lower intake thermodynamics conditions. As it was showed previously that ozone enables to advance the combustion phasing, maintaining a constant location of the CA50 may be achieved by reducing either the intake pressure or the intake temperature or again both intake thermodynamic parameters. As a result, when the ozone concentration seeded becomes important, intake conditions can be drastically reduced. Moreover, generally observing these combustion areas, it may see that they move in parallel towards lower intake temperatures. Indeed, compared to the initial combustion area of isooctane, the use of 10 ppm enables to shift this region with 50 °C less and 40 ppm with 90 °C less. Similar impacts were observed in the literature [10], [11]. Finally, as previously observed, ozone advanced rapidly the combustion phasing and according to previous values discussed, low

ozone enables to strongly decrease the intake temperature while higher ozone concentrations continue allowing reducing the intake temperature but the shift is less pronounced. Further experiments were therefore performed under lower intake temperatures than those necessary to autoignite without any oxidizing chemical species to highlight the effect of the ozone on the isooctane combustion.

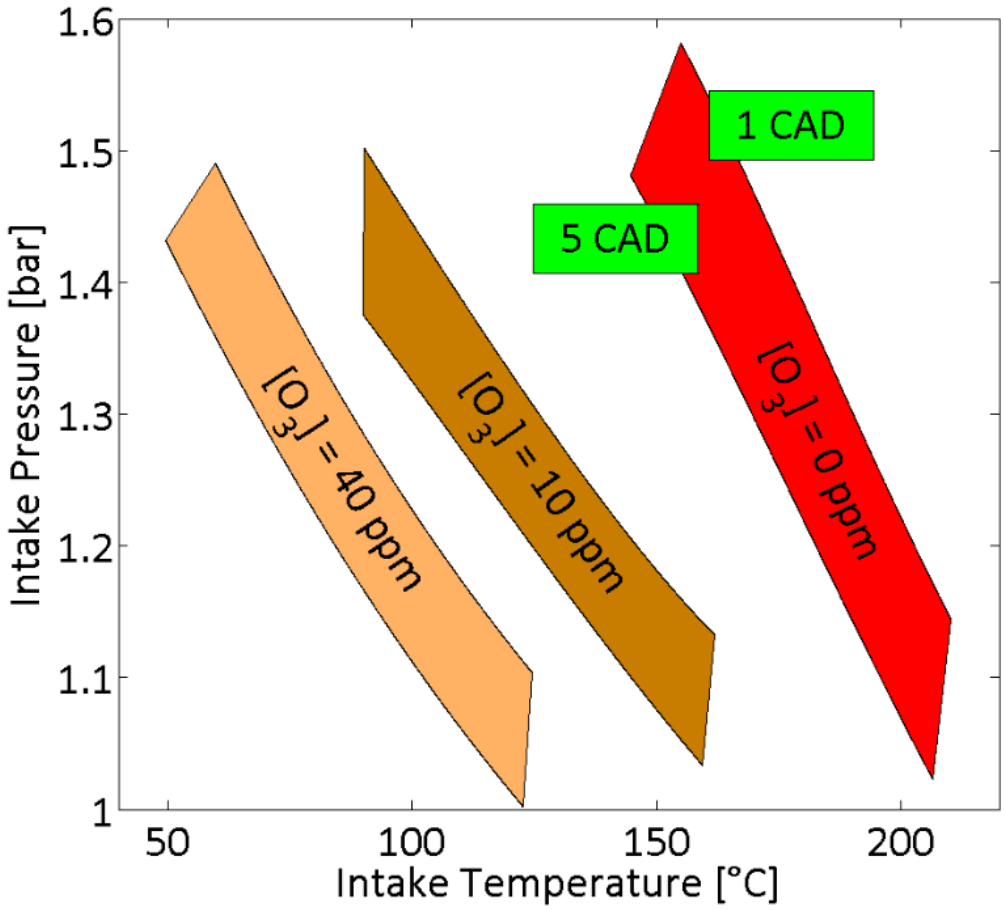

Figure 60. *"Optimum" combustion area for isooctane as fuel for different fixed ozone concentrations as a function of the intake pressure and the intake temperature.*

4.2. Combination of intake temperature with ozone

According to previous results obtained under unfavorable conditions to achieve isooctane combustion, further experiments were performed at a constant pressure (1 bar), with several temperatures lower than the temperature needed to enable the combustion at this pressure (200 °C) and by varying the ozone concentration seeded in the intake of the engine, from 0 to 140 ppm. Results are presented in Figure 61.

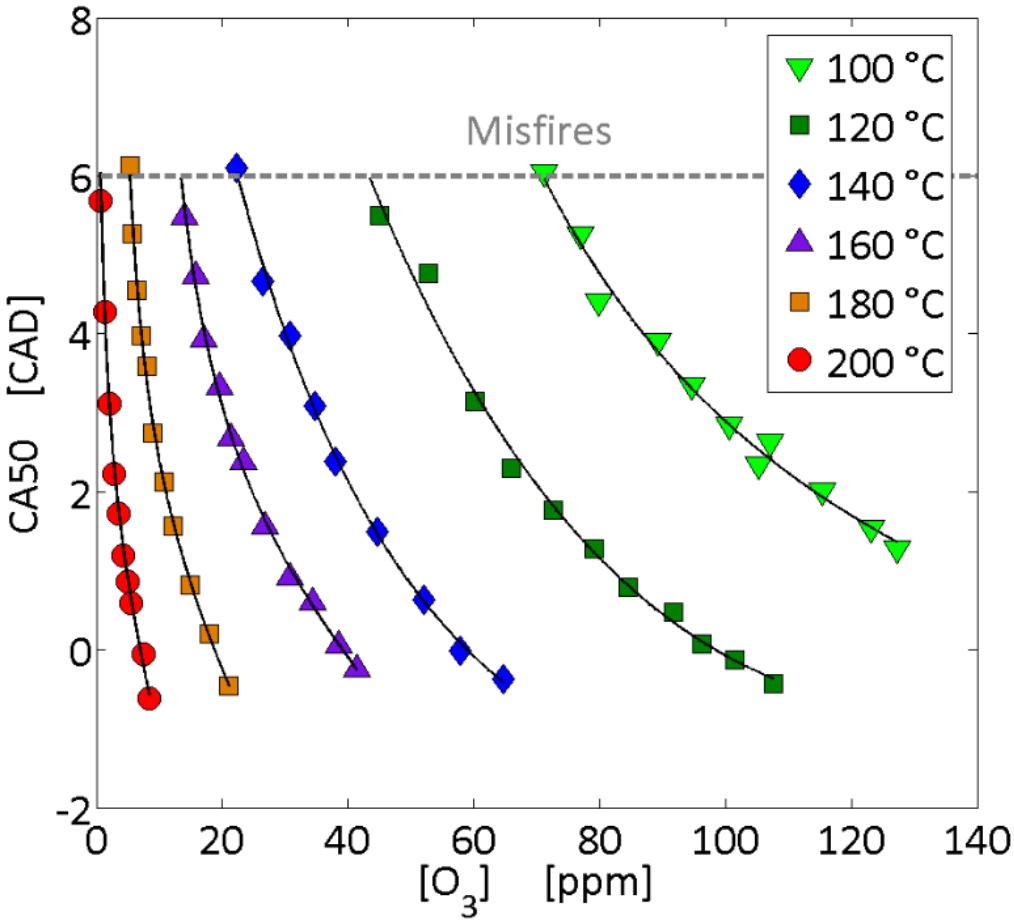

Figure 61. *Evolution of the CA50 as a function of ozone concentrations for different intake temperatures at a constant pressure of 1 bar.*

The results show that isooctane can burn under lower temperatures but a minimum ozone concentration is needed to initiate the combustion. Moreover, this initial concentration of ozone must increase exponentially with the decrease of the intake temperature and, more generally, the same observation can be made for maintaining a constant phasing. Regarding the advance of the combustion phasing temperature by temperature, less than 10 ppm are necessary at 200 °C to move the CA50 of at least 6 CAD while at an intake temperature of 120 °C, an increase of approximately 60 ppm is required to observe a similar advance. This result clearly shows that the combustion phasing is less sensitive to the ozone when the intake temperature decreases. Indeed, the ozone decomposition is mainly affected by temperature, a high temperature rapidly breaks down ozone which produces O-atoms. In turn, O-atoms rapidly oxidize the fuel. Under lower temperatures, the phenomenon is less pronounced and high concentrations of this chemical species are needed to achieve a similar advance of the combustion phasing.

As a results, the overall results previously obtained for isooctane as fuel demonstrate that the HCCI combustion may be easily control under a wide range of

conditions and in particular, with temperatures variations. Moreover, as the CA50 is less sensitive under lower temperatures, a better control of the combustion phasing can be considered.

4.3. Cool flame occurrence

Most of the time, the HCCI combustion of isooctane into internal combustion engines presents a single stage ignition [27]. However, previous studies showed that isooctane is affected by a cool flame oxidation [37]. According to previous results with ozone seeding, no cool flame appears on heat release rate traces and it was considered that this oxidizing chemical species directly acts on the main combustion stage. Nevertheless, in the case of combustion assisted by ozone seeding under lower intake temperature than one necessary to achieve the combustion without ozone, isooctane may show two-stage ignition

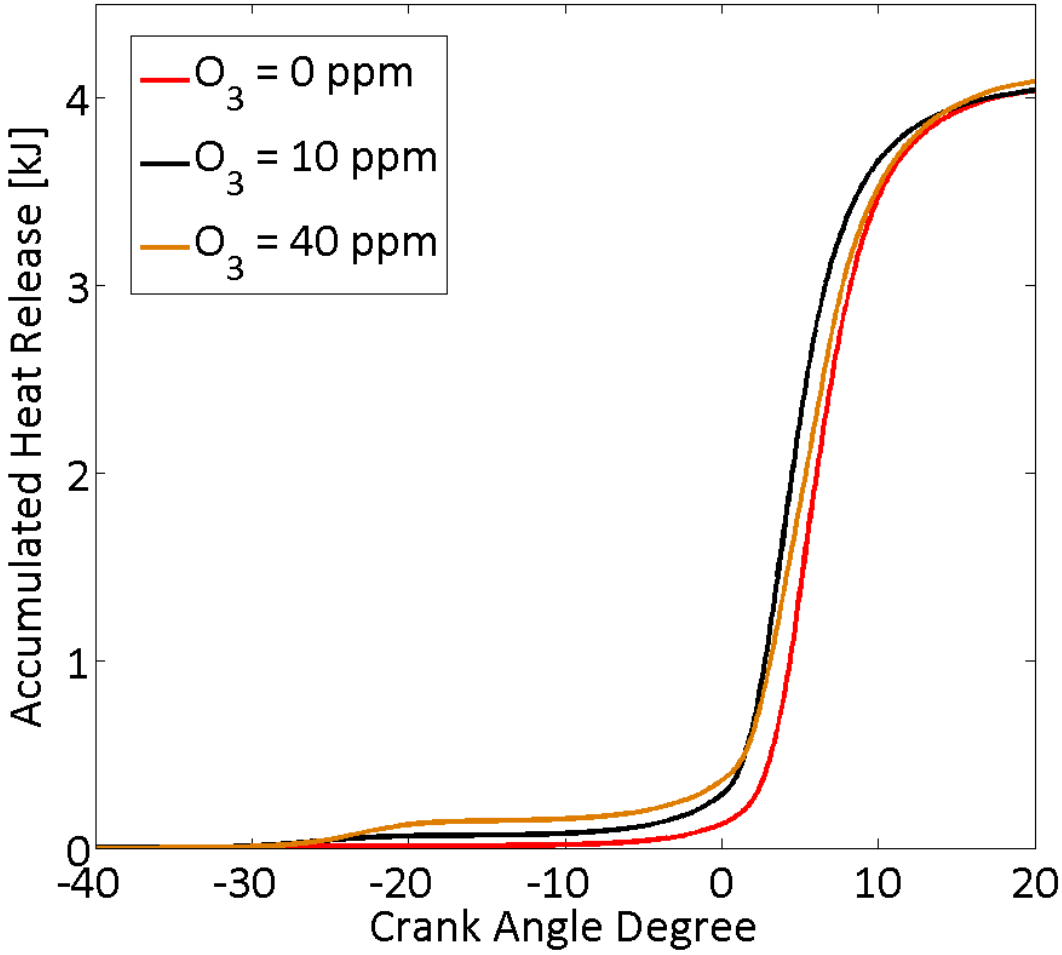

Figure 62. *Heat release rate evolutions for different ozone concentrations at a constant intake pressure of 1.3 bar and a constant CA50 of 5 CAD.*

as observed in Figure 62. These results are presented for heat release rate traces with a constant CA50 around 5 CAD, a constant intake pressure of 1.3 bar and for three ozone concentrations of 0, 10 and 40 ppm (therefore with intake temperatures of 167 °C, 105 °C and 66 °C, respectively).

Without ozone, heat release rate shows only one ignition stage while under lower intake temperature and with ozone addition, a cool flame ignition occurs progressively. As the intake temperature is weaker, the cool flame reactions have enough time to establish and demonstrate experimentally that ozone modifies the start of the combustion since the energy released during the cool flame increases. Moreover, such results are confirmed through kinetics computations. By using the same methodology than one previously presented, ignition timing of the cool flame was computed. Simulations showed that ignition timing are in agreement with the experimental results observed. When the temperature decreases, the ignition timing is delayed but increasing the amount of ozone leads strongly to a shortened ignition timing. Therefore, the ozone effect is higher than the temperature effect. Finally, according to experimental results and computational results, reduce the temperature and inject ozone enable to achieve cool flame occurrence.

As a conclusion, these results on isooctane combustion showed that the use of ozone might help controlling the HCCI combustion phasing under a wide range of conditions. Moreover, last results demonstrate that the combination of using low intake temperatures with ozone injections clearly showed that ozone influences the beginning of the fuel oxidation. It could therefore enable to examine the onset of the cool flame and its effect on the overall HCCI combustion into internal combustion engines.

5. Ozone, nitric oxide and nitrogen dioxide seeding (Article III)

The impact of ozone was previously examined and further experiments with isooctane as fuel demonstrate that controlling the HCCI combustion through the use of this oxidizing chemical species may be achieved. Most of the time, ozone is produced from dielectric barrier discharge systems [159], [163]–[166]. To ensure ozone production without any other undesired oxidizing chemical species, such devices must be supplied by neat oxygen. However, considering that this kind of appliances may be integrated into conventional vehicles, supplying it with air will be most appropriate. Unfortunately, the use of air may produce nitrogen oxides at the intake of the engine, in particular nitric oxide and nitrogen dioxide [167]–[170]. These two nitrogen oxides can also react with ozone as observe into the literature and strongly reduce the impact of ozone. Moreover, nitrogen oxides may also be present into the combustion chamber through residuals (iEGR) of the previous combustion cycle or through an EGR loop (Figure 63). Considering that, experiments and kinetics computations were therefore performed to compare their respective effect with that of ozone in the case of isooctane as fuel. Then, the case when nitric oxide and ozone seed together the intake of the engine was investigated because nitric oxide is the main nitrogen oxide presents inside exhaust gases and because it is the initial nitrogen oxide generated by dielectric barrier discharge.

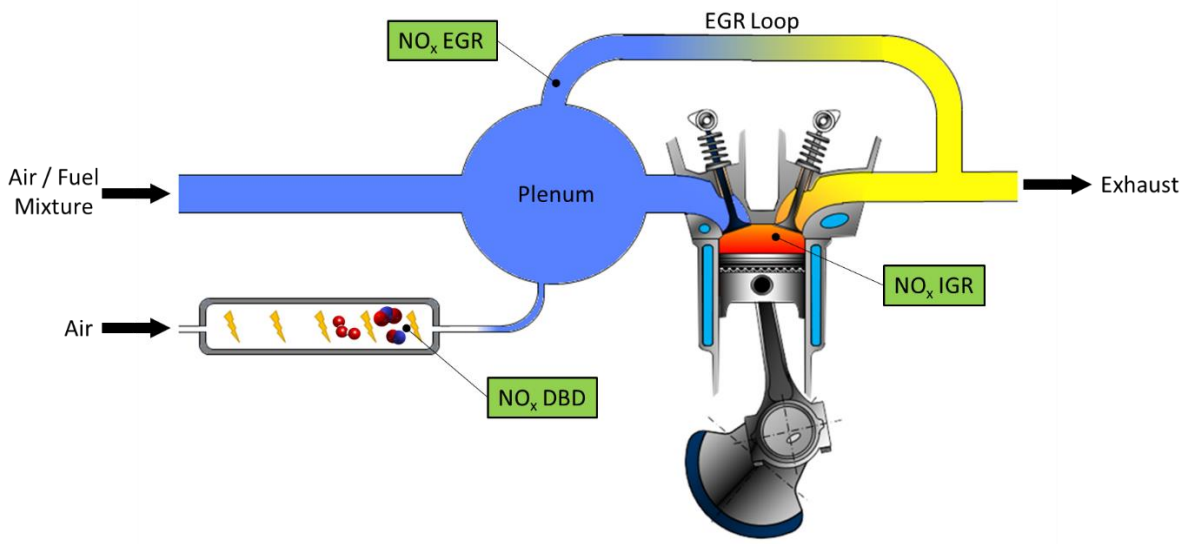

Figure 63. *Scheme of the different sources of NO_x into an engine using an ozone generator.*

5.1. Comparison between ozone, nitric oxide and nitrogen dioxide

5.1.1. Experimental results

These three chemical species are all oxidizing ones and may improve the HCCI combustion. Their respective impact on the isooctane combustion was therefore investigated by starting from a combustion without any seeding of oxidizing chemical species

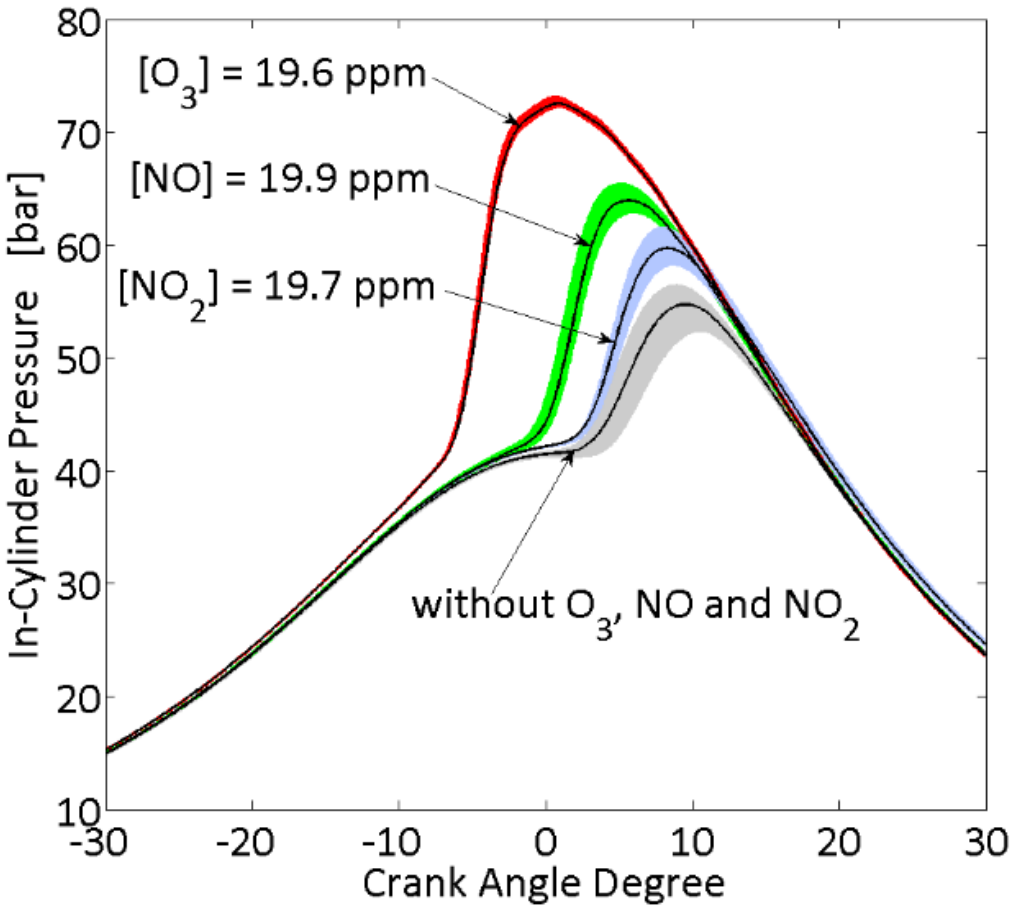

Figure 64. A. *In-cylinder pressure traces without any species seeded and with 20 ppm of each oxidizing chemical species (O_3: ozone, NO: nitric oxide and NO_2: nitrogen dioxide) separately injected.*

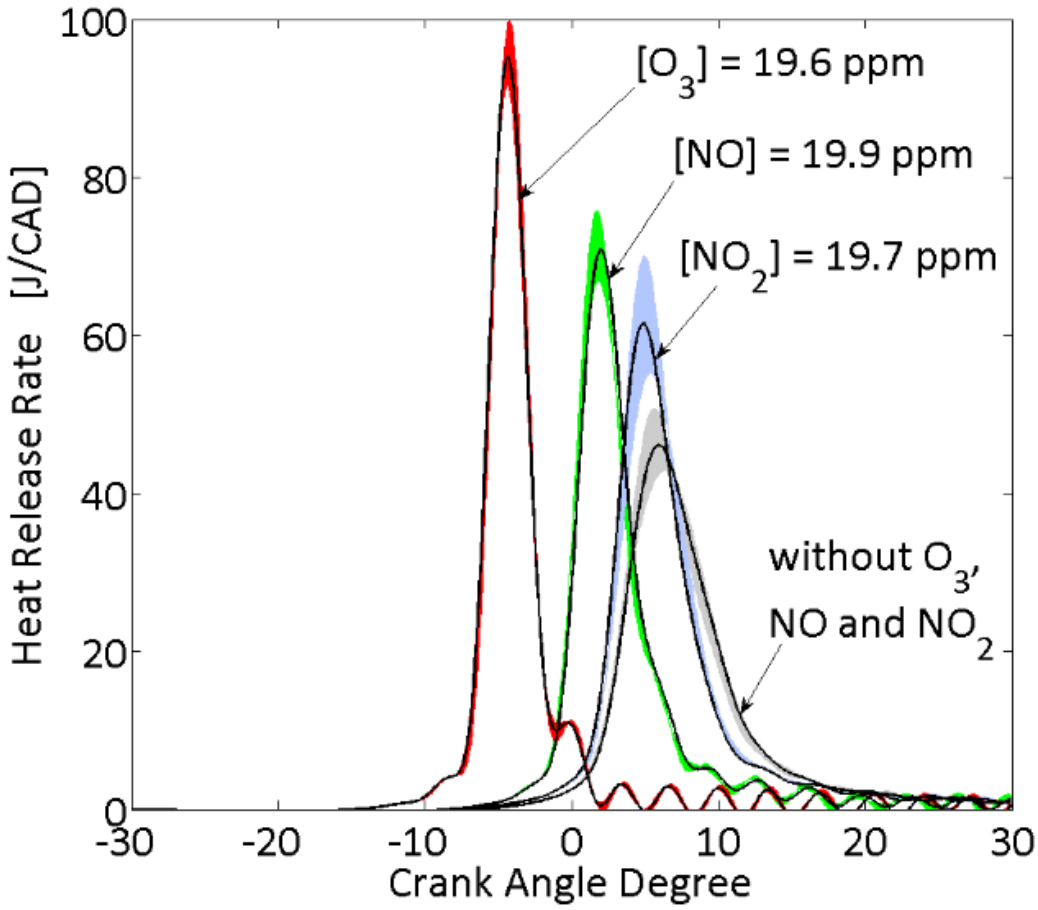

Figure 64. B. *Heat release rate traces without any species seeded and with 20 ppm of each oxidizing chemical species (O_3: ozone, NO: nitric oxide and NO_2: nitrogen dioxide) separately injected.*

at the intake and near misfires. Intake conditions were selected according to first results presented in this chapter for the combustion of pure PRFs. The intake pressure has been set at 1.2 bar and the intake temperature at 175 °C. The other engine parameters, the rotation speed and the equivalence ratio, has been tuned at constant values of N =1500 rpm and φ = 0.3, respectively. For this investigation, the three species selected were injected separately in the intake of the engine and their effect compared. The amount of ozone varied from 0 to 25 ppm while nitrogen oxides concentrations ranged between 0 and 100 ppm. The limit in ozone concentration was fixed according to previous experiments and the limit for nitrogen oxides was fixed based on the maximum NO_x levels permitted [112], [171], [172]. Results for in-cylinder pressure and heat release rate traces in the case of a seeding of 20 ppm of each oxidizing chemical species are presented in Figure 64. As previously shown, black curves correspond to the average of the 100 cycles recorded and shaded areas to the minimum and maximum variation of the same 100 cycles recorded. Generally, evolutions of these two parameters show that all the three oxidizing chemical species studied improve the combustion and advance its phasing. Indeed, in reference to the in-cylinder pressure traces without any seeding, the maximum pressure increases and move towards the top dead center. Similarly, the maximum of the heat release rate increases and its location advances. Moreover, this result was also confirmed regarding the IMEP. This parameter increases with the injection of these oxidizing chemical species. The covariance of the IMEP was also assessed and results show a decrease of the covariance, leading to a better stability of the combustion. The stability of the combustion may be also clearly observed with the variations of the in-cylinder pressure and heat release rate traces over the 100 cycles recorded. Similar results were also observed in the literature for nitric oxide and nitrogen dioxide additions [123], [124]. Finally, comparing the effect of each species for a constant concentration, ozone shows the best improvement while nitrogen dioxide the lowest.

To better appreciate the impact of these oxidizing chemical species, the CA50 of each experiments performed has been determined from the cumulative heat release rate traces. Results in Figure 65 show the shift of the CA50 in reference to that without any oxidizing chemical species injected. It may easily be observed that all these chemical species advance the HCCI combustion of isooctane and it is confirmed that ozone gives the most important advance phasing and nitrogen dioxide the lowest. Moreover, regarding the trends, it can be seen that ozone provides an exponential effect for the overall concentrations injected. In the case of nitric oxide, results also showed an exponential impact for amounts up to 40 ppm but lower than ozone and then, a linear decrease of the CA50. Finally, nitrogen dioxide leads to a linear advance of the combustion phasing for all the range of concentrations tested.

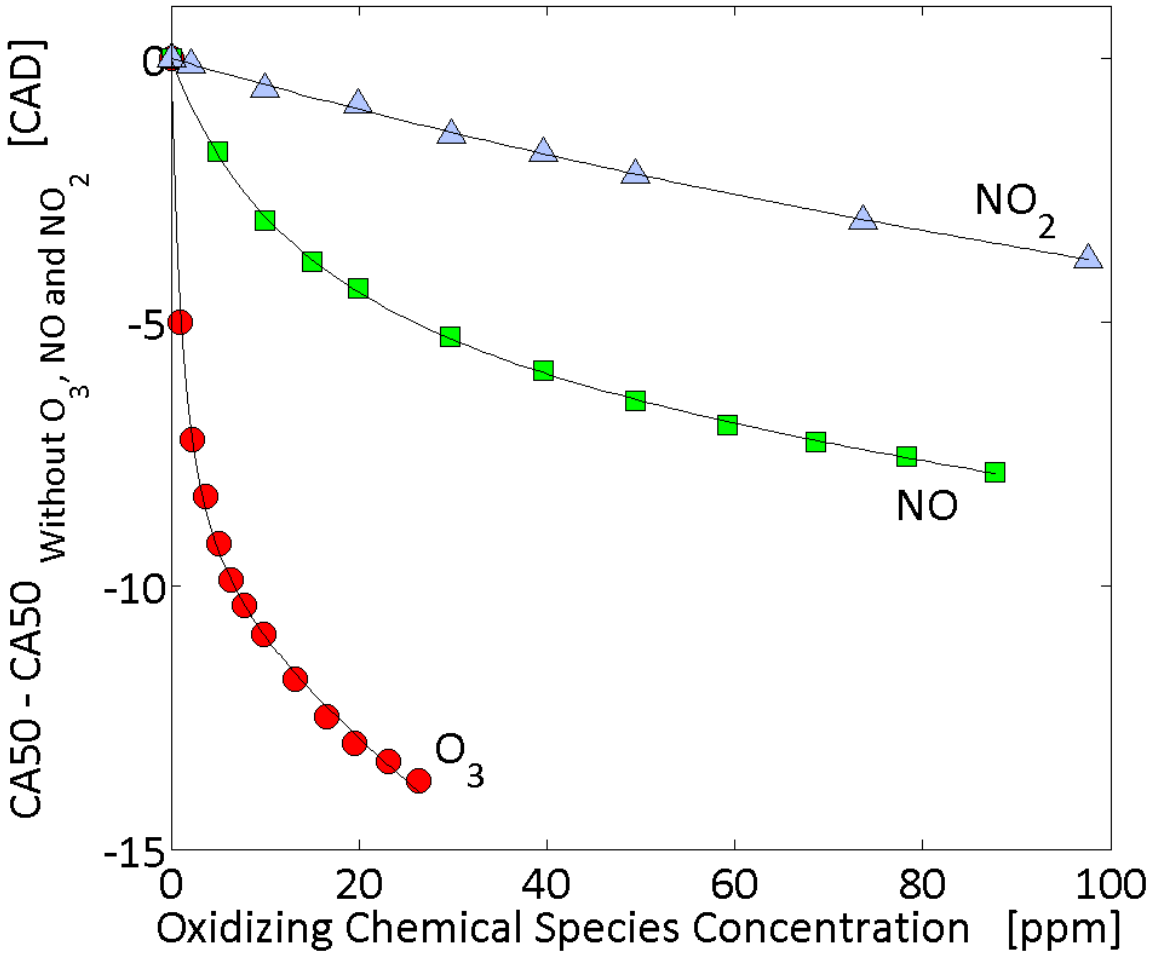

***Figure 65**. Shift of the CA50 as a function of the three oxidizing chemical species (O_3: ozone, NO: nitric oxide and NO_2: nitrogen dioxide) when they are separately injected.*

5.1.2. Kinetics results

Similarly to the investigation of the ozone effect, computations were run to further describe and compare the impact of these three oxidizing chemical species. The mechanism used here is based on the PRFs mechanism [30] to which two sub-mechanisms were added: one for ozone [132] and one for nitrogen oxides [158]. As previously, this new kinetics scheme has been validated from the computation of ignition delays. Simulations were therefore run for two case: with the PRFs mechanism alone and with the addition of both sub-mechanisms. Results obtained with the presence of these two sub-mechanism are identical to those obtained without their presence and this new kinetics scheme was validated. From now, simulations to study the respective impact of ozone, nitric oxide and nitrogen dioxide were run.

Computations were conducted on ignition delays for the three oxidizing chemical species. In the present case, initial conditions were fixed in agreement with the experimental

results. Equivalence ratio was fixed at 0.3, the initial pressure at 40 bar (pressure observed on the in-cylinder pressure evolutions prior to the auto-ignition), the initial temperature ranged from 650 K to 1000 K and concentrations of the oxidizing chemical species were all fixed at 20 ppm. Results are presented in Figure 66.

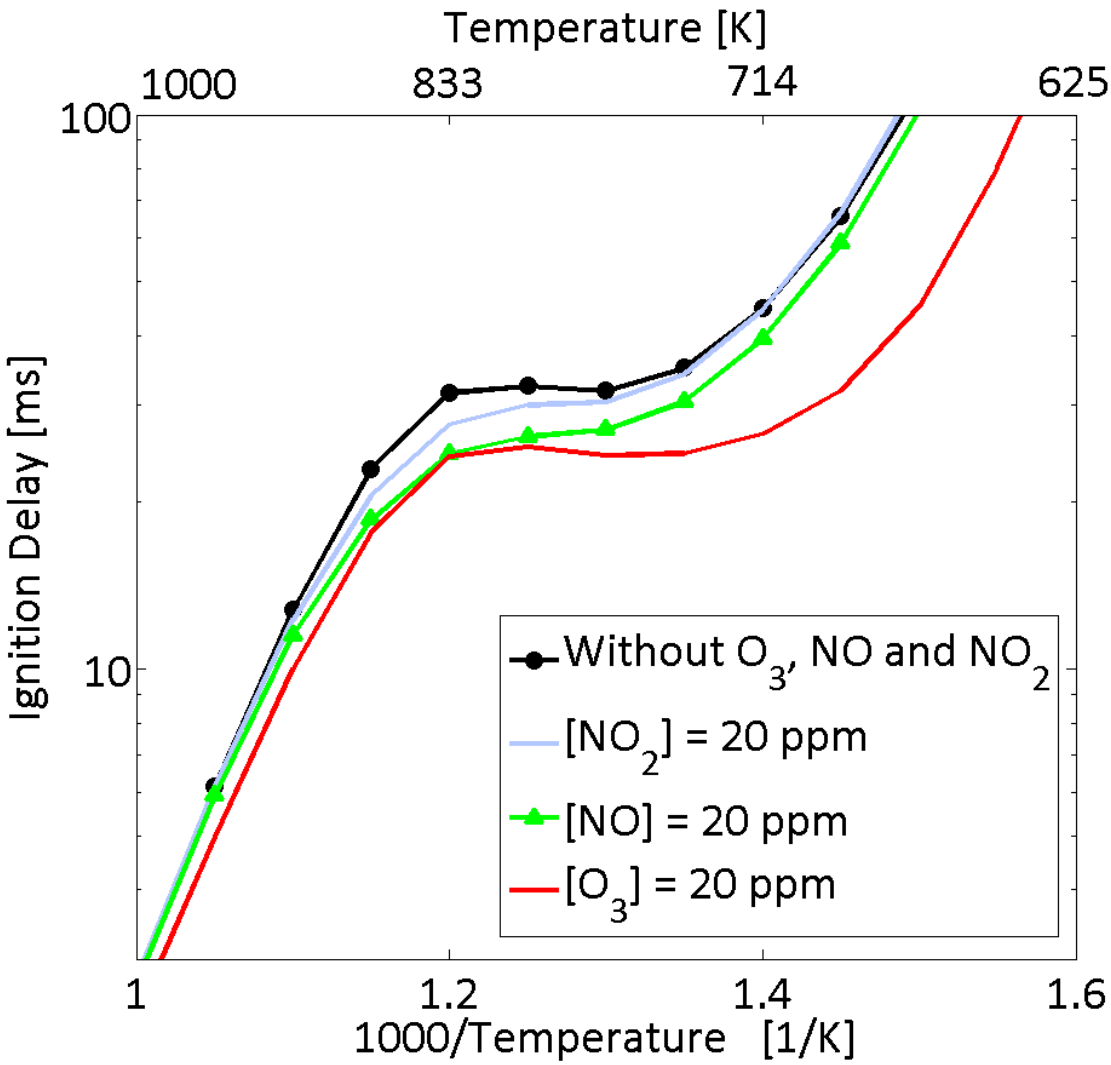

Figure 66. *Ignition delays computed over a large temperature range, for isooctane as fuel with an equivalence ratio of 0.3, for an initial pressure of 40 bar and 20 ppm of each oxidizing chemcial species studied.*

As already observed, ozone reduces the ignition delay on all the temperature ranges and mainly during the low temperature regime also corresponding to the cool flame domain. Nitric oxide also shows a decrease of the ignition delay but its effect on the cool flame domain is less pronounced than ozone and the main impact is visible on the negative temperature coefficient (NTC) temperature range. In the case of nitrogen dioxide, there is no impact on the cool flame domain and only a slight advance of the ignition delay during the NTC regime is visible. Finally, it may conclude that the ignition delays computed are in

agreement with experimental observations. Ozone well leads to the ignition delays the most shortened and nitrogen dioxide to the lowest.

Regarding the rates of consumption (ROC) for each oxidizing chemical species according to the previous computations, the impact of ozone previously described is not modified. Indeed, ozone mainly decomposes into oxygen molecules and O-atoms (R-29) which in turn directly oxidize the fuel and lead to the formation of OH radicals (R-30). Then, OH radicals rapidly consume the fuel (R-31) and the combustion occurs.

$$C_8H_{18} + O \rightarrow C_8H_{17} + OH \qquad \text{R-30}$$

$$C_8H_{18} + OH \rightarrow C_8H_{17} + H_2O \qquad \text{R-31}$$

In the case of nitric oxide, this oxidizing chemical species does not react with the fuel but with HO_2 radicals (R-32) resulting from the first oxidation of the fuel (R-33). This reaction leads to the formation of OH radicals which finally react with the fuel through reaction R-31. Instead of ozone which enables a fast consumption of the fuel through O-atoms prior to any reactions with the fuel, nitric oxide needs to wait for a first oxidation with molecular oxygen and the availability of a HO_2 radical. As a result, the earlier formation of OH radicals which enhance the fuel oxidation and the advance of the ignition timing is postpones.

$$NO + HO_2 \rightarrow NO_2 + OH \qquad \text{R-32}$$

$$C_8H_{18} + O_2 \rightarrow C_8H_{17} + HO_2 \qquad \text{R-33}$$

Similarly to nitric oxide, nitrogen dioxide does not react directly with the fuel and also needs the presence of HO_2 radicals coming from the reaction R-33 or the presence of methyl radicals (CH_3) to improve the combustion. As a result, the improvement of the combustion with nitrogen dioxide seeding comes from the following reaction system. The nitrogen dioxide which reacts with a CH_3 radical produces a nitric oxide (R-34) and then, nitric oxide leads to a OH radical through reaction R-32. However, the main pathway leading to the formation of OH radicals and to the combustion enhancement comes from reactions R-35 and R-36 with an intermediate radical. As a result, the need of a HO_2 radical explains that nitrogen dioxide has less impact than ozone on the HCCI combustion of isooctane and the presence of intermediate species explains that combustion improvement is lower than nitric oxide one. Indeed, further analyses on the rate of consumption showed that reactions R-35 and R-36 take place later than reaction R-32.

$$NO_2 + CH_3 \rightarrow NO + CH_3O \qquad \text{R-34}$$

$$NO_2 + HO_2 \rightarrow HONO + O_2 \qquad \text{R-35}$$

$$HONO + M \rightarrow NO + OH + M \qquad \text{R-36}$$

Finally, the improvement of the HCCI isooctane combustion through the use of these three different oxidizing chemical species may be summarized by Figure 67.

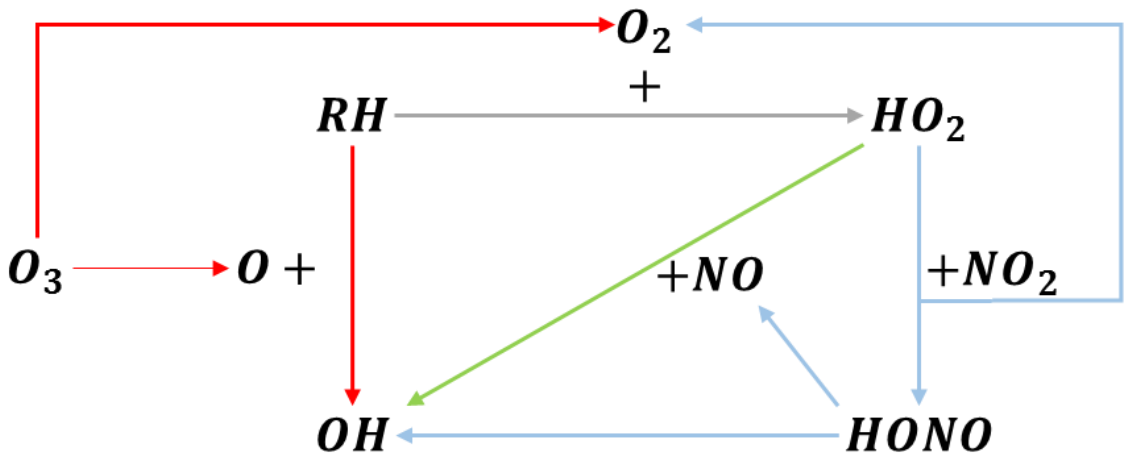

Figure 67. *OH radicals production in the presence of ozone, nitric oxide and nitrogen dioxide.*

5.2. Simultaneous seeding of ozone and nitric oxide

Previous results considered the impact of ozone, nitric oxide and nitrogen dioxide when they are separately injected into the intake of the engine. The two first species showed the most important impact on the combustion of isooctane. Moreover, nitric oxide is mainly present in exhaust gases when nitrogen oxides are detected and is the first nitrogen oxides produce from dielectric barrier discharge supplied by oxygen/nitrogen blend. In the present part, an injection of these two oxidizing chemical species together was considered through experiments followed by computations.

5.2.1. Experimental results

Experiments were performed according to the same conditions than those previous tuned, i.e. a rotation speed of 1500 rpm, an equivalence ratio of 0.3 and intake conditions of 1.2 bar and 175 °C. Both oxidizing chemical species, ozone and nitric oxide, were injected for concentrations from 0 to 55 ppm and from 0 to 70 ppm, respectively. The investigation was organized according to several repeated experiments by seeding alone a constant nitric oxide concentration and by varying the ozone concentration. Results obtained are presented in Figure 68 for in-cylinder pressure and heat release rate traces in the case without any seeding of ozone and nitric oxide (reference case) and in the case of a constant nitric oxide injection with several ozone concentrations. It can be seen that an injection of nitric oxide without ozone increases and advances both maximum in-cylinder pressure and maximum

heat release rate. Then, with a weak ozone injection, the combustion timing is slightly delayed and finally, continuing to raise the ozone concentration improves the isooctane combustion. There is therefore an

As for the results previously presented when ozone and nitric oxide were injected separately, the shift of the CA50 for the present experiments was plotted in reference to the case without any seeding. Results are presented in Figure 19. It may be observed that nitric oxide well advances the combustion phasing when no ozone is injected. Then, when the ozone addition starts, the combustion timing is slightly delayed but always advanced compared to the reference and finally, as soon as the ozone concentration reaches approximately the half concentration of nitric oxide, the CA50 strongly advances according to an exponential trend. Referring to literature observation, ozone and nitric oxide may easily react together through the reaction R-37 [160], [163]–[165], [168]–[170]. Therefore, when the nitric oxide is seeded alone, it is the only species which improves the combustion timing. With a small addition of ozone, ozone is consumed with a part of the nitric oxide through the reaction R-37 for generating nitrogen dioxide. As a result, it remains a lower concentration of nitric oxide than one initially introduced with low extra nitrogen dioxide amounts. As the concentration of nitric oxide decreases and as the impact of nitrogen dioxide is lower than one of the other oxidizing chemical species, the presence of both species in the mixture may explained the advance compared to the reference case and the short delay observed compared to a nitric oxide injected alone. Finally, for the last part of the trend observed in Figure 69, the exponential decrease is quite similar to the effect of seeding only ozone meaning that a part of the ozone is not consumed with nitric oxide and is available to strongly improve the isooctane combustion impact when both oxidizing chemical species seed together the intake of the engine.

$$O_3 + NO \rightarrow NO_2 + O_2 \qquad \text{R-37}$$

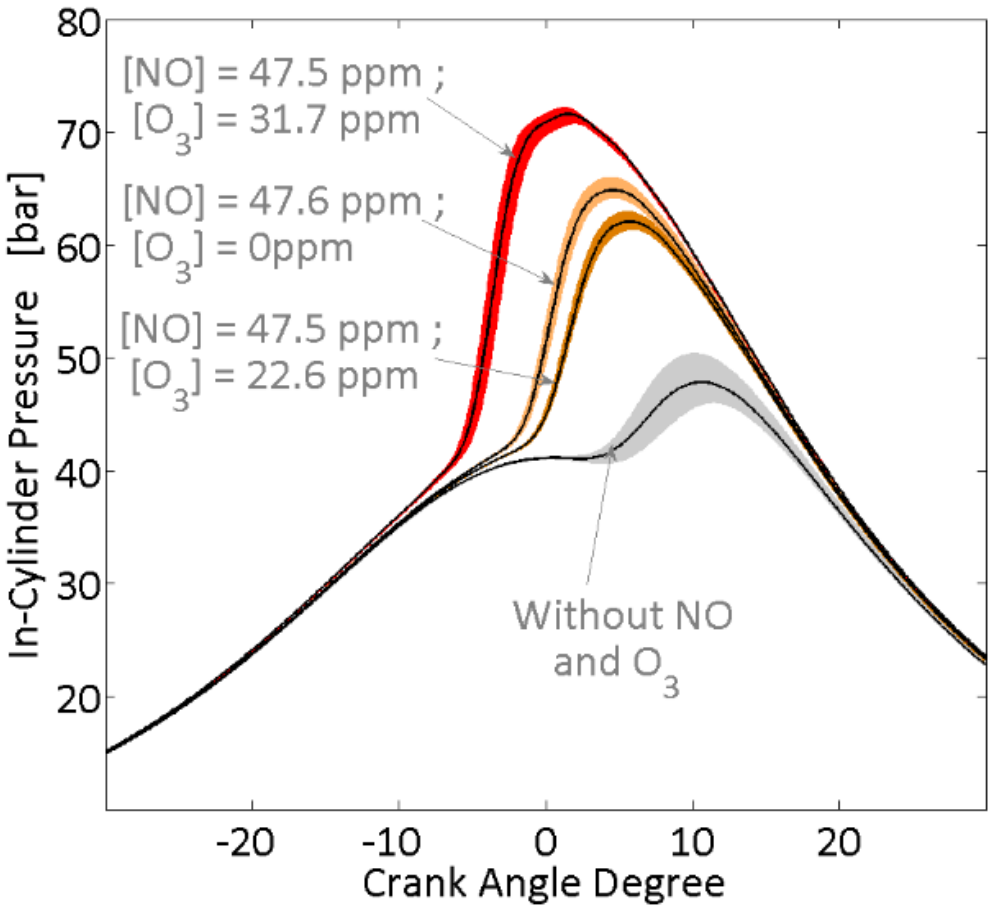

Figure 68. A. *In-cylinder pressure traces as a function of the crank angle degree for several couple of concentration in ozone and nitric oxide simultaneously seeded in the intake of the engine.*

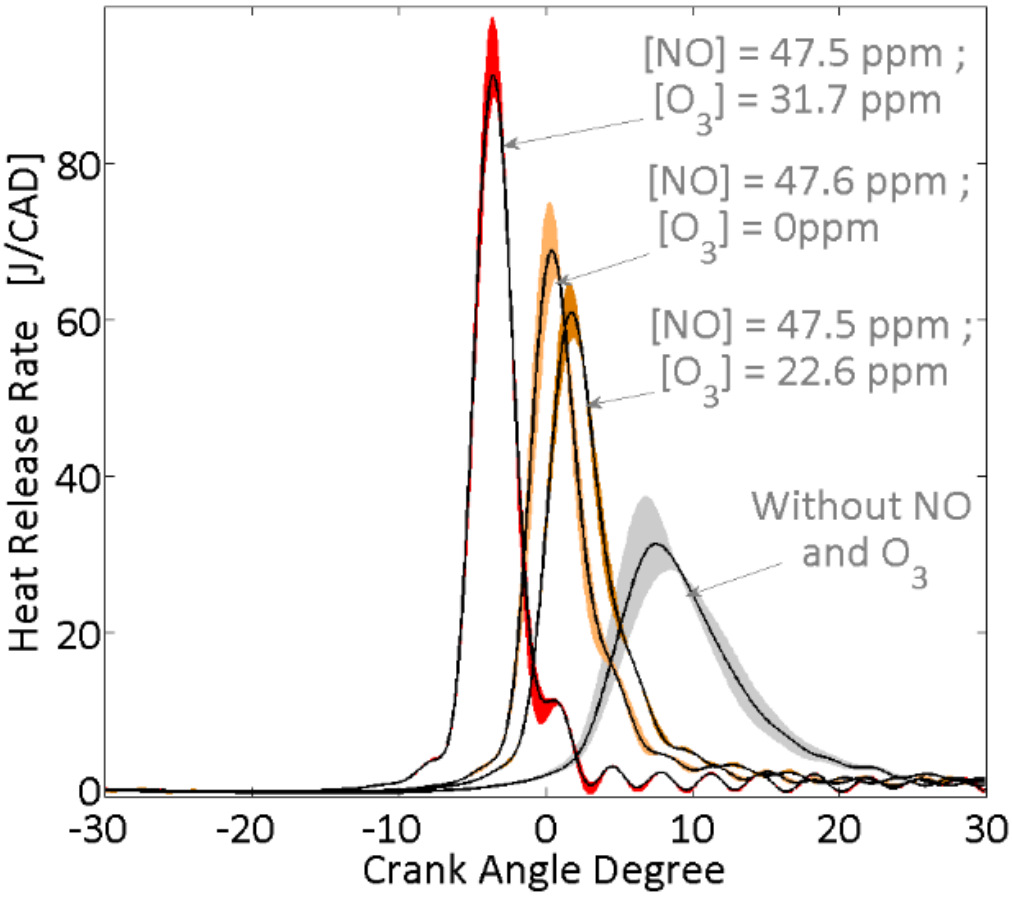

Figure 68. B. *Heat release rate traces as a function of the crank angle degree for several couple of concentration in ozone and nitric oxide simultaneously seeded in the intake of the engine.*

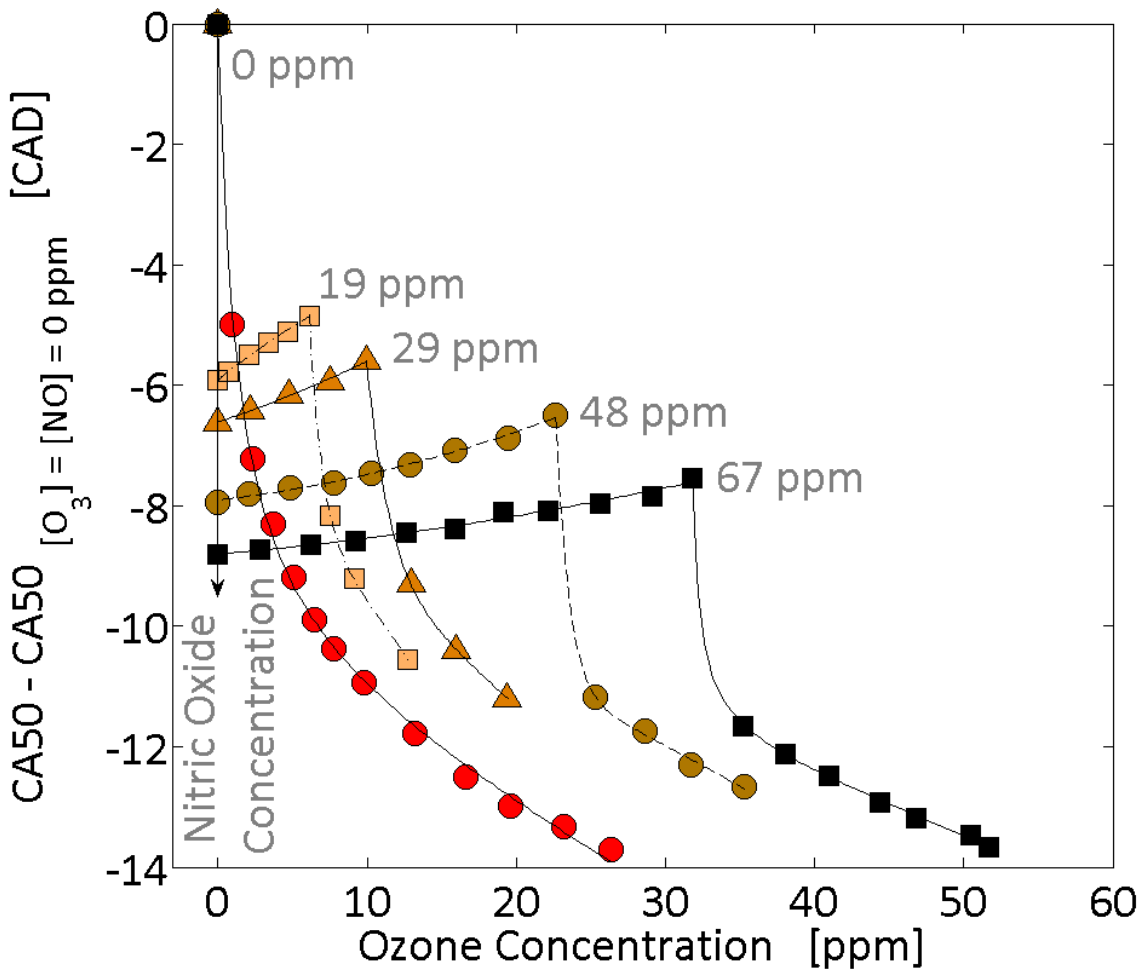

Figure 69. *Shift of the CA50 in reference to the case without any seeding as a function of the nitric oxide (concentrations in grey on the graph) and ozone when the two oxidizing chemical species seed simultaneously the intake of the engine.*

5.2.2. Kinetics results

Further analyzes of the effect of nitric oxide and ozone when they seed together the intake of the engine were carried out by running computations. Simulations were conducted by using the same kinetic scheme than that previously used for separately analyzing the impact of the three oxidizing chemical species. Initial conditions were chosen identical than previous computations achieved, i.e. for an equivalence ratio of 0.3, an initial pressure of 40 bar, a wide range of initial temperatures and by varying the initial concentrations of nitric oxide and ozone. Results obtained are presented in Figure 70 for concentrations of 50 ppm and 20 ppm for nitric oxide and ozone, respectively. These volume fractions were selected in accordance with in-cylinder pressure and heat release rate traces presented in Figure 68. It may be observed that when both oxidizing chemical species are separately added, their respective effect is well reproduced. Nevertheless, for the case where they are together

present into the initial mixture, ozone and nitric oxide show a combined effect on the computed ignition delays and the result poorly reproduced the experimental observation. Ideally the curve must be upper than the trend observed for only nitric oxide addition. Moreover, this combined effect was confirmed regarding the rate of consumption of these two oxidizing chemical species. For each of them, the main reaction pathways are the same than that described above when they are added separately and no reaction involving both species appeared. The lack of this reaction therefore explains the results observed in Figure 70.

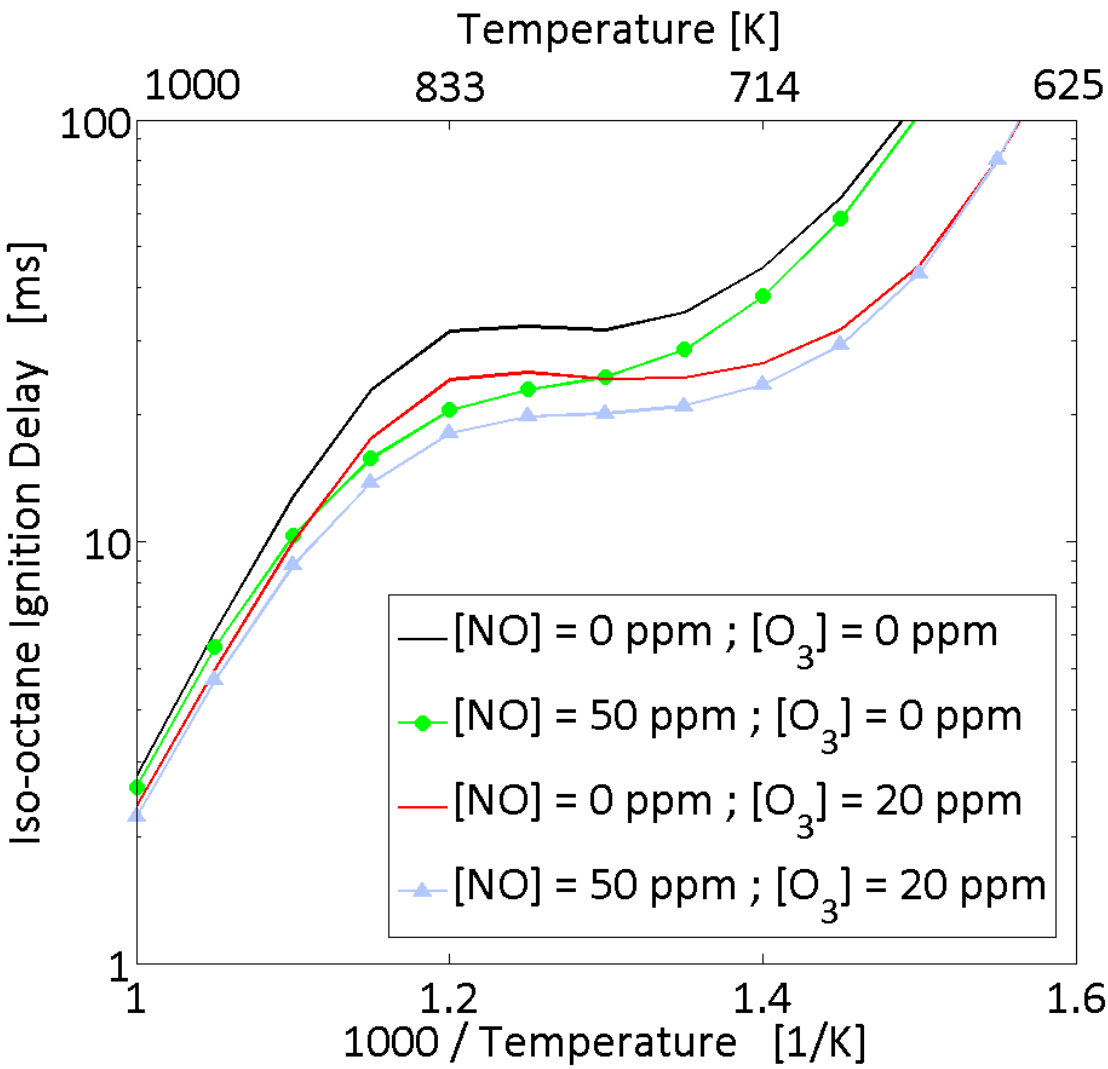

Figure 70. *Ignition delays computed over a large temperature range in the case without any seeding, when nitric oxide is seeded alone, when ozone is seeded alone and when both oxidizing chemical species are together present.*

According to the literature, the ozone and nitric oxide may react together under low temperature such as ambient temperature [160]. With the help of further experiments, the ozone concentration was measured at the intake of the engine when both species are injected simultaneously without any fuel. The results showed that ozone concentrations

decrease almost linearly with the increase of the nitric oxide and as soon as the injected concentration of each of them is equal, the ozone concentration measured is zero (Figure 71). As a result, ozone and nitric oxide rapidly react together before their entrance into the combustion chamber and it can be assumed that the mixture may contain ozone, nitric oxide and nitrogen dioxide during experiments.

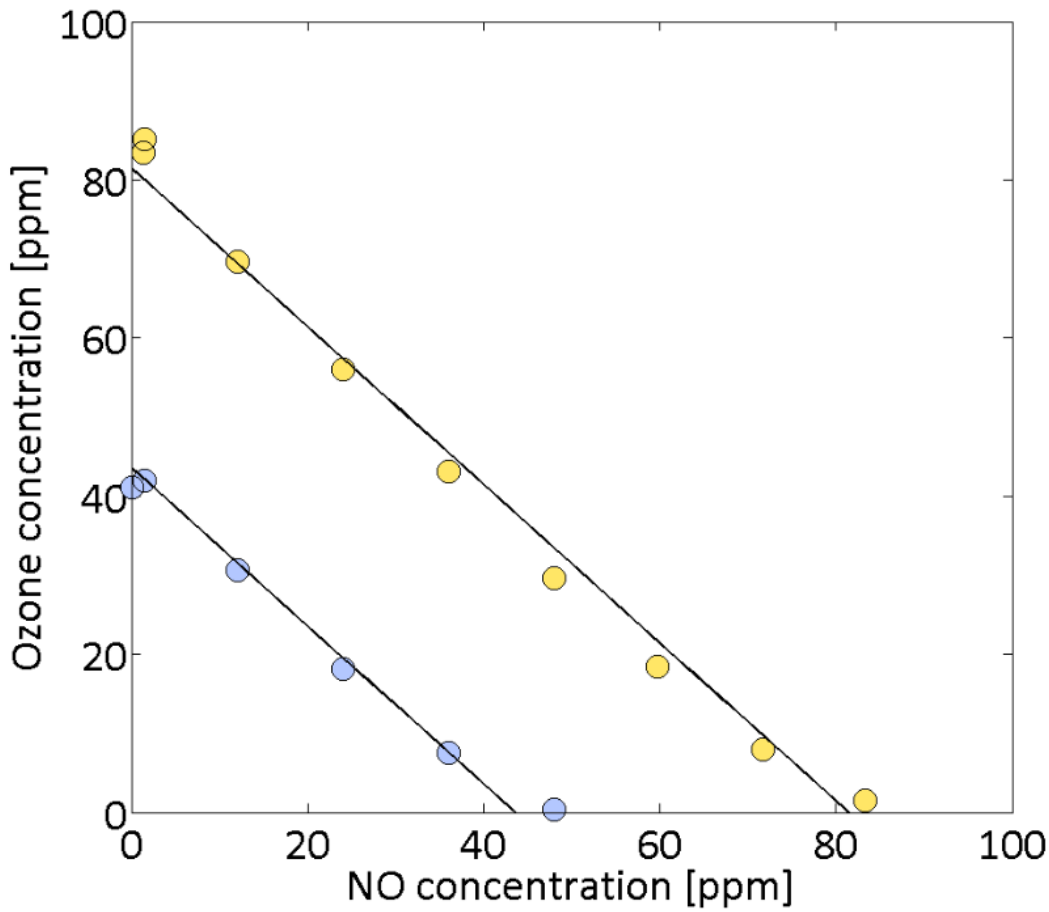

Figure 71. *Ozone concentrations measured at the intake of the engine as a function of the nitric oxide concentration injected into the plenum for two different initial concentration of ozone. Blue markers correspond to an initial ozone concentration of approximately 40 ppm and yellow markers to an initial ozone concentration around 80 ppm.*

Therefore, a new approach for computations was implemented and consists of carry out simulations in two steps (Figure 72). The aim of the first step is to compute the intake of the engine, more precisely the plenum, according to the residence time (τ) of the homogeneous mixture inside this volume ($\tau \sim$ 4s) and constant intake thermodynamic conditions. Then, these output results are used as initial conditions for the second step of the computation and finally, enable to run simulations of the ignition delays, similar to those previously conducted, for an initial pressure of 40 bar (in-cylinder pressure observed before the combustion occurs) and over a wide range of temperature.

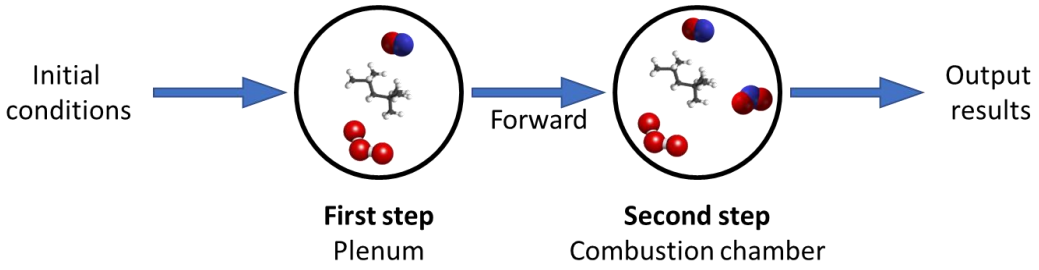

Figure 72. *Scheme of the two-step computation.*

According to this new approach, computations under various initial concentrations of nitric oxide and ozone were carried out in the conditions cited above and for an equivalence ratio of 0.3. Results at the end of the first step showed that both oxidizing chemical species rapidly react together (less than 1s) and produce nitrogen dioxide.

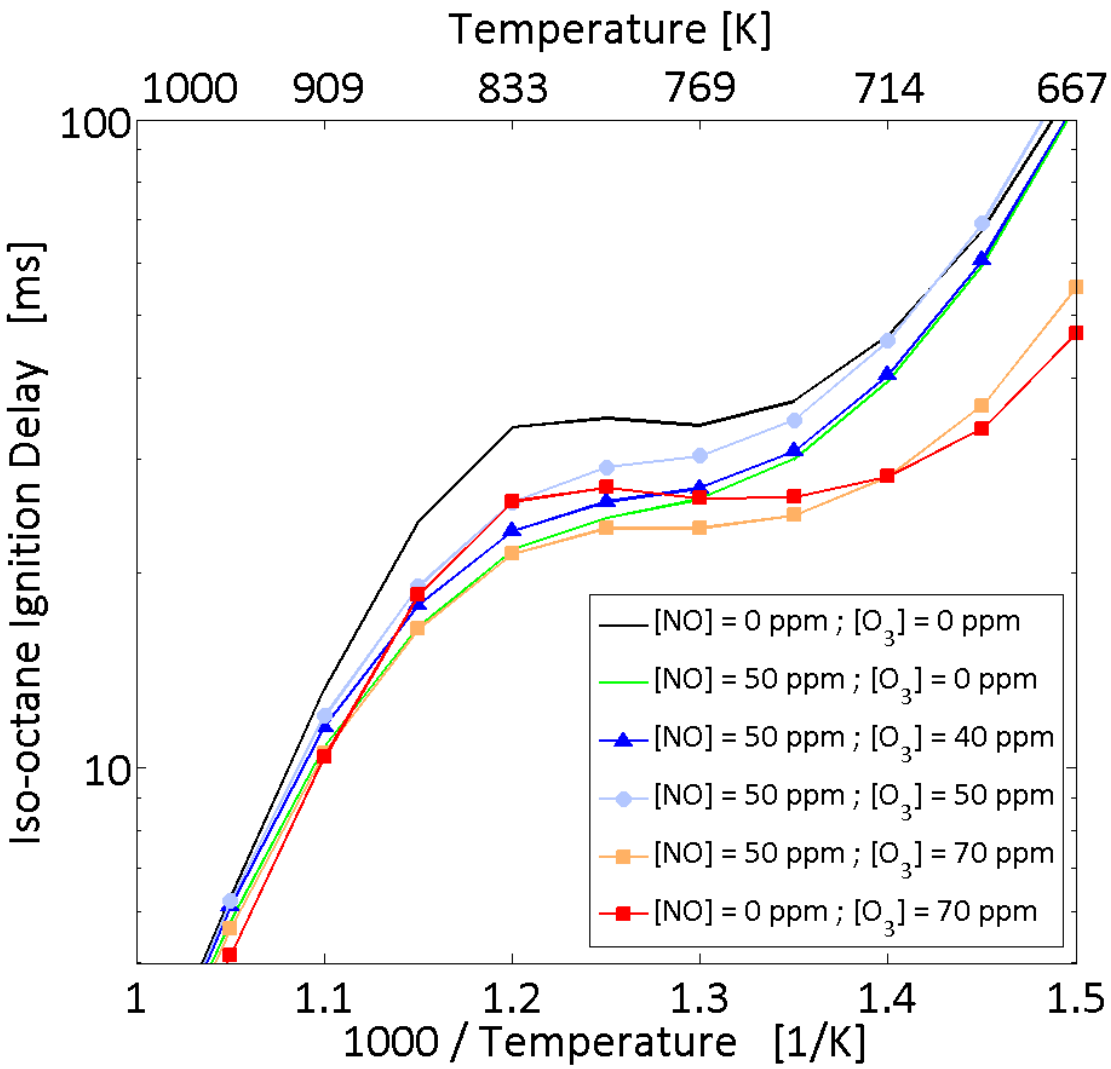

Figure 73. *Ignition delays computed in two steps over a wide range of temperature and under various nitric oxide and ozone concentrations.*

Depending of the initial concentrations, several cases take place. If the concentration in nitric oxide is greater than that of ozone, ozone is fully consumed and replaced by nitrogen dioxide according to the reaction R-37 ($O_3 + NO \rightarrow NO_2 + O_2$). The second step of the computation therefore starts with amounts of nitrogen dioxide (NO_2) and a part of the nitric oxide NO which did not react during the first step. Inversely, when ozone concentration is greater than that of nitric oxide, NO is entirely consumed to generate NO_2 and some ppm of ozone remain. However, after the total consumption of nitric oxide, ozone decomposes by itself due to the temperature but this effect stays moderated and a part of this chemical species remains for the second step of the computation. Finally, ignition delays are obtained after the second step of the computations. Results are presented in Figure 73. It may observe that when nitric oxide is seeded alone, the ignition delay is well advance compared to the reference without seeding. Then, with an ozone concentration lower than the concentration of nitric oxide, the ignition delays computed are slightly delayed but always in advance compared to the reference and finally, when ozone amount becomes greater than that of nitric oxide, the ignition delays strongly decreases. In the case where nitric oxide and ozone are with the same initial concentration, there is only nitrogen dioxide during the second step of the computation. These last results were compared with a simulation with only nitrogen dioxide and for the same initial concentration. Outputs show a weak variation which can be neglected.

Finally, the results obtained according to this two-step computation satisfactorily explain the experimental observations. However, during experiments, the transition on CA50s with the increase of the ozone and a constant concentration of nitric oxide has been observed when the ozone amount is approximately the half of nitric oxide amount while during computations, the transition occurs when the ratio between these two species is about 1. This effect was attributed to a partial stratification which may take place inside the plenum during the injection of the oxidizing chemical species and before the entrance of the fresh gases into the combustion chamber. As a result, there is less nitrogen dioxide produce experimentally than during computations. However, it was also observed that nitrogen dioxide may consumed ozone into the plenum (Figure 74). A reaction between ozone and nitrogen dioxide could compete with the reaction between ozone and nitric oxide leading to a higher nitric oxide concentration into the combustion chamber. This assessment may considered when the CA50 is delayed with a nitric oxide injection and a small ozone concentration (Figure 69) but does not explain the strong advance observed on the CA50 when a higher ozone concentration seeds the intake of the engine. According to the trend observed with our experimental results, it may assume that the impact comes from chemical interactions between ozone and isooctane. Under these intake temperatures, fuels may be partially oxidized [113], [114], [173] and may lead to the advance observed. Therefore, there is probably a competition between ozone consumed by nitric oxide and ozone which breaks down to O-atom which finally oxidizes the fuel. This assumption on a competition between

these reactions is likely the main reason leading to the phenomenon observed. In front of this issue, our experimental setup used here is not appropriated to study such chemical interactions and further investigations with another experimental setup such as a flow reactor are needed.

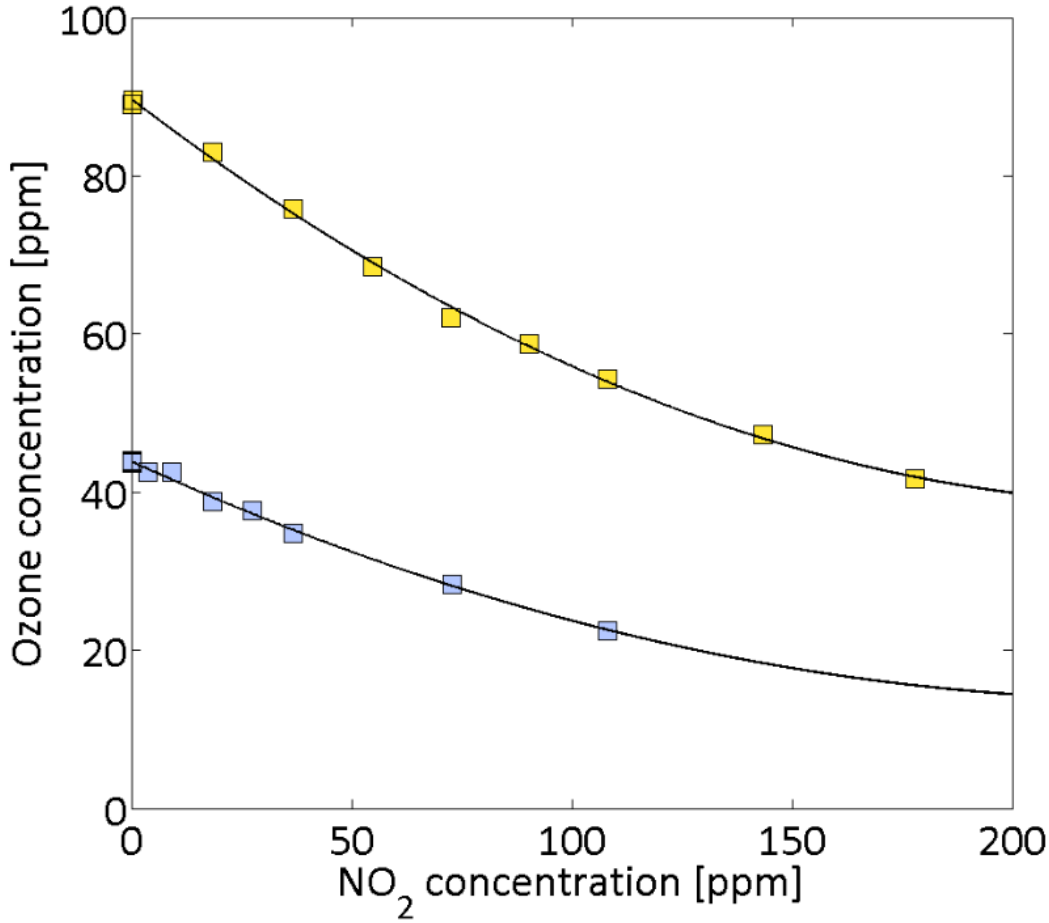

Figure 74. *Ozone concentrations measured at the intake of the engine as a function of the nitrogen dioxide concentration injected into the plenum for two different initial concentration of ozone. Blue markers correspond to an initial ozone concentration of approximately 40 ppm and yellow markers to an initial ozone concentration around 90 ppm.*

6. Application case (Article IV)

The impact of several oxidizing chemical species, which may be produced by ozone generators, was previously examined and showed a potential for controlling HCCI combustion process. The following investigation takes place to highlight the impact of using an ozone generator by considering a real application for automotive vehicles. The effect on all the engine outputs was observed with isooctane as fuel and finally, a dynamic control of the combustion was achieved and corresponds to the final achievement of this Thesis.

For studying the effect on engine outputs, the use of two different gases supplying an ozone generator was compared. 1) The first was pure oxygen which avoided the formation of nitrogen oxides species and 2) the second was air, which could be more suitable for an application on board a real vehicle. Moreover, before achieving a dynamic control of the HCCI combustion, the injection position of the oxidizing chemical species was examined also following two different cases: an injection into the plenum located upstream the intake of the engine and an injection into one of the engine pipes (Figure 75).

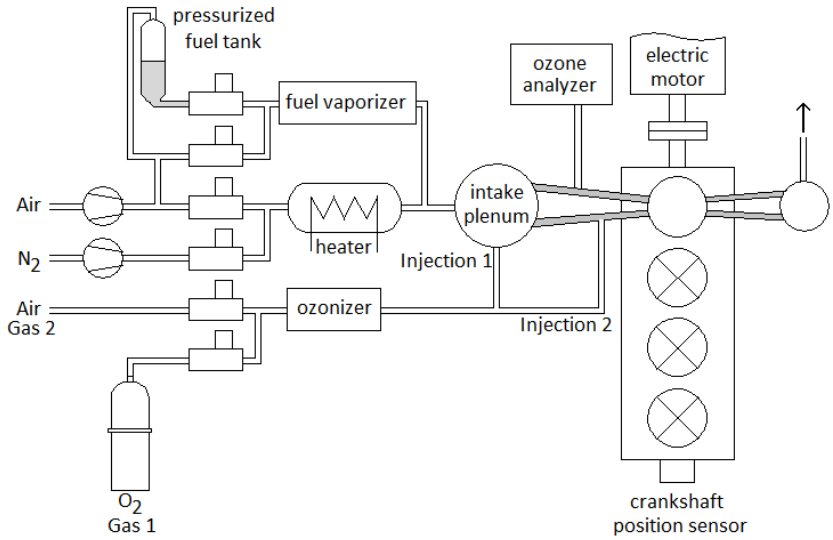

Figure 75. *Scheme of the experimental setup for the application case. The ozone generator may be supplied either by pure oxygen or air and the ozone produced can be injected either inside the plenum or into one of the intake pipes.*

6.1. Ozone calibration

Before running combustion experiments, calibrations were performed to estimate the ozone concentrations generated and injected into the combustion chamber. The quantification was carried out under motoring operations for both supply gases studied and for three intake temperatures selected, i.e. 100 °C, 150 °C and 200 °C. The sample for analyzing the ozone concentrations into the mixture was taken on one of the engine intake pipes while the ozone was injected inside the intake plenum upstream the intake pipes to

enable a homogeneous mixture with ozone (injection 1 on Figure 26). Results for the ozone concentration are presented as a function of the ozone generator capacity in Figure 76.

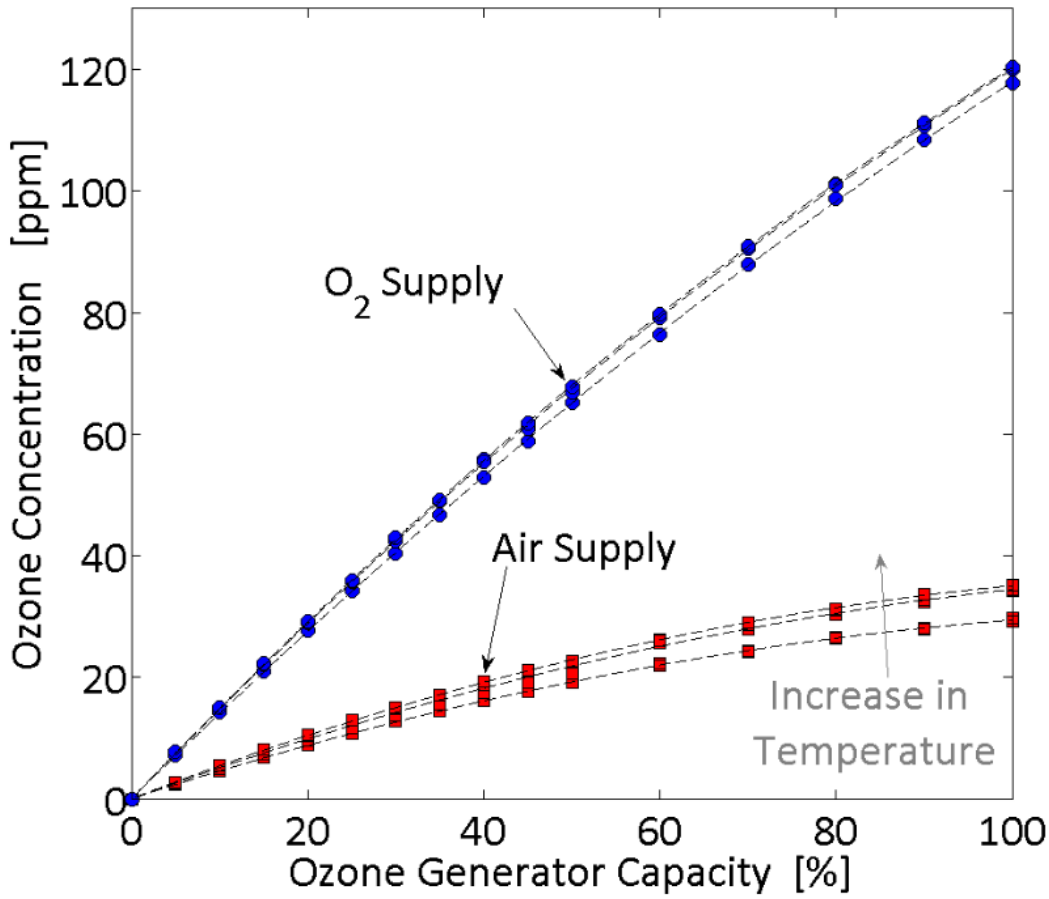

Figure 76. *Calibration of the ozone concentration measured at the intake of the engine as a function of the gas supply (pure oxygen and air) and for three different intake temperatures (100 °C, 150 °C and 200 °C).*

Results show that increasing the ozone generator capacity rises the ozone concentration injected into the combustion chamber. Moreover, depending on the increase of the temperature, it may be also observed an increase of the O_3 concentrations. This growth is explained by the fact that the ozone generator is supplied with a constant flow meaning that the ozone production is kept constant and the increase of the temperature at the intake results in a decrease of the total volumetric flow. Therefore, the ozone is less diluted and the concentration increases. However, for temperatures of 150 °C and 200 °C, there is a very slight difference of the trends which is due to the high intake temperature. Indeed, ozone is particularly sensitive to the temperature which exponentially breaks down ozone and strongly reduce its half-life time when it increases and therefore leads to a depletion of ozone. Finally, comparing the ozone concentration for the two different gases supplying the ozone generator, the same conclusions may be achieved except that for an air

supply, the ozone concentration is lower than for a pure oxygen supply. Indeed, it is normal to observe a lower ozone concentration as the oxygen fraction is approximately 21% in the air. However, even if there is a ratio of five in oxygen between both gases selected, the concentration of ozone is not five times lower but between three and four times lower. Similar results were already observed in ozone generation studies [160], [163], [173], [174]. As a result, the ozone production strongly depends on the ozone generator but also on the intake temperature of the engine and the nature of the gas supply.

For the case of the injection near the intake valve (injection 2 on the Figure 26), measurements of the ozone concentration were not available as the ozone has not enough time to be well mixed with the main flow and it was impossible to carry out a sample. Therefore, results as a function of ozone concentrations will be presented from the calibration performed with the first injection. Only the study on the impact of the gas supply will use the ozone concentration and, most of the time, the ozone generator capacity will be used instead.

6.2. Comparison of the gas supply

According to the results on the calibration of the ozone generator, the most efficient gas supply is the pure oxygen but for an automotive application, air will be more appropriated. The aim here is to compare the impact of the gas supply on the combustion results, more precisely on the combustion phasing from the observation of the maximum pressure location. Experiments were conducted for isooctane as fuel, under a constant intake pressure of 1 bar and for three intake temperature of 100 °C, 150 °C and 200 °C, respectively. Ozone was injected inside the plenum and was respectively produced from pure oxygen in a first time and then from air. Results for an increase of the ozone generator capacity on the combustion phasing can be observed in Figure 77.

Results are presented for both gas supply selected and were plotted referring to the ozone generator capacity tuned and then from the ozone concentration estimated previously. As previously observed in previous experiments, ozone allows advancing the maximum pressure location towards the top dead center according to an exponential trend. Applying a low capacity on the ozone generator results in a significant advance of the combustion phasing while with a high capacity, the combustion phasing moves slightly. Moreover, this effect is particularly pronounced for high temperatures. For lower temperatures, a minimum ozone concentration is required and the exponential trend is kept but with less impact. Depending on the nature of the gas supply, it may see that air has a lower impact for a same ozone generator capacity due to the lower ozone concentration generated and injected. The tuned capacity must be therefore strongly increased with air as gas supply to achieve a similar phasing than with oxygen as gas supply. Nevertheless, air can be used to ensure the HCCI combustion of isooctane.

Finally, observing the maximum pressure location trends according to the ozone concentration estimated previously, it might conclude that there is no dependence of the gas supply. It is also possible to conclude that the use of air with the present ozone generator leads to only an ozone production and avoids the formation of nitrogen oxides. Measurements of nitric oxide and nitrogen dioxide were conducted at the intake of the engine and did not exceed 1 ppm. Their presence has been neglected. However, it is important to note that the ozone generator used for this study was designed to avoid the production of such unfavorable species but their formations could not be omitted in the case of an ozone generator with malfunctions or for an onboard automotive ozone generator. Therefore, the ozone generator which will be implemented into a vehicle must be developed to suit such an application. Moreover, as the maximum ozone concentration achieved for an air supply is less than 40 ppm, no results are available at 100 °C. Indeed, ozone concentration needed to start the combustion is approximately of 50 ppm and the ozone generated is insufficient. Moreover, the limit for maintaining the isooctane combustion near misfires with the ozone capacity tuned to the maximum was established experimentally at 120 °C.

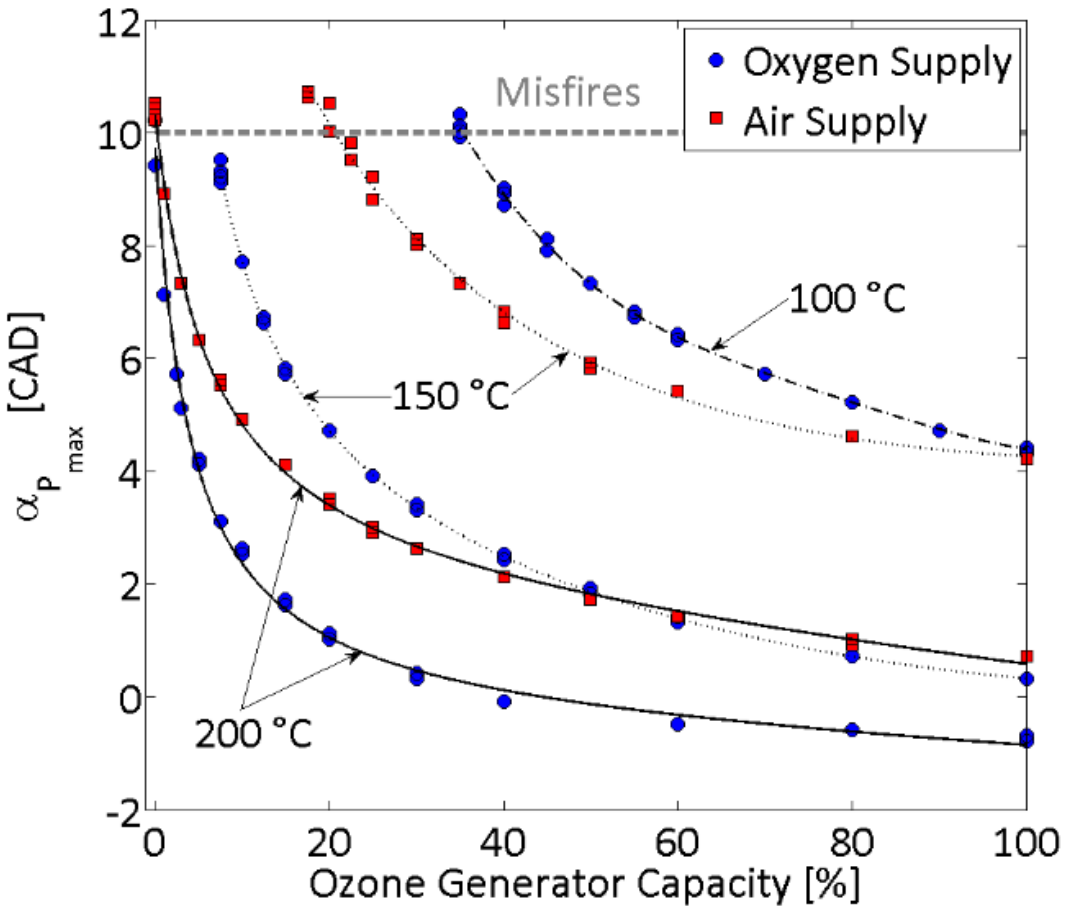

Figure 77. A. *Phasing of the maximum pressure location as a function of the ozone generator capacity for an oxygen supply and an air supply*

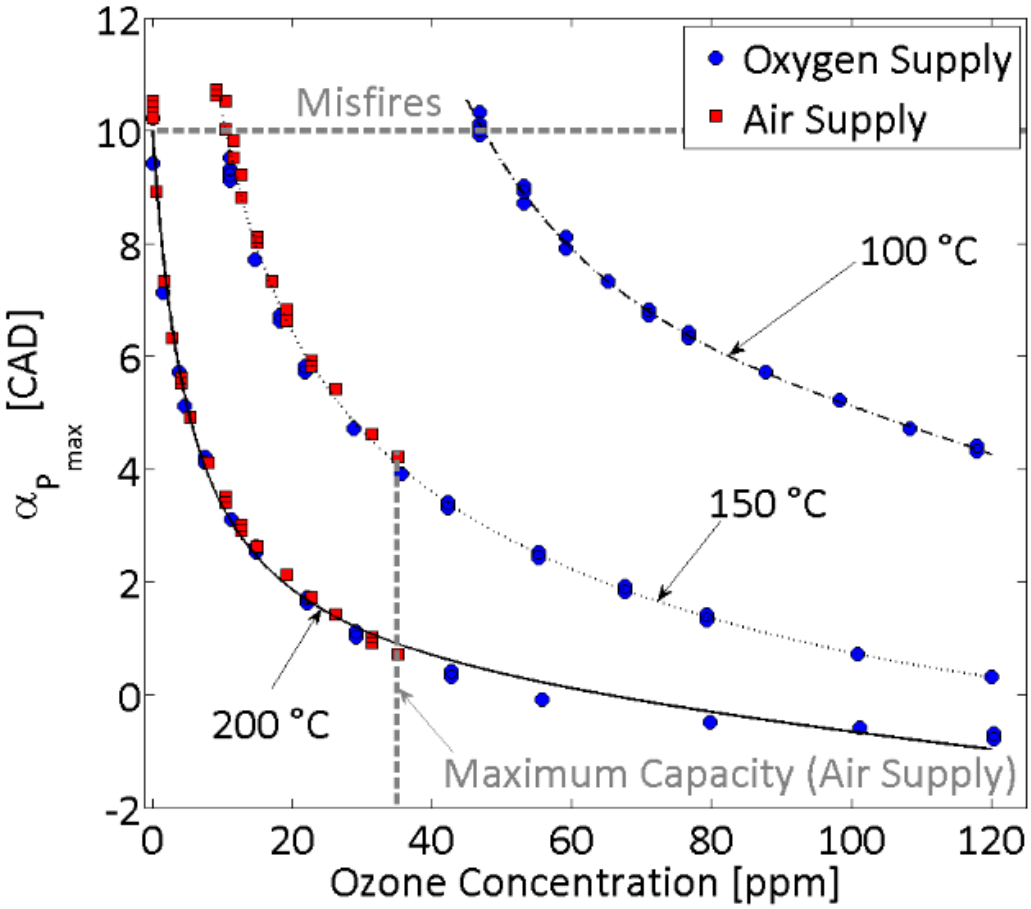

Figure 77. B. *Phasing of the maximum pressure location as a function of the ozone concentration for an oxygen supply and an air supply.*

6.3. Comparison of the injection position

As introduce in the beginning of this application case part, the aim is also to compare the impact of the injection position for ozone. According to the experimental setup, two kinds of injection were carried out: an injection inside the plenum and an injection inside one of the pipes near the intake valve of the engine. The first enables to let enough time to create a homogeneous mixture with the ozone while the second will probably lead to a stratification of the ozone into the combustion chamber. Experiments were performed under the same conditions than those previous used for investigating the impact of the gas supply and the maximum pressure locations for each condition were analyzed.

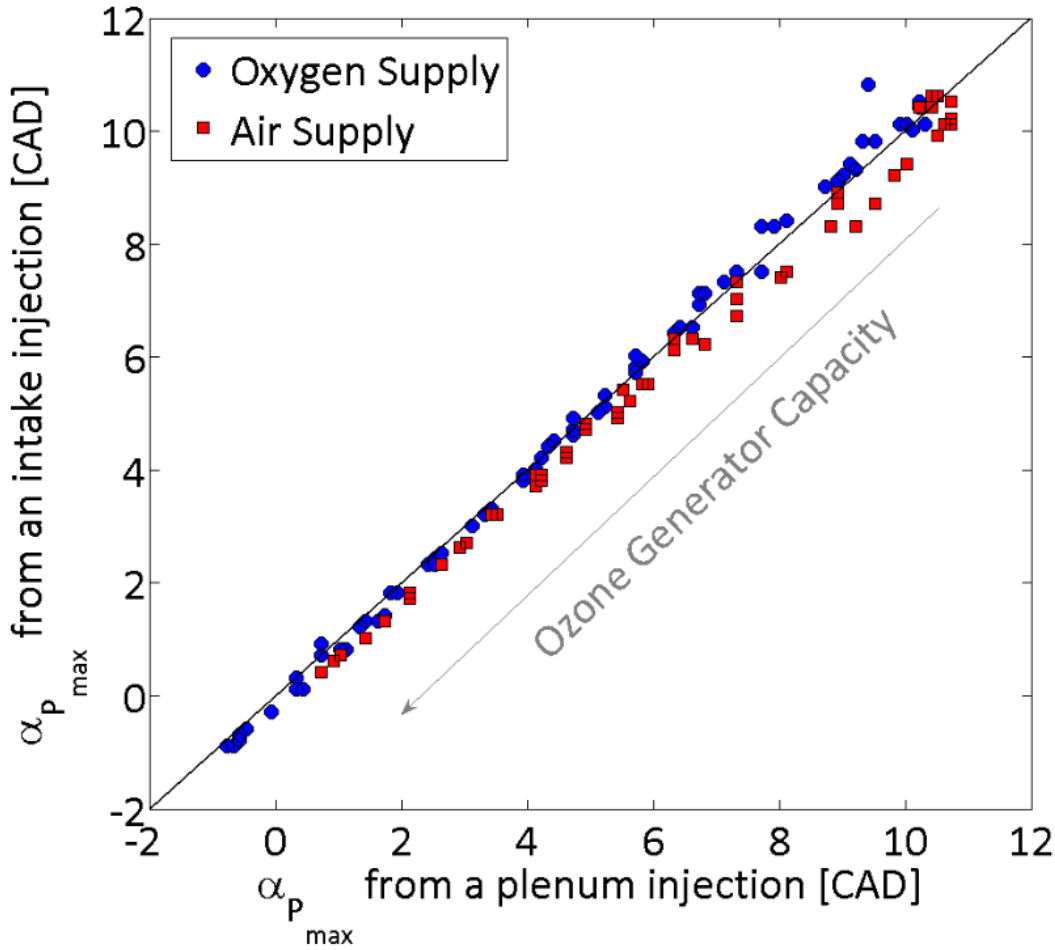

Figure 78. *Effect of the ozone generator capacity on the maximum cylinder pressure for the two different injection positions, for the two different gases supplying the ozone generator (neat oxygen and dry air) and for the three intake temperatures selected (100 °C, 150 °C and 200 °C).*

Figure 78 presents the trends of the maximum pressure location for an injection into the intake of the engine as a function of the same parameter for a plenum injection with the same ozone generator capacity tuned, for the three intake temperatures selected and for the two different gas supply previously studied. Results clearly showed that there is no

difference between the two injection positions and there is also no difference by changing the gas supplying the ozone generator. The results mean that the ozone is efficiently mixed with the air/fuel mixture inside the combustion chamber. As a consequence, these results are particularly interesting for a future dynamic control of the HCCI combustion with such a technique. Indeed, by injecting the ozone very near the intake valve of the engine, the residence time between the ozone production and its injection inside the combustion chamber is strongly reduced. Controlling cycle-to-cycle the HCCI combustion is therefore possible.

6.4. Experimental results

Previous results showed that the HCCI combustion process of isooctane may be controlled efficiently by using an ozone generator. Moreover, air may supply such a device and leads to ozone concentrations without any nitrogen oxides and finally, the injection may be performed near the intake valve of the engine to achieve a cycle-to-cycle control of the combustion. Considering this injection position, the other engine outputs were analyzed for both kind of gas supply chosen. The goal here is to go further in our investigations, as there is no impact on the results in term of ozone concentrations by using either pure oxygen or air. All these results are presented as a function of the maximum pressure location since varying the ozone generator capacity may control this parameter.

6.4.1. Engine outputs

6.4.1.1. Combustion phasing

Combustion phasing is here represented from CA10, CA50 and CA90 determined from the cumulative heat release rate traces. As a function of the maximum cylinder pressure location (Figure 79), all the parameters showed a linear decrease with the increase of the ozone generator capacity, especially for a maximum pressure crank angle located between the top dead center and 10 CAD after this position. Beyond 10 CAD, the deviation observed is related to the occurrence of misfires over the 100 cycles recorded, i.e. that some cycles present a negative IMEP. Prior to the top dead center, the other deviation is related to an advance of the auto-ignition of the isooctane while the maximum pressure location cannot advance more due to the motion of the piston. Similar results were already observed into the literature and it was assumed that this curve followed third order polynomial trends [52]. Moreover, it can also be noted that there is no dependence to the intake temperatures on the evolution of these combustion phasing as well as no effect of the gas supplying the ozone generator. Finally, as the CA10 and CA90 evolve linearly with two different slopes, it may conclude that the combustion duration also evolves linearly and it declines with the increase of the ozone concentration injected.

Consequently, these results demonstrated that controlling the ozone generator capacity and the ozone concentration injected allow to manage the maximum pressure phasing as well as the combustion phasing.

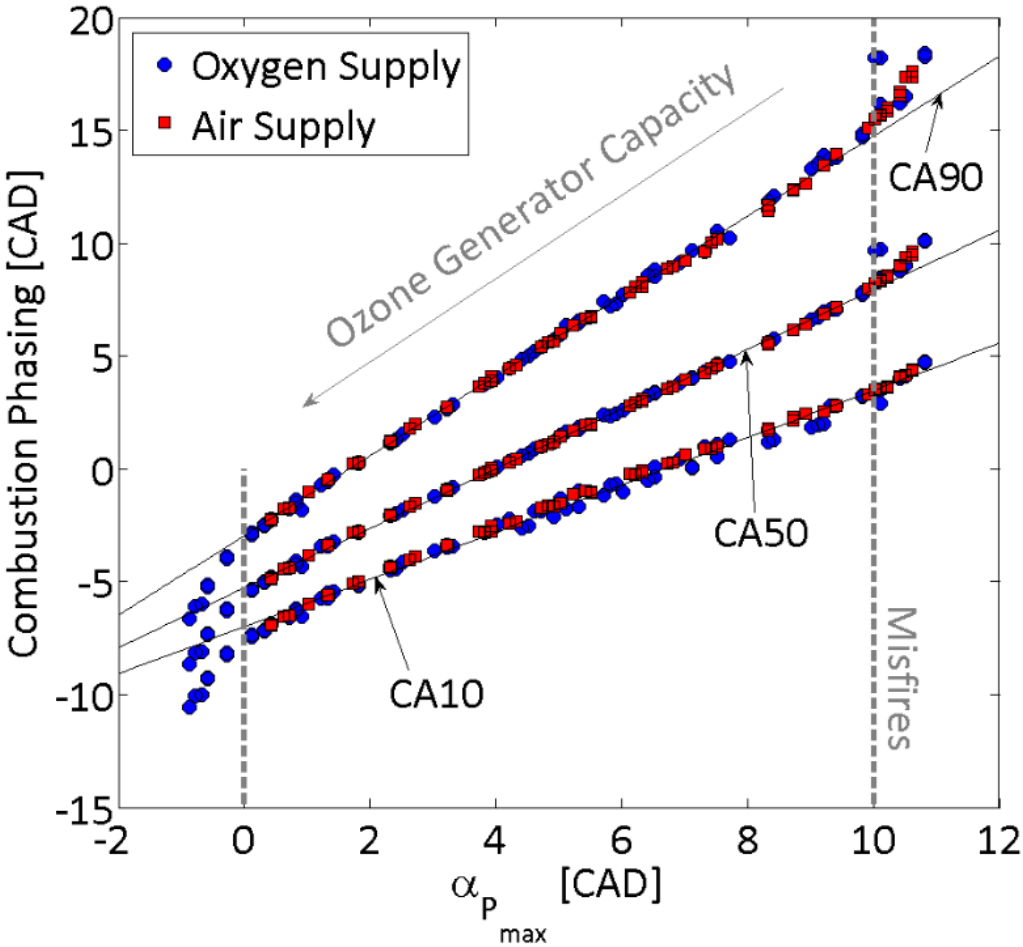

Figure 79. *CA10, CA50 and CA90 as a function of the maximum pressure location for both types of gas supply, for an injection inside the intake pipe and the three intake temperatures tuned.*

6.4.1.2. Indicated mean effective pressure

The indicated mean effective pressure (IMEP) was determined from the in-cylinder pressure traces and the results are showed in Figure 80. It can be observed that this parameter evolves following parabolic curves and therefore it presents a maximum value. According to the results, this value is reached between 2 CAD and 4 CAD and is variable with the intake temperature tuned. Decreasing the intake temperature allows to increase the IMEP as the fuel mass or the energy introduced inside the combustion is more important. Similar trends were also already observed in the literature. Finally, it may also conclude that this parameter could be controlled by varying the ozone generator capacity and tuning the intake temperature of the engine.

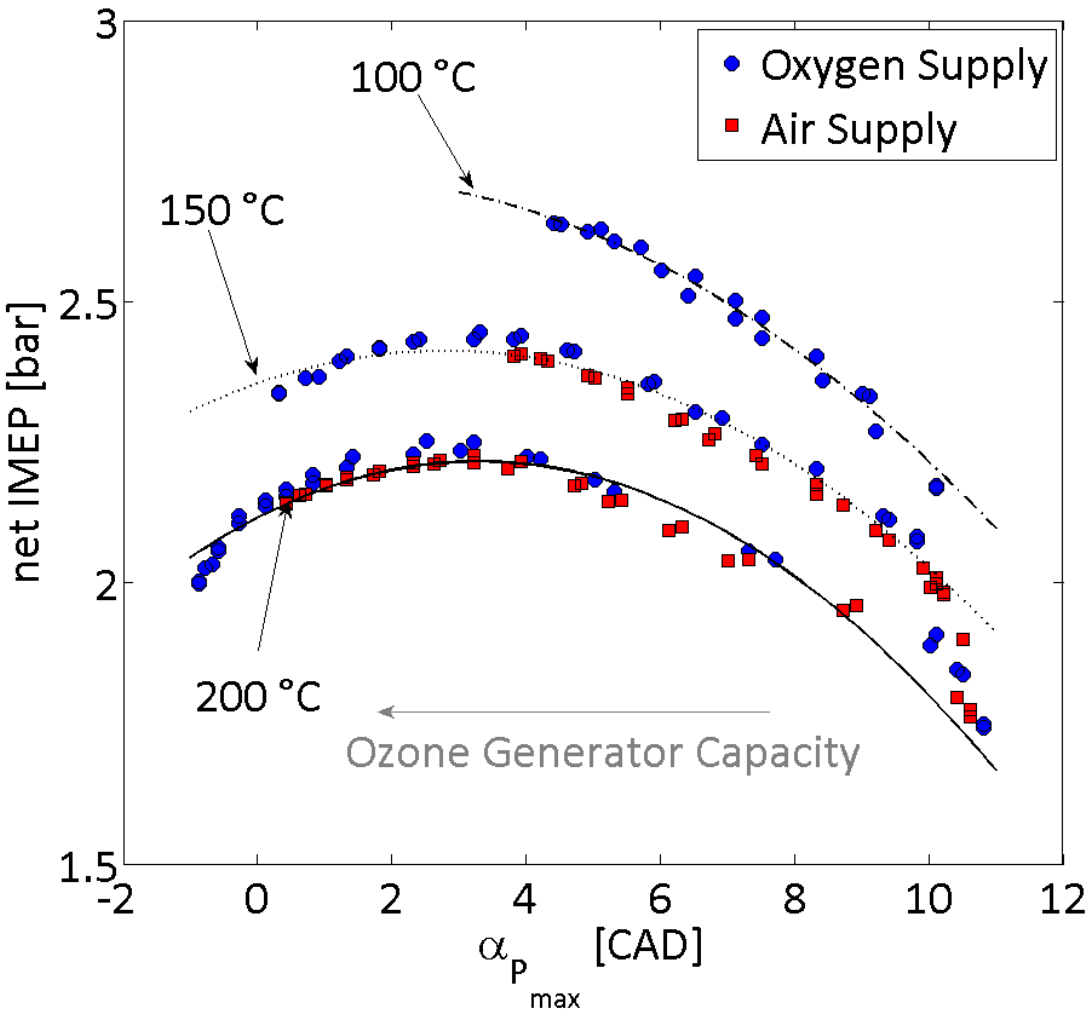

Figure 80. *Net indicated mean effective pressure as a function of the maximum pressure location for both types of gas supply, an injection inside the intake pipe and the three intake temperatures.*

6.4.1.3. Maximum pressure rise rate

The last engine output observed was the maximum pressure rise rate (MPRR) which is one of the major issues which need to be overcome before HCCI engines become operational. Results are presented in Figure 81. As a function of the maximum pressure position, this parameter increases following a linear trend with no impact of the intake temperature. Therefore, raise the ozone concentration injected leads to a higher MPRR and an increase of the noise level. Regarding the experimental values quantified, this parameter reaches a maximum value of 8 bar/CAD. In practical case, the limitation of pressure rise rate to avoid any damages is below 10 bar/CAD and is therefore never exceeded in the present results [175], [176]. Finally, as all the previous engine outputs discuss above, the combustion may also be managed by controlling the ozone injected.

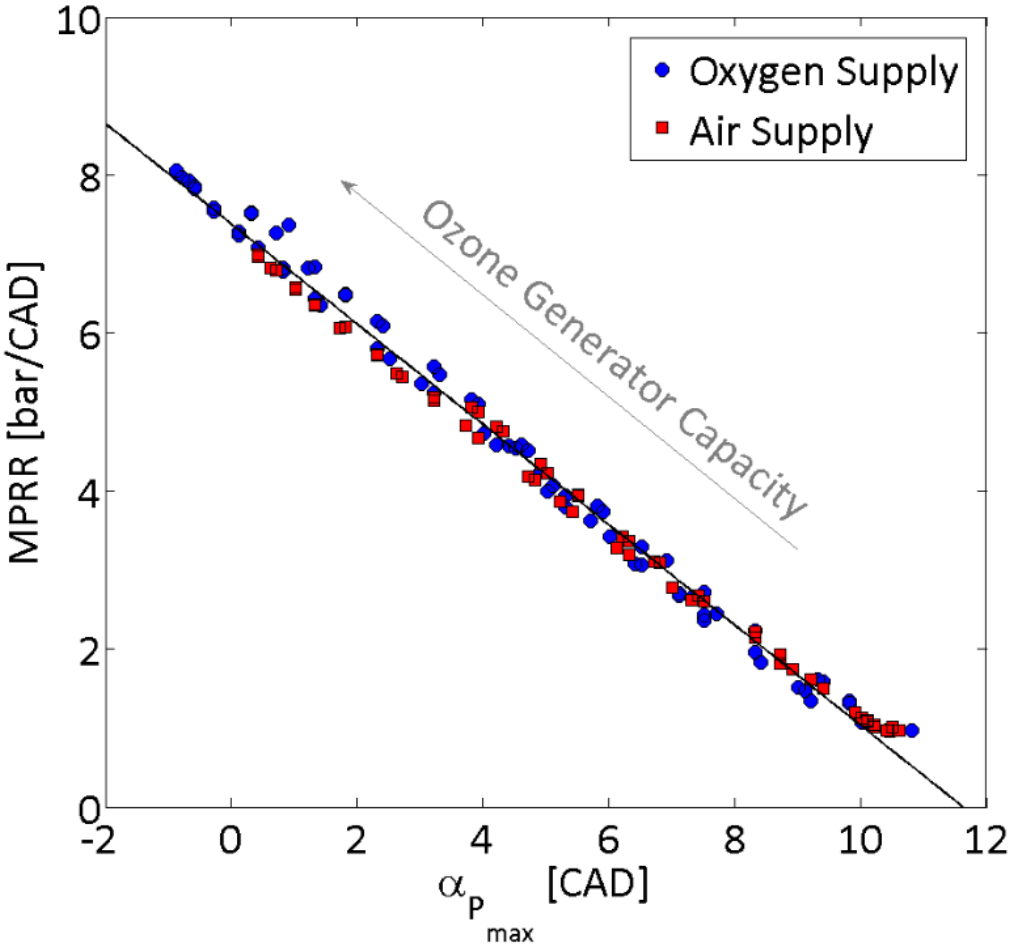

Figure 81. *Maximum pressure rise rate as a function of the maximum pressure phasing for both types of gas supply, an injection inside the intake of the engine and the three intake temperatures selected.*

6.4.2. Pollutants emissions

During these experiments, pollutants were measured according to the conditions tuned. Results obtained are presented above.

6.4.2.1. Carbon monoxide emissions

Carbon monoxide results are presented in Figure 82. Generally, it may see that this pollutant decrease with the increase of the ozone injected. As the isooctane combustion is improved, higher internal temperatures within the combustion chamber are reached and a better oxidation of carbon monoxide occur [110], [177], [178]. Moreover, it may also be observed that there is an impact of the intake temperature. Later is the combustion and lower is the intake temperature, higher are the carbon monoxide emissions. The important amounts of carbon monoxide are due to the late oxidization of this pollutant over the combustion cycle and the low internal temperature inside the combustion chamber [33]. With an increase of the intake temperature, oxidation starts earlier in the cycle and with

higher internal temperatures which explain the decrease of the emissions. Finally, all these results converge towards a unique value when the ozone concentrations increase because the combustion is improved. The combustion is advanced and therefore the oxidation of carbon monoxide occurs earlier with an ideal internal temperature. However, the final value remains important mainly due to the shape of the piston [179], i.e. the squish volume, and a thermal stratification which establishes [42], [43], [180]. As we work with a Diesel engine, the homogeneous mixture is trapped into areas where the combustion is not very intensive or even missing [82], [86].

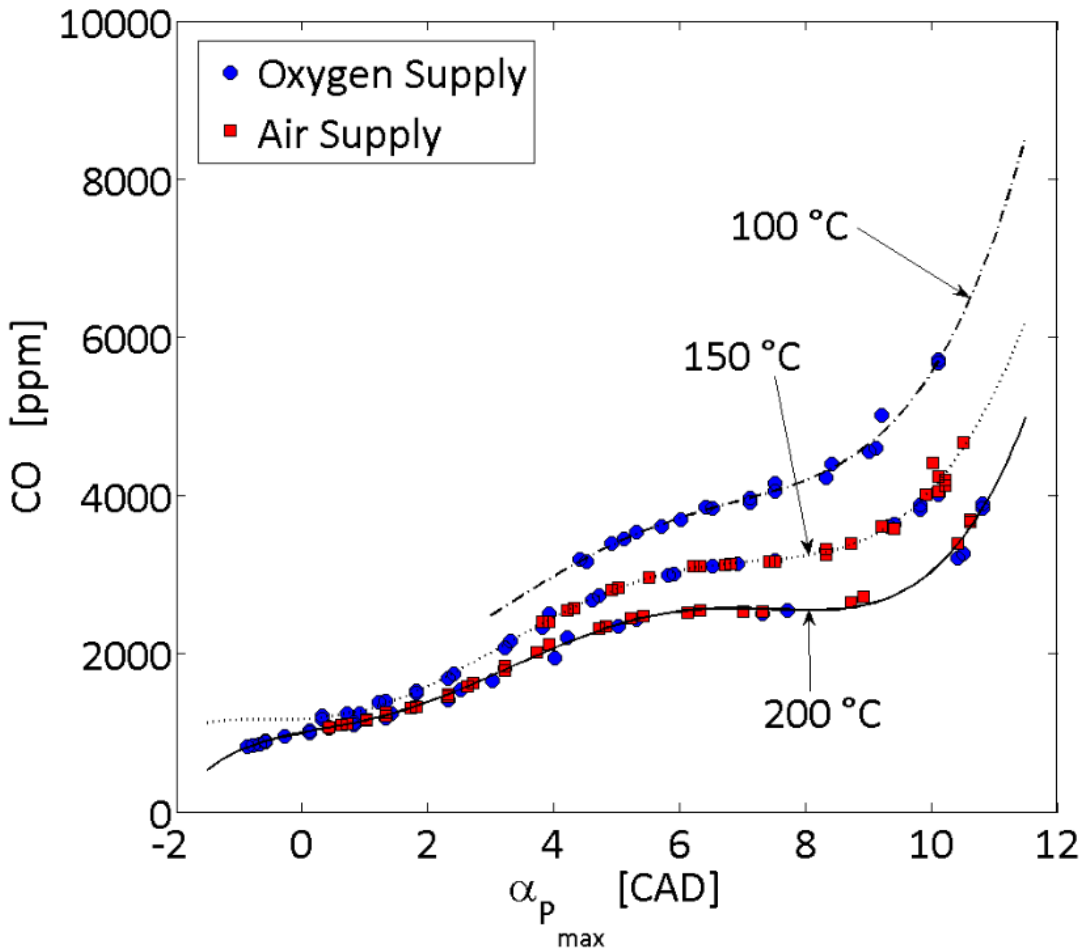

Figure 82. *Carbon monoxide trends as a function of the maximum in-cylinder pressure location for the three intake temperatures tuned.*

6.4.2.2. Unburned hydrocarbons emissions

Similarly to carbon monoxide emissions, unburned hydrocarbons emissions are plotted in Figure 83 as a function of the maximum pressure location. With the increase of the ozone, this pollutant decreases due to the improvement of the combustion and the highest in-cylinder temperature reached [178]. However, as the oxidation of this pollutant starts very earlier in the cycle, no dependence of the intake temperature was observed.

Finally the lower value achieved remains high for the same reason than that for the carbon monoxide emissions, i.e. that a part of the mixture is trapped inside the squish volume [179] and mainly because this pollutant is formed near the wall and the crevices [82], [86], [181].

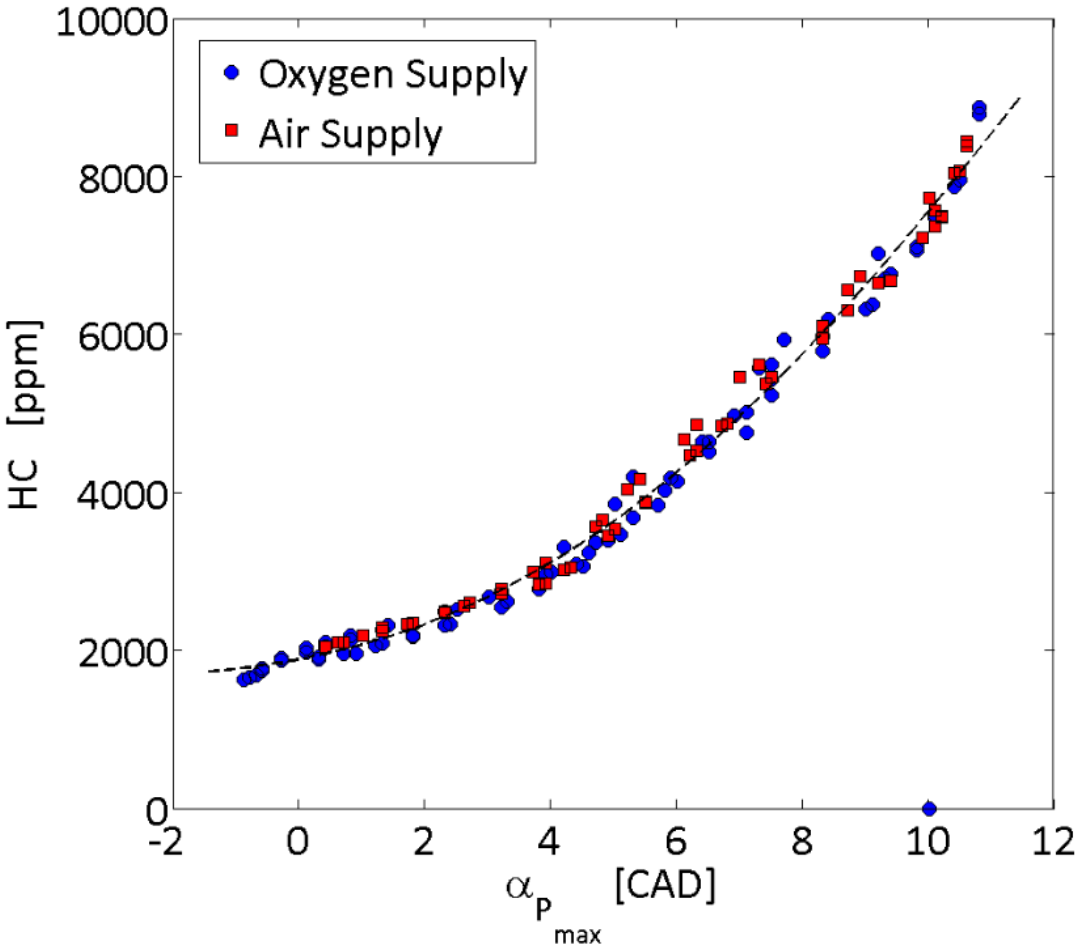

Figure 83. *Unburned hydrocarbons trends as a function of the maximum pressure location for both gas supply and the three intake temperatures tested.*

6.4.2.3. Nitrogen oxides emissions

The last pollutant measured was nitrogen oxides. Results are presented in Figure 84. All the values did not exceed 5 ppm and stay relatively low. However, with the increase of the ozone generator capacity, it may observed a slight rise due to the internal temperatures reached which are at around 1800 K maximum in average [18]. Moreover, these results showed that we can expect to a negligible impact of NO_X with the ozone injected since the highest concentrations measured in the exhaust are low (approximately of 5 ppm) and the residuals were estimated at around 6 % for this engine [151] In other words, NO_x trapped into the combustion chamber do not exceed 0.3 ppm and reactions between NO_x and ozone may be entirely overlooked.

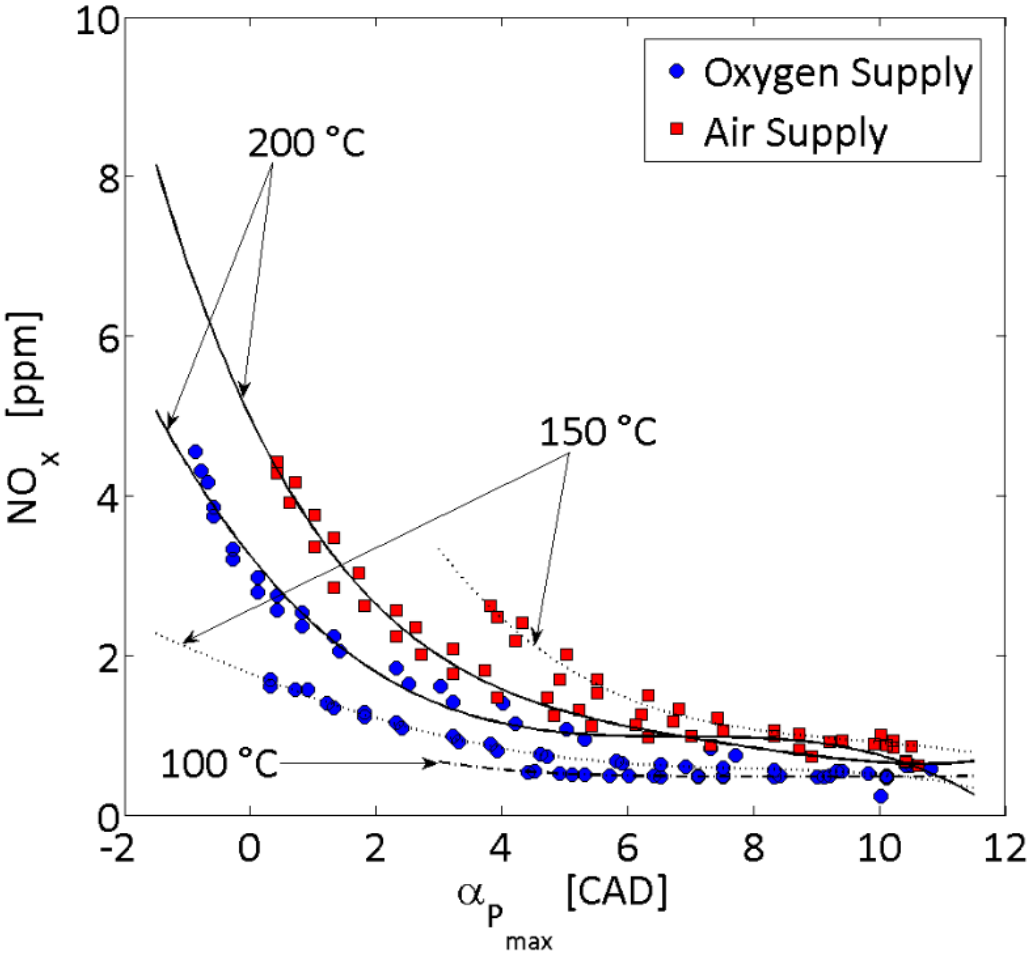

Figure 84. *Nitrogen oxides trends as a function of the maximum pressure location.*

6.5. Towards a cycle-to-cycle control

All the previous results obtained highlighted that isooctane combustion can easily be controlled by using an ozone generator supplied by air. Based on these previous experiments, an application case has been developed to demonstrate that a cycle-to-cycle is possible. These last results will correspond to the final achievement of this work. Moreover, this approach will enable us to identify the main ways to improve before achieving an on-road vehicle with such an application. The configuration retained for the present investigation was that with an injection near the intake valve and with air as gas supply. Finally, several parameters will be selected to monitor the combustion phasing and the maximum pressure location was selected in the present case due to the presence of the in-cylinder pressure sensor on the experimental setup. Note that a future control may use either pressure sensor [182], [183], or conventional sensors already integrated into vehicles [162], [184] or again new sensors such as ion current probes [185], [186].

6.5.1. Cycle-to-cycle approach

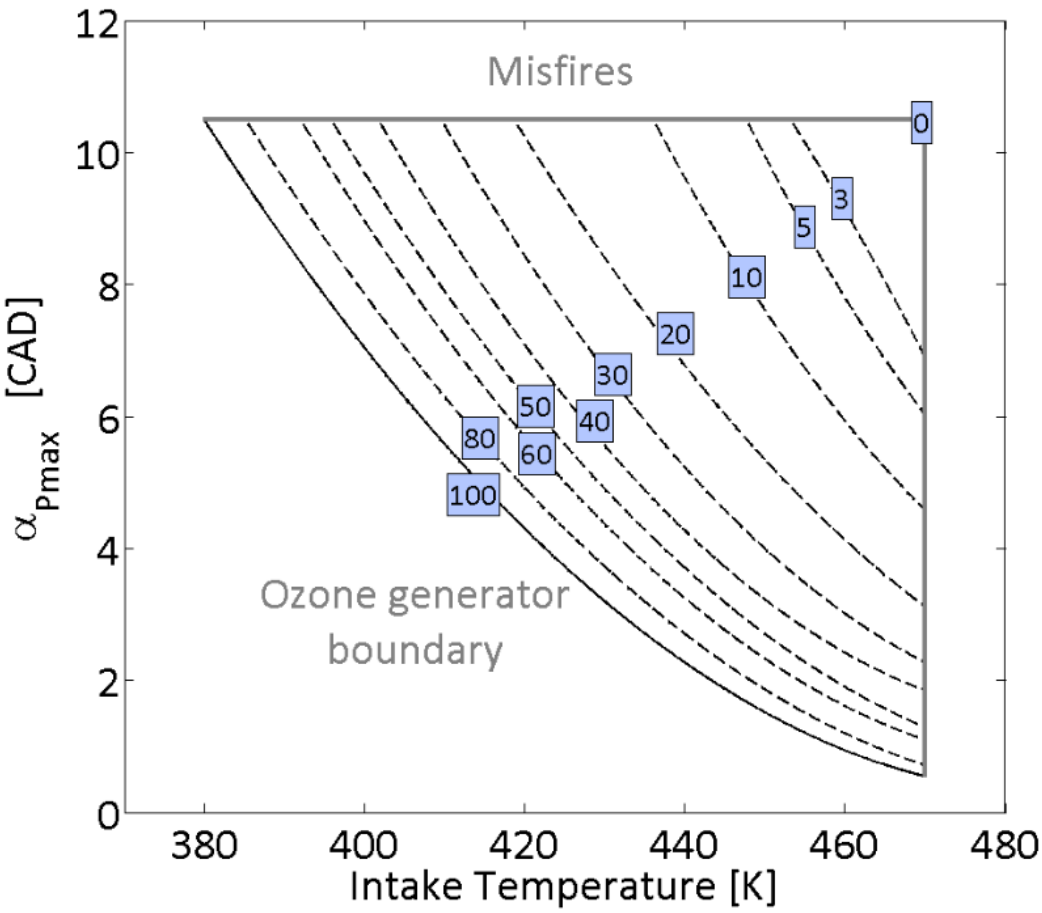

Figure 85. *Cartography of the ozone generator capacity needed to achieve a maximum pressure location under various intake temperatures of the engine. This map is based on all the experimental data previously obtained with air as gas supply for the ozone generator and with extra ones near the boundaries displayed.*

The cycle-to-cycle variation using the ozone generator to control the combustion process of isooctane was investigated first. From the previous results presented on the maximum pressure location by varying the ozone generator capacity and extra experiments, a cartography of the ozone needed to achieve a maximum pressure location setpoint under various intake temperatures has been established (Figure 85). Finally, a fit of the data used to build this map was carried out and the polynomial expression of the ozone generator capacity based on the maximum pressure location required and the instantaneous intake temperature has been implemented. Such an approach enables us to select a maximum pressure position as target and the amount of ozone needed is automatically produced and injected. The cycle-to-cycle variation has been studied following two approaches: the first by delaying the phasing and the second by advancing it. Results are showed in Figure 86 for 100 consecutive cycles. It may be observed that the transition between two maximum pressure

locations set takes place in two steps. Both steps were identified. The first, where the signal applied on the ozone generator is modified and where the phasing remains constant, corresponds to the carrier time of the ozone from the outlet of the ozone production area and the entrance of the engine. The second, where the maximum pressure location moves towards its target value, was attributed to the residence time of the flow inside the cell generating ozone. As this volume is particularly high, the flow takes a long time to cross the entire cell and corresponds to the approximately 10 cycles needed for the transition. Nevertheless, knowing the constant flow crossing the ozone generator and the rotation speed of the engine which is 1500 rpm, the transition time was estimated at less than 1s.

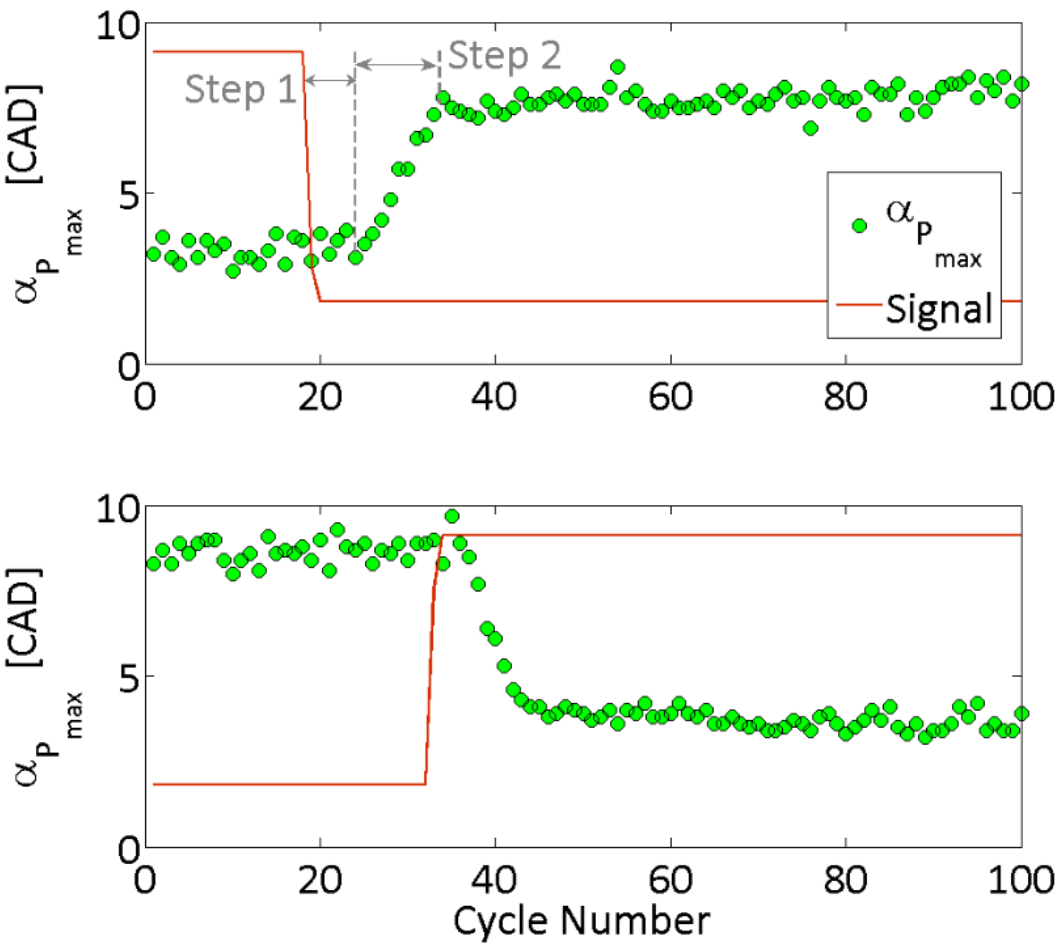

Figure 86. *Cycle-to-cycle variations for an increase and a decrease of the combustion phasing. Dots correspond to the maximum pressure phasing at each cycle and lines correspond to the signal on the ozone generator. Step 1 and step 2 correspond to the transitional time.*

These results highlighted the ways to improve in order to achieve an ideal control of the HCCI combustion by using an ozone generator. First, it is necessary to reduce the carrier time between the output of the generator and the intake valve of the engine. One solution could be to connect directly these output and input. Such a setup will result in a direct

injection of the ozone inside the combustion chamber. Another way will be to reduce the cell enabling to generate this oxidizing chemical species or again, increase the flow which crosses this volume. With all these improvements, the transition could be reduce to a very short time and could eventually take 1 cycle. However, additional works are needed due to the tradeoff between the flow and the ozone generator capacity. Indeed, raise the flow reduce the ozone concentration produced and the ozone generator capacity has to increase if we want to maintain a constant concentration of oxidizing chemical species. Additionally to these experiments performed to observe the transition time when the maximum pressure location changes, experiments with an increase and a decrease of intake temperature were carried out. Results are presented into Article IV and showed that this approach allows to maintain a constant combustion phasing by controlling the ozone generator capacity while the intake temperature changes.

6.5.2. Dynamic control

6.5.2.1. Open-loop control

According to the previous results on the cycle-to-cycle control of the combustion, a dynamic control of the phasing has been achieved by using the previous approach, i.e. by automatically applying the ozone generator capacity as a function of the maximum pressure location target. This is a first approach but this method could also be replaced by a direct use of the previous data with linear interpolations instead of the cartography established. Figure 87 sums up this open-loop control of the engine.

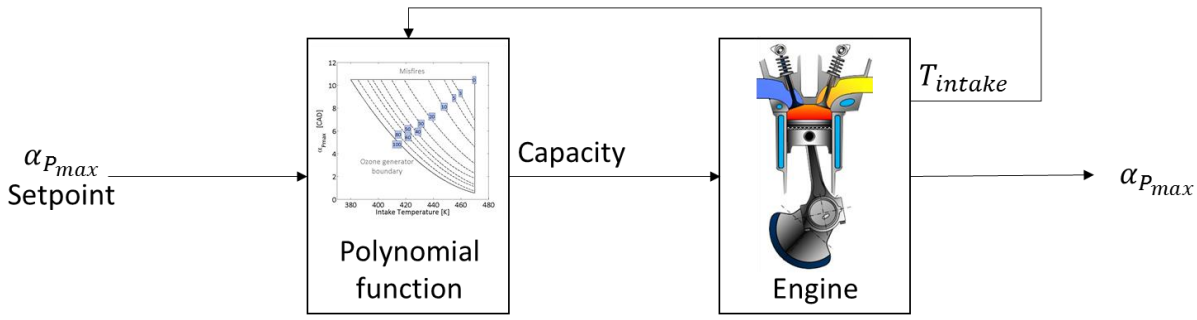

Figure 87. *Scheme of the open-loop control.*

For this case, experiments were carried out by only asking a phasing of the combustion and all the other conditions, i.e. intake pressure, intake temperature, rotation speed and equivalence ratio, were kept constant. Results obtained are showed in Figure 88. Generally, depending on the maximum pressure location asked, the system gives us very rapidly the required value. Nevertheless, most of the time, results showed offsets more or less important. These offsets are attributed to the correlation applied for tuning the capacity on the ozone generator which has been established from steady combustion experiments. Furthermore, by requiring a combustion phasing near the top dead center, the ozone generator reaches its maximum capacity and the combustion cannot advances more.

Inversely, by requiring a too late combustion phasing, the ozone production shuts down and the combustion is lost. Therefore, under these conditions, the presence of ozone is necessary to maintain the combustion. Finally, this dynamic control demonstrated that ozone generator may be applied to control quickly the HCCI combustion but this methodology has a lack of accuracy.

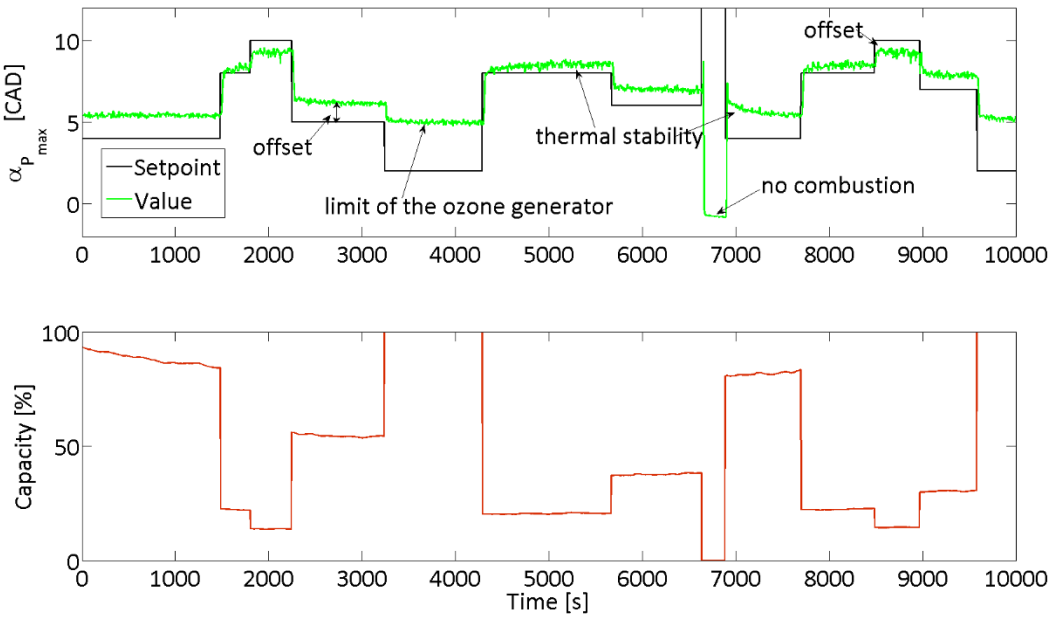

Figure 88. *Dynamic control of the combustion phasing via a cartography approach for an intake temperature of 150 °C.*

6.5.2.2. Closed-loop control

In parallel to the previous approach which consists of using a function between the maximum pressure phasing and the capacity applied to the ozone generator, an approach by controlling the combustion with the help of a PID was tested. Such an approach corresponds to a closed-loop control of the combustion timing of the engine and is summarized by Figure 89.

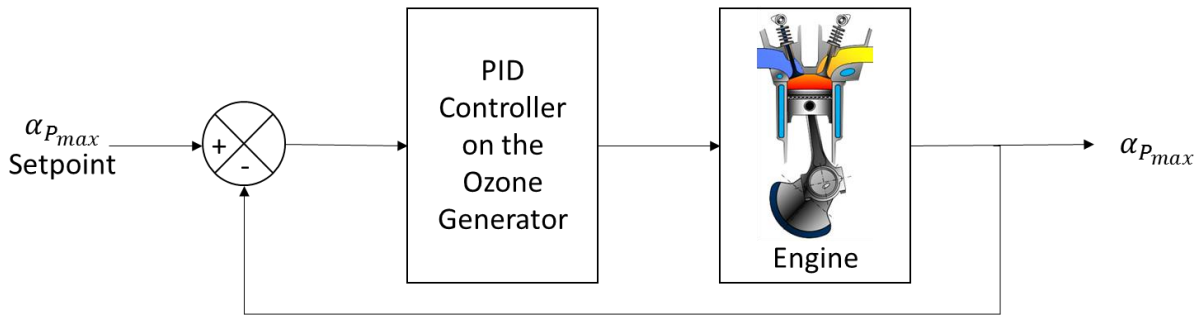

Figure 89. *Scheme of the closed-loop control.*

Experiments were performed by randomly varying the maximum pressure phasing in the same conditions than those selected for the cartography approach. Results are presented in Figure 90. It may observe that the system quickly responds in the beginning and finally increase or decrease slowly to achieve the setpoint. Inversely to the cartography approach, this system is slower but accurate. However, optimizations could be made by modifying the parameters of the control loop with respect of the tradeoff between accuracy and speed. Otherwise, another solution will be to combine both approach [162], the cartography for its speed of operation and the close loop control for its accuracy.

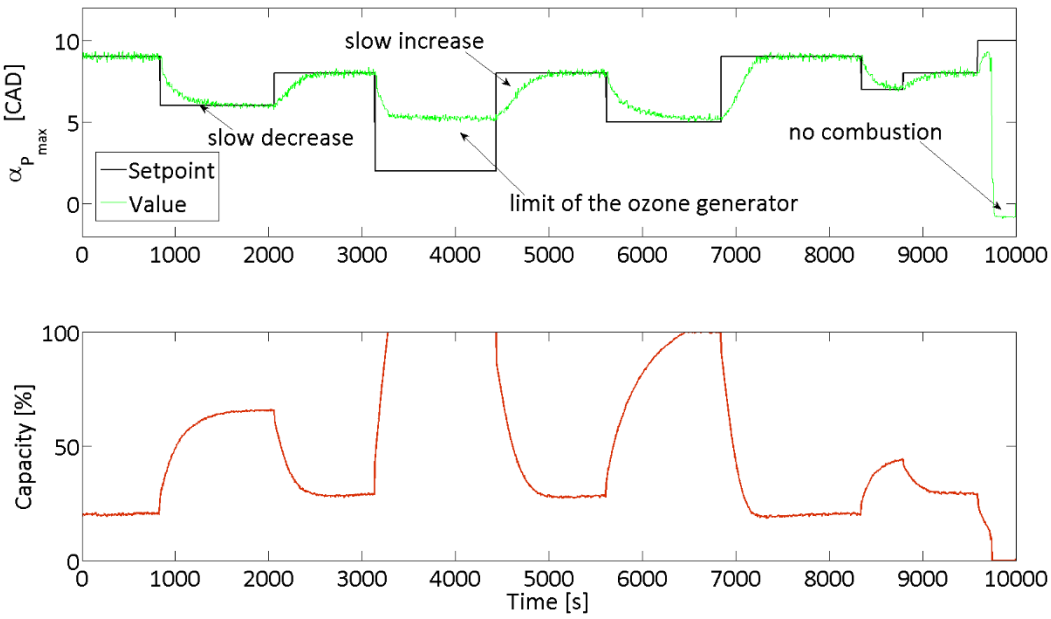

Figure 90. *Dynamic control of the combustion phasing via a closed loop control approach an intake temperature of 150 °C.*

7. Conclusion on Primary Reference Fuels

To summarize, the present chapter focused on the HCCI combustion of Primary Reference Fuels mainly with ozone seeding. Investigations were performed on a HCCI engine bench and results obtained were coupled with kinetics computations. All the experiments were carried out for a constant rotation speed, N= 1500 rpm, and a constant equivalence ratio, φ = 0.3. Intake conditions were set depending on the fuel used and from a prior study where the "optimum" combustion regions of each fuel selected was determined.

The impact of ozone was studied for each fuel selected by starting experiments from the most difficult intake conditions encountered, i.e. the minimum intake temperature and the minimum intake pressure allowing the combustion to autoignite with a phasing near misfires, due to the oxidizing potential of ozone. From these points, ozone was seeded for concentrations up to 50 ppm for each fuel except for isooctane where concentrations do not exceed 10 ppm. Generally, results showed that ozone is able to improve the HCCI combustion of all the PRFs selected as well as advance their combustion phasing. Observing parameters such as cool and main flame phasing, CA05 or CA50 as a function of ozone, it was noted that this oxidizing chemical species allows to advance exponentially the combustion phasing and acts on the beginning of the combustion, therefore, early in the combustion process. Furthermore, for all the PRFs except for isooctane, ozone provides the same effect: a rapid advance of the phasing with less than 20 ppm and then continuing increasing the concentration injected results in a less pronounced linear advance. The energy released during the cool flame regime was also studied and results confirm that ozone improve the combustion earlier in the HCCI combustion process due to the linear increase of the cool flame energy ratio observed as a function of the cool flame phasing. In the case of isooctane, no cool flame was observed and ozone acts directly on the main flame, resulting in a stronger and faster improvement of the combustion and advance of its phasing than the other fuels with very low ozone concentration (less than 10 ppm). Experimental results were then discussed with computations of the kinetics run with a new validated kinetics scheme and a constant volume model. Ozone decomposition into the combustion chamber was investigated first and it was observed that increase the intake temperature leads to an earlier decomposition of ozone while the intake pressure has no effect. This last result explained the similar trends observed for n-heptane and mixtures of n-heptane and isooctane as experiments were performed under the same intake temperature and with a different intake pressure. Moreover, the impact of the temperature on ozone breakdown also explained the stronger sensitivity on isooctane as the experiments were conducted under a high intake temperature. Finally, last simulations showed that ignition delays computed are in agreement with the experimental results observed on the combustion phasing and kinetics analysis showed that ozone is not directly responsible of the improvement of the combustion. The earlier oxidation of the n-heptane and isooctane

comes from an initiation reaction with O-atom coming from the ozone decomposition instead of the normal oxidation with oxygen molecule. Lastly, in the case of a mixture of both fuels, n-heptane may oxidized earlier than isooctane because it is less resistant to the ignition and its presence into PRFs surrogate explained that these fuels may autoignite under the lowest intake temperature with the same effect of the ozone.

Following these first results, further investigations were conducted for isooctane as fuel. Due to the significant impact of ozone on its combustion, it was investigated the possibility of reducing the intake temperature towards more conventional ones and use the oxidizing potential of ozone to make the combustion possible. It was showed that ozone may easily maintain the combustion under intake conditions unfavorable normally. By decreasing the intake temperature, a minimum ozone concentration is needed to start the isooctane combustion and this value must increase exponentially when the intake temperature decreases. It was also observed that, under lower intake temperatures, isooctane is less sensitive to ozone and therefore confirm the effect of the temperature on ozone decomposition. As a result, ozone has the potential to control the combustion phasing under a wide range of intake conditions and it may also be used for cool starting of the engine. Moreover, these results also confirmed that ozone modified the occurrence of the combustion since an analysis on heat release rate curves showed the presence of the isooctane cool flame.

As ozone showed that it may control the combustion phasing of a HCCI engine, the possibility of generate it and use it for a real application was investigated. For creating ozone, an ozone generator is needed. Such a device tends to become increasingly small and may achieve sizes really interesting for vehicle implementation. However, the ideal gas for this apparatus and this application would be air but such a gas could result into the production of NO_x, mainly nitric oxide and nitrogen dioxide. Both species can altered the impact of ozone. Besides, NO_x may also be present into residuals or with the use of EGR. Their impact on the HCCI combustion was therefore compared with that of ozone for isooctane as fuel. Results showed that the three chemical species have all an oxidizing potential since they allow advancing the combustion. Among the three, ozone presents the highest effect while nitrogen dioxide the lowest. These results were explained by using a kinetics scheme. Computations indicated that ozone allows directly oxidizing the fuel through a reaction involving an O-atom while both NO_x need the presence of radicals coming from the normal oxidation of fuels before allowing to improve the chain branching reactions. Moreover, there is also additional intermediate reactions in the case of nitrogen dioxide which explain that this oxidizing chemical species provide the lowest effect. Finally, as nitric oxide is the most present NO_x into EGR or residuals or from the ozone generator, its impact combines with that of ozone was investigated. Results displayed that when both oxidizing chemical species are seeded together, the isooctane combustion phasing is always advanced compared to a reference case without seeding but the species lead to a delay compared to

the case when they are injected separately. The delay occurs due to a significant reaction involving both ozone and nitric oxide in front of the combustion chamber. This reaction leads to nitrogen dioxide species which in turn advance the combustion but has less effect on the combustion phasing than both others.

Finally, a real application case was considered using an ozone generator supplied with air. Prior experiments consisted of measuring the concentration of ozone at the entrance of the engine and showed that such a device may achieve suitable levels of ozone for applications. Furthermore, NO_x concentrations were also quantified and the level remained negligible. However, it is important to note that the ozone generator used is a commercial one configured to produce only ozone. There is not ozone generator developed for automotive application from now and the interaction between ozone and NO_x should be considered for implementing such device into a vehicle. New experiments similar to those previously performed were then carried out and indicated that such a device can be used to control the combustion phasing as well as other engine outputs and levels of pollutants. Moreover, based on the results obtained, a dynamic control was developed through an open-loop control approach and through a closed-loop control approach. The first allows a rapid control but with a lack of accuracy while the second presents the inverse and finally, the improvements which can lead to an on-board application of such device were identified.

From now, the investigation focused only on PRFs but HCCI engines may consider the use of other fuels. The impact of ozone was therefore investigated on alternative fuels for automotive and results are presented in the next chapters.

Chapitre 4 / Chapter 4

Résultats sur la combustion de carburants gazeux

Results on the combustion of gaseous fuels

Résumé

Ce quatrième chapitre est ciblé sur la combustion des carburants gazeux. Suite aux précédents résultats obtenus sur la combustion des PRFs, une approche scientifique similaire a été mise en place et consiste à étudier l'impact de l'ozone sur ces autres carburants, en particulier sur des carburants relativement proches du gaz naturel. Les résultats présentés font référence à un travail publié :

- Article V : J-B. Masurier, F. Foucher, G. Dayma, P. Dagaut, *Effect of Additives on Combustion Characteristics of a Natural Gas Fueled HCCI Engine*, SAE Technical Paper 2014-01-2662, 2014.

Les carburants gazeux sélectionnés pour cette étude ont été le méthane, le propane et l'hydrogène. Grâce à son potentiel oxydant, l'ozone a démontré une aptitude à autoinflammer l'isooctane alors que les conditions appliquées au moteur ne l'auraient pas permis en temps normal. Le méthane a donc été sélectionné en raison de sa très forte résistance à l'autoinflammation et dans le but de voir si cette espèce chimique sera capable d'améliorer la combustion de ce carburant. Le propane a quant à lui été retenu en raison de ses propriétés d'auto-inflammation relativement proches de celles de l'isooctane. Enfin, l'hydrogène est lui aussi un carburant difficile à autoinflammer et est considéré comme un carburant n'émettant pas de CO_2.

De manière analogue à l'étude menée sur les PRFs, des essais expérimentaux sans ensemencement ont été effectués. Les résultats ont montré que le propane présente des tendances similaires à celles de l'isooctane. Dans le cas de l'hydrogène, ses propriétés le décrivent comme étant difficile à autoinflammer mais en réalité, dans le cadre de sa combustion en moteur HCCI, ce gaz peut s'autoinflammer bien plus facilement que l'isooctane. Finalement, des essais ont aussi été tentés jusqu'aux limites des conditions d'admission du moteur avec le méthane mais malheureusement, ce carburant nécessite des conditions encore bien plus importantes. Compte tenu de l'absence de combustion dans le cas du méthane, une injection d'ozone a été effectuée afin de réduire sa résistance à l'autoinflammation. Cependant, malgré la présence d'une quantité significative de cette espèce oxydante, la combustion du méthane reste inexistante. En conséquence et en considérant que le méthane n'est jamais employé pur, l'étude s'est finalement portée sur des mélanges essentiellement composés de méthane avec propane ou hydrogène.

D'une manière générale, les résultats ont montré des tendances similaires à celles déjà obtenues lors de la combustion des PRFs : une amélioration de la combustion avec une avance de son phasage. Dans le cadre des expériences menées avec un mélange méthane-propane, les résultats ont montré qu'il est bien possible de réduire les conditions de pression et de température à l'admission du moteur tout en maintenant le contrôle de la

combustion par l'ozone. Ainsi, il est possible de contrôler les paramètres du moteur tel que la pression moyenne indiquée, le niveau de bruit ou encore le déroulement de la combustion. De plus, les niveaux de polluants ont aussi été évalués et leurs tendances ont confirmé une amélioration de la combustion. Toutefois, en raison des fortes conditions d'admission, d'importants niveaux de NO_x ont été relevés. Dans le cas des expériences avec les mélanges méthane-hydrogène, la variation des fractions volumiques de chaque carburant a démontré des résultats similaires à ceux obtenus en dégradant les conditions d'admission du moteur. Ainsi, l'ozone a donc le potentiel de maintenir le contrôle d'un carburant malgré des conditions d'admission non favorables à son autoinflammation en l'absence de cette espèce chimique oxydante. De plus, il donne aussi la possibilité d'adapter le carburant, d'utiliser des mélanges avec des fractions volumiques variables, en fonction de l'objectif à atteindre sur le moteur. Finalement, ces expériences ont été couplées avec des simulations de cinétique chimique où l'impact de l'ozone sur chaque carburant pure a été analysé. Les résultats ont indiqué que ces carburants sont oxydés d'une manière identique à celle observé pour les PRFs.

Abstract

The fourth chapter is centering on the combustion of gaseous fuels. Following the previous results obtained on the combustion of PRFs, a similar scientific approach was made and consists in studying the impact of ozone on these fuels, in particular on fuels closed to the natural gas. Results introduced refer to the following article:

- Article V: J-B. Masurier, F. Foucher, G. Dayma, P. Dagaut, *Effect of Additives on Combustion Characteristics of a Natural Gas Fueled HCCI Engine*, SAE Technical Paper 2014-01-2662, 2014.

Gaseous fuels selected for this study was methane, propane and hydrogen. Thanks to its oxidizing potential, ozone showed it was able to autoignite isooctane while the conditions applied to the engine do not enable normally. Methane was therefore selected due to its high resistance to the autoignition and in the aim to see if ozone will be able to improve the combustion of this fuel with its promoting effect. Propane was selected due to its autoignition properties closed to those of isooctane. Finally, hydrogen is also a fuel difficult to autoignite and is considered as a clean fuel.

Similarly to the study conducted on PRFs, experiments without seeding were performed. Results showed that propane has trends similar to those of isooctane. In the case of hydrogen, its properties described it as a fuel difficult to autoignite, but in the case of HCCI combustion, this gas may autoignite more easily than isooctane. Finally, experiments were carried out up to the limits of the intake conditions of the engine with methane as fuel but unfortunately, this fuel needs more important intake conditions. As there is no combustion for methane, an ozone injection was performed to reduce its resistance to the autoignition. However, despite the significant amount of this oxidizing species, methane combustion does not exist. Consequently and by considering that methane is never used pure, the study was made on fuel blends with high ratios of methane and complemented with propane or hydrogen.

Generally, results showed similar trends than those obtained for the combustion of PRFs: an improvement of the combustion coupled to an advance of its phasing. For experiments performed with methane/propane as fuel, results showed that it was possible to reduce either the intake pressure or the intake temperature or these two parameters while keeping the control of the combustion by using ozone. As a result, it is possible to control engine outputs such the indicated mean effective pressure, the noise level or again the combustion process. Moreover, pollutants were also measured and their trends confirmed the improvement of the combustion. However, due to the too high intake conditions, significant levels of NO_x were measured. In the case of methane/hydrogen as fuel, ranging the ratios of each fuel showed similar results than those obtained by reducing

the intake conditions of the engine. Ozone has therefore the potential to maintain the control of a fuel despite unfavorable intake conditions for the autoignition when ozone is missing. Moreover, it gives also the possibility to adapt the fuel, to use blends with variable ratios, as a function of the aim to achieve on the engine. Finally, experiments were coupled with computations of kinetics where the impact of ozone for each fuel used pure was analyzed. Results indicated that fuels are oxidized similarly to PRFs.

1. Introduction on gaseous fuels (Article V)

Previous chapter discussed about the impact of using ozone generators to control the combustion of primary reference fuels. In particular, a wide part was focused on the impact of the oxidizing chemical species generated by such devices on the combustion of isooctane. Last results showed that the ozone generator used produces only ozone and achieving a dynamic control is possible with an ozone generator. Considering these prior results and the possibility that HCCI engines and future advanced combustion engines can use other fuels than the conventional ones, the impact of ozone has been investigated on alternative fuels such as gaseous fuels. This study was also reinforced by the fact that ozone may auto-ignite fuels under unfavorable conditions. Therefore, as gaseous fuels are often more resistant to the self-ignition than isooctane, the use of ozone could help to achieve the combustion of such fuels.

The aim of the present part is to investigate the effect of ozone on gaseous fuels. Fuels retained were methane because it is the most difficult fuel to auto-ignite, propane due to its properties similar to those of isooctane and hydrogen due to its ability to be a clean fuel and normally also difficult to auto-ignite.

2. Combustion of gaseous fuels

Similarly to the investigation on the combustion of primary reference fuels, this first part of this study examines the combustion of gaseous fuels without oxidizing chemical species. Experiments were conducted under a constant rotation speed and a constant equivalence ratio of 1500 rpm and 0.3, respectively. The intake pressure and the intake temperature varied to determine the "optimal" combustion area of each gaseous fuels selected. The results obtained are presented in Figure 91 and showed the isoCA50s when the combustion phasing is located at the top dead center (0 CAD).

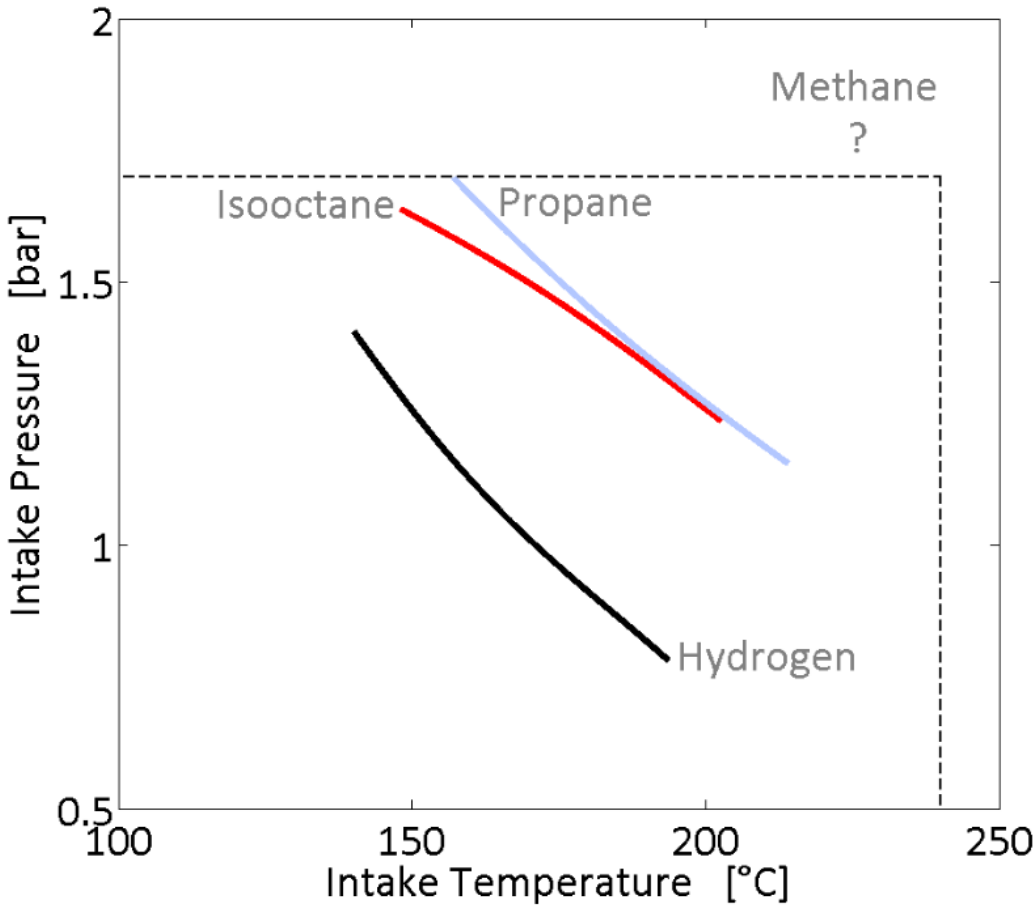

Figure 91. *IsoCA50s located at the top dead center for the gaseous fuels selected as a function of the intake pressure and intake temperatures, an equivalence ratio of 0.3 and a rotation speed of 1500 rpm. Dotted lines correspond to the operating limits of the engine bench.*

It may observe that no results are available for methane. During experiments, increase the intake conditions of pressure and temperature up to their respective limits, i.e. 1.7 bar and 240 °C, did not enable us to auto-ignite methane. In fact, this fuel is known to be the most difficult fuel to auto-ignite according to its octane number [187]. It is therefore

normal that no combustion appears. Propane has an octane number similar to that of isooctane and is mainly assimilated to this PRF but under gaseous phase. Regarding the results, it may observe that the isoCA50 for propane is really closed to that of isooctane. Finally, the last gaseous fuel selected, hydrogen, presents an octane number higher than 100. Therefore, from the results on the same diagram observed for PRFs and from the other gaseous fuels tested, hydrogen must present an isoCA50 line upper than that of isooctane. Unfortunately, results obtained showed that the isoCA50 line for hydrogen is lower than one for isooctane by the fact that hydrogen is more reactive than other gaseous fuels tested. Indeed, RON and MON are mainly defined for spark ignition engines [188], [189] and studies showed that the burning velocities of this fuel are very significant [190], resulting in high indexes. For HCCI combustion, there is no flame velocity, instead, the kinetics allows a quite homogeneous mixture and as a consequence, octane number is not the only parameter to consider to conclude on the combustion of fuels into HCCI engines [46], [47], [70].

According to previous results on isooctane combustion under HCCI conditions assisted by ozone injections, it was observed that the presence of ozone may help to auto-ignite fuels under conditions where the combustion does not exist. It was therefore decided to focus on the possibility of using ozone to enable the HCCI combustion of methane.

3. Effect of ozone on gaseous fuels

First, experiments were performed with pure methane and pure hydrogen for a rotation speed of N = 1500 rpm and an equivalence ratio of φ = 0.3. Intake pressure and intake temperature were fixed respectively at 1 bar and 155 °C for hydrogen, limit of the misfires for this fuel, and at the operating limits of the experimental setup for methane because previous results do not display any combustion for methane as fuel. From these initial conditions, ozone was injected into the intake of the engine to observe its effect. Results for hydrogen as fuel are plotted in Figure 92 and compared to those of isooctane.

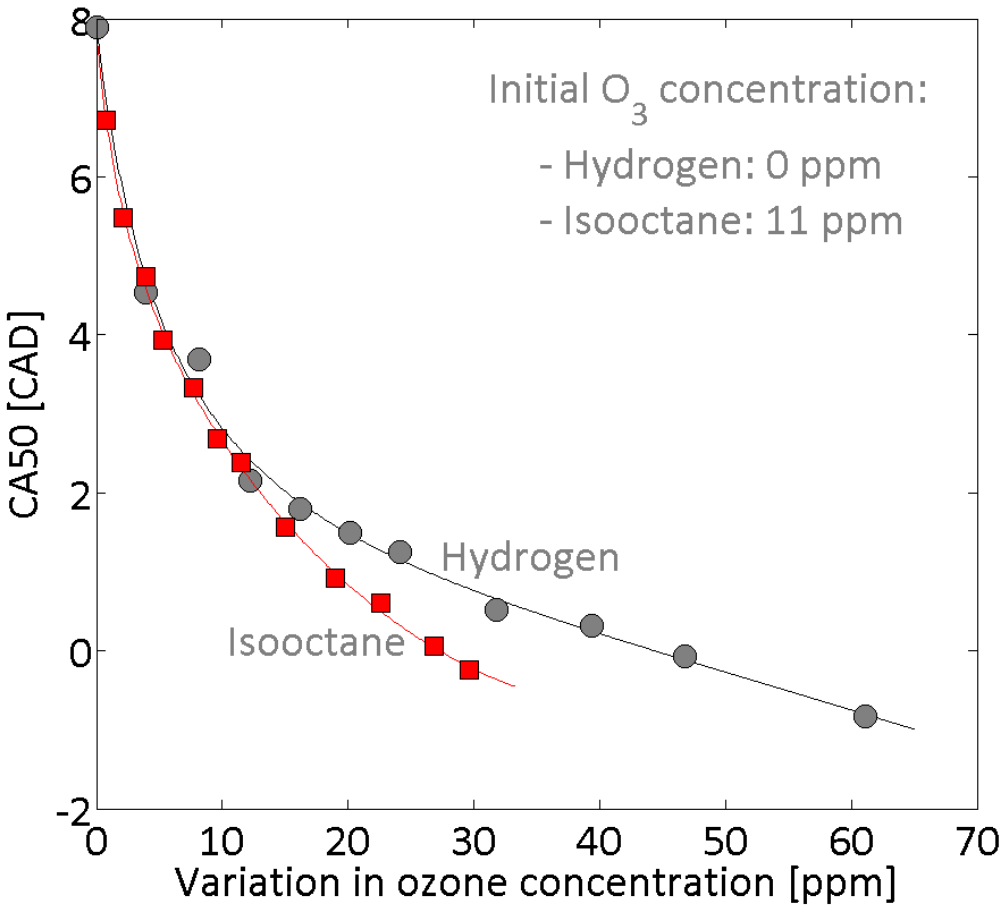

Figure 92. *Effect of ozone on hydrogen and isooctane combustions for intake conditions fixed at 1 bar and 155 °C. Results for isooctane need a minimum ozone concentration to auto-ignite under these conditions. The ozone concentration axis for isooctane results were therefore shifted and adapted to start with the same initial CA50. The two trends must be therefore analyzed as a function of a variation of the ozone concentration.*

Similarly to PRFs, hydrogen showed that its combustion timing is also advanced with ozone injection and by comparison with isooctane results, hydrogen showed that it is less influenced. Note that results for isooctane need a minimum ozone concentration and that

these results were shifted. Its trend is therefore displayed according to a variation of the ozone added. The highest impact on isooctane comes from its chemical structure which enables an easier oxidation by oxygen atom resulting from the breakdown of ozone. This result means that the chemical structure of the fuel is of main importance for applying ozone and observing a significant impact.

For methane, the initial conditions do not permit the autoignition of this fuel but previous results on PRFs and in particular on isooctane combustion showed that the fuel oxidation may occur under lower temperatures than those necessary by seeding ozone into the intake of the engine. Ozone was therefore directly applied under these conditions and unfortunately, no results were available, even by pushing the ozone generator to its maximum capacity. The main issue comes from the ozone seeding which was limited to a very low concentration while previous results in the literature showed that at least 600 ppm of ozone is needed to initiate natural gas combustion [12]. Moreover, experiments were also performed by increasing the equivalence ratio but here again, no combustion occurs. Referring to practical case using methane, this fuel is always blended with other compounds. For instance, natural gas is mainly composed of methane but depending of its source in the world, it is mixed with other small fuel fractions of ethane, propane or again butane [191]. Another example is hythane which is referred as a blend of 80 % of natural gas with 20 % of hydrogen [192]. Finally, there is also biogas which mainly consists of methane and carbon dioxide [193], [194]. Therefore, the present investigation on the impact of ozone did not consider pure methane as fuel but blends of methane with propane and methane with hydrogen.

3.1. Combustion of methane/propane surrogate

Combustion of a mixture of methane and propane in the volume fraction of 95 % and 5 %, respectively, was investigated first. These respective amounts of fuels were selected to be representative of a synthetic natural gas. The study was conducted with combustion experiments on the engine bench and then, with computations using a detailed kinetics scheme.

3.1.1. Experimental results

Experiments were performed on the engine bench for a fixed mixture of methane and propane with an equivalence ratio remained constant at $\varphi = 0.4$ and a constant rotation speed of N = 1500 rpm. The impact of ozone on such a fuel is first studied under constant intake conditions and then by separately varying the intake pressure and the intake temperature.

3.1.1.1. In-cylinder pressure, temperature and heat release rate trends

For studying the impact of ozone on this fuel, experiments were carried out for intake conditions on the engine allowing the first autoignition of this methane/propane mixture, i.e. a combustion which is at the limit of misfiring. The intake pressure and the intake temperature were therefore fixed at 1.5 bar and 495 K, respectively. Ozone was finally injected into the plenum and ranged from 0 to approximately 40 ppm. Experiments stopped at this limit value due to the high level of noise on the experimental bench and because the combustion phasing took place before the top dead center. Results on in-cylinder pressure, in-cylinder temperature and heat release rate traces are presented in Figure 93. Black curves correspond to the average of the 100 cycles recorded and shaded areas which surround each average represent the variations over the same 100 cycles.

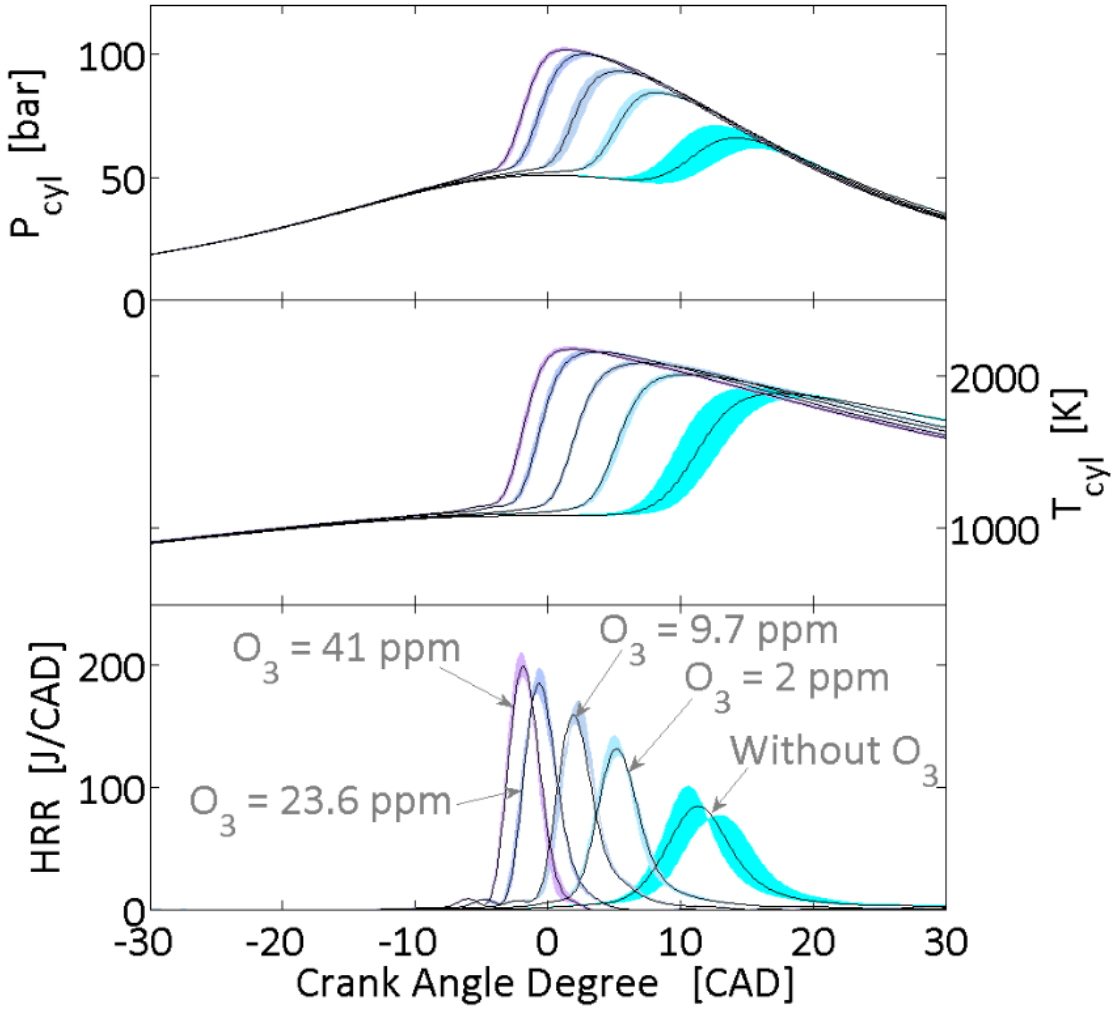

Figure 93. *In-cylinder pressures, in-cylinder temperatures and heat release rates traces as a function of the ozone concentrations with an intake pressure of 1.5 bar and an intake temperature of 495 K.*

Observing these results, ozone showed that it is an excellent promoter of the HCCI combustion. When no ozone is injected, the combustion is near misfiring, the maximum in-

cylinder pressure occurs late and combustion is difficult to stabilize. As soon as few ppm of ozone are added to the air/fuel mixture, the combustion immediately gained in intensity. The maximum pressure increases and moves towards the top dead center which may be summarized as an improvement of the HCCI combustion. Moreover, regarding the variation of the combustion, it may also be observed that the use of ozone leads to a better stabilization. Finally, similarly to the results observed on PRFs, a low concentration of ozone conducts to a rapid improvement of the combustion while continuing increasing the amount of ozone continues to enhance the combustion but with a lower effect. This observation can be conduct on each traces presented in Figure 93. Moreover, observing the heat release rates, the combustion is particularly long without ozone and the addition of this oxidizing chemical species finally allows shortening the combustion process. Similar results were already observed in the literature with a natural gas as fuel [11], [12] and other fuels [9], [13]. Further experiments were then conducted under variations of the intake pressure and the intake temperature.

3.1.1.2. Combustion characteristics under intake pressure variation

To initiate the HCCI combustion in the engine used for the previous mixture of methane and propane, an intake pressure and an intake temperature of 1.5 bar and 495 K are needed, respectively. Similarly to the results presented for isooctane in the previous chapter, it was tested the possibility of reducing the intake conditions by maintaining the combustion with the help of ozone. First, it was investigated a decrease of the intake pressure with a constant intake temperature. Intake pressure was decreased from 1.5 bar to 1.2 bar by step of 0.1 bar while the temperature was kept at 495 K. For these experiments, ozone ranged from 0 to 120 ppm (Limit of production for the ozone generator under these conditions). Figure 94 showed the engine outputs obtained, i.e. the indicated mean effective pressure (IMEP), the maximum pressure rise rate (MPRR), the CA50 and the combustion duration.

By comparing the results observed with those obtained with isooctane as fuel, it may conclude that ozone clearly enable to maintain the combustion of the methane/propane blend selected under conditions where the combustion does not take place. Moreover, it is also needed to seed a minimum concentration of ozone to auto-ignite the fuel. This value must increase with the decrease of the intake pressure. Finally, compare to previous results obtained with isooctane, the impact of ozone is less pronounced on methane/propane combustion since higher concentrations of this oxidizing chemical species are needed to strongly advance the combustion phasing. Besides, the operating conditions were selected higher than those tested for isooctane meaning that under the same conditions, ozone will have more influence on isooctane. This result may be explained by the fact that the chain carbon is not long enough to ease the combustion and that the chemical

structure is of main importance. For example, all the H from methane are primary while for isooctane, some H are secondary.

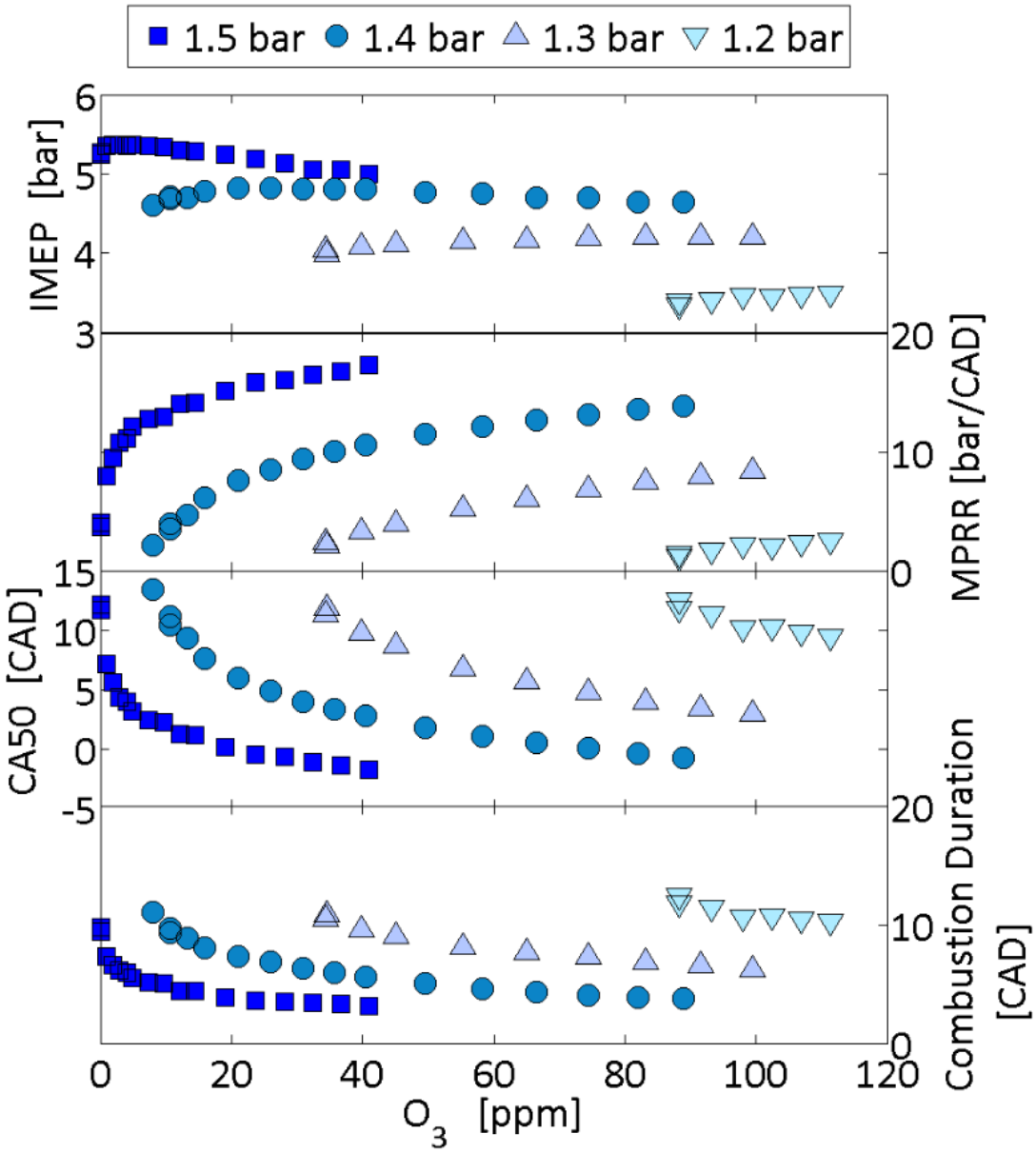

Figure 94. *Engine outputs (IMEP, maximum pressure rise rate, CA50 and combustion duration) as a function of the ozone injected under various intake pressures and a constant intake temperature of 495 K.*

Regarding the results presented in Figure 94, the IMEP showed several trends. At 1.5 bar, IMEP rapidly increases to achieve a maximum value and finally decreases by continuing injecting ozone due to an early auto-ignition and combustion phasing. Moreover, in this condition, this fuel is particularly sensitive to the ozone. A similar trend may be observed at 1.4 bar except that the effect is less pronounced. Finally, for the two last intake pressure fixed, only a growth of the IMEP is seen because the combustion phasing is too late and the ozone concentration is not sufficient to further investigate its impact. According to

the values observed, the maximum IMEP for each conditions fixed decreases. This decrease is due to the constant equivalence ratio used. As the intake pressure decreases, the mass or energy eligible inside the combustion chamber also decreases and therefore leads to a lower work. The MPRR was also examined. Similarly to the IMEP, this parameter showed that it is very sensitive to the ozone addition. Most of the time, the MPRR reaches values higher than 10 bar/CAD meaning that the combustion is particularly noisy. With ozone, a fast combustion occurs and rapidly raises the in-cylinder pressures as observed in Figure 93. Finally, the intake pressure must be strongly reduce for achieving low level of noise. The last engine outputs determined were the CA50 and the combustion duration. Both parameters decrease as a function of the ozone injected meaning that the combustion is advanced and the energy is quickly released. Under high intake pressures, these two parameters are very sensitive and showed exponential decrease up to a finite value. Therefore, in these cases, continuing increasing the ozone concentration will not provide additional advance of the combustion. Under lower intake pressures, the effect is less pronounced and high concentration of ozone are necessary to maintain the combustion.

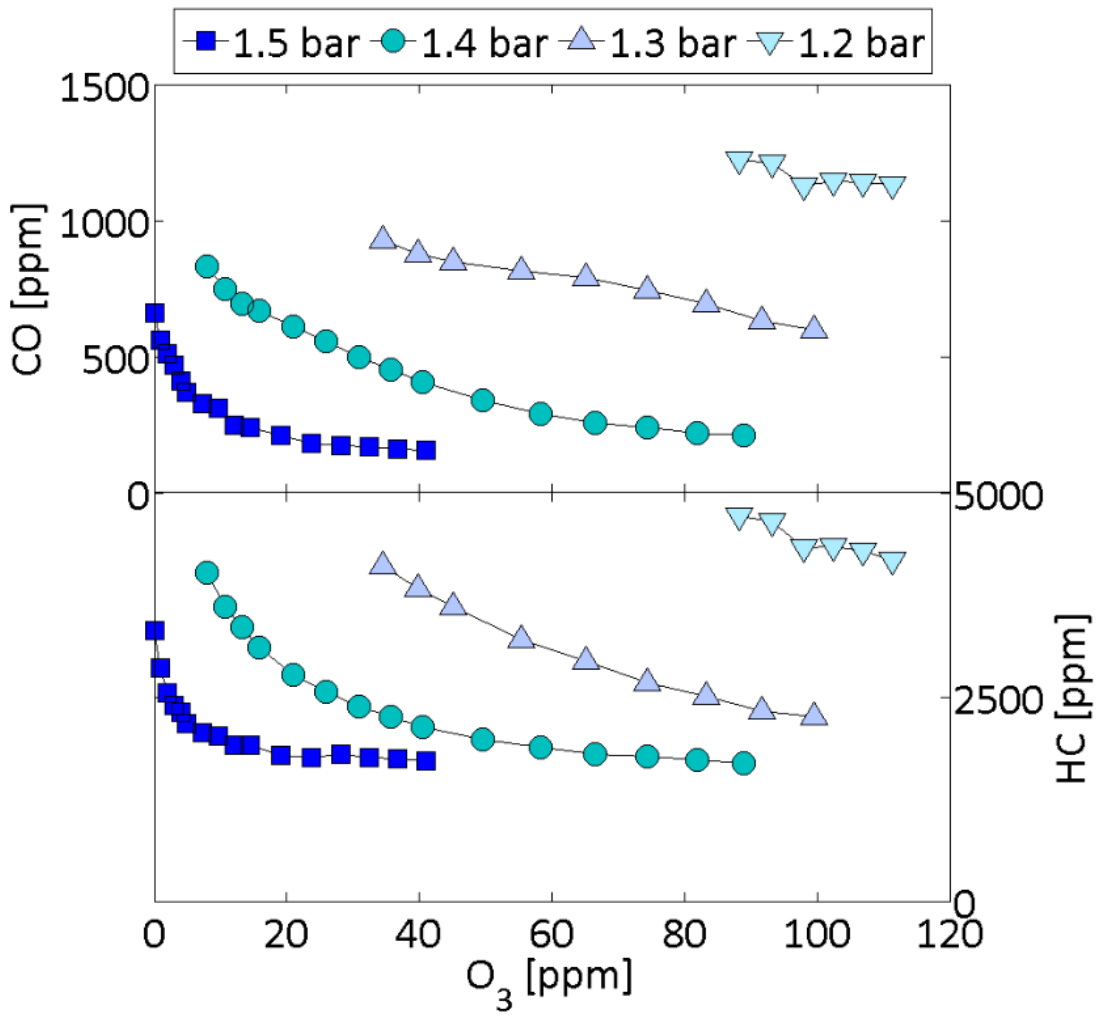

Figure 95. *Carbon monoxide and unburned hydrocarbons emissions as a function of the ozone injected under various intake pressures and a constant intake temperature of 495 K.*

3.1.1.1. Pollutants under intake pressure variation

Additionally to the engine outputs, pollutants (carbon monoxide (CO), unburned hydrocarbons (HC) and nitrogen oxides (NO_x)) were also measured and are analyzed above.

3.1.1.1.1. Carbon monoxide and unburned hydrocarbons

Generally, it may be observed that the ozone seeding results in a decrease of the CO and HC levels (Figure 95). These two pollutants present a similar decrease except that the quantified values are different and they finally finish to achieve a minimum and finite value. These high levels are due to the intake conditions fixed (closed to misfiring cycle) which are not favorable for achieving ideal cylinder temperatures and combustion timing of this fuel [178], [181]. Moreover, the high levels of CO and HC are also due to the shape of the piston which is a diesel one. Such a shape leads to a squish volume [179] and crevices [82] which traps part of the fresh gases and avoid their combustion. Finally, both trends demonstrate that ozone is responsible of an improvement of the combustion since lower are these pollutants, higher is the combustion efficiency.

3.1.1.1.2. Nitric oxides

For NO_x, results showed an increase of this pollutant. Levels are quite low under unfavorable conditions while with the enhancement of the combustion, high level may be achieved (Figure 96). Such a level is due to the in-cylinder temperatures which may reach temperatures closed to 2200 K and are particularly high due to the intake conditions selected [18]. However, under the lowest intake pressure tested (1.2 bar), NO_x are strongly reduced and we find all the benefits of using homogeneous combustion.

Compare to isooctane combustion in the previous chapter where the levels of NO_x can be neglected, the high amount measured with methane/propane blend must be discussed. According to Figure 96, NO_x range from 0 to 1000 ppm and means that NO_x trapped into the clearance volume of the engine may be estimated up to 60 ppm [151]. In this case, the intake pressure was fixed at 1.5 bar and the ozone ranged from 0 to 40 ppm. As the NO_x concentration is higher than ozone one, it could be assumed that all the ozone should be consumed by reaction between these oxidizing species. Nevertheless, such an assumption does not allow us to explain the promoting effect on the combustion since oxidizing species produced from reactions between ozone and NO_x have less effect than ozone alone. The main reason of these results comes from the difference of pressure between the intake and the exhaust which are respectively of 1.5 bar and 1.0 bar. As a result, there is a swept of the hot residuals and therefore of the residuals NO meaning that the reaction between O_3 and NO during the induction stroke can still be neglected in the present case. However, the possibility of ozone breakdown in front of the intake pipe with the elevated intake temperature have not to be neglected [159], [160]. Such a prior decomposition could lead to prior oxidation of the fuel and there will also be no time for

competition between reactions leading to the decomposition of ozone and reactions which involve ozone and NO_x. Moreover, according to this assumption, NO_x should not consumed with ozone and perhaps these residuals also contribute to the improvement of the combustion in this case [124]. This strengthens the need of studying with a more suitable experimental setup the reactions which may come in such a case between the fresh gases before their entrance into the combustion chamber.

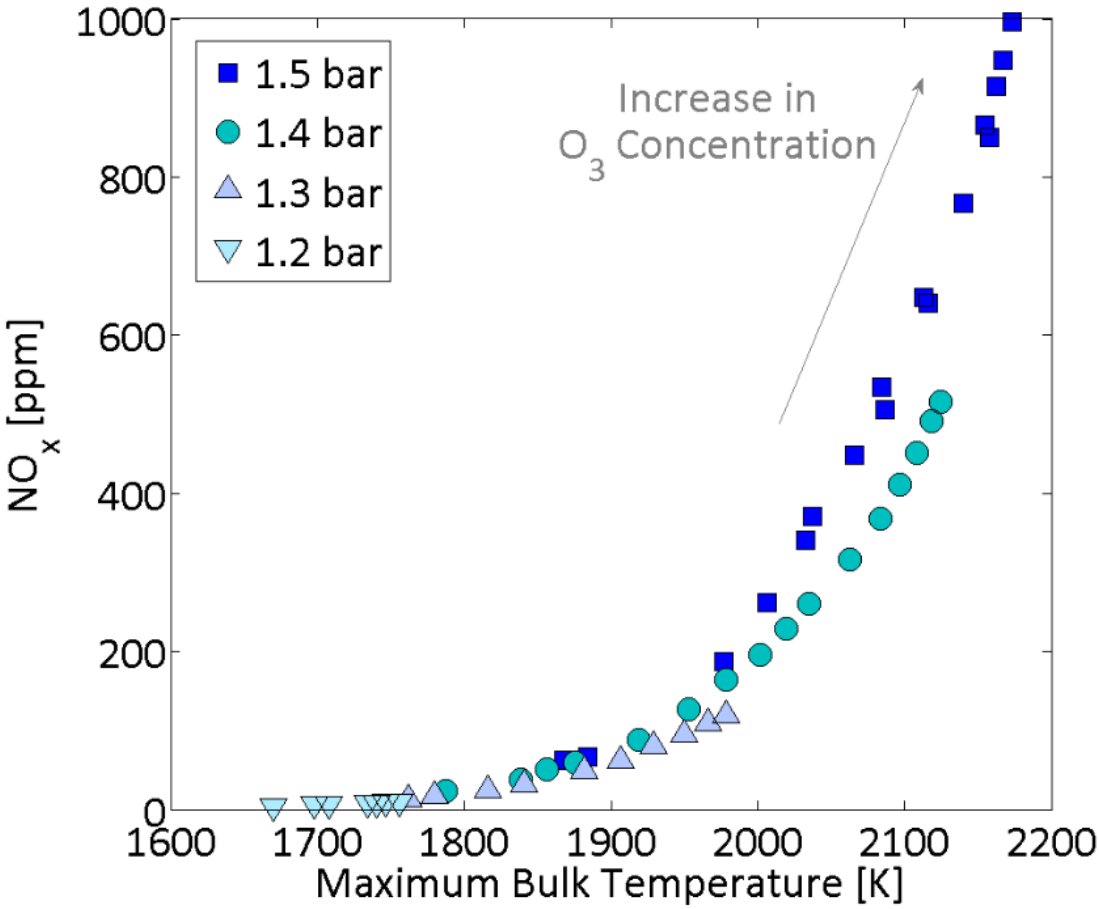

Figure 96. *Nitric oxides measured at the exhaust of the engine as a function of the maximum bulk temperature estimated under various intake pressures and a constant intake temperature of 495 K.*

3.1.1.2. Combustion characteristics under intake temperature variation

Previous investigation examined the possibility of degrading the intake pressure and use ozone for controlling HCCI combustion of the methane propane fuel selected. In this part, the same investigation was performed but by reducing the intake temperature of the engine while the intake pressure is kept constant. Four intake temperatures were selected ranging from 448 K to 495 K. The intake pressure was fixed at 1.5 bar and experiments were conducted by varying the ozone concentration. Engine outputs are presented in Figure 97.

Generally and similarly to the previous results under unfavorable intake pressures, engine outputs showed that to maintain the combustion, a minimum ozone concentration is also needed. This initial value exponentially increases with the decrease of the intake temperature since the bulk mass temperature reached lower levels.

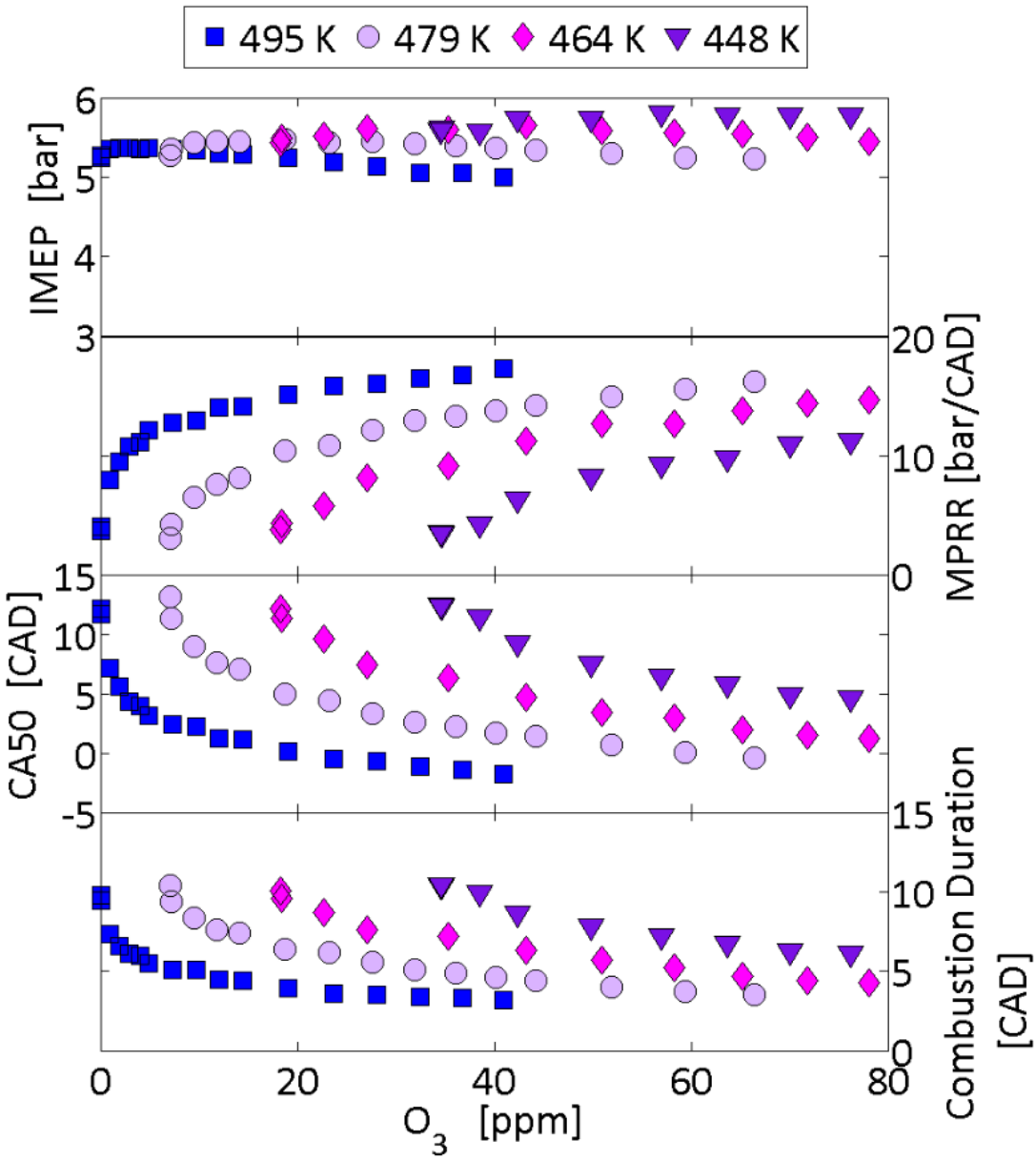

Figure 97. *Engine outputs (IMEP, maximum pressure rise rate, CA50 and combustion duration) as a function of the ozone injected under various intake temperatures and a constant intake pressure of 1.5 bar.*

Inversely to the intake pressure reduction, decreasing the intake temperature results in a growth of the IMEP. As the temperature decrease, the mass introduced inside the combustion is more important and therefore, a more significant IMEP may be obtained. Nevertheless, the trend of this parameter stays similar to previous one, i.e. the IMEP increases, reaches a maximum and finally decreases. Observing the MPRR, a slight decrease

may be visible under lower temperatures than those necessary. However, even if we apply lower intake temperatures, the combustion noise remains very high. Reducing the intake temperature is therefore less efficient than reducing the intake pressure. Finally, for CA50 and combustion duration, trends are also similar to those observed previously but the impact of the ozone demonstrate in all the cases that continuing to raise the ozone concentration have no effect as they present a minimum and finite value.

3.1.1.3. Pollutants under intake temperature variation

Pollutants during experiments under lower intake temperatures were also measured and were analyzed hereafter.

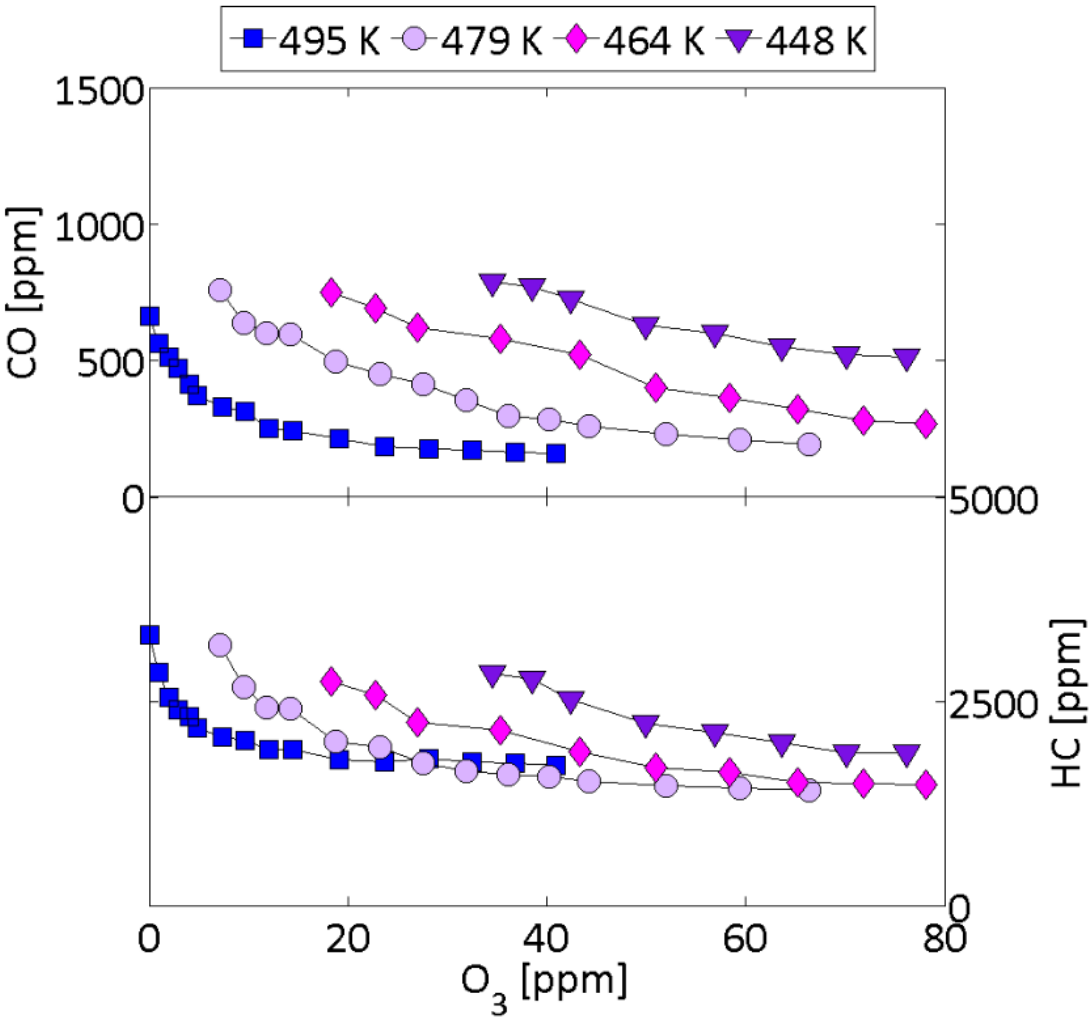

Figure 98. *Carbon monoxide and unburned hydrocarbons emissions as a function of the ozone injected under various intake temperatures and a constant intake pressure of 1.5 bar.*

3.1.1.3.1. Carbon monoxides and unburned hydrocarbons

Emissions of carbon monoxide and unburned hydrocarbon measured at the exhaust of the engine are presented in Figure 98. Here again, similar trends than those observed under intake pressure variation were observed. CO and HC simultaneously decrease with

ozone additions meaning that ozone well enable to improve the combustion under these conditions. Moreover, both pollutants seem to achieve a unique finite value which seems function of the intake pressure and which may achieve with the ozone. However, levels remain high due to the shape of the piston.

3.1.1.3.2. Nitric oxides

For emissions of nitric oxides, the increase is due to the in-cylinder temperatures reached which are higher than the minimum temperature corresponding to the occurrence of NO_x in such conditions [18]. Decreasing the intake temperature allows to reduce these emissions but unfortunately, they do not achieve zero because of the elevated intake pressure (1.5 bar) which make possible high temperatures within the combustion chamber (Figure 99). Such emissions could be strongly reduced by decreasing the inlet temperature. Nevertheless, an intake temperature too low will result in misfires as the ozone needed to

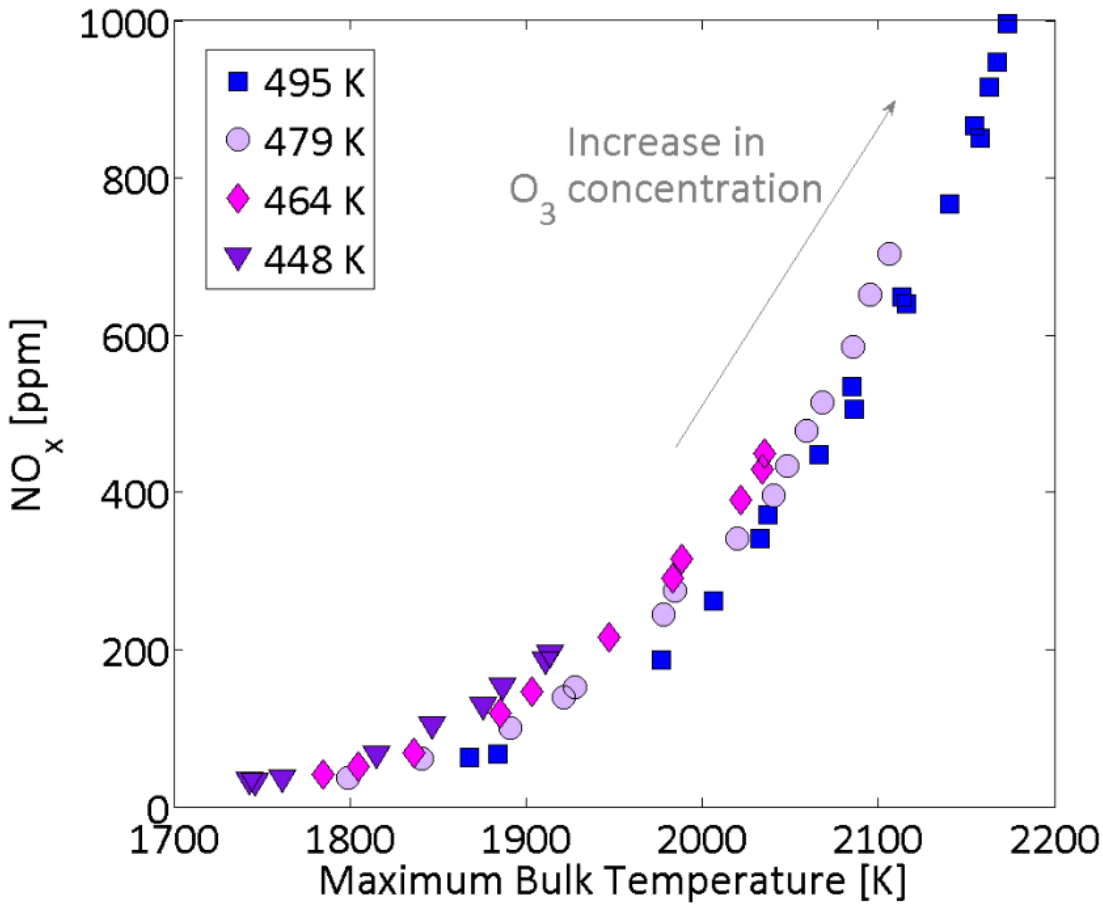

Figure 99. *Emissions of nitric oxide measured at the exhaust of the engine as a function of the maximum bulk temperature estimated under a wide range of intake temperature and for a constant intake pressure of 1.5 bar.*

maintain the combustion will be limited by the ozone generator. Finally, the intake temperature has less impact than the intake pressure on these pollutants since lower in-cylinder pressures were reached by decreasing the intake pressure. Additionally, the levels of NO_x measured here must be also considered but the promoting effect on the combustion previously observed is probably due to the ozone breakdown alone. Again, in the present case, there is a higher intake pressure (1.5 bar) than the exhaust pressure (1.0 bar) meaning that hot residuals are swept by fresh gases, therefore limiting the reactions involving NO_x and O_3 during the induction stroke. However, possible ozone decomposition and fuel oxidation in front of the intake pipes have not to be neglected due to the high intake temperature tuned.

To conclude, the experiments performed on the methane/propane fuel selected showed that ozone is able to keep the control of the HCCI combustion even when the intake conditions, pressure and temperature, are not favorable for achieving an ideal phasing. Moreover, it is also possible to control the entire engine outputs as well as pollutants.

3.1.2. Kinetics interpretation

As for PRFs, present experimental results on gaseous fuels were coupled with computational results to further investigate the impact of ozone on the oxidation of gaseous fuels. These simulations were also run with the help of the Chemkin package and the constant volume model. The kinetic scheme selected was that presented in Chapter 2 where the ozone sub-mechanism has been added.

3.1.2.1. Assessment of the kinetic scheme

The kinetic scheme consists of the combination of a gaseous fuels scheme with an ozone sub-mechanism. The scheme for gaseous fuels is that validates for hydrogen, carbon monoxide and C1 to C4 species proposed by *Wang et al.* [155] and the ozone sub-mechanism is that previously used and proposed by *Halter et al.* [132]. Both mechanisms were validated separately and it is therefore needed to evaluate this new scheme. Ignition delays were therefore computed in the case of pure methane and pure propane as fuels without ozone for the mechanism with and without the presence of the ozone sub-mechanism. Conditions were fixed at 40 bar and for an equivalence ratio of 0.4 while computations were run by ranging the temperature. Results showed no difference with and without the addition of the ozone sub-mechanism.

3.1.2.2. Ignition delays

Computations of the ignition delays were simulated first by varying the temperature for pure methane, pure propane and for a mixture of both gaseous fuel without ozone and with concentrations of 1, 10 and 100 ppm of this oxidizing chemical species. Conditions were took in agreement with the values observed during experiments, i.e. a pressure of 40 bar

and an equivalence ratio of 0.4 observed just before the ignition into the combustion chamber. Results are plotted in Figure 100.

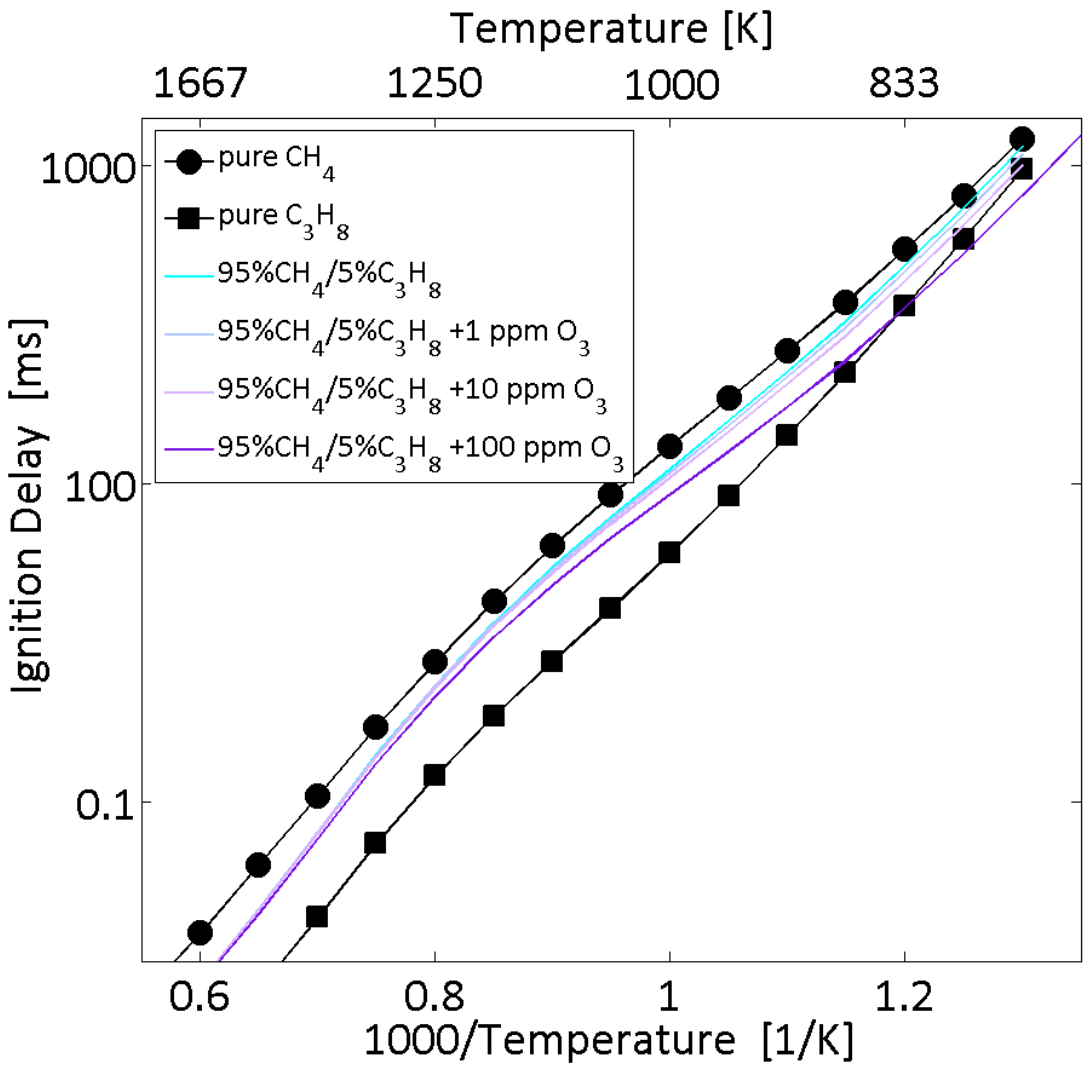

Figure 100. *Ignition delays as a function of the inverse temperature of pure methane, pure propane and a mixture of both fuels without ozone and with mole fraction of 1, 10 and 100 ppm of ozone.*

Results showed that pure methane is well the most difficult to auto-ignite and pure propane the easier. These results are therefore in agreement with those observed during experiments. For the use of a mixture of 95 % of methane and 5 % of propane, the ignition delays computed are slightly lower than pure methane ones. This blend may therefore auto-ignite more easily than pure methane due to the presence of propane and explain that this natural gas surrogate can burn into the engine and not the neat methane. By applying ozone, the ignition delays computed are reduced. The impact is clearly visible for temperature lower than 1250 K (higher than 0.8 in Figure 100). Moreover, the trends showed that ozone concentrations added exponentially advance the ignition delay.

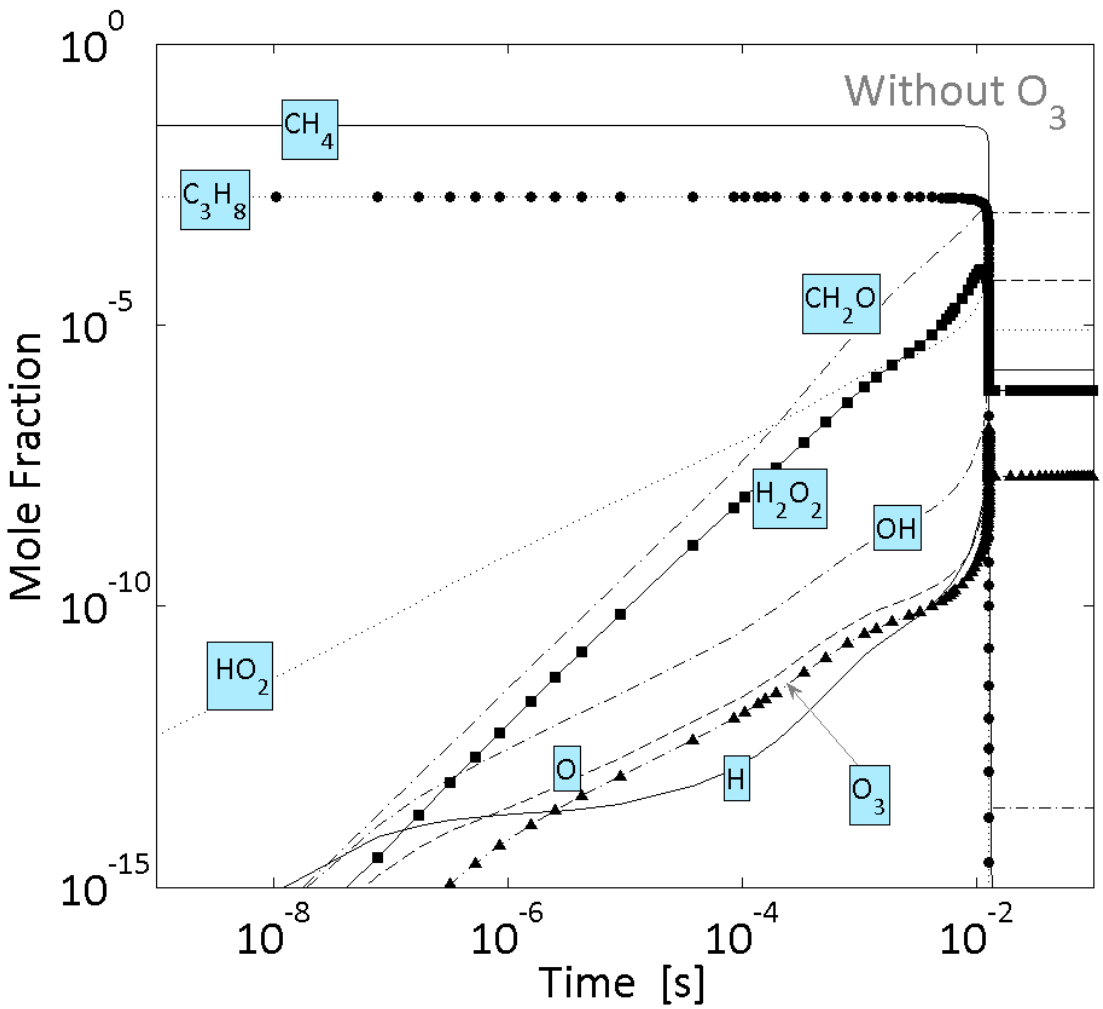

Figure 101. A. *Mole fractions for a mixture of methane and propane (95/5) without ozone.*

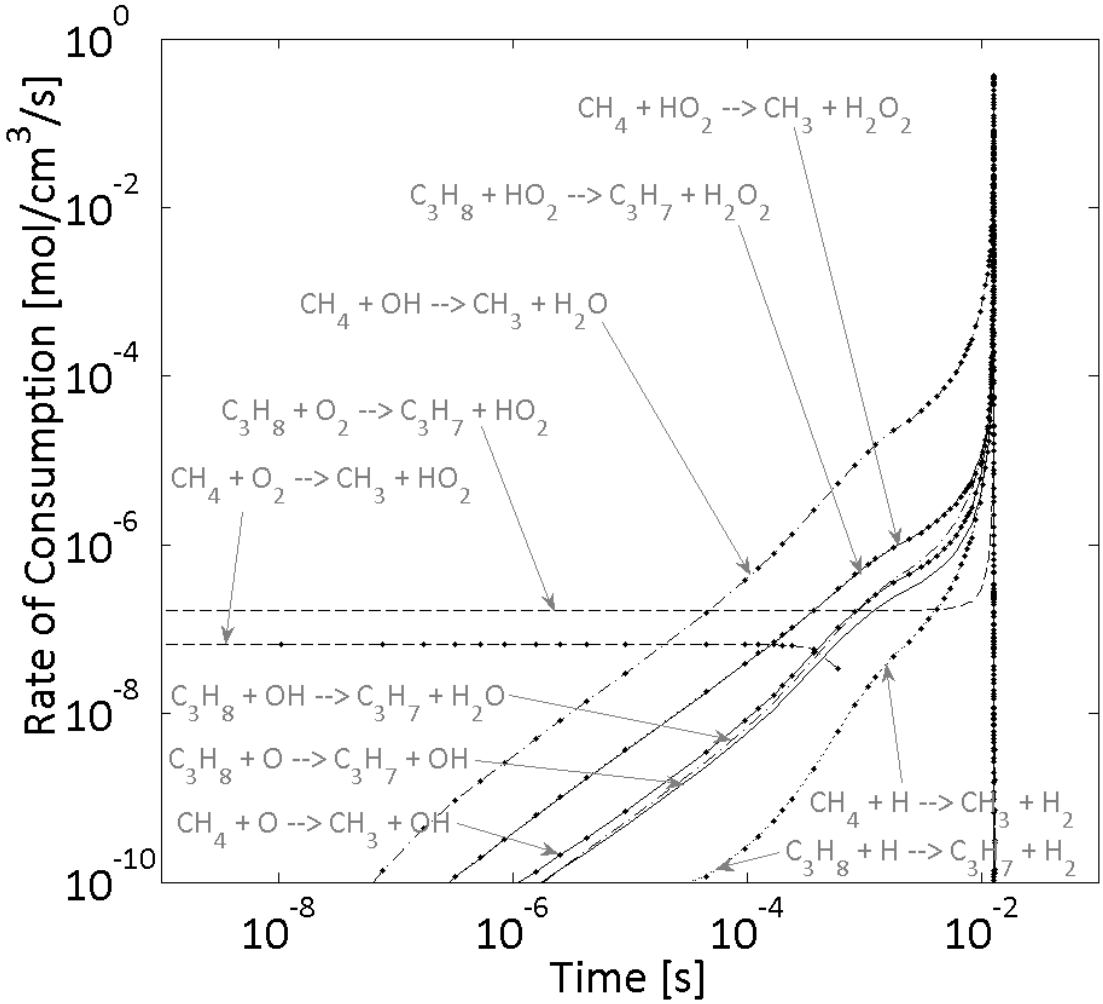

Figure 101. B. *Rate of consumption for a mixture of methane and propane (95/5) without ozone.*

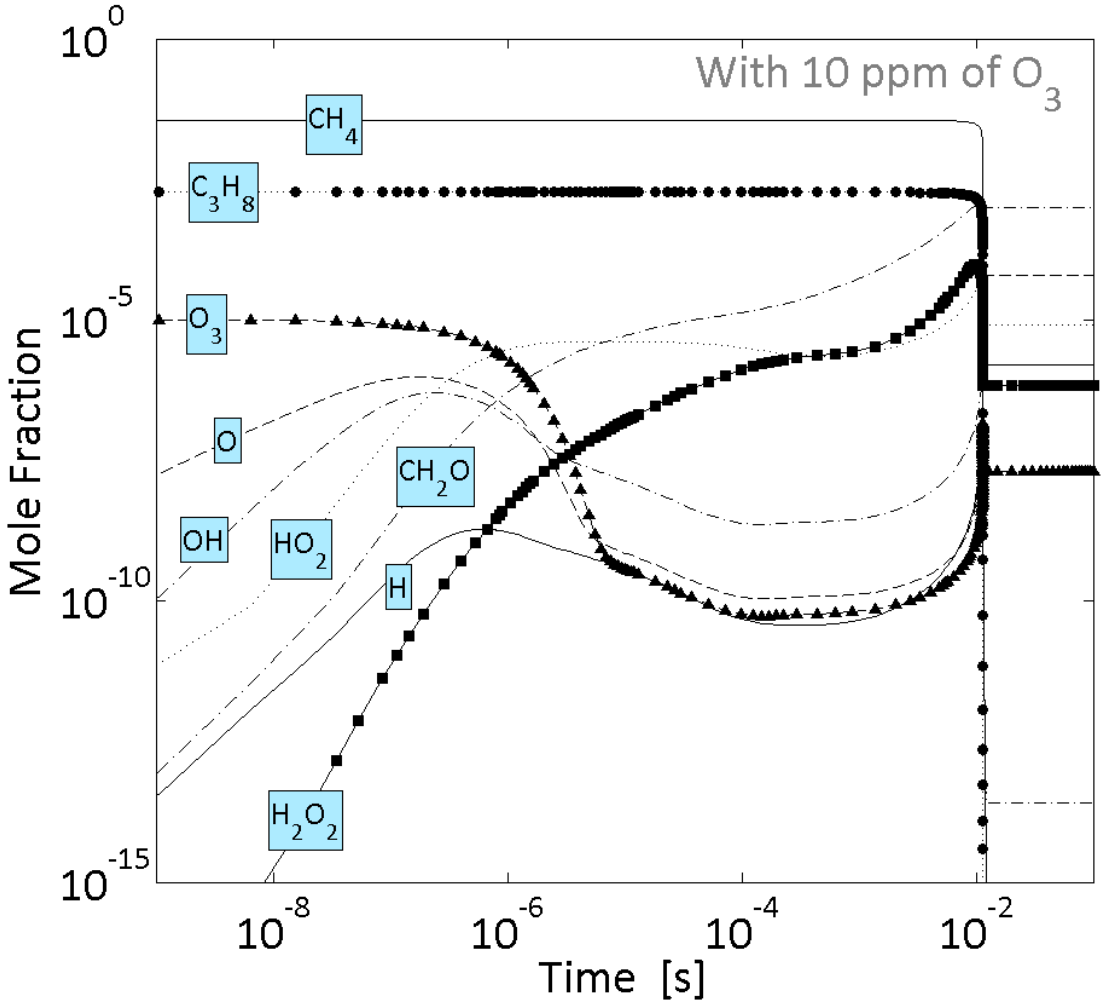

Figure 101. C. *Mole fractions for a mixture of methane and propane (95/5) with 10 ppm of ozone.*

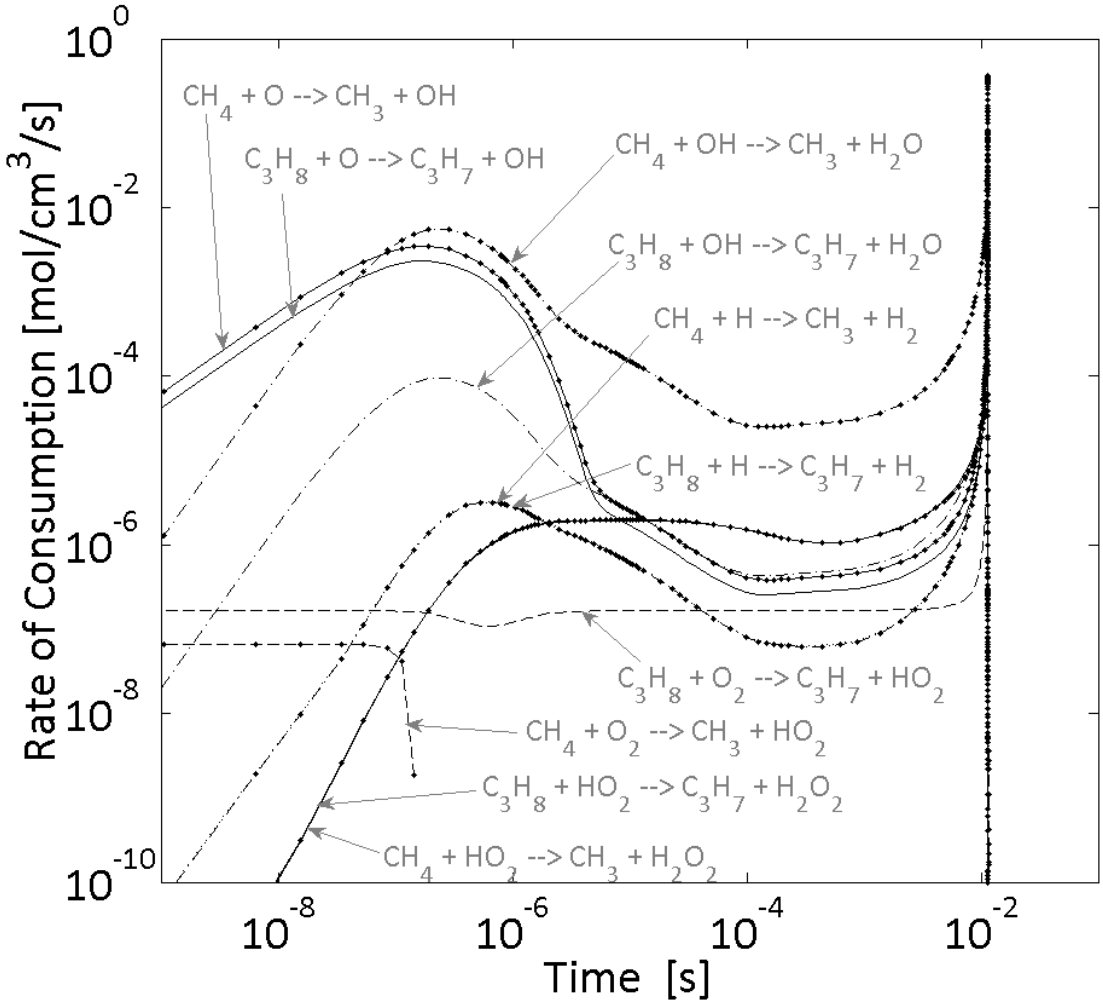

Figure 101. D. *Rate of consumption for a mixture of methane and propane (95/5) with 10 ppm of ozone.*

3.1.2.1. Rates of consumption

Following the computations of ignition delays, the oxidation pathways of methane propane fuel selected were studied in two conditions: without ozone and for a concentration of 10 ppm. Results for mole fractions of the main radicals and rate of consumption for methane and propane are showed in Figure 101.

The impact of ozone on methane and propane was separately investigated. Without ozone, it may be observed that the oxidation of methane starts by a reaction involving the oxygen molecule (R-38). This reaction leads to the formation of a methyl radical (CH_3) and a hydroperoxyl radical (HO_2).

$$CH_4 + O_2 \rightarrow CH_3 + HO_2 \qquad \text{R-38}$$

Following this initiation reaction, methane is mainly consumed through reactions with hydroxyl radicals (OH) (R-39) and HO_2 radicals (R-40). The first one dominates and leads to the combustion.

$$CH_4 + OH \rightarrow CH_3 + H_2O \qquad \text{R-39}$$

$$CH_4 + HO_2 \rightarrow CH_3 + H_2O_2 \qquad \text{R-40}$$

According to the analysis of the reactions, OH radicals are produced from the following reaction system (R-41 to R-45).

$$H_2O_2 \rightarrow OH + OH \qquad \text{R-41}$$

$$CH_3 + O_2 \rightarrow CH_2O + OH \qquad \text{R-42}$$

$$CH_3 + HO_2 \rightarrow CH_3O + OH \qquad \text{R-43}$$

$$H + O_2 \rightarrow O + OH \qquad \text{R-44}$$

$$H + HO_2 \rightarrow OH + OH \qquad \text{R-45}$$

In this system, the H_2O_2 radical is produced from two HO_2 radicals via reaction R-46.

$$HO_2 + HO_2 \rightarrow H_2O_2 + O_2 \qquad \text{R-46}$$

while H comes from the reactions R-47 and R-48.

$$H_2 + O \rightarrow OH + H \qquad \text{R-47}$$

$$H_2 + OH \rightarrow H_2O + H \qquad \text{R-48}$$

On the other hand, the oxidation of propane also starts with an initiation reaction involving an oxygen molecule and results in the production of an alkyl radical of the propane and a HO_2 radical (R-49).

$$C_3H_8 + O_2 \rightarrow C_3H_7 + HO_2 \qquad \text{R-49}$$

Then, propane is mostly consumed by OH and HO_2 radicals through the following reactions which lead to the combustion.

$$C_3H_8 + OH \rightarrow C_3H_7 + H_2O \qquad \text{R-50}$$

$$C_3H_8 + HO_2 \rightarrow C_3H_7 + H_2O_2 \qquad \text{R-51}$$

Similarly to the methane, OH radicals in the case of propane come from the system involving the reactions R-41, R-42, R-42 and R-52.

$$aC_3H_5 + HO_2 \rightarrow OH + C_2H_3 + CH_2O \qquad \text{R-52}$$

where H_2O_2 comes from the reaction R-46 as previously determined and the other radicals, i.e. CH_3 and aC_3H_5, come from direct and indirect decompositions of propane.

Finally, when we consider the surrogate of natural gas, the oxidation starts with an initiation reaction of the propane which reacts more easily than the oxidation of methane with the oxygen molecule. Then, the low concentration of radicals produced allows consuming both fuels with chain branching reaction up to the occurrence of the combustion.

When ozone is injected, the oxidation pathway is modified. Instead of reacting with oxygen molecule, these two fuels react with O-atoms through reactions R-53 and R-54 and results into a direct formation of OH radicals.

$$CH_4 + O \rightarrow CH_3 + OH \qquad \text{R-53}$$

$$C_3H_8 + O \rightarrow C_3H_7 + OH \qquad \text{R-54}$$

These O-atoms comes from ozone decomposition which occurs earlier than usual oxidation of the fuels through reaction R-55.

$$O_3 + M \rightarrow O_2 + O + M \qquad \text{R-55}$$

Then, the direct production of OH radicals allows to rapidly oxidize fuels, leading to earlier chain branching reactions and an earlier auto-ignition. The impact of ozone through a kinetics analysis may therefore be summarized as in Figure 102.

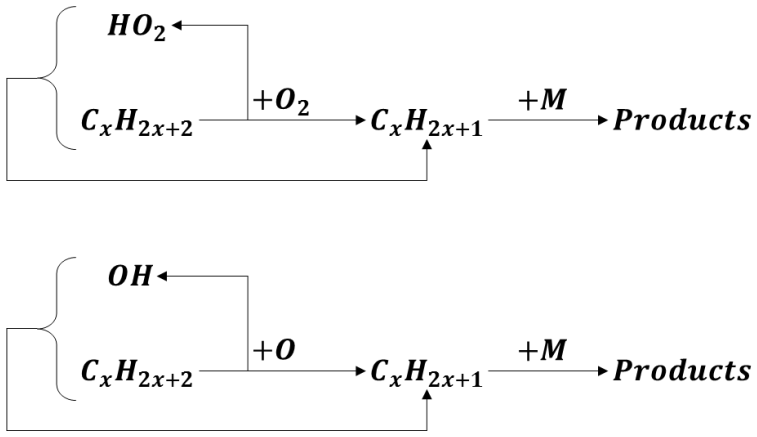

Figure 102. *Initial reactions involving gaseous fuel oxidation in the case without ozone seeding (on the top) and with ozone seeding (on the bottom).*

3.2. Combustion of methane/hydrogen surrogate

Previous study considered a natural gas surrogate composed of methane and propane. In the present part, propane was replaced by hydrogen and was mixed in various volumetric fractions with methane. The investigation was also conducted through experiments on the engine test bench and with the same computational method than one used for previous results.

3.2.1. Experimental results

For this fuel, experiments were performed by varying the proportion of hydrogen in the fuel and by varying the ozone concentration seeded. All the other conditions, i.e. the intake pressure, the intake temperature, the rotation speed and the equivalence ratio were kept similar to those fixed in the previous part. As a reminder, intake pressure was 1.5 bar, intake temperature was 495 K, rotation speed was 1500 rpm and equivalence ratio was 0.4.

3.2.1.1. In-cylinder pressure, temperature and heat release rate trends

The impact of ozone was investigated under these conditions for a mixture of methane and hydrogen. It was observed experimentally that keeping the 95 % of methane and replacing the 5 % of propane by the same amount of hydrogen does not allow to auto-ignite this surrogate. However, previous results without ozone showed that pure hydrogen auto-ignites earlier than propane and unfortunately, a similar fraction of hydrogen does not help the fuel to auto-ignite. In fact, hydrogen does not provide enough radicals to oxidize the methane which in turn react as an inhibitor due to the high temperature needed to self-

ignite it. Volumetric fractions of each gas were therefore modified to enable to obtain the combustion. The new fuel found is a mixture of 80 % methane and 20 % hydrogen which can be related to hythane. Considering it, experiments were conducted by ranging ozone from 0 up to approximately 40 ppm. Results are presented in Figure 103 for in-cylinder pressure, in-cylinder temperature and heat release rate traces. Black curves represent the average on 100 cycles recorded while shaded areas correspond to the variation of the same 100 cycles.

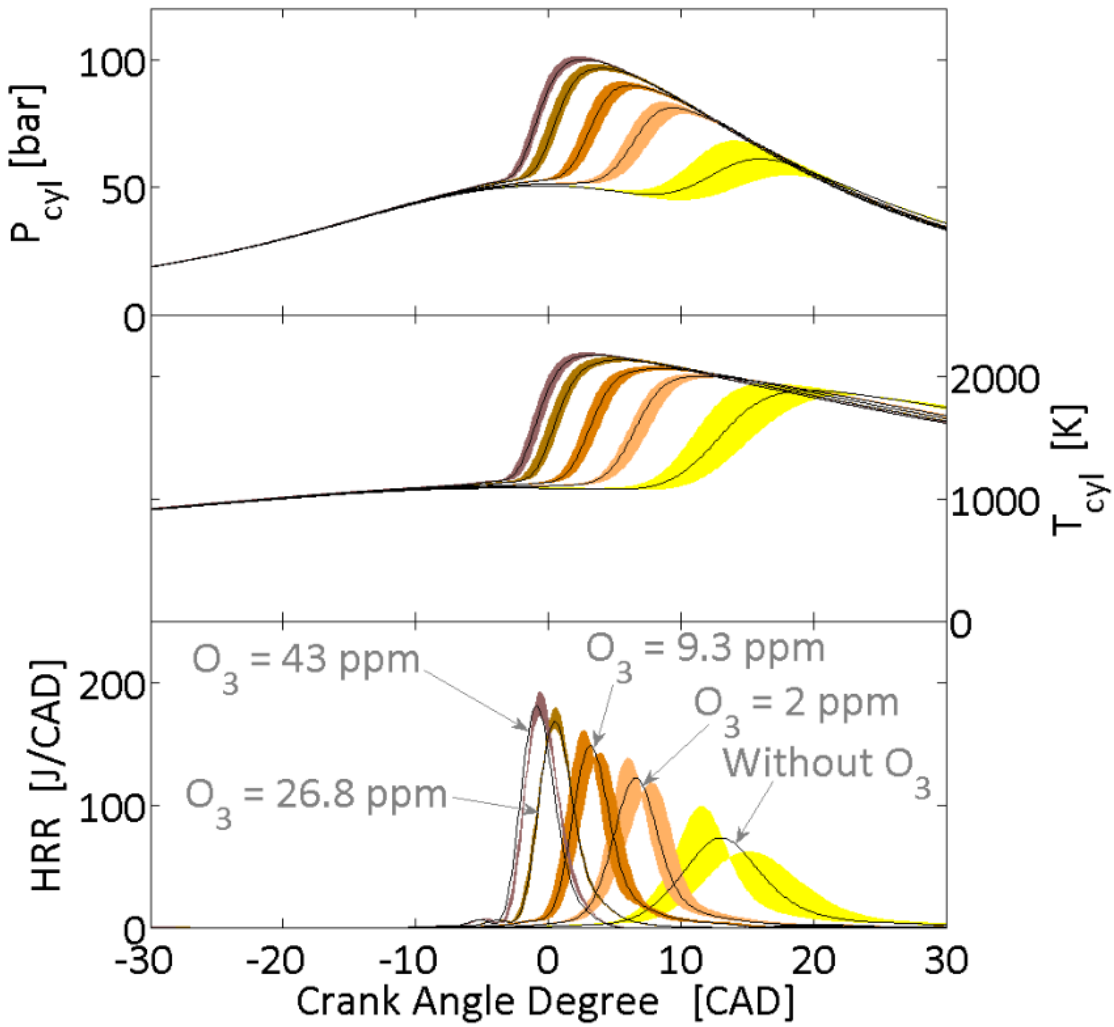

Figure 103. *In-cylinder pressures, in-cylinder temperatures and heat release rates traces as a function of the ozone concentration for a mixture of methane and hydrogen (80/20), an intake pressure of 1.5 bar and an intake temperature of 495 K.*

As already observed in our previous results and in literature [9], [11]–[13], ozone leads to an improvement and an advance of the combustion of the methane hydrogen mixture selected. All the traces presented showed an increase of their maximum value coupled with an advance of their respective location towards the top dead center. Moreover, the combustion duration is reduced when increasing the concentration of this oxidizing chemical species and finally, observing the shaded areas, a better stabilization of the HCCI combustion can be achieved.

3.2.1.2. Combustion characteristics

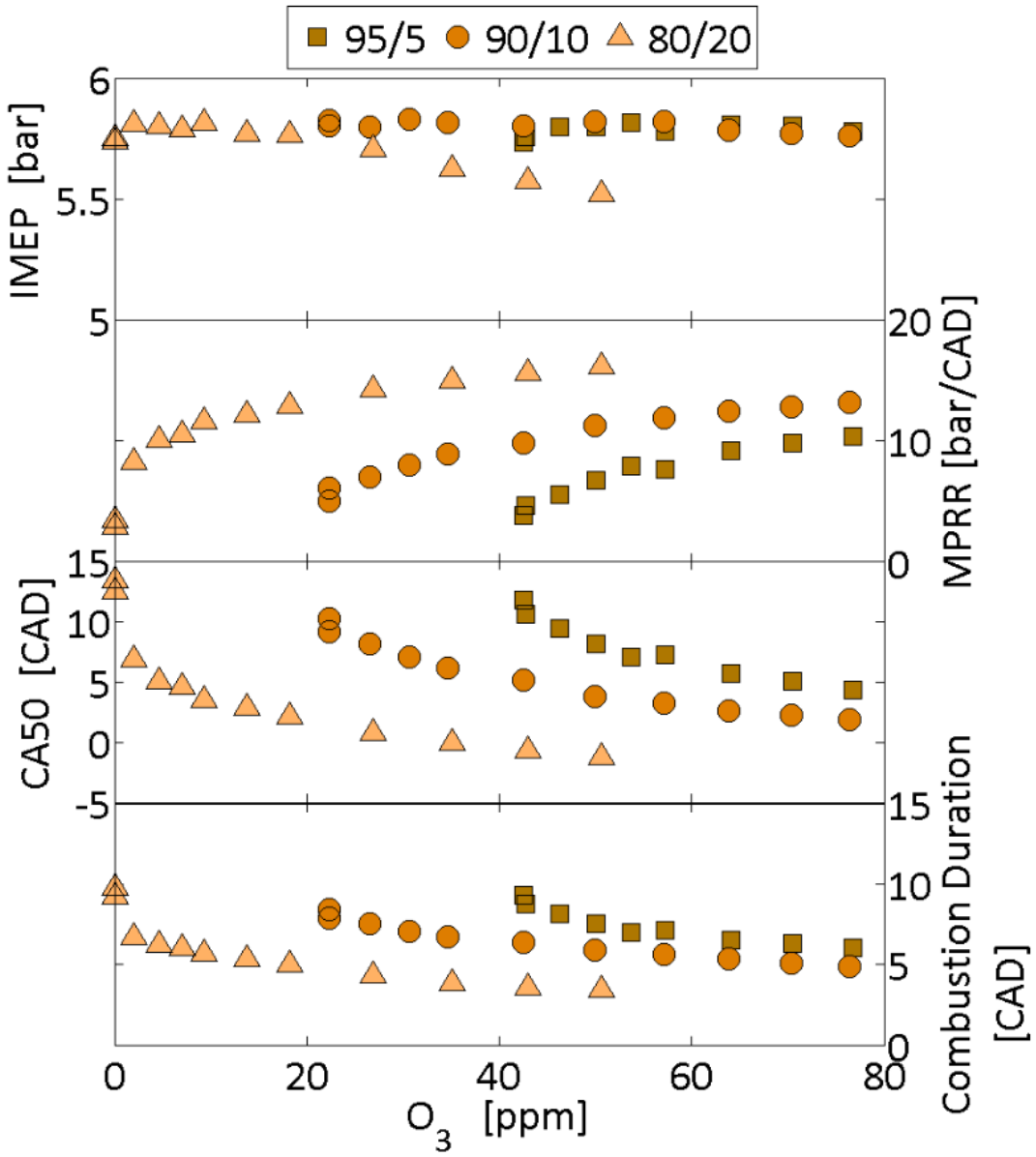

Figure 104. *Engine outputs (IMEP, maximum pressure rise rate, CA50 and combustion duration) as a function of the ozone concentration under various mixtures of methane and hydrogen.*

The impact of ozone on a blend of gases (methane/propane and methane/hydrogen) was previously investigated and showed a high potential to control the HCCI combustion phasing. Moreover, it was also revealed that combustion under unfavorable intake conditions can be maintained. The present part focused on the use of ozone to auto-ignite fuels whose the properties do not allow their self-ignition. It was therefore investigated the impact of ozone on mixture of methane and hydrogen with lower volumetric fractions than one previously studied. Mixtures selected are summarized in Table 7. For all these fuels, experimental conditions were kept constant under the values

previously cited. Only ozone concentrations were ranged from 0 to approximately 80 ppm. The results on engine combustion characteristics are plotted in Figure 104.

Table 7. *Mixtures of methane and hydrogen selected.*

Fuels	Methane [%]	Hydrogen [%]
A	80	20
B	90	10
C	95	5

Engine outputs showed that IMEP increases briefly and decreases rapidly with the ozone concentration. Similar trends may be observed for other mixtures but the effect is less pronounced. However, it can be seen that the work produced by the engine is fairly constant. Regarding the trends on MPRR, increasing the ozone concentration results in a

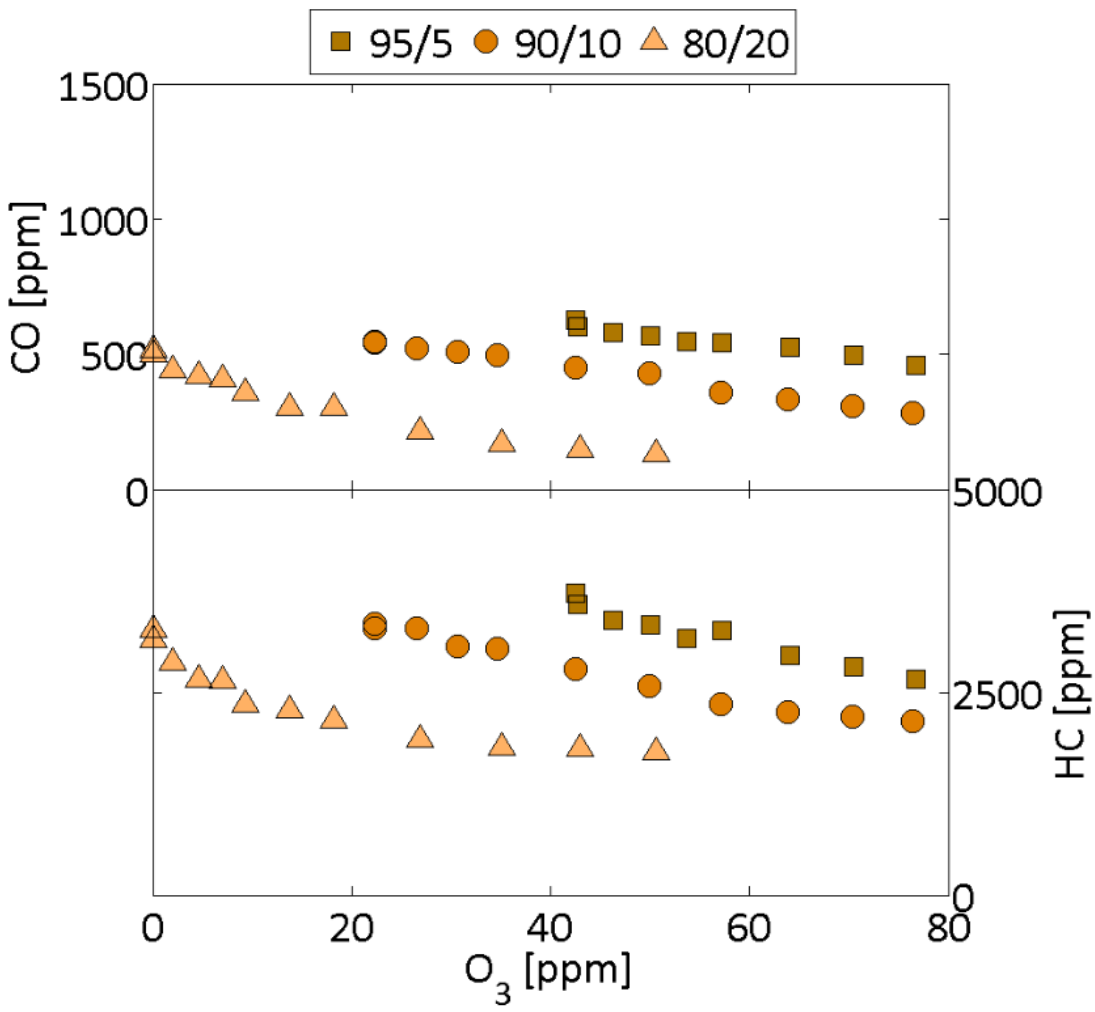

Figure 105. *Carbon monoxide and unburned hydrocarbon emissions as a function of the ozone concentration under various mixtures of methane and hydrogen.*

high level of noise. Even if the value is moderated for the mixture with the lowest hydrogen fraction, it remains too important due to the high intake pressure and temperature tuned. Finally, the combustion phasing and the combustion duration well showed that ozone allows to advance the HCCI combustion and that the combustion process occurs more rapidly. Controlling such combustion is therefore possible by using this oxidizing chemical species. Moreover, as a function of the fuels, these parameters seem to tend towards a finite and constant value and continuing injected more ozone will not improve much the combustion.

3.2.1.1. Pollutants

Additionally to the engine outputs, pollutants at the exhaust of the engine for these methane/hydrogen surrogates were also measured and analyzed.

3.2.1.1.1. Carbon monoxides and unburned hydrocarbons

Trends for carbon monoxide and unburned hydrocarbon are plotted in Figure 105 and showed evolutions very similar to those observed for a mixture of methane and propane, i.e. a decrease of both pollutants when the ozone increases. Here again, CO and HC reach a finite value which remains high mainly due to the squish volume of the piston. However, by comparing with previous measurements carried out with methane/propane as fuel, lower levels of CO were achieved. These low concentrations of CO measured are due to the use of hydrogen which does not contain C-atoms into its own structure.

3.2.1.1.2. Nitric oxides

NO_x emissions were finally also measured for methane/hydrogen fuels and high levels of this pollutant were observed (Figure 106). Here again, the important concentrations of NO_x are due to the intake conditions of pressure and temperature needed to auto-ignite these fuels which are very high and allow to reach significant in-cylinder temperatures (up to 2200 K) [18]. Compare to the results for methane/propane as fuel, concentrations of NO_x are upper with methane/hydrogen while the maximum bulk temperature is quite the same. This higher concentration is due to the determination of the maximum bulk temperature which is an average and means that local temperature into the combustion chamber could be even higher due to the high reactivity of hydrogen. Finally, the interaction between NO_x and ozone must be also considered since the fraction of this species trapped into the clearance volume should be higher. Nevertheless, as discussed with methane/propane as fuel, the difference between the intake pressure and the exhaust pressure which are 1.5 bar and 1.0 bar, respectively, means that NO_x residuals are swept, reducing possible reactions between O_3 and NO during the induction stroke. However, with the high intake temperature, ozone may break down earlier and prior reactions into the intake with the fuel must not be neglected.

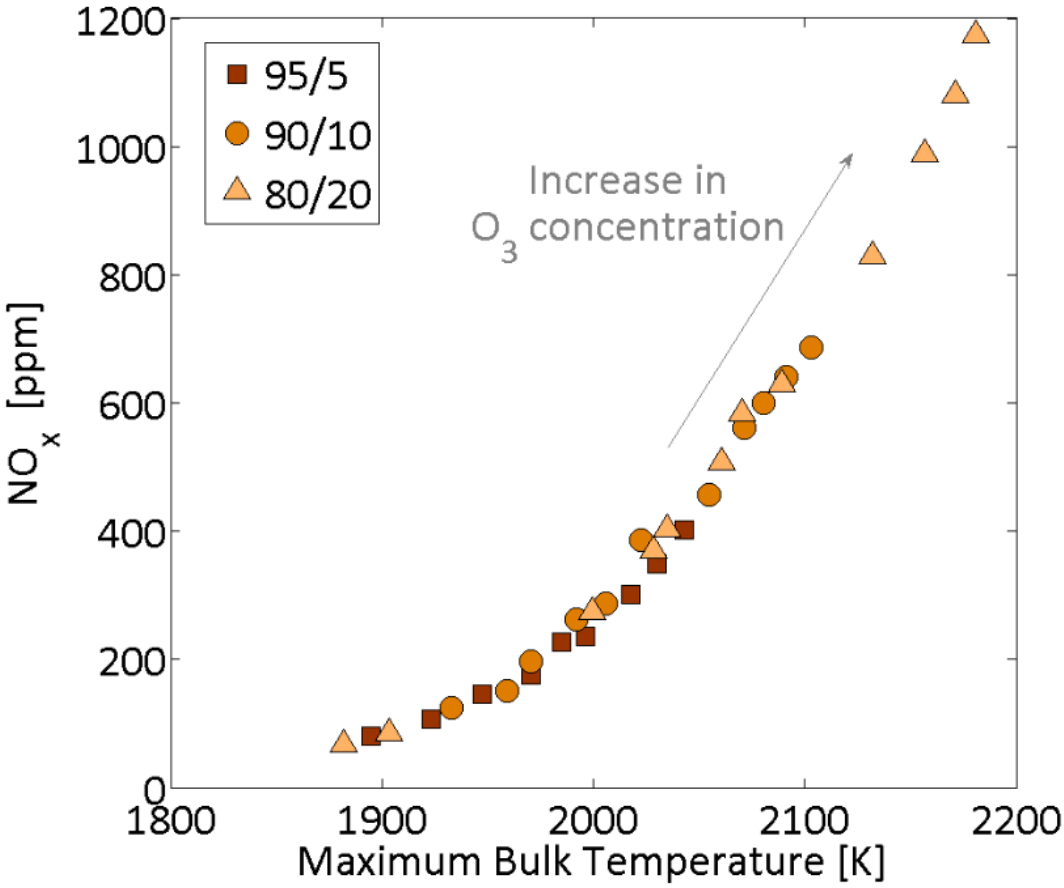

Figure 106. *Nitric oxides emissions as a function of the maximum bulk temperature under various mixtures of methane and hydrogen*

To conclude on methane/hydrogen fuels, all these results demonstrate that ozone has the potential to control HCCI combustion parameters of various mixtures of fuels. In particular, ozone is very useful to help auto-ignite fuels whose combustion does not occur.

3.2.2. Kinetics interpretation

To complete the experimental results on the combustion of methane/hydrogen mixture into the HCCI engine, computations were run. The kinetic scheme was that used previously to investigate the impact of ozone on the oxidation of methane/propane mixture. In this part, the simulations were only focused on a mixture of 80 % methane and 20 % hydrogen.

3.2.2.1. Ignition delays

Ignition delays were computed first under the same conditions than those used for ignition delays of the methane/propane mixture. Additionally, ignition delays for pure methane and pure hydrogen were computed with the simulations of the hythane surrogate

and the different ozone concentrations applied (0, 1, 10 and 100 ppm). Results are presented in Figure 107.

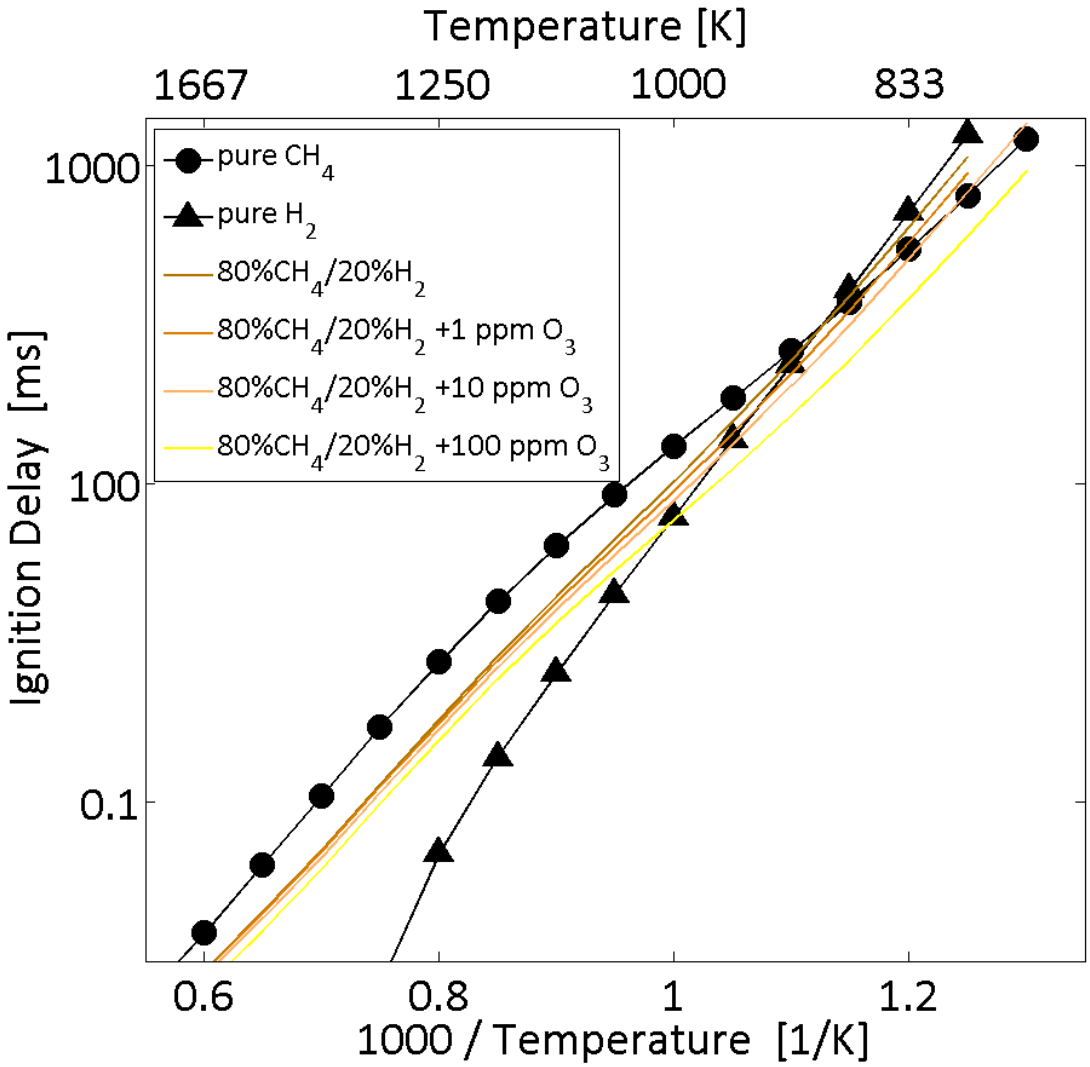

Figure 107. *Ignition delays as a function of the inverse temperature for pure methane and pure hydrogen as well as mixture of methane and hydrogen with varying ozone concentrations.*

According to the trends observed and by comparing these results with previous ignition delays computed, in particular that of propane, it may be seen that hydrogen auto-ignites later than propane for temperatures lower than 1100 K (0.9 in Figure 100 and Figure 107). This can explain the more significant volume fraction of hydrogen needed to auto-ignite methane. Moreover, by comparing with methane ignition delays, it may observe that hydrogen auto-ignite easily as soon as the temperature reaches approximately 900 K (i.e. an inverse temperature of 1.1). As the beginning of the combustion starts at temperatures near 1000 K, the fraction of hydrogen into the fuel is responsible of the combustion. According to the impact of ozone, it may observe that here again, this molecule leads to a decrease of the ignition delays computed. The effect is mainly visible for low temperatures and it may also

conclude that a low concentration of this species strongly improve the autoignition while higher concentrations continue to advance this parameter but with an effect less pronounced.

3.2.2.2. Rates of consumption

To further investigate the impact of ozone on the methane/hydrogen mixture selected, an analysis of the main pathways leading to the combustion was conducted. Two cases were studied: without ozone added and with 10 ppm of ozone. Results on the mole fractions of the fuels and the main radicals as well as the main rate of consumption of the fuels are presented in Figure 108. The impact on methane was previously studied and do not change by replacing propane by hydrogen. Therefore, only the pathways for hydrogen were analyzed. Its oxidation starts with an initiation reaction with the help of the oxygen molecule (R-56).

$$H_2 + O_2 \rightarrow H + HO_2 \qquad \text{R-56}$$

Then, the combustion is achieved through the reactions R-57 and R-58 and mainly by the reaction involving OH radicals.

$$H_2 + OH \rightarrow H + H_2O \qquad \text{R-57}$$

$$H_2 + HO_2 \rightarrow H + H_2O_2 \qquad \text{R-58}$$

OH and HO_2 radicals are mainly produced from the system including reactions R-7, R-8 and R-10. Finally, as hydrogen has a better reactivity than methane, it promotes the entire combustion with a production of OH radicals. In the case of the presence of ozone, the initiation reactions of each fuel start with an O-atom instead of the oxygen molecule (R-47 and R-53) where this atom comes from the ozone decomposition. O-atom allows creating earlier and directly OH radicals which therefore lead to an advance of the combustion. Finally, the impact of ozone on the methane/hydrogen fuel may also be summarized according to the pathways in Figure 102.

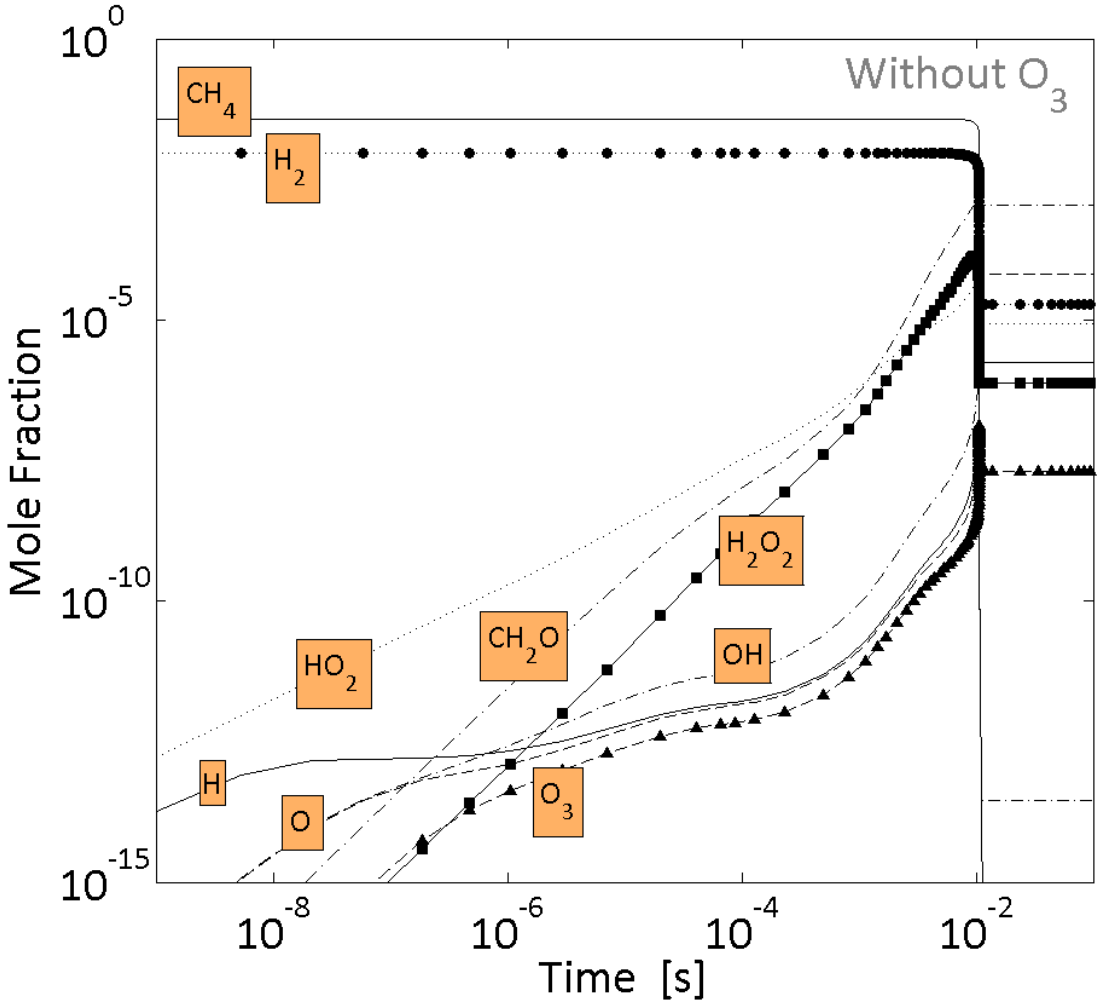

Figure 108. A. *Mole fractions of the main radicals for a mixture of methane and hydrogen (80/20) without ozone.*

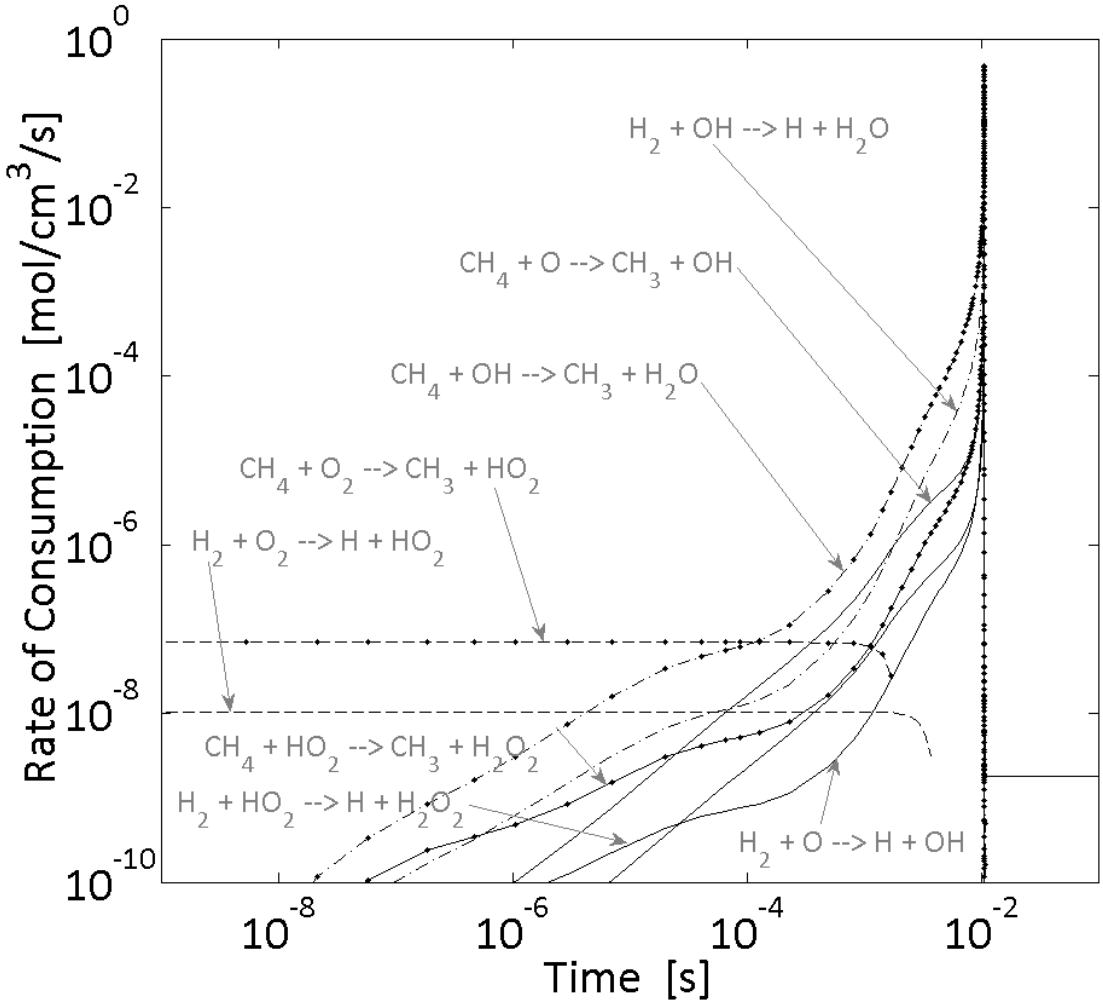

Figure 108. B. *Rate of consumption for a mixture of methane and hydrogen (80/20) without ozone.*

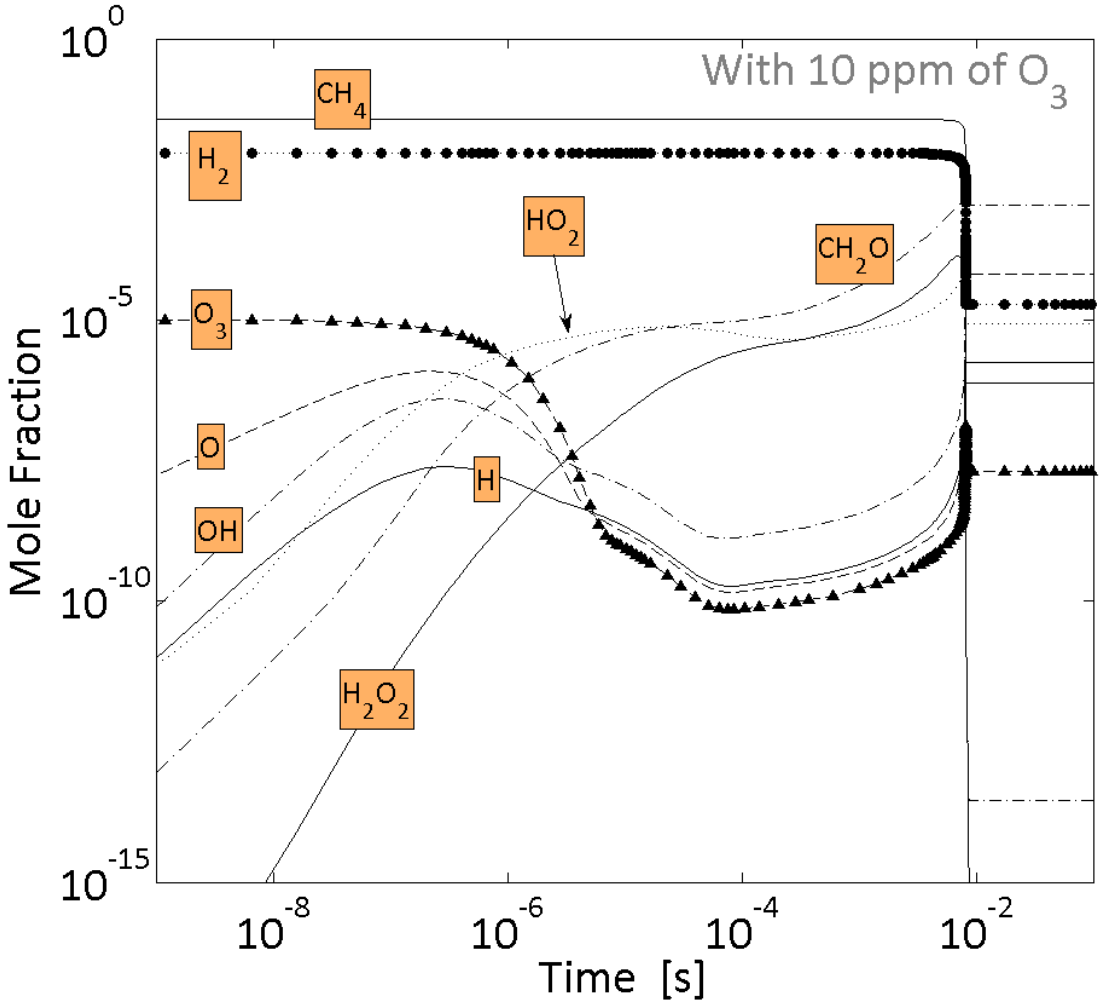

Figure 108. C. *Mole fractions of the main radicals for a mixture of methane and hydrogen (80/20) with 10 ppm of ozone.*

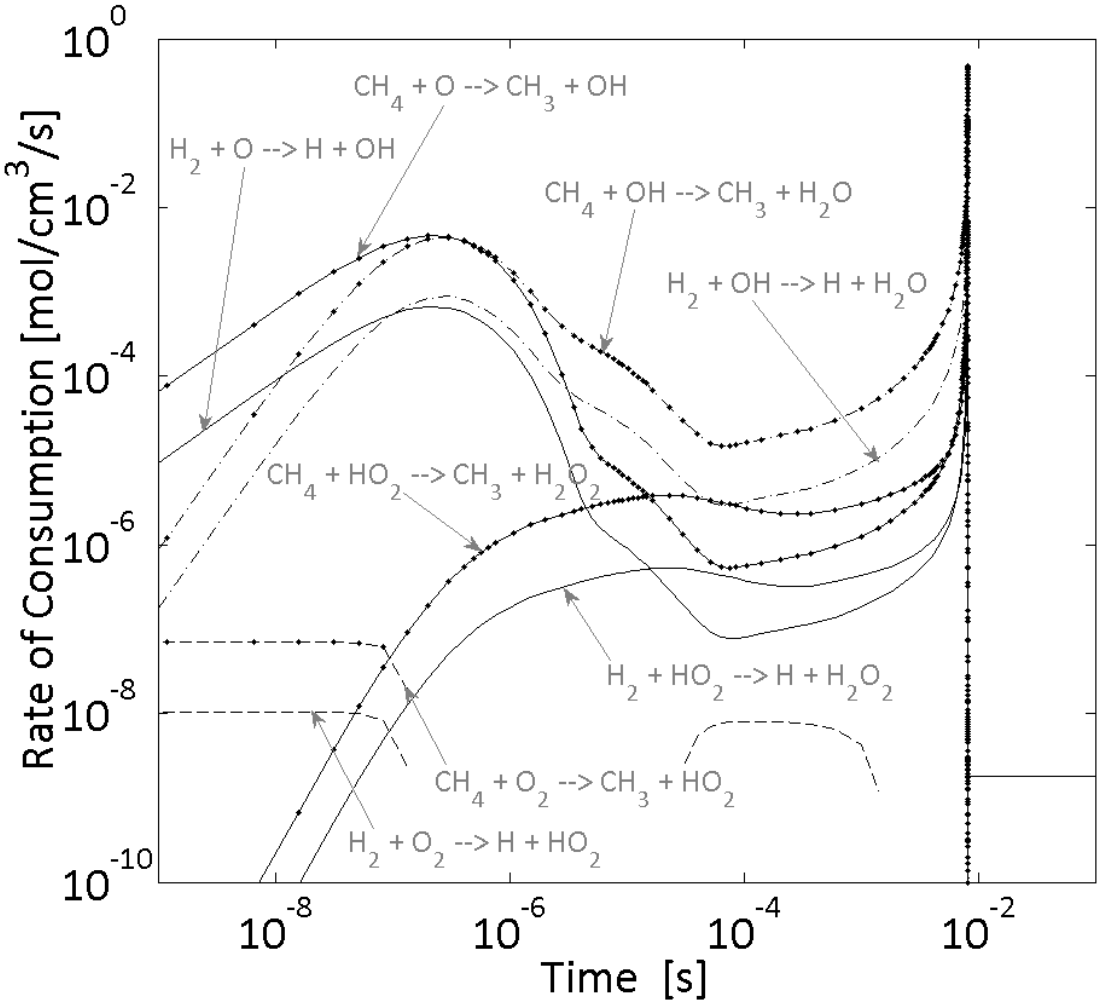

Figure 108. D. *Rate of consumption for a mixture of methane and hydrogen (80/20) with 10 ppm of ozone.*

4. Conclusion on gaseous fuels

In the present chapter, the combustion of gaseous fuels with ozone seeding was investigated. A prior series of experiments without this oxidizing chemical species showed that propane leads to similar trends than isooctane due to its properties near than those of the reference fuel. Hydrogen, despite its high octane number, indicated that it can self-ignite easily than isooctane due to its high reactivity. Finally, methane as fuel for HCCI engines was studied but unfortunately, no results were obtained due to the very high autoignition resistance. Extra experiments were performed at the limit of the engine intake conditions but even with ozone addition, methane does not burn. As a result, the study focused on the combustion of a methane-propane mixture and methane-hydrogen mixtures with ozone additions.

The first part with a methane-propane mixture demonstrated that ozone leads to an enhancement of the combustion of this fuel as well as an advance of its phasing. Additionally, experiments conducted by decreasing either the intake pressure or the intake temperature confirmed that this oxidizing chemical species can be used to manage the HCCI combustion. Therefore, parameters such as IMEP, combustion process, efficiencies, level of noise and pollutants can be controlled by monitoring the ozone concentration injected. In the second part, experiments with methane-hydrogen mixtures were performed also by varying the ozone concentration but instead of reducing the intake conditions, three different volumetric ratios of both fuels were selected. Similar conclusions were achieved meaning that it is possible to choose a fuel adapted to the engine and control its combustion process by setting the ozone seeded. Finally, computations carried out to complete experiments displayed the same results than PRFs. Fuels, either methane or propane or hydrogen, are all oxidized first by the O-atom coming from the ozone decomposition which results in an earlier ignition providing the improvement of the overall combustion.

Chapitre 5 / Chapter 5

Résultats sur la combustion des carburants de la famille des alcools

Results on the combustion of alcohol fuels

Résumé

Ce dernier chapitre sur les résultats obtenus au cours de la thèse traite des carburants de faisant partis de la famille des alcools. Comme dans le chapitre précédent, seul l'impact de l'ozone sur ces carburants a été étudié et les résultats présentés font référence à un travail déjà publié :

- Article VI : J-B. Masurier, F. Foucher, G. Dayma, P. Dagaut, *Ozone Applied to the Homogeneous Charge Compresssion Ignition Engine to Control Alcohol Fuels Combustion*, Applied Energy, 2015.

De manière similaire aux études précédentes, l'effet de l'ozone a aussi été étudié sur la combustion des carburants de type alcool. Trois carburants ont été sélectionnés : le méthanol, l'éthanol et enfin le butanol. Une étude préliminaire sans ensemencement a été effectuée afin de déterminer les conditions d'admission idéales à imposer pour obtenir un phasage optimum de la combustion de chacun de ces carburants. Les résultats ayant montrés une convergence de leurs phasages respectifs, un couple unique pression-température d'admission a été retenu pour analyser expérimentalement l'impact de l'ozone. Comme dans le cas des PRFs, il a été observé que l'ozone permet d'améliorer la combustion des alcools et d'avancer leur phasage. Par comparaison entre eux, le butanol est le carburant le plus impacté par l'ozone et le méthanol le moins en raison de leur structure chimique. Cependant, par rapport aux PRFs, malgré des tendances similaires en fonction de la concentration d'ozone, les alcools sont beaucoup plus résistants à son potentiel oxydant étant donné que des concentrations bien supérieures sont nécessaires pour obtenir une même avance sur le phasage. De plus, ces carburants ont eux aussi démontré la possibilité de contrôler le phasage de leur combustion, ainsi que l'ensemble des paramètres moteur (pression moyenne indiquée, durée de la combustion) moyennant le contrôle de la quantité d'ozone injectée. Toutefois, afin d'aboutir à un phasage optimal permettant l'optimisation sur un maximum de paramètres du moteur, un mélange de ces trois carburants de la famille des alcools serait probablement idéale. Finalement, en complément des résultats expérimentaux, des simulations de cinétique chimique à l'aide d'un nouveau schéma basé sur l'oxydation des alcools auquel a été ajouté le sous mécanisme de l'ozone ont été réalisées et ont permis d'aboutir aux mêmes conclusions que celles pour les PRFs et les carburants gazeux. D'une manière générale, l'oxydation des alcools commence par une réaction d'initiation avec la molécule d'oxygène tandis que dans le cas où l'ozone est injecté, les alcools sont consommés via une réaction impliquant l'oxygène atomique résultant de la décomposition de l'ozone. Cette première réaction qui prend place bien plus tôt que les voies d'oxydation normales permet finalement d'aboutir aux avances observées lors des expériences.

Abstract

This last chapter of results is about alcohol fuels. As in the previous chapter, only the impact of ozone on these fuels was investigated and the results presented are referred to the following article:

- Article VI : J-B. Masurier, F. Foucher, G. Dayma, P. Dagaut, *Ozone Applied to the Homogeneous Charge Compresssion Ignition Engine to Control Alcohol Fuels Combustion*, Applied Energy, 2015.

Similarly to the previous studies, the effect of ozone was also study on the combustion of alcohol fuels. Three different fuels were selected: methanol, ethanol and finally n-butanol. A prior study without seeding was carried out to determine the optimum conditions to set in order to obtain an ideal phasing of their respective combustion. Results showed a convergence of their respective phasing and therefore, a unique couple of intake pressure and temperature was chosen for analyzing through experiments the impact of ozone on these fuels. As for PRFs, it was observed that ozone enables to improve the combustion of alcohols and advance their phasing. By comparing them, n-butanol is the most affected by ozone and methanol the least due to their chemical structure. However, compare to PRFs, despite the similar trends observed as a function of the ozone concentration, alcohols are more resistant to the oxidizing potential of ozone since higher concentrations were needed to achieve the same combustion phasing. Moreover, these fuels also showed the possibility to control the combustion phasing as well as all the engine outputs (indicated mean effective pressure, combustion duration) by managing the amount of ozone injected. However, to achieve an optimal phasing and an optimization of the engine outputs, a blend of these three alcohol fuels will be probably ideal. Finally, to complement the experimental results, computations were carried out with a scheme based on the oxidation of alcohol fuels where it was added the ozone sub-mechanism. Results allowed to achieve the same conclusions than those for PRFs and gaseous fuels. Generally, alcohol oxidation starts with an initiation reaction involving the oxygen molecule while in the case of an ozone injection, alcohol fuels are consumed through reaction involving the oxygen atom coming from the ozone break down. This reaction occurs very earlier than by the normal oxidation pathways and finally lead to the advances of the combustion observed during the experiments.

1. Introduction on alcohol fuels (Article VI)

In previous chapters, experimental and numerical results showed that ozone has the potential to control the HCCI combustion phasing of different kinds of fuels, in particular PRFs and gaseous fuels. Moreover, it was also observed that this oxidizing chemical species provide the same initial pathways on these fuels. Currently, other fuels present a wide interest for engine applications and may use as alternative fuels. Alcohol fuels are good candidates and were widely investigated [157], [195]. They already showed that they may replace conventional automotive fuels as for instance ethanol. These fuels have for properties to include an oxygen atom in their respective structure which may alter the impact of ozone.

Ozone was already applied on fuel with oxygen atom in its structure [13] but never on alcohol fuels. The aim of the present part is therefore to study the impact of ozone on the combustion of alcohol fuels into a HCCI engine. Similarly to previous investigations carried out, the effect of this oxidizing chemical species was studied through experiments on the engine bench coupled with computations. Fuels selected were methanol (MeOH), ethanol (EtOH) and n-butanol (BuOH) because they present properties closed to that of isooctane.

2. Combustion of alcohol fuels

Similarly to the study on PRFs and gaseous fuels, the combustion of the alcohol fuels selected without seeding of ozone or any oxidizing chemical species was investigated first. Here again, the main objective was to determine the "optimum" regions were the combustion of our three alcohol fuels take place. Therefore, experiments were performed under the same conditions than previous ones. As a reminder, the rotation speed and the equivalence ratio were respectively maintained constant at 1500 rpm and 0.3. The aim was to determine the areas where the CA50 is located between 0 and 6 CAD, i.e. from a combustion located at the top dead center up to a combustion located near misfires, by monitoring the intake pressure and the intake temperature. Results are presented in Figure 109.

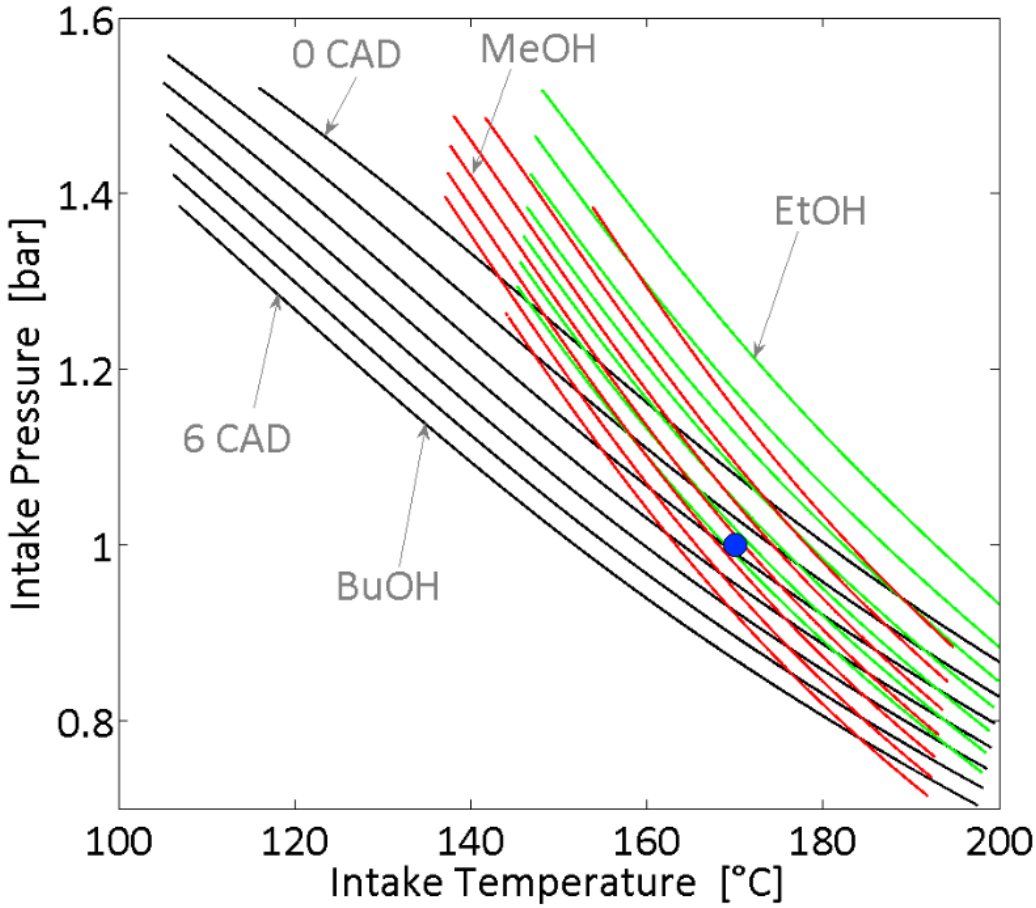

Figure 109. *IsoCA50s from 0 to 6 CAD for the three alcohol fuels selected (MeOH, EtOH and BuOH) as a function of the intake pressure and the intake temperature of the engine, for an equivalence ratio of 0.3 and a rotation speed of 1500 rpm.*

It can be observed that BuOH is the alcohol fuel which auto-ignites the most readily among the three fuel selected and EtOH is the most difficult. For MeOH, this fuel showed

that it has a behavior similar to that of EtOH. This trend may be interpreted according to the respective RON, MON and ON of each fuel [187]. BuOH has an ON of 91.5, the lowest of the alcohol fuels selected, MeOH and EtOH holding ON of 99 and 99.5, respectively. The ON therefore explains that BuOH is the most easily fuel to auto-ignite and as both other fuels have ON rather similar, it was normal to see that combustion area of MeOH is very close to that of EtOH. However, there is a slight difference which results in a later combustion phasing for EtOH. Similar results were already observed for both fuels in the literature [52] and are in agreement with our results. Finally, it can also be noted that in the case of high intake temperatures, isoCA50s converge for all the fuels studied. This convergence was attributed to the sensitivity of each fuel which is defined as the difference between the RON and the MON of each fuel [46]. Fuels have respectively a sensitivity of 20 for MeOH, 19 for EtOH and 13 for BuOH. The closed sensitivity of MeOH and EtOH explain both fuels present similar trends, even parallel. Moreover, by observing a unique isoCA50 with an increase of the intake temperature, both fuels present a higher slope than BuOH due to their higher values on this parameter.

3. Effect of ozone

Starting from the previous results on the HCCI combustion of alcohol fuels without oxidizing chemical species seeding, the effect of ozone was studied by performing experiments and computations.

3.1. Experimental results

3.1.1. In-cylinder pressure and heat release rate traces

Results in Figure 1 showed that without ozone injection and by varying the intake conditions of the engine, the respective MeOH, EtOH and BuOH "optimum" combustion regions converge. Therefore, the experiments with ozone were performed for a unique couple of intake pressure and intake temperature to compare the impact of this oxidizing chemical species on these three fuels. The intake pressure was fixed at 1 bar and consequently, the intake temperature was monitored at 170 °C. This temperature corresponds to the minimum intake temperature needed to allow the combustion of the most difficult fuel to autoignite, i.e. EtOH at a combustion timing of 6 CAD. From this point, experiments were performed by ranging the ozone concentration from 0 to approximately 130 ppm (upper limit with the ozone generator). Moreover, data were recorded by increasing the ozone concentration from the minimum up to the maximum and then, by decreasing the concentration. The objective was to show the good stability and repeatability of the results. The evolutions of the in-cylinder pressures recorded and the heat release rates calculated are presented in Figure 110 as a function of the ozone concentrations. Here again, black curves represent the average of the 100 cycles recorded and colored envelopes correspond to the maximum variations, upper and lower limits, of the same 100 cycles.

Generally, we may observe that results are quite similar to those obtained for ozone seeding with PRFs and gaseous fuels. They are also in agreement with prior results observed in the literature [9], [11]–[13]. Regarding the in-cylinder pressure traces, increasing the ozone concentration at the intake of the engine allow to increase the maximum pressure and the combustion is advanced for all the alcohol fuels selected. In the same way, the heat release rate traces also showed an increase of their maximum values meaning that ozone allows to improve the combustion of alcohol fuels and advance its phasing. Moreover, this result was confirmed observing the value of the IMEP. This parameter raises from 2.40 to 2.55 bar, from 2.10 to 2.36 bar and 2.30 to 2.39 bar for MeOH, EtOH and BuOH, respectively. Finally, it may also be observed from the colored areas and the covariance of the IMEP that ozone enables to stabilize the combustion.

Additionally to the observations provide by in-cylinder pressure and heat release rate traces as a function of ozone, it is possible to give a first comparison of the impact of this oxidizing chemical species on the three alcohol fuels selected. Thus, from the difference between the maximum in-cylinder pressure without ozone seeding and the maximum

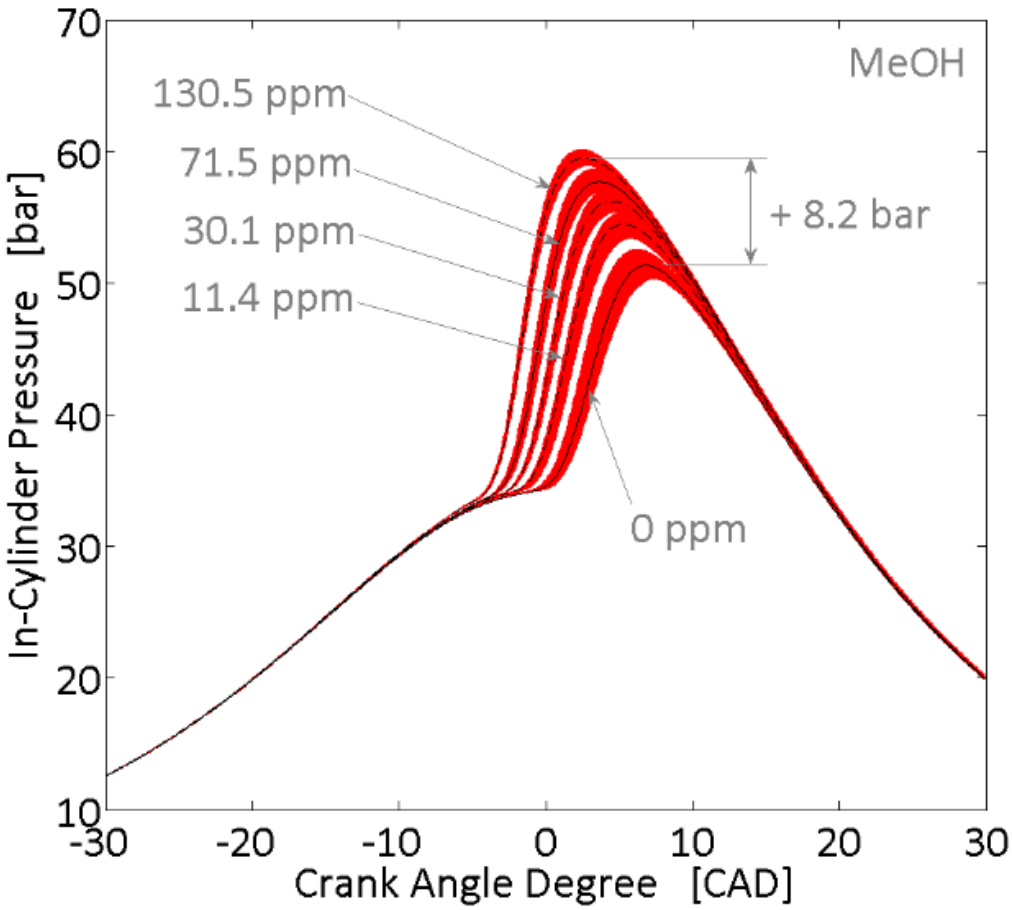

Figure 110. A. *In-cylinder pressure traces as a function of the ozone seeded for MeOH as fuel. Black curves correspond to the average of 100 cycles recorded and gray areas represent the variation of the same 100 cycles (the upper and the lower limits obtained).*

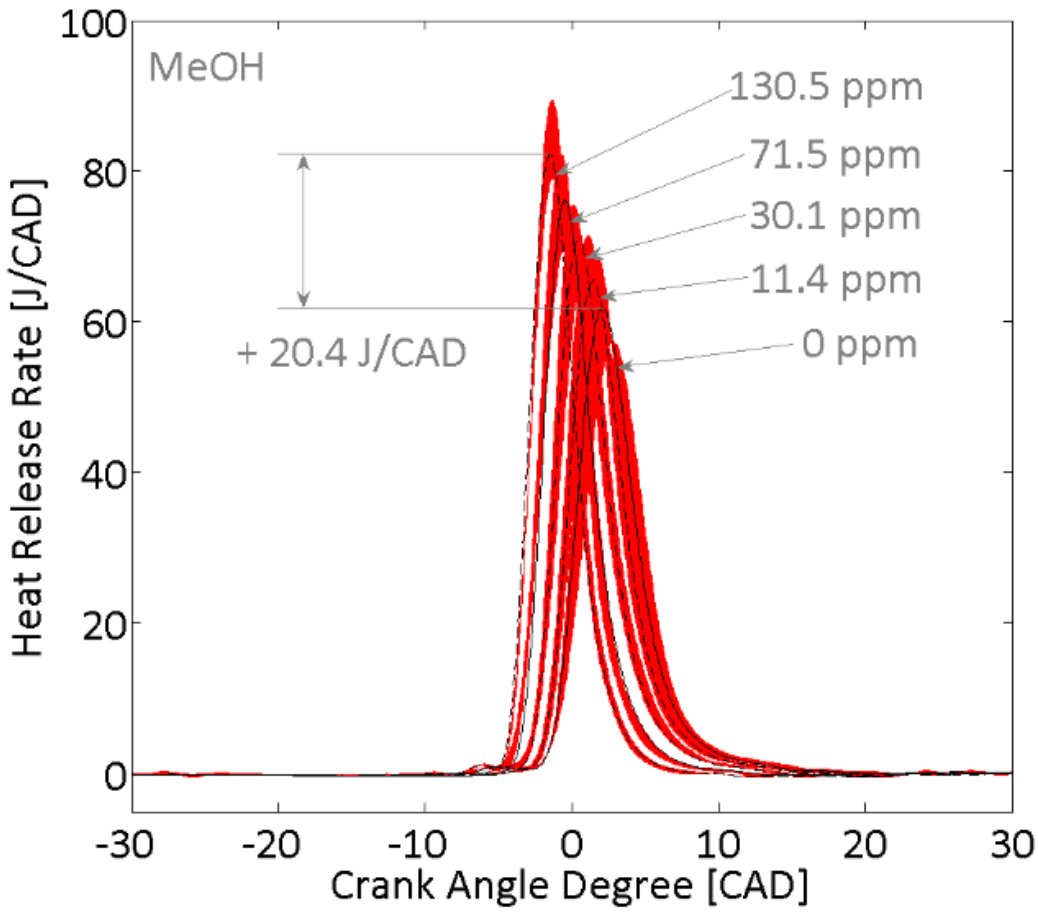

Figure 110. B. *Heat release rate traces as a function of the ozone seeded for MeOH as fuel. Black curves correspond to the average of 100 cycles recorded and gray areas represent the variation of the same 100 cycles (the upper and the lower limits obtained).*

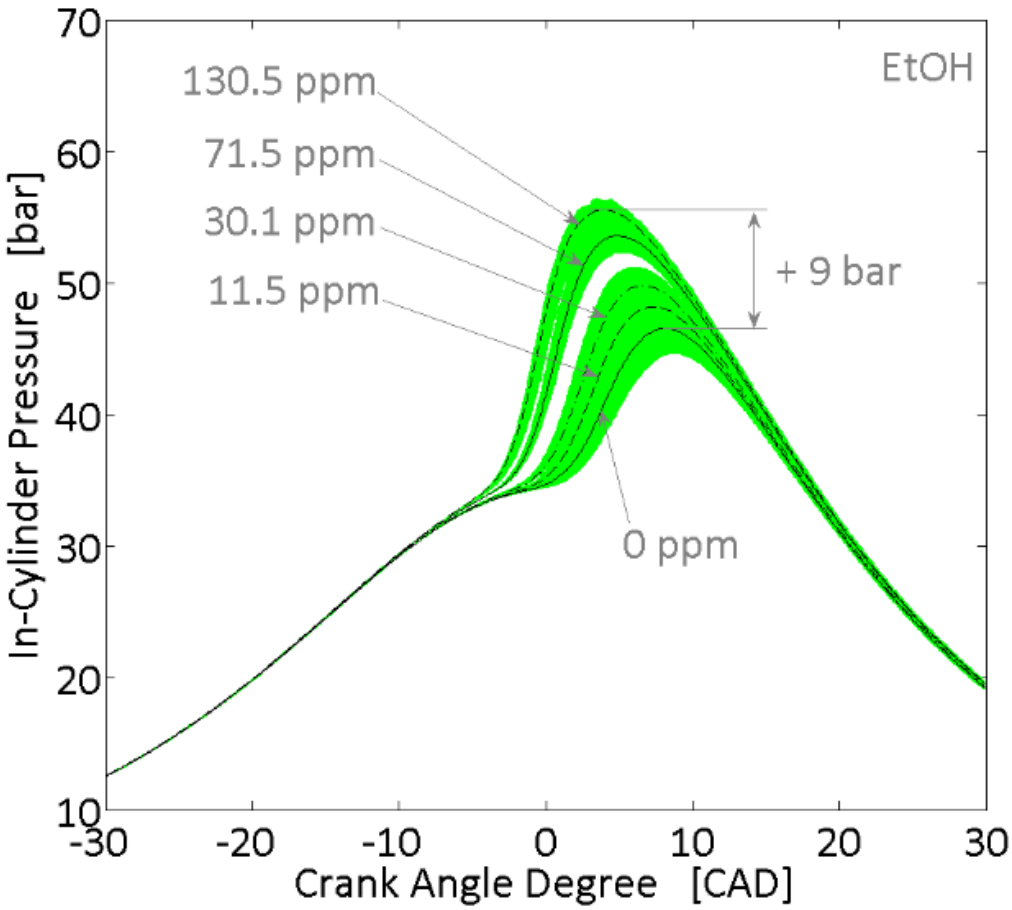

Figure 110. C. *In-cylinder pressure traces as a function of the ozone seeded for EtOH as fuel. Black curves correspond to the average of 100 cycles recorded and gray areas represent the variation of the same 100 cycles (the upper and the lower limits obtained).*

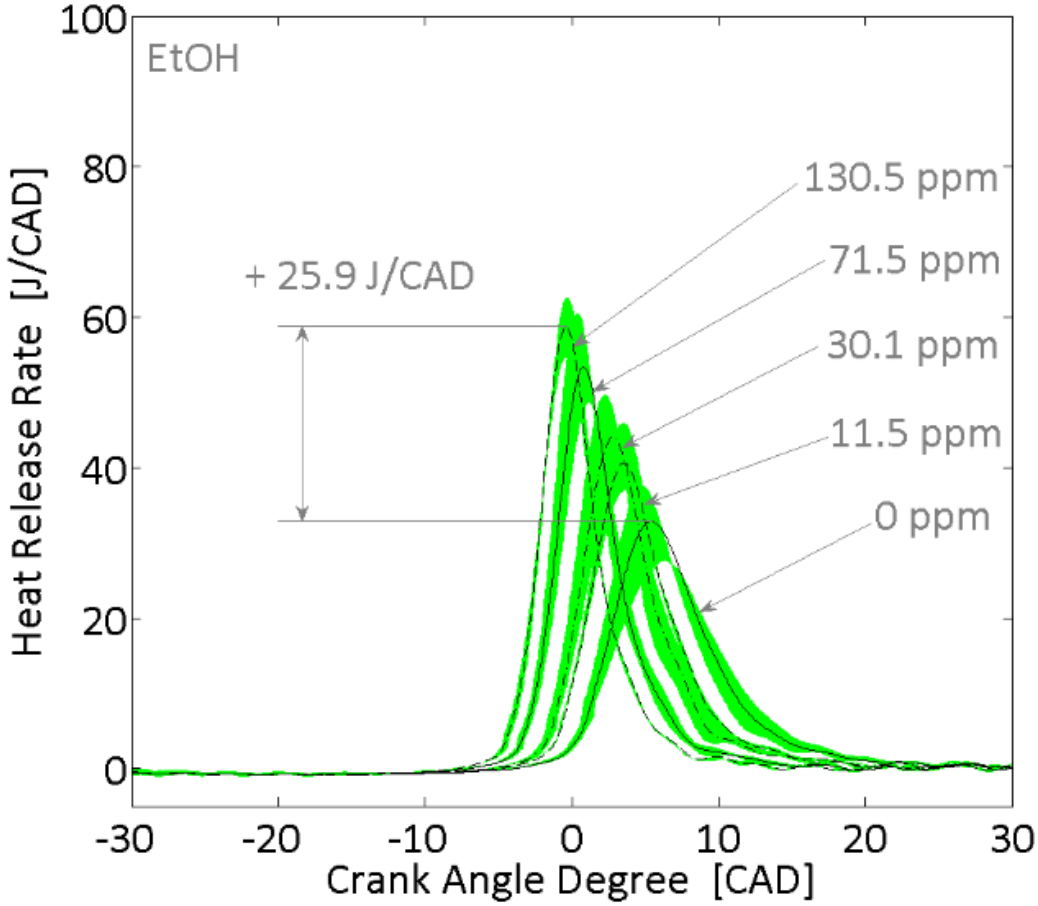

Figure 110. D. *Heat release rate traces as a function of the ozone seeded for EtOH as fuel. Black curves correspond to the average of 100 cycles recorded and gray areas represent the variation of the same 100 cycles (the upper and the lower limits obtained).*

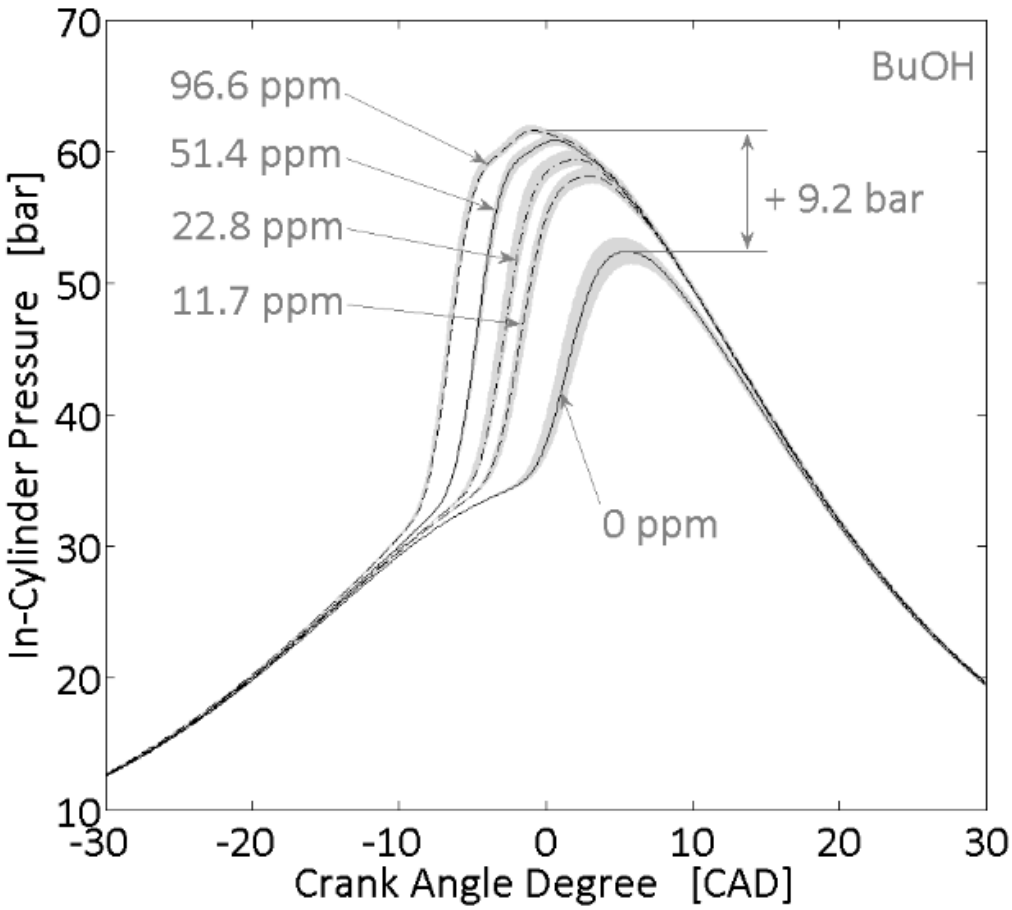

Figure 110. E. *In-cylinder pressure traces as a function of the ozone seeded for BuOH as fuel. Black curves correspond to the average of 100 cycles recorded and gray areas represent the variation of the same 100 cycles (the upper and the lower limits obtained).*

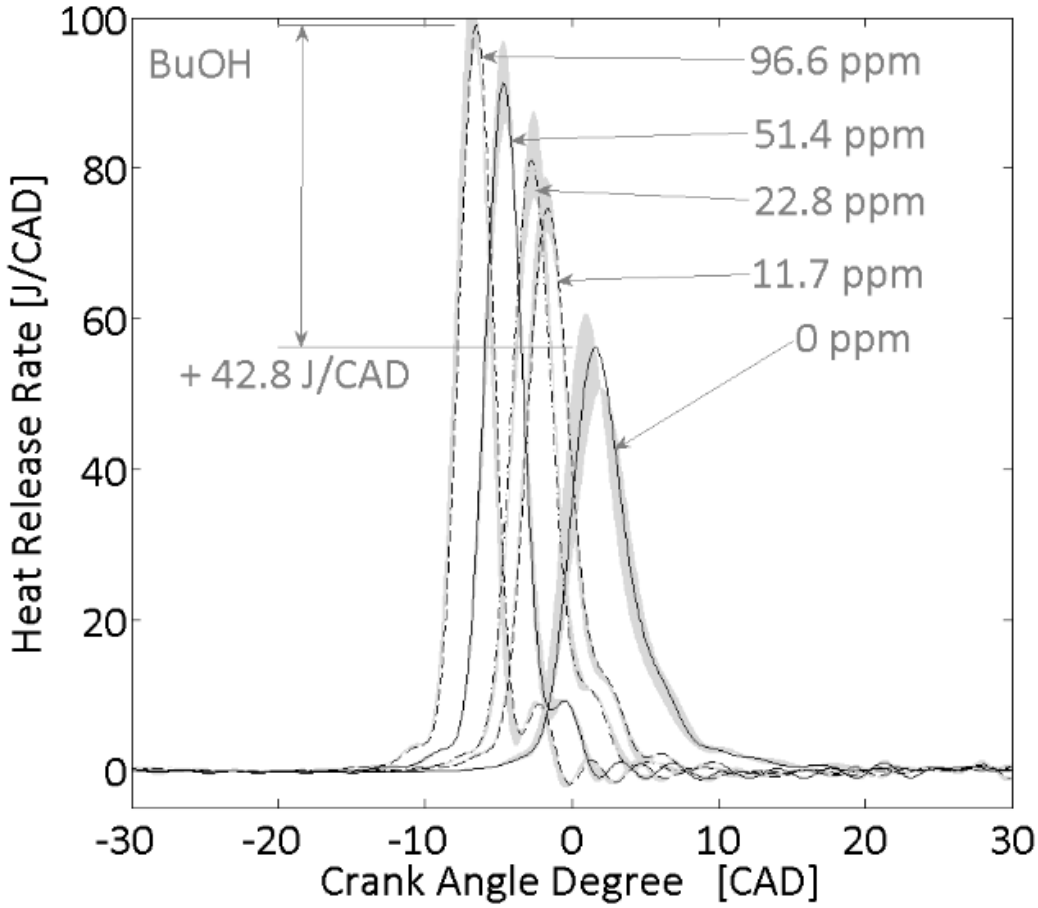

Figure 110. F. *Heat release rate traces as a function of the ozone seeded for BuOH as fuel. Black curves correspond to the average of 100 cycles recorded and gray areas represent the variation of the same 100 cycles (the upper and the lower limits obtained).*

pressure with the highest ozone concentration injected or from the same difference in the case of heat release rates, it may conclude that the highest impact of ozone is on BuOH while MeOH presents the lowest.

3.1.2. Engine outputs

To further compare the impact of ozone on the three alcohol fuels selected, engine outputs were analyzed. In particular, the parameters observed were combustion phasing, IMEP and combustion duration.

3.1.2.1. Combustion phasing

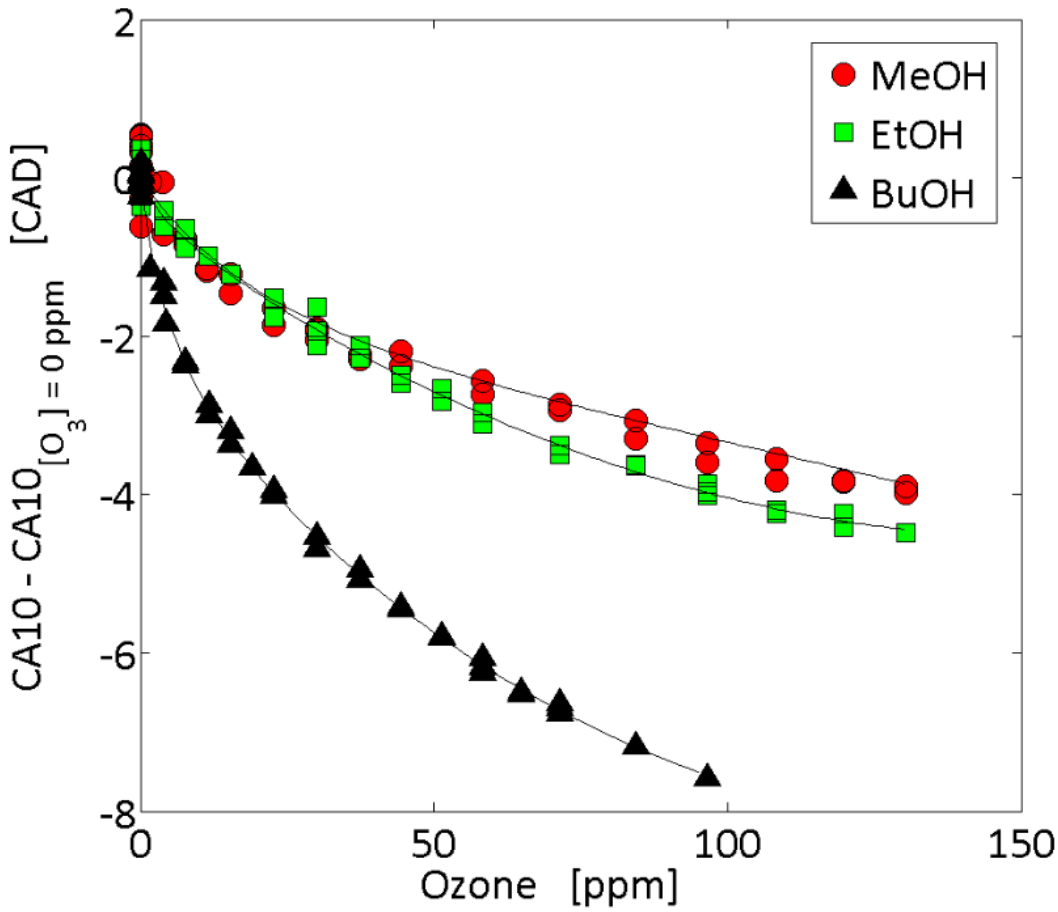

Figure 111. *Effect of ozone on the shift of the CA10 with respect to the CA10 without ozone for the three alcohol fuels selected. Symbols represent the experiments and dashed lines the trends.*

The combustion phasing was first analyzed to compare the impact of ozone on MeOH, EtOH and BuOH. Parameters selected were CA10 and CA50 determined from the cumulative heat release rate evolutions. In order to be able to achieve a good comparison

between the three fuels, the shift of these two parameters were plotted in reference to their respective value when no ozone is injected. Results obtained are presented in Figure 111 and Figure 112 respectively for the CA10 and the CA50.

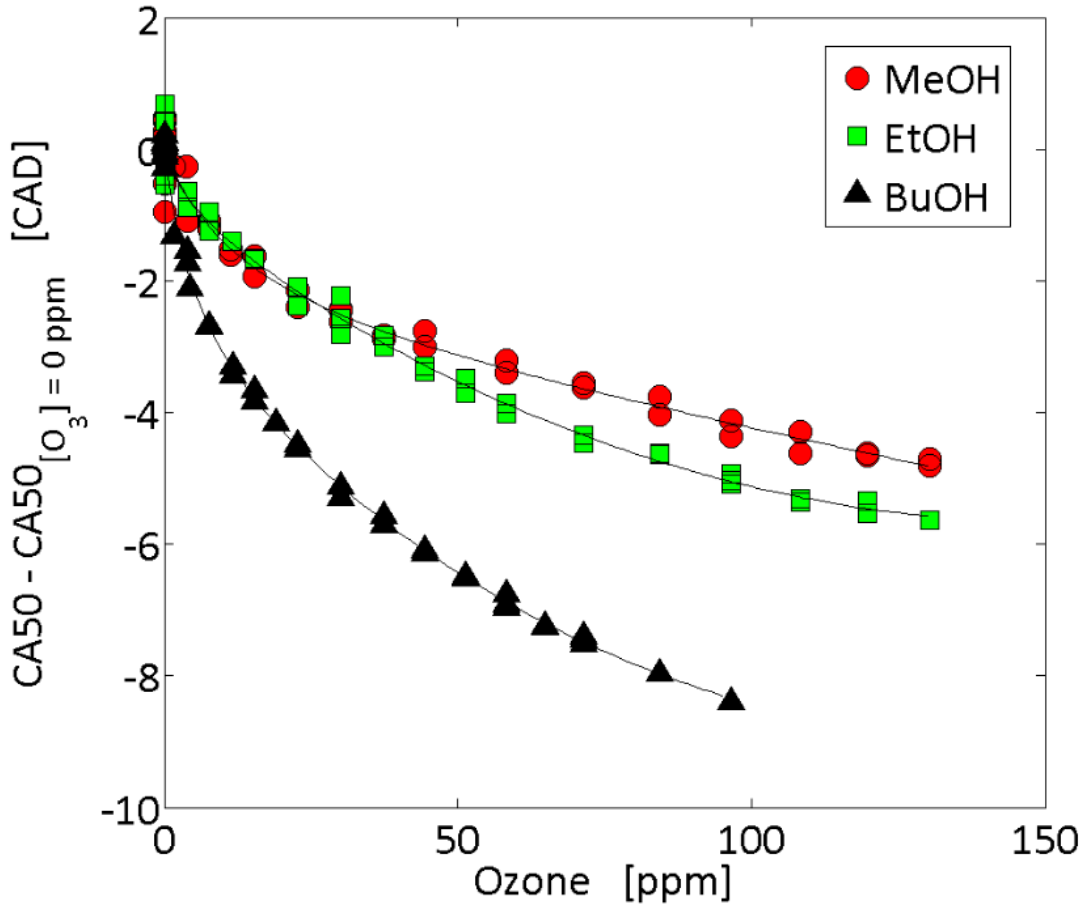

Figure 112. *Effect of ozone on the shift of the CA50 with respect to the CA50 without ozone for the three alcohol fuels selected. Symbols correspond to the experiments and dashed lines to the trends.*

Regardless of the fuel, it may observe from both parameters that ozone has well the potential to advance the combustion and the phasing may be controlled by managing the concentration seeded. Among the three fuel selected, it is well confirmed that BuOH is the most impacted by ozone and MeOH the least due to their respective chemical structure and in particular due to their carbon chain. Indeed, BuOH is the fuel with the longest carbon chain (4 carbons) and it is therefore the easiest fuel to oxidize while MeOH which has only one carbon is the most difficult. These results clearly showed that the fuel structure is of main importance. Furthermore, all the trends showed that ozone acts exponentially on the combustion phasing. In particular, a high impact may be observed for concentrations lower than 50 ppm. For higher concentrations, the impact is less pronounced and curves seem to tend towards a constant value. Comparing the effect on both CA10 and CA50, ozone

provides the same evolutions. As we can consider CA10 as the phasing of the ignition, the trend observed on CA10 means that ozone also modifies the beginning of the combustion in the case of alcohol fuels. For CA50 trends, these results may be compared to the previous results obtained for PRFs and gaseous fuels. It was concluded that ozone has a lower impact on alcohol fuels. Studies with PRFs and gaseous fuels showed that less than 50 ppm are needed to strongly advance the combustion phasing while in the present case, seeding reaches amounts up to 130 ppm. In the case of BuOH, the combustion may advance of approximately 8 CAD while for PRFs, in particular for isooctane under the same intake temperature, shifts of 10 CAD were measured with less ozone.

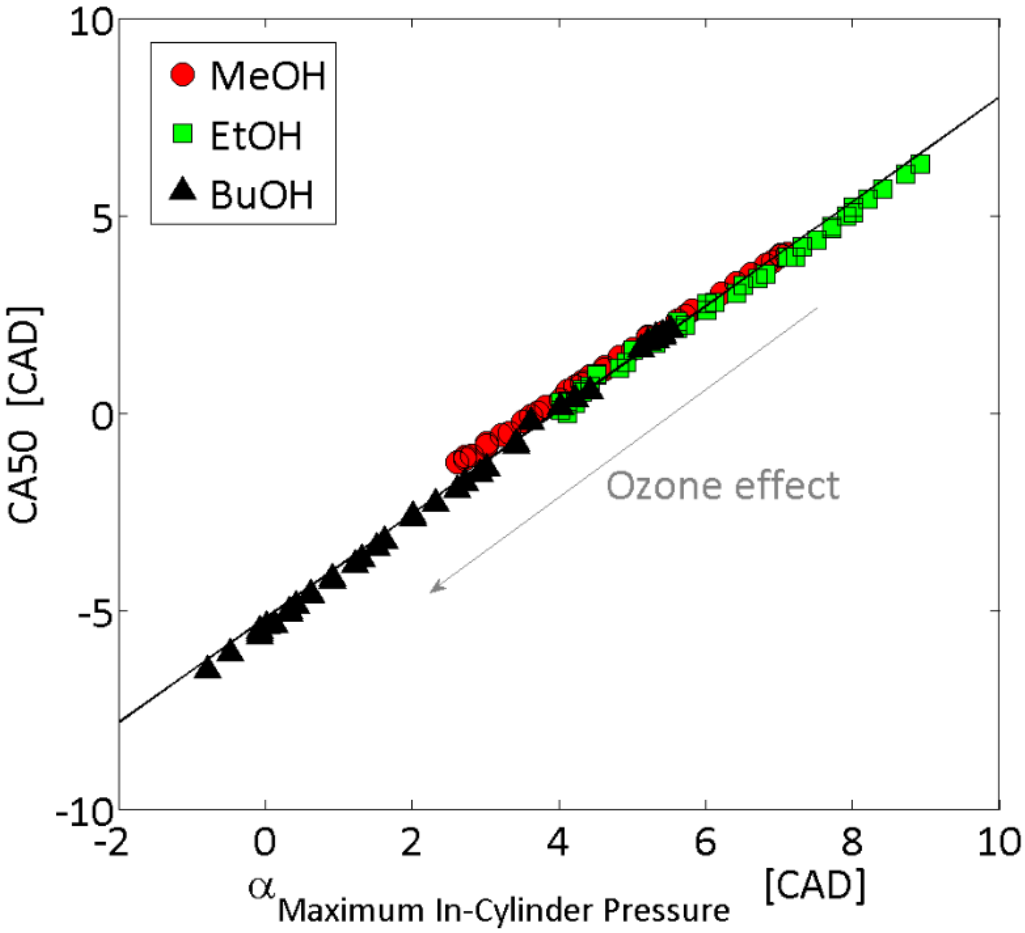

Figure 113. *CA50 phasing as a function of the maximum in-cylinder pressure and the ozone injected for the three alcohol fuels selected. Symbols represent the experiments and dashed line the trend.*

The maximum in-cylinder pressure phasing was also investigated. From the in-cylinder pressure traces, it can be observed that this location also advances exponentially towards the top dead center as low concentration of ozone strongly improve the combustion and continuing to inject higher concentrations results into a lower effect of ozone. The phasing of the maximum in-cylinder pressure was therefore compared to the

CA50 and the results are showed in Figure 113. Independently of the alcohol fuel selected, the CA50 evolves linearly as a function of the maximum pressure location. As a result, the combustion phasing may either control by monitoring the maximum pressure phasing or the CA50 and the value of the other parameter will be known. Moreover, such results are particularly interesting because any of the fuels selected may be used to focus on a specific phasing. It is therefore just necessary to manage the ozone concentration injected. Finally, as EtOH is the fuel with the latest autoignition and BuOH with the earliest, a mixture of these alcohol fuels studied could help to control the combustion phasing on a wide range of crank angle degrees.

3.1.2.2. Indicated mean effective pressure

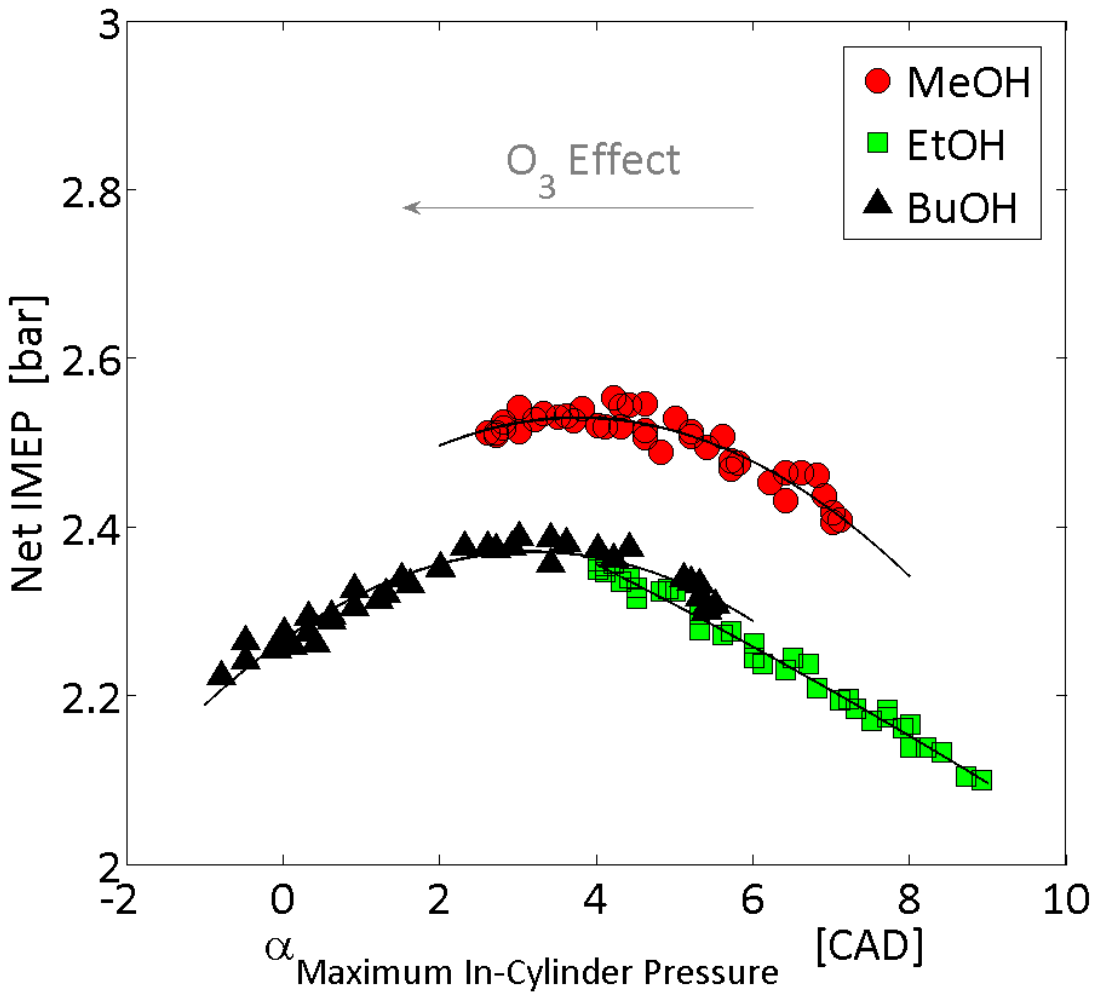

Figure 114. *Net indicated mean effective pressure as a function of the maximum in-cylinder pressure and the ozone seeded for the three alcohol fuels selected. Symbols represent experiments and dashed lines the evolutions.*

The IMEP was also determined and analyzed. Results obtained for this parameter are plotted as a function of the maximum in-cylinder pressure location and the ozone

concentration in Figure 114. Trends follow parabolic curves allowing the possibility of achieving a maximum value. As BuOH is the fuel which autoignites the easiest into our HCCI engine due to the intake conditions fixed, the evolution of its IMEP rapidly reaches its maximum with the increase of the ozone. Inversely in the case of EtOH, only an increase of the IMEP was observed because it is the most difficult to autoignite and because we cannot inject more ozone. The limit of the generator was achieved. Finally, for the last fuel, MeOH, the parabolic trend is well visible and the maximum IMEP was reached just before the limit in ozone concentration. Therefore, a maximum IMEP may be achieved for each alcohol fuel selected, even for EtOH if the limit of the ozone generator was higher. Furthermore, independently of the fuel, the maximum IMEP may be achieved for a maximum in-cylinder pressure position located between 3 and 4 CAD or with respect to the CA50, between -1.2 and the top dead center. These results showed that using a blend of these three fuels as previously proposed will be very useful to work around the maximum IMEP and finally ozone may help controlling the IMEP through the control of the combustion phasing.

3.1.2.3. Combustion duration

Combustion duration was the last parameter studied in this part. Results are presented in Figure 115 for each alcohol fuels selected as a function of the CA50. Basically, regardless to the fuel, ozone enables to limit the burning time while advancing the phasing. Moreover, all the trends follow linear evolutions for CA50s ranging from -5 to 5 CAD. Out of this range, the sensitivity changes due to misfires (CA50 upper than 5 CAD) or because the combustion is too advance and present some artefacts on the heat release rate trace (CA50 lower than -5 CAD). Misfires were observed only for EtOH due to the intake conditions fixed. Indeed, it is the fuel the most difficult to autoignite and these intake pressure and temperature only enable it to burn near misfiring. Inversely, BuOH is the only fuel to present combustions particularly advanced for the same reasons and due to the impact of ozone which strongly improve its combustion process. Finally, the linear trends may be gathered into a unique linear slope because of the standard variations on these parameters.

3.2. Kinetics results

As a complement to the experimental results, computations for the three alcohol fuels selected were conducted. Simulations were run with the constant volume model described in Chapter 2 and with a kinetic scheme containing our fuels [156] and including the ozone sub-mechanism [132]. To ensure agreement with the experiments, ignition delays were computed by tuning the equivalence ratio at 0.3, for a pressure of 35 bar (pressure prior to the combustion into the engine) and by varying the temperature. Computations were therefore carried out first to validate the new kinetic scheme built which include the ozone sub-mechanism. Then, the impact of ozone from a chemical analysis was investigated through ignition delays and reaction pathways.

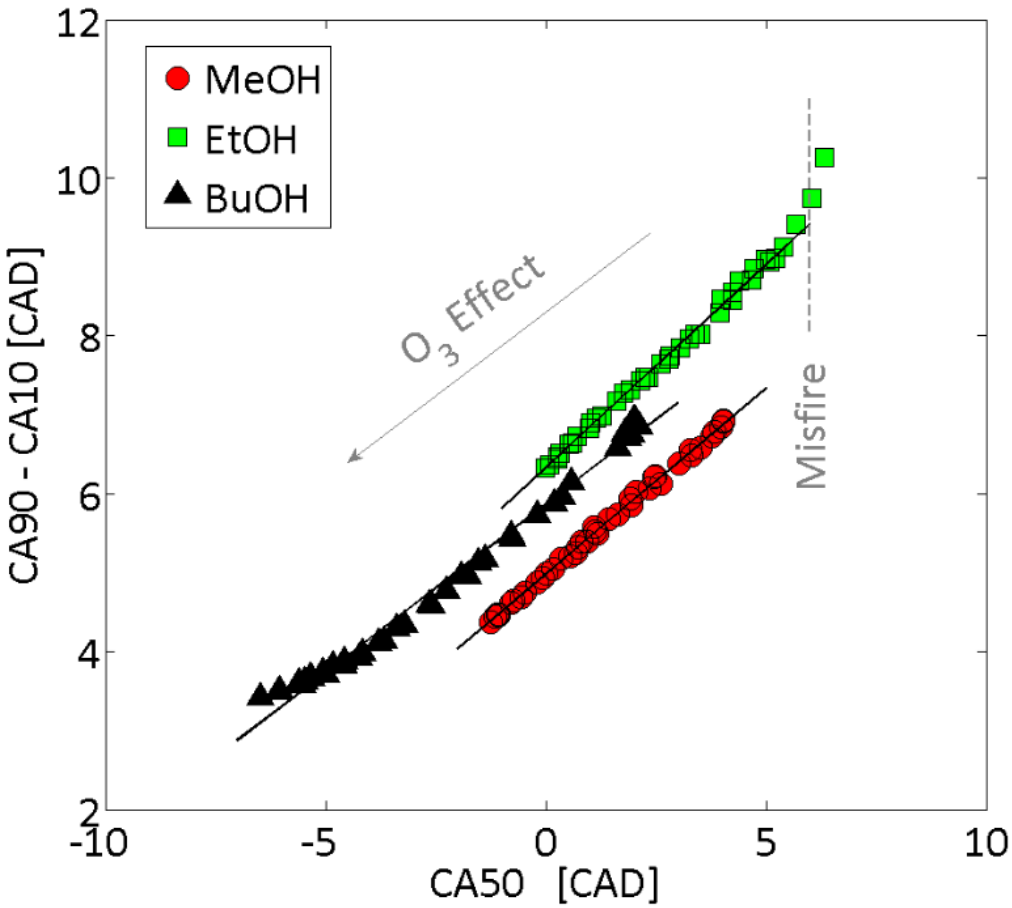

Figure 115. *Combustion duration as a function of the CA50 and the ozone seeded for the three alcohol fuels selected. Symbols correspond to the experiments and dashed lines to the trends.*

3.2.1. Assessment of the kinetic scheme

The kinetic scheme built to study the impact of ozone on the combustion of alcohol fuels consists of an alcohol fuel scheme and an ozone sub-mechanism. Both mechanisms were separately validated and their combination must be also assessed before investigating the impact of this oxidizing chemical species through a kinetic interpretation. Computations were therefore performed for ignition delays for two cases, with the presence of the ozone sub-mechanism and without. Results obtained are presented in Figure 116.

As observe, results with and without the use of the ozone sub-mechanism are in good agreement. The presence of the ozone does not affect the ignition delays computed of the three alcohol fuels meaning that it is validated and can be used for our study. Additionally, it may see that computational results well match with the first experimental results presented without ozone seeding. Before 950 K, i.e. for temperatures similar than those observed at the ignition of the fuels into the engine when the intake temperature is

tuned to its minimum, BuOH is the easiest fuel to autoignite while two other fuels, MeOH and EtOH, present very closed ignition delays. Furthermore, for temperatures higher than 950 K, the three fuels also showed a convergence of their respective ignition delays.

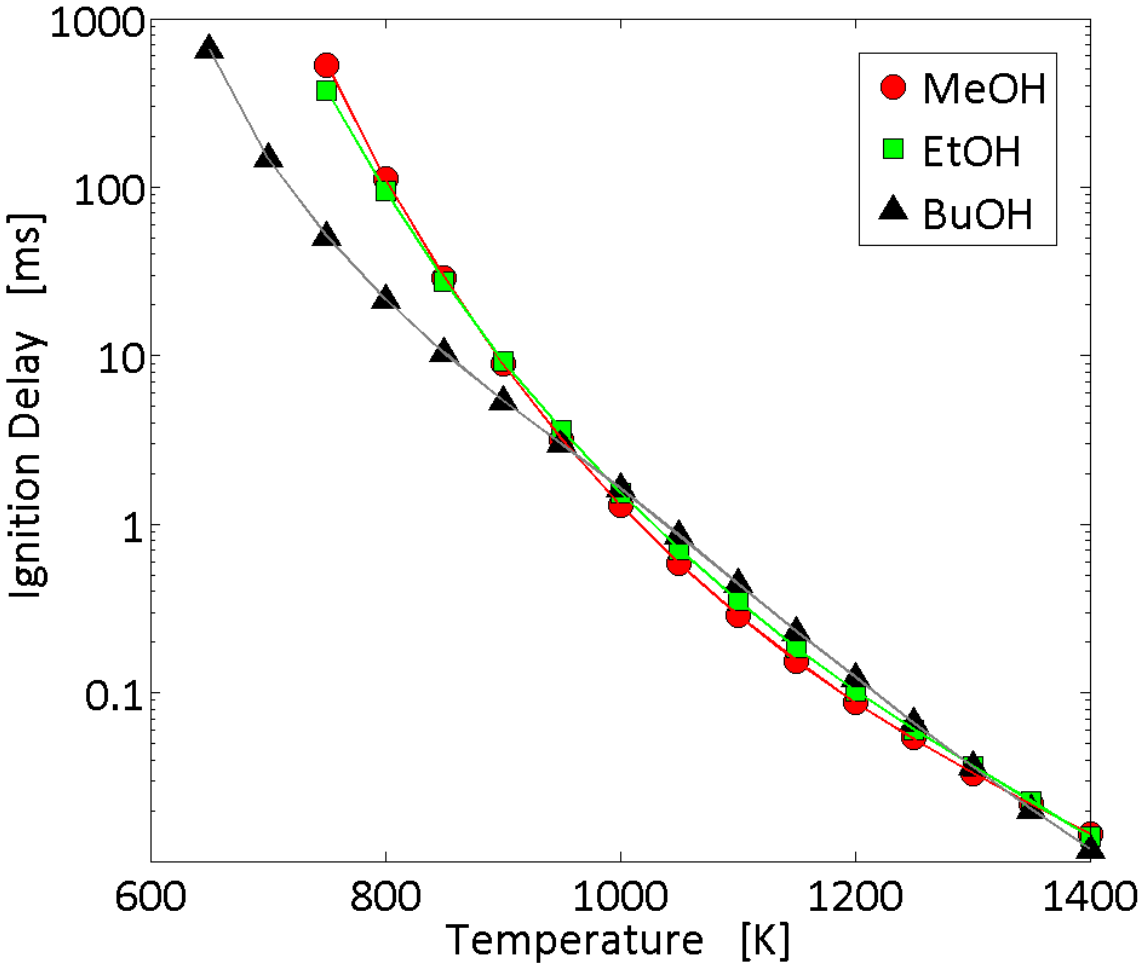

Figure 116. *Ignition delays computed as a function of the temperature for the three alcohol fuels selected under a pressure of 35 bar and an equivalence ratio of 0.3. Symbols represent the results obtained in the case of the scheme without the ozone sub-mechanism and dashed lines the results with the ozone sub-mechanism.*

3.2.2. Ignition delays

From this new kinetic scheme, computations were run to investigate the impact of ozone on alcohol fuel oxidation. These simulations were conducted under the same conditions than those previously used and by varying the ozone concentrations. Three ozone concentrations were fixed (1 ppm, 10 ppm and 100 ppm) and the results on the ignition delays computed are showed in Figure 117. The computations showed that BuOH is the most impacted by ozone and MeOH the least. These results well match with our experimental results on the combustion phasing. Moreover, the effect is particularly

pronounced for low temperatures due to the oxidizing potential of this chemical species while for high temperatures, natural oxidation enables to achieve a fast ignition even with the presence of ozone. For MeOH, results are quite different due to its high resistance to the oxidation and therefore, ozone provides it a higher effect under high temperatures. Finally, as the ignition delays are representative of the onset of the combustion, it may conclude that ozone mainly improves the beginning of the alcohol fuels oxidation. Nevertheless, previous results and studies assess the effect of this oxidizing chemical species and conclude that it is not the ozone which modifies the onset of the combustion but the O-atom coming from the ozone decomposition. Additional computations were therefore performed with the

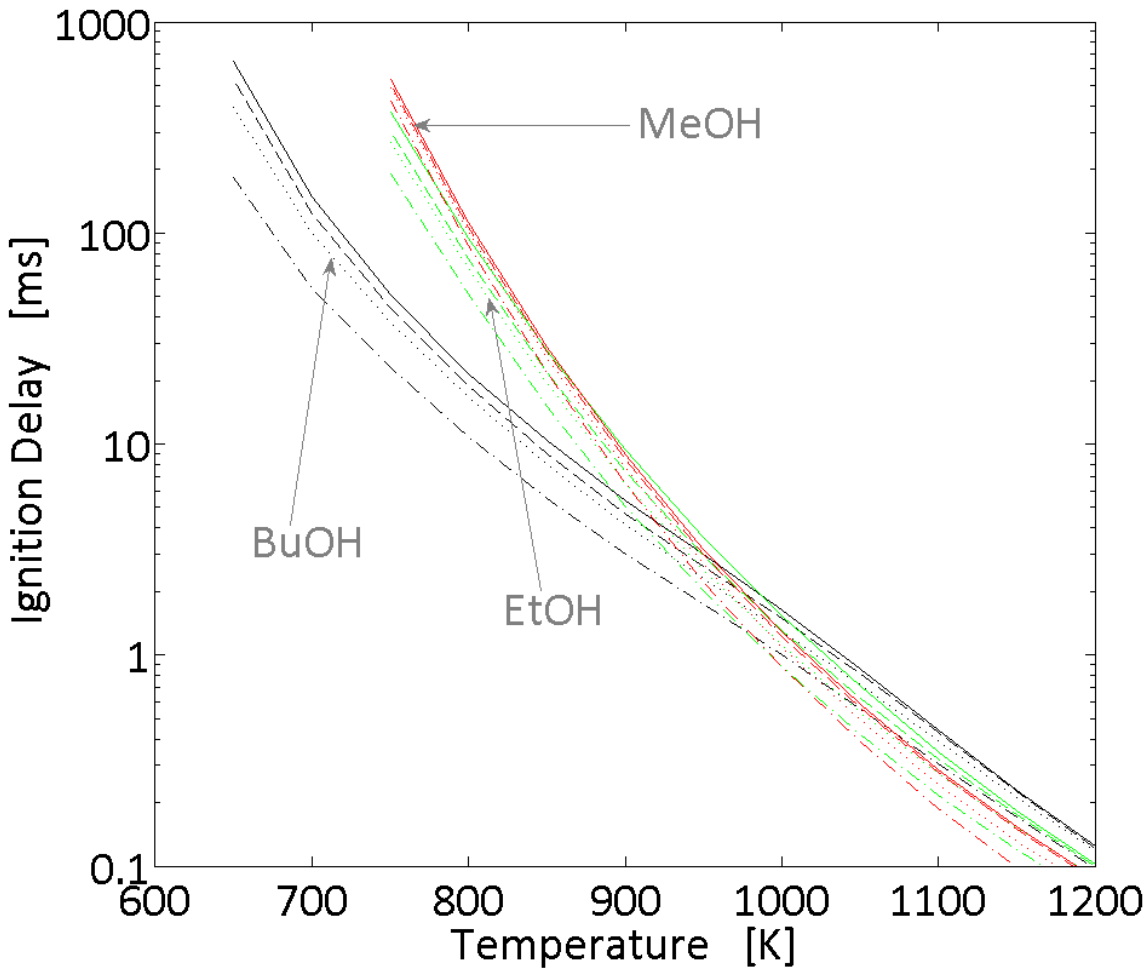

Figure 117. *Ignition delays computed as a function of the temperature and the ozone concentration for the three alcohol fuels studied, for a pressure of 35 bar and an equivalence ratio of 0.3. Solid lines correspond to a concentration of 0 ppm, dashed lines to a concentration of 1 ppm, dotted lines to a concentration of 10 ppm and dash-dot lines to a concentration of 100 ppm.*

same conditions than those used for the ozone but by replacing ozone by O-atom. Results showed the same traces than those observed for ozone and confirm that the improvement of the combustion is due to the presence of O-atom.

3.2.3. Kinetic analysis

To finalize our investigation on the effect of ozone on the combustion of alcohol fuels, a kinetic analysis was conducted for each fuel selected. The results are well described into the Article VI and as the effect is independent to the fuel used, only a summary is provided here. Figure 118 presents the global oxidation of an alcohol fuel when no ozone is injected and with the presence of this oxidizing chemical species.

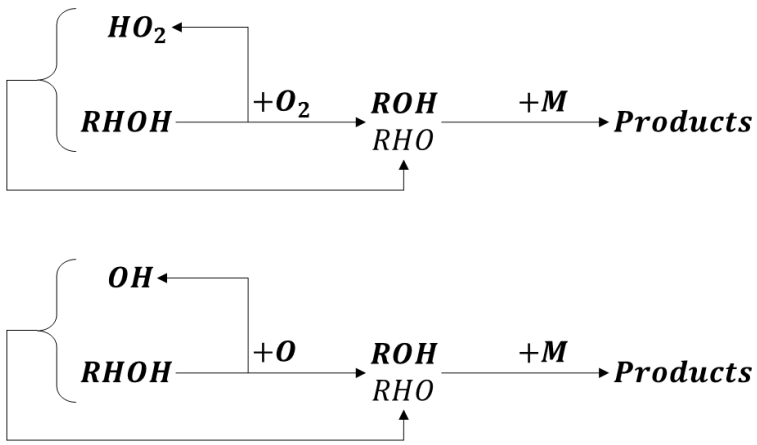

Figure 118. *Summary of the alcohol fuels oxidation without ozone (on the top) and with ozone seeding (on the bottom).*

Globally, when no ozone is injected, alcohol fuels oxidation is initiated by a reaction which involves an oxygen molecule and produces an alcohol radical (ROH or RHO, the first being the most produced) and an HO_2 radical. The HO_2 radical then oxidizes the fuel and leads to the combustion according to the reaction pathways described by *Sarathy et al.* [157]. With an ozone seeding, only the initial reaction is changed. Instead of an oxygen molecule, alcohol fuel is directly oxidized by an O-atom coming from the ozone decomposition. This O-atom leads to the formation of an OH radical and, as a result, the earlier formation of OH radicals finally allows to achieve an advance of the ignition timing as well as the improvement of alcohol fuels combustion.

4. Conclusion on alcohol fuels

This last chapter considered the use of alternative alcohol fuels for HCCI engines and the impact of ozone on their respective combustion was examined. Similarly to previous chapter, the study was conducted through experiments coupled with kinetics computations.

All the experiments were performed for a constant rotation speed of N = 1500 rpm and an equivalence ratio fixed at φ = 0.3. A prior study without ozone seeding allowed determining the optimum combustion regions of each alcohol fuel. The results were consistent with the properties of the fuels, octane number and sensitivity. Moreover, these first results showed a convergence of the regions and therefore, a unique couple of intake pressure and intake temperature was held for observing the impact of ozone. Concentrations of ozone were ranged up to 130 ppm and results showed that increase the ozone seeding leads to an improvement of the combustion and an advance of their respective phasing. By comparing them, it was displayed that butanol is the most impacted by ozone and methanol the least due to their chemical structure. Moreover, these results matched with PRFs results for the trends but ozone concentrations must be significant to achieve a similar advance in alcohol fuels phasing. Finally, engine outputs were also observed and showed that ozone has a good potential for controlling HCCI combustion of these alcohol fuels (CA50, maximum pressure location, IMEP, combustion duration) or a mixture of the three fuels selected.

Additionally to the experiments, computations were performed with a new kinetics scheme based on a validated alcohol fuels mechanism and an ozone sub-mechanism. Results on ignition delays are in agreement with experimental observations and an analysis of the reaction pathways showed that ozone oxidizes indirectly alcohol fuels as in the case of PRFs. Instead, the earlier oxidation of the fuel is due to O-atom coming from the ozone breakdown.

Conclusion

Version française / French version

Les principaux objectifs dans le domaine de l'automobile sont de réduire la consommation en carburants des véhicules, réduire les émissions de CO_2 ainsi que les polluants tout en maintenant de hauts rendements. Ces dernières années ont vu l'émergence de nouveaux modes de combustion automobiles qui pourrait dans un avenir proche remplacé les modes de combustion conventionnels, à savoir le moteur à allumage commandé et le moteur à allumage par compression, afin de mieux répondre à ces objectifs. Parmi eux, de nombreuses études se sont portées sur le mode de combustion « Homogeneous Charge Compression Ignition ». En dépit de son fort potentiel, le développement de ce nouveau mode de combustion est encore très limité du fait que plusieurs défis restent à surmonter. Le problème majeur est de trouver un moyen efficace de contrôler son processus de combustion, entièrement gouverné par la cinétique chimique, sur un large domaine d'utilisation, en termes de charges et de régimes.

Dans le cadre du projet ERC 2G-CSafe, un des objectifs scientifiques est d'étudier l'impact de l'injection d'espèces chimiques oxydantes sur le déroulement de la combustion au sein des moteurs tel que les nouveaux modes de combustion et en particulier, la combustion HCCI. Cela permettra d'apporter à la communauté scientifique de nouvelles données et analyses sur l'impact chimique de diverses espèces oxydantes en vue de participer à la compréhension des phénomènes observés lors de combustions homogènes. Finalement, ces travaux participeront aussi à dresser de nouvelles stratégies de contrôle pour l'automobile et participeront à la création de technologies innovantes. Les présents travaux de thèse portent ainsi sur l'effet d'un ensemencement à l'admission d'un moteur HCCI par des espèces chimiques minoritaires oxydantes provenant de générateurs à décharges plasma et les possibilités applicatives de tels dispositifs pour un véhicule automobile.

La première partie de ce manuscrit s'est donc intéressée en détail à la combustion HCCI et a permis de mettre en évidence les avantages et inconvénients de ce mode de combustion. Il en résulte que le problème majeur de ce type de combustion est que le manque d'un moyen efficace pour contrôler l'intégralité de son processus de combustion sur une large plage d'utilisation est le facteur limitant de son développement. Une étude bibliographique a démontré qu'il existe de nombreuses possibilités et paramètres à contrôler qui pourrait permettre de lever ce verrou. D'une manière générale, chacun de ces leviers ont leurs propres avantages et inconvénients et il est fort à parier que le développement de futurs moteurs fonctionnant sur le mode de combustion HCCI intégrera plusieurs d'entre eux. Compte tenu que ce mode de combustion est entièrement régit par la

cinétique de la combustion, des études récentes se sont portées sur l'impact de l'ajout de diverses espèces chimiques oxydantes. Bon nombre d'entre elles influencent clairement le processus de combustion mais toutes ne peuvent pas aboutir à de réels cas d'applications. Finalement, il en résulte que l'ozone, qui est par ailleurs une des espèces les plus oxydantes, sera probablement la plus à même à contrôler efficacement le processus de combustion HCCI et pourrait être produite au sein de réels véhicules puisque les dispositifs la générant deviennent de plus en plus petit. Jusqu'à présent, les études avaient seulement démontré son impact sans pour autant considérer de vrais cas d'applications. Ainsi, deux objectifs principaux ont été définis :

1. Evaluer le potentiel applicatif des générateurs d'ozone pour contrôler la combustion HCCI. Ces dispositifs produisent majoritairement de l'ozone mais d'autres espèces telles que les oxydes d'azote peuvent aussi être formés compte tenu des conditions d'utilisation. Il était donc important de caractériser leur impact respectif et leurs interactions. De plus, puisque l'ozone dispose de temps de vie assez limité, l'influence de la température a aussi été considérée.
2. Etudier l'impact de l'ozone sur la combustion d'une grande variété de carburants. Puisque les moteurs HCCI ont la particularité d'être flexible sur l'utilisation des carburants, divers carburants référencés comme conventionnels et alternatifs et leur oxydation en présence d'ozone doit faire l'objet de recherche et pourra ces résultats pourront être comparé.

Afin de répondre concrètement à ce double objectif, les différents moyens expérimentaux et outils de simulation utilisés tout au long de ces travaux de thèse ont été définis dans la deuxième partie de ce manuscrit. Les études ont principalement été conduites sur un banc moteur monocylindre expérimental adapté pour un fonctionnement HCCI. Celui-ci a été décrit dans sa totalité ainsi que la méthodologie d'acquisition des données. De plus, un nouveau programme a été développé tout au long de la thèse pour permettre l'analyse des résultats et a été entièrement présentée. Finalement, en plus des résultats expérimentaux, des simulations de cinétique chimique ont été effectuées au moyen du package Chemkin II et de l'exécutable Senkin en vue d'appréhender les phénomènes relatifs à l'ajout d'ozone dans le moteur. Le modèle retenu a été présenté ainsi que les différents mécanismes et sous-mécanismes sélectionnés pour ces travaux.

Une importante partie des essais a été réalisé avec pour carburant les « Primary Reference Fuels » et en particulier l'isooctane en vue de répondre au premier objectif de ces travaux. Initialement, l'impact de l'ozone sur la combustion de plusieurs PRFs a été déterminé, permettant une comparaison avec des résultats issus de la littérature et d'étendre l'analyse de l'ozone sur leur combustion. Les résultats ont clairement mis en évidence l'effet promoteur de cette espèce chimique oxydante. D'une manière générale, l'ozone a démontré qu'il permet d'améliorer la combustion, de la rendre plus stable ainsi

que d'avancer son phasage. Une analyse approfondie des résultats sur le phasage de la combustion a aussi mis en évidence que l'ozone a un effet promoteur exponentiel sur la combustion HCCI des PRFs. De très faibles concentrations injectées à l'admission permettent d'avancer considérablement le phasage de l'ensemble du processus de combustion tandis que de plus importantes concentrations continuent de promouvoir la combustion mais avec une influence moins prononcée. Par comparaison entre les différents PRFs sélectionnés, l'ozone conduit à un effet similaire pour l'ensemble d'entre eux excepté pour l'isooctane. Cela est dû à la présence de n-heptane dans ces carburants qui permet l'autoinflammation à des températures d'admission ambiantes. Pour l'isooctane, la principale raison vient de sa difficulté à s'autoinflammer qui nécessite l'emploi d'une température d'admission significative. Ce paramètre a une forte influence sur la durée de vie de l'ozone et résulte en une décomposition prématurée de cette espèce chimique oxydante. Cela permet ainsi d'oxyder le carburant bien plus tôt et donc d'augmenter brutalement le phasage de la combustion. Par ailleurs, ces essais expérimentaux ont montré que l'ozone agissait sur l'intégralité du processus de combustion et particulièrement au début. Les analyses ont montré que le phasage de la flamme froide des PRFs avance dans le cycle et que l'énergie libérée pendant cette étape augmente conduisant à une augmentation de températures dans le cycle et donc aussi à une avance de la combustion principale. Néanmoins, dans le cas de l'isooctane qui ne présente pas de flamme froide, l'ozone influence directement le début de la combustion principale. Cet effet promoteur de l'ozone a aussi été mis en évidence à l'aide de simulations de cinétique chimique sur l'isooctane. Les résultats ont démontré que l'ozone influence bien l'initiation de la combustion mais de manière indirecte. C'est en réalité l'atome d'oxygène issu de la décomposition de l'ozone qui permet l'oxydation directe du carburant et la formation de radicaux hautement réactifs menant très rapidement à la combustion.

Etant donné que les premiers résultats ont montré que l'ozone permet d'avancer le phasage de la combustion en initiant l'oxydation des carburants à de plus faibles températures et étant donné que sa décomposition est fortement influencée par la température, une étude supplémentaire a été effectuée avec l'isooctane. Les résultats ont clairement démontré que l'ozone a le potentiel de contrôler la combustion HCCI moyennant des variations des conditions d'admission du moteur. L'emploi de cette molécule oxydante serait donc bénéfique pour résoudre une autre problématique de la combustion HCCI, à savoir, le démarrage à froid. De plus, cette étude a aussi permis de confirmer que l'ozone agit sur le début de la combustion puisqu'une apparition de la flamme froide a été observée.

L'ozone a ainsi démontré son potentiel d'utilisation pour une application automobile. Néanmoins, l'intégration des dispositifs le générant peut amener d'autres problématiques. Ceux-ci nécessitent l'utilisation d'oxygène pour assurer la production d'ozone mais dans le cadre d'une application automobile, employer l'oxygène contenu dans l'air sera plus adapté. Toutefois, d'autres espèces oxydantes telles que les oxydes d'azote

pourraient aussi être produites. De plus, ces espèces peuvent être présentes dans les résiduels ou avec l'EGR et pourraient interagir avec l'utilisation d'un générateur d'ozone, renforçant ainsi l'intérêt d'une telle étude. L'impact de ces différentes espèces a donc été comparé et il a été mis en évidence que toutes ces espèces chimiques améliorent la combustion et avancent le phasage de la combustion. Par comparaison de leur influence respective, l'ozone est le plus oxydant et le dioxygène d'azote le moins. Cela a été justifié à l'aide de la cinétique chimique et par une analyse de la production des espèces les plus réactives et conduisant à la combustion. Finalement, l'ajout simultané de l'ozone et du monoxyde d'azote, l'oxyde d'azote le plus présent dans les gaz d'échappement, a été étudié. Les résultats ont ainsi montré qu'il existe des interactions résultant en un retard de la combustion. Ces réactions prennent place à l'admission du moteur bien avant l'admission des gaz frais dans la chambre de combustion. Toutefois, ces phénomènes ont été expliqués à l'aide de la cinétique chimique mais le problème reste assez complexe. D'autres études basées sur l'utilisation de dispositifs expérimentaux mieux adaptés seraient nécessaires pour approfondir la compréhension des phénomènes prenant place dans l'admission du moteur.

Finalement, une dernière étude a permis de finaliser l'évaluation du potentiel applicatif des générateurs d'ozone à l'aide de la mise en place d'un contrôle dynamique dans de réelles conditions d'utilisation. Tout d'abord, il a été observé que le générateur d'ozone employé produit uniquement de l'ozone et aucunes espèces chimiques indésirables. Cela est dû au générateur d'ozone utilisé pour notre étude qui a été conçu pour se focaliser sur une production d'ozone tandis que dans le cas d'une potentielle application automobile, l'hypothèse de possibles interactions entre l'ozone et les oxydes d'azote n'est pas à mettre de côté. Finalement, il a été démontré qu'il est possible de contrôler le phasage de la combustion ainsi que l'ensemble des paramètres moteur moyennant la gestion du générateur d'ozone et la gestion de la température d'admission. En conséquence, deux types de contrôle dynamiques ont été testés, permettant clairement de montrer qu'un générateur d'ozone peut être employé pour un contrôle efficace de la combustion HCCI.

Suite à l'ensemble de ces résultats prouvant le potentiel applicatif des générateurs d'ozone, plusieurs séries d'expériences ont été conduites en utilisant des carburants autres que les carburants conventionnels et en considérant uniquement l'ozone comme espèce oxydante. Face au potentiel oxydant de cette molécule permettant de réduire les températures de début d'oxydation des carburants, son influence sur des carburants très difficiles à autoinflammer a été effectuée. Le meilleur candidat pour une telle étude était bien évidemment le méthane. Malheureusement, les concentrations injectées étant faibles, seul des mélanges à fortes teneurs en méthane ont pu être étudiés. Par comparaison avec les précédents résultats et en particulier ceux de l'isooctane, l'impact de l'ozone reste identique toutefois, des concentrations bien plus importantes sont nécessaires pour atteindre des avances significatives de la combustion malgré que la température d'admission était bien plus importante. La principale raison vient donc de la structure du carburant et de

la longueur de sa chaîne carbonée. Plus cette dernière est longue et plus l'oxydation du carburant par l'oxygène atomique est facile. Le carburant a sélectionné pour une combinaison avec l'ozone est donc crucial afin de couvrir une large plage d'utilisation.

En plus de carburants à hautes teneurs en méthane, d'autres carburants alternatifs possédant une structure chimique différente ont été sélectionnés pour étudier l'impact de l'ozone. Le choix s'est porté sur trois carburants de la famille des alcools, le méthanol, l'éthanol et le n-butanol. Etant donné que ces carburants peuvent s'autoinflammer moyennant les mêmes conditions moteur, une étude comparative a pu être établit. L'ozone a montré une influence similaire aux carburants précédemment sélectionnés, pour rappel, une avance et une amélioration de la combustion. Toutefois, il a été observé que le n-butanol était bien plus impacté par l'ozone que le méthanol. Cela a ainsi mis en évidence que la structure chimique du carburant est importante si l'on souhaite obtenir une influence plus ou moins importante de l'ozone. De plus, par comparaison avec l'isooctane, ce dernier est bien plus influencé pour des conditions similaires moteur du fait que sa chaine carbonée la plus importante contient plus d'atomes de carbone que le n-butanol mais aussi en raison de l'absence de la structure alcool. Finalement, l'ensemble de ces résultats a permis de mettre en évidence l'impact de l'ozone sur la combustion HCCI de différents carburants et que la structure du carburant est un facteur important a considéré.

Conclusion

Version anglaise / English version

The main objectives in the automotive field are reducing fuel consumption of vehicles, reducing CO_2 emissions as well as pollutants while maintaining high efficiencies. In recent years, advanced combustion modes emerged and may replace in the near future conventional combustion modes, i.e. spark ignition and compression ignition engines, in order to meet these requirements. Among them, lots of investigations were made on the Homogeneous Charge Compression Ignition mode. In spite of its strong potential, the development of this new combustion mode is still very limited as there are many challenges to address. The main problem is finding an effective means for controlling the combustion process, entirely governed by kinetics, on a wide operating range, in terms of rotation speeds (N) and loads (φ, P, T).

One scientific aim of the ERC 2G-CSafe project is investigating the impact of minor oxidizing chemical species on the combustion process into engines such as the advanced combustion engines and in particular, the HCCI combustion. This investigation will allow bringing the scientific community new data and analysis on the chemical impact of various oxidizing species in order to participate to the understanding of the phenomena observed during homogeneous combustions. Finally, these works will also participate to the built of new control strategies for automotive and to the design of innovative technologies. The present Thesis consists in investigating the effect of seeding the intake of a HCCI engine with minor oxidizing chemical species coming from devices generating plasma discharges and showing the possible applications of such a device onboard a vehicle.

The first part of the Thesis consisted in a review on the HCCI combustion which allows us highlighting the advantages and drawbacks of this combustion mode. It was therefore observed that the main issue of the HCCI combustion is that an efficient means for controlling the whole combustion process is needed and therefore limits the development of such an engine. A state of the art on the HCCI combustion showed that there is many possibilities and parameters to control in order to overcome this problem. Generally, each of them has its own pros and cons and the development of future HCCI engines will probably use several of them. As this combustion mode is entirely governed by kinetics, recent investigations were made on the impact of the addition of different oxidizing chemical species. Many of them influence clearly the combustion process but only some of these species may be consider for real applications. Finally, ozone, one of the strongest oxidizing species, will be probably the most powerful species used for controlling the overall HCCI combustion process. Moreover, it could be generated onboard a vehicle since devices generating it become increasingly small. Up to now, studies only observed the impact of

ozone without considering real application cases. As a result, two main objectives were drawn:

1. Assess the potential of applying ozone generators to control the HCCI combustion. These devices mainly generate ozone but other species could be produced such as nitrogen oxides depending in the conditions of use. It was therefore important to characterize their respective impact and their interactions. Moreover, since ozone has a short life time which decreases with the temperature, the influence of temperature was also considered.
2. Investigate the impact of ozone on the combustion of a wide range of fuels. Since HCCI engine is fuel flexibility, many fuels referred as conventional and alternative fuels were studied as well as their own oxidation in the presence of ozone. Finally, these results are compared.

In order to meet these objectives, the experimental setup and the numerical tools used during these works were defined in the second chapter of the Thesis. The investigations were mainly carried out on a single cylinder engine adapted to work under HCCI conditions. It was entirely described as well as the methodology to acquire the data. Moreover, a new program has been developed all along the Thesis to allow the determination and analysis of the results and was introduced. Finally, in complement to the experimental results, kinetics computations were performed with the help of the Chemkin II package and the Senkin executable to bring the understanding of the phenomena observed due to the ozone seeding at the intake of the engine. The model retained was introduced as well as the mechanism and sub-mechanisms selected.

A major part of the experiments was performed with Primary Reference Fuels (PRFs) and in particular isooctane to meet the first objective of these works. First, the impact of ozone on the combustion of several PRFs was determined, allowing a comparison with results found in the literature and to extend the analysis of ozone on the combustion. Results clearly highlighted the promoting effect of ozone. Generally, ozone showed that it allows to improve the combustion, to stabilize it as well as advance its phasing. A deeper analysis of the results on the combustion phasing also highlighted that ozone leads to an exponential effect on the HCCI combustion of PRFs. Low concentrations injected at the intake allow to strongly advance the phasing of the overall combustion process while higher concentrations continue to promote the combustion but the influence is less pronounced. By comparing the PRFs selected, ozone leads to a similar effect for all of them except for isooctane as fuel. The similar impact observed is due to the presence of n-heptane in all the PRFs which allows the autoignition under ambient temperatures. For isooctane as fuel, the main reason comes from its difficulty to autoignite which need the use of a significant intake temperature. The temperature strongly influences the ozone lifetime and results in an earlier breakdown of ozone which finally allows to oxidize very earlier the fuel and therefore

to increase rapidly the combustion phasing. Furthermore, these experimental results showed that ozone modified the overall combustion process and in particular the beginning. Analysis showed that the phasing of the PRFs cool flame advance in the cycle and that the energy released during this step increases, leading to an increase of the in-cylinder temperatures into the cycle and therefore, also to the advance of the main combustion step. Nevertheless, in the case of isooctane where no cool flame occurs, ozone influences directly the beginning of the main combustion. The promoting effect of ozone was also highlighted through the help of kinetics computations with isooctane as fuel. These last results showed that ozone impacts the start of the combustion but not directly. The improvement is due to the oxygen atom coming from the ozone breakdown ($O_3 \rightarrow O_{atom} + O_2$) which enables a direct oxidation of the fuel and the formation of highly reactive radicals leading very rapidly to the combustion.

As the first results showed that ozone allows advancing the combustion phasing by starting the oxidation of fuels under lower temperatures and as the breakdown of ozone is strongly influenced by the temperature, an extra study has been carried out with isooctane. Results displayed that ozone has the potential to manage the HCCI combustion with variations of the intake conditions of the engine. The use of this oxidizing species will be also useful to solve another issue of the HCCI combustion: the cold start. Moreover, this study also allowed confirming that ozone acts on the beginning of the combustion as a cool flame occurred.

Ozone therefore showed its potential for an automotive application. Nevertheless, the implementation of devices generating ozone may bring other problems. These generators need the use of pure oxygen to ensure a high production of ozone but for automotive applications, use oxygen contained in the air will be more suitable. However, other species such as nitrogen oxides could also be produced in the ozone generator. Moreover, these species could also be present into residuals or with the use of EGR and may react with the use of an ozone generator, supporting such an investigation. The impact of all these different species was therefore compared and it was highlighted that each of them improve the combustion and advance the combustion phasing. Ozone showed that it is the species which influences the most the combustion and nitrogen dioxide (NO_2) the least. These results were justified through kinetics computations and by an analysis of the more reactive radicals produced leading to the combustion. Finally, the simultaneous injection of ozone (O_3) and nitric oxide (NO), the nitrogen oxide the most encountered into the combustion products, was studied. Results showed that there are interactions which lead to a delay of the combustion. These reactions take place in front of the combustion chamber before the entrance of the fresh gases into the combustion chamber. These phenomena were explained through kinetics but the problem remains complex. Other studies based on the use of other experimental setups more appropriate will be needed to examine deeply the understanding of these phenomena into the intake of the engine.

Finally, a last study with isooctane allowed assessing the possible application of ozone generators through a dynamic control in real conditions of use. First, it was observed that the ozone generator used, only produced ozone, and no undesirable chemical species. In fact, the ozone generator used, which is a commercial device, focuses only on an ozone production while in the case of an automotive application, the assumption of possible interactions between ozone and nitrogen dioxide are not forgotten. Finally, it was showed that it is possible to control the combustion phasing as well as all the engine parameters by managing 1) the ozone generator capacity and 2) the intake temperature. Consequently, two kinds of dynamic controls were performed, showing that ozone generator could be implemented for efficiently controlling the HCCI combustion.

Following all these results showing the potential application of ozone generators, lots of experiments were performed by using other fuels than conventional ones and by considering only ozone as oxidizing chemical species. As ozone allows to reduce temperatures of the start of the oxidation of fuels, it influence on fuels highly difficult to autoignite was carried out. The best fuel for such a study is obviously methane. Unfortunately, the concentrations injected were low and only mixtures of fuels with high fractions of methane have been studied. By comparing with previous results and in particular with isooctane ones, the impact of ozone is similar. However, higher concentrations are needed to achieve significant advances of the combustion in spite of the highest intake temperatures set. The main reason comes from the structure of the fuel. Longer the carbon chain is, easier the fuel oxidation is. The fuel selected for a use with ozone is therefore crucial and must enable to cover a wide operating range.

Additionally to the fuels with high ratios of methane, other alternative fuels with a different chemical structure were selected for investigating the ozone impact. Three alcohol fuels were selected: methanol, ethanol and n-butanol. As these fuels may autoignite through the same intake conditions, a comparative study was established. Ozone showed a similar influence than with previous fuels selected, an advance and an improvement of the combustion. However, it was observed that n-butanol is the most impacted by ozone and methanol the least. It was highlighted that the fuel structure is of main importance if we want to obtain an influence more or less important with the use of ozone. Moreover, by comparing with prior results, isooctane is more influenced by ozone under the same engine conditions due to its carbon chain, which is longer than that of n-butanol, but also due to the absence of the alcohol structure. Finally, all these results allowed highlighting that the impact of ozone on the combustion of a wide range of fuels and that the structure of the fuel is a significant parameter to consider.

Futures recherches

Version française / French version

Jusqu'à présent, les études sur la combustion HCCI avec l'ozone avaient considéré seulement son effet promoteur pour contrôler le phasage de la combustion. La présente étude a considéré le potentiel applicatif de l'utilisation de l'ozone et a permis une comparaison de l'impact de cette molécule chimique oxydante sur divers carburants. Bien évidemment, ces résultats participent à la communauté scientifique en apportant de nouvelles données et analyses pour le développement de tels dispositifs dans le cadre d'applications automobiles pouvant intégrer divers nouveaux modes de combustion. Ces approches étant innovantes, de nombreuses recherches restent encore à effectuer et font partis des perspectives de la présente thèse.

L'ozone a démontré aisément qu'il est possible de contrôler le phasage de la combustion HCCI en ajustant les concentrations injectées. Néanmoins, les essais menés au cours de la présente étude se sont limités à un seul régime moteur et une seule richesse pour les mélanges air/carburant. Afin de pouvoir remplacer les moteurs conventionnels, le mode de combustion HCCI doit pouvoir être contrôlé efficacement sur un large domaine d'opérations. Des recherches supplémentaires sont donc nécessaires afin de déterminer si l'ozone peut être utilisé sur un large domaine de régimes et de charges et finalement déterminer les limites applicatives du dispositif générant cette espèce chimique oxydante.

Afin d'étendre le domaine d'utilisation de la combustion HCCI, de forts taux d'EGR sont employés. Les résultats ont montré que des espèces minoritaires comme les oxydes d'azote présents en très faibles concentrations peuvent altérer le phasage de la combustion HCCI par des réactions avec l'ozone intervenant bien avant l'admission du mélange homogène dans la chambre de combustion. L'EGR est composé de bien d'autres espèces chimiques dont les fractions sont plus ou moins importantes et qui pourrait réagir avec l'ozone, annihilant son potentiel oxydant. Il est donc important de considérer les différentes interactions pouvant survenir lors d'une combinaison entre l'utilisation d'importants niveaux d'EGR et de l'ozone.

Certaines réactions pouvant intervenir dans l'admission du moteur, il est crucial d'étudier la décomposition de l'ozone et les différentes réactions pouvant intervenir entre les différents composés. Cela permettra de caractériser les éventuelles oxydations entre l'ozone et les espèces majoritaires et minoritaires issues de l'EGR ainsi que les hypothétiques réactions de pré-oxydation du carburant. Cependant, de telles études ne peuvent pas utiliser un banc moteur. A la place, un nouveau réacteur chimique est nécessaire et de nombreuses études pourraient être menées pour apporter une meilleure compréhension de ces

différents phénomènes et éventuellement participer au développement d'un nouveau mécanisme de combustion avec l'ozone. De manière additionnelle, ce type d'expérience pourrait permettre de caractériser l'intégralité des réactions en amont de la chambre de combustion mais la majeure partie des réactions conduisant à la combustion prennent place au sein du moteur. Des études en moteurs optiques sont donc nécessaires afin d'évaluer la décomposition de l'ozone dans la chambre de combustion. Cela demeure néanmoins un réel challenge compte tenu que les fractions de cette espèce chimique sont extrêmement faibles pour être détectées par des techniques optiques. D'autres essais optiques pourraient permettre d'observer la formation prématurée des radicaux hydroxyles mais il pourrait être difficile de distinguer ceux produits par l'oxydation directe du carburant avec l'oxygène atomique issu de la décomposition de l'ozone de ceux provenant de l'oxydation normale du carburant. Finalement, l'ensemble des résultats obtenus au cours de ces travaux ainsi que ceux pouvant être obtenu via ces perspectives pourraient activement participés au développement et à l'amélioration de modèles de simulation de la combustion HCCI.

Un autre facteur important mis en évidence au cours de ces travaux est le carburant. Il peut s'autoinflammer avec plus ou moins de difficultés et les études préliminaires de cette étude ont clairement mis en évidence le besoin d'établir des propriétés caractérisant son comportement en combustion HCCI. Toutefois, dans le cadre de cette étude, il semble que la structure chimique des carburants soit cruciale et l'ozone peut conduire à une influence plus ou moins importante sur leur combustion. De plus, sachant que les carburants conventionnels tel que l'essence ou le diesel sont constitués de plusieurs centaines de composés différents, il est important d'étudier l'impact de l'ozone sur des carburants avec une structure chimique différente encore de celles déjà testées. De plus, l'ozone a montré une aptitude à contrôler la combustion sur un large domaine de température. Cependant dans le cas de l'isooctane, cette température était encore élevée comparée à celles rencontrées en moteur à combustion interne. Ainsi, des carburants légèrement moins difficiles à autoinflammer que l'isooctane proche de l'essence devrait être étudiés pour démontrer un plus large domaine d'opérations.

La combustion HCCI a été très étudiée ces dernières années mais encore aujourd'hui, son développement demeure limité. Toutefois, d'autres nouveaux modes de combustion pourraient favorablement remplacer les moteurs conventionnels. Ces derniers présentent des phénomènes similaires à la combustion HCCI et les études sur ce mode de combustion participent activement à leur développement. Les présents résultats peuvent donc permettre d'appréhender le potentiel impact de l'ozone sur d'autres modes de combustion tel que le mode de combustion PCCI ou RCCI et des études expérimentales avec ces derniers devraient être effectuées concrètement.

Enfin, dans le cadre de ces études, un générateur d'ozone commercial a été utilisé. Celui-ci est peu adapté pour des applications automobiles mais d'autres déjà existants sont

réellement très petits, très performants et pourrait être intégrer à de vrais véhicules. Toutefois, un tel dispositif doit être optimisé pour répondre à un cahier des charges en adéquation avec son utilisation. Dans le cas d'une application automobile, ce générateur devra se focaliser sur une production d'ozone uniquement comme cela a été observé au cours de ces travaux, devra être le moins énergivore possible lors de l'utilisation de ses capacités maximales et finalement devra atteindre de hautes productions d'ozone et ce en un laps de temps imparti pouvant être relativement court.

Future research

Version anglaise / English version

Up to now, investigations on the HCCI combustion with ozone only considered its promoting effect for controlling the combustion phasing. The present Thesis considered the potential use of ozone by implementing ozone generator onboard vehicles and allowed a comparison of the impact of this oxidizing chemical species on a wide range of fuels. Obviously, these results bring new data and analysis to the scientific community for developing such devices for automotive applications working with advanced combustion mode. These approach are innovative, more research must be still carried out and are outlined in the present prospects of the Thesis.

Ozone showed that it can easily control the HCCI combustion phasing by managing the concentrations injected. Nevertheless, experiments performed during this work were limited to only one rotation speed (N=1500 rpm) and only one equivalence ratio (φ = 0.3). Before a widespread use of HCCI engine, this mode must be controlled under a wide operating range. Further research is therefore needed to determine if ozone can be used on a wide range of rotation speed and load and finally, determine the application limits of such a device generating this oxidizing chemical species.

To expand the field of action of the HCCI combustion, high EGR ratios are used. Results showed that minor species such as nitrogen oxides found in low concentrations may alter the combustion phasing by reactions involving ozone and occurring before the induction of the fresh gases into the combustion chamber. EGR consists in many chemical species whose the fractions are more or less important and could react with ozone, inhibiting ozone's promoting effect. It is therefore of a main importance to consider the different interactions which may occur through the simultaneous use of EGR and ozone.

Some reactions may appear into the intake of the engine, it is crucial to study the breakdown of ozone and the different reactions which can occur between the different compounds. Such an investigation will allow characterizing the potential oxidations between ozone and minor and major species coming from EGR as well as the hypothetical reaction of pre-oxidation of the fuels. However, such investigations cannot be performed with an engine bench. Instead, a new chemical reactor is needed and lots of experiments must be performed to bring a better understanding of the different phenomena and could also participate in the development of a new mechanism for the ozone-assisted combustion. Additionally, this kind of experiment could allow characterizing the whole reactions in front of the combustion chamber but the main part of reactions leading to the combustion occurs into the engine. Studies with optical access engines are therefore needed to assess the

ozone breakdown into the combustion chamber but it is still a significant challenge since the fractions of this oxidizing chemical species are extremely small for detections with optical techniques. Other optical measurements could allow to observe the prior formation of hydroxyl radicals (OH) but it could be difficult to differentiate those generated by 1) the direct reaction involving the fuel and the oxygen atom coming from the ozone decomposition or 2) those resulting to the normal oxidation of the fuel. Finally, the entire results obtained during these works as well as those which could be obtained through these perspectives could participate to the development and the improvement of computational models for the HCCI combustion.

Another key factor highlighted in these works is the fuel. The fuel may autoignite more or less easily and prior studies in the Thesis clearly highlighted the need of establishing properties describing the behavior under HCCI combustion. However, for this study, it seems that the chemical structure of the fuel is of a significant importance and ozone may lead to an influence more or less important. Moreover, knowing that conventional fuels such as gasoline or diesel consist in several hundreds of components, it is important to investigate the impact of ozone on fuels whose the chemical structure is still different to those already tested. Moreover, ozone showed that it was able to control the combustion under a wide range of temperature. Unfortunately, in the case of isooctane (RON = 100), the temperature was still high compared to those encountered into an internal combustion engine. As a result, fuels slightly less difficult to autoignite than isooctane and closed to gasoline should be investigated in order to apply ozone under a wide range of operating.

The HCCI combustion was studied in last years and even today, HCCI development is still growing. However, other advanced combustion modes could slowly replace conventional engines. These advanced combustion modes present similar phenomena than those of the HCCI combustion and studies on HCCI combustion play an important role into the development of future internal combustion engines. The present results may therefore allow understanding the potential impact of ozone on other combustion modes such as PCCI or RCCI combustions and experimental studies with these advanced combustion modes must be conducted.

Finally, in the present Thesis, a commercial ozone generator has been used. This apparatus is not suitable for automotive applications but other devices already exist, are very small, are very powerful and could be implemented onboard real vehicles. However, such a device must be optimized for answering to specifications in accordance with its use. For automotive application, this generator should focus only on an ozone production as it was observed during our experiments, but also must be less energy-consuming during the use of its maximal capacities and finally, must also allow to achieve high levels of ozone with a time consistent with one engine cycle.

References

[1] U.S. Energy Infromation Administration, “International Energy Outlook 2013,” 2013.

[2] U.S. Energy Information Administration, “Annual Energy Outlook 2015 with projections to 2040,” 2015.

[3] U.S. Energy Information Administration, “Annual Energy Outlook 2014 with projections to 2040,” 2014.

[4] Department of Social and Economic Affairs, “World Population Prospects 2015,” 2015.

[5] International Energy Agency, “World Energy Outlook 2012,” 2012.

[6] Ertrac, “Energy Carriers for Powertrains,” pp. 1–110, 2014.

[7] J. D. Miller and C. Façanha, “The State of Clean Transport Policy - A 2014 Synthesis of Vehicle and Fuel Policy Developments,” *Int. Counc. Clean Transp.*, 2014.

[8] Parlement européen and Conseil de l’union européen, “RÈGLEMENT (CE) No 715/2007 DU PARLEMENT EUROPÉEN ET DU CONSEIL du 20 juin 2007 relatif à la réception des véhicules à moteur au regard des émissions des véhicules particuliers et utilitaires légers (Euro 5 et Euro 6) et aux informations sur la réparation,” 2007.

[9] F. Foucher, P. Higelin, C. Mounam-Rousselle, and P. Dagaut, “Influence of ozone on the combustion of n-heptane in a HCCI engine,” *Proc. Combust. Inst.*, vol. 34, no. 2, pp. 3005–3012, 2013.

[10] S. M. Aceves, D. Flowers, J. Martinez-Frias, F. Espinoza-Loza, W. J. Pitz, and R. Dibble, “Fuel and Additive Characterization for HCCl Combustion,” *SAE Tech. Pap.*, 2003.

[11] A. Mohammadi, H. Kawanabe, T. Ishiyama, M. Shioji, and A. Komada, “Study on combustion control in natural-gas PCCI engines with ozone addition into intake gas,” *SAE Tech. Pap.*, 2006.

[12] H. Nishida, “Homogeneous Charge Compression Ignition of Natural Gas / Air Mixture with Ozone Addition,” *J. Propuls. Power*, vol. 22, no. 1, pp. 151–157, 2006.

[13] H. Yamada, M. Yoshii, and A. Tezaki, “Chemical mechanistic analysis of additive effects in

homogeneous charge compression ignition of dimethyl ether," *Proc. Combust. Inst.*, vol. 30 II, no. 2, pp. 2773–2780, 2005.

[14] R. Stone, *Introduction to Internal Combustion Engines*. 1992.

[15] J. E. Dec, "Advanced compression-ignition engines - Understanding the in-cylinder processes," *Proc. Combust. Inst.*, vol. 32 II, no. 2, pp. 2727–2742, 2009.

[16] R. D. Reitz, "Directions in internal combustion engine research," *Combust. Flame*, vol. 160, no. 1, pp. 1–8, 2013.

[17] H. Bendu and S. Murugan, "Homogeneous charge compression ignition (HCCI) combustion: Mixture preparation and control strategies in diesel engines," *Renew. Sustain. Energy Rev.*, vol. 38, pp. 732–746, 2014.

[18] T. Kitamura, T. Ito, J. Senda, and H. Fujimoto, "Mechanism of smokeless diesel combustion with oxygenated fuels based on the dependence of the equivalence ration and temperature on soot particle formation," *Int. J. Engine Res.*, vol. 3, no. 4, pp. 223–248, 2005.

[19] G. D. Neely, S. Sasaki, Y. Huang, J. a Leet, and D. W. Stewart, "New Diesel Emission Control Strategy to Meet US Tier 2 Emissions Regulations Reprinted From : Diesel Exhaust Emission Control 2005," *Sae Pap. 2005-01-1091*, vol. 2005, no. 724, 2005.

[20] M. P. B. Musculus, P. C. Miles, and L. M. Pickett, "Conceptual models for partially premixed low-temperature diesel combustion," *Prog. Energy Combust. Sci.*, vol. 39, no. 2–3, pp. 246–283, 2013.

[21] S. L. Kokjohn, R. M. Hanson, D. a. Splitter, and R. D. Reitz, "Fuel reactivity controlled compression ignition (RCCI): a pathway to controlled high-efficiency clean combustion," *Int. J. Engine Res.*, vol. 12, no. 3, pp. 209–226, 2011.

[22] R. D. Reitz and G. Duraisamy, "Review of high efficiency and clean reactivity controlled compression ignition (RCCI) combustion in internal combustion engines," *Prog. Energy Combust. Sci.*, 2014.

[23] S. Saxena and I. D. Bedoya, "Fundamental phenomena affecting low temperature combustion and HCCI engines, high load limits and strategies for extending these limits," *Prog. Energy Combust. Sci.*, vol. 39, no. 5, pp. 457–488, 2013.

[24] M. Yao, Z. Zheng, and H. Liu, "Progress and recent trends in homogeneous charge compression ignition (HCCI) engines," *Prog. Energy Combust. Sci.*, vol. 35, no. 5, pp. 398–437, 2009.

[25] X. Lu, D. Han, and Z. Huang, “Fuel design and management for the control of advanced compression-ignition combustion modes,” *Prog. Energy Combust. Sci.*, vol. 37, no. 6, pp. 741–783, 2011.

[26] J. M. Bergthorson and M. J. Thomson, “A review of the combustion and emissions properties of advanced transportation biofuels and their impact on existing and future engines,” *Renew. Sustain. Energy Rev.*, vol. 42, pp. 1393–1417, 2015.

[27] M. Sjöberg and J. E. Dec, “Comparing late-cycle autoignition stability for single- and two-stage ignition fuels in HCCI engines,” *Proc. Combust. Inst.*, vol. 31 II, pp. 2895–2902, 2007.

[28] M. M. Hasan and M. M. Rahman, “Homogeneous charge compression ignition combustion: Advantages over compression ignition combustion, challenges and solutions,” *Renew. Sustain. Energy Rev.*, vol. 57, pp. 282–291, 2016.

[29] H. J. Curran, P. Gaffuri, W. J. Pitz, and C. K. Westbrook, “A comprehensive modeling study of n-heptane oxidation,” *Combust. Flame*, vol. 114, no. 1–2, pp. 149–177, 1998.

[30] H. J. Curran, P. Gaffuri, W. J. Pitz, and C. K. Westbrook, “A comprehensive modeling study of iso-octane oxidation,” *Combust. Flame*, vol. 129, no. 3, pp. 253–280, 2002.

[31] P. Dagaut, M. Reuillon, and M. Cathonnet, “High Pressure Oxidation of Liquid Fuels From Low to High Temperature. 1. n-Heptane and iso-Octane,” *Combust. Sci. Technol.*, vol. 95, pp. 233–260, 1994.

[32] P. Dagaut, M. Reuillon, and M. Cathonnet, “High Pressure Oxidation of Liquid Fuels From Low to High Temperature. 2. Mixtures of n-Heptane and iso-Octane,” *Combust. Sci. Technol.*, vol. 103, pp. 315–336, 1994.

[33] A. Dubreuil, F. Foucher, and C. Mounaim-Rousselle, “Effect of EGR Chemical Components and Intake Temperature on HCCI Combustion Development,” *SAE Int.*, pp. 776–790, 2006.

[34] X.-C. Lü, W. Chen, and Z. Huang, “A fundamental study on the control of the HCCI combustion and emissions by fuel design concept combined with controllable EGR. Part 2. Effect of operating conditions and EGR on HCCI combustion,” *Fuel*, vol. 84, no. 9, pp. 1084–1092, 2005.

[35] H. Machrafi and S. Cavadias, “An experimental and numerical analysis of the influence of the inlet temperature, equivalence ratio and compression ratio on the HCCI auto-ignition process of Primary Reference Fuels in an engine,” *Fuel Process. Technol.*, vol. 89, no. 11, pp.

1218–1226, 2008.

[36] C. Cinar, A. Uyumaz, H. Solmaz, F. Sahin, S. Polat, and E. Yilmaz, “Effects of intake air temperature on combustion, performance and emission characteristics of a HCCI engine fueled with the blends of 20% n-heptane and 80% isooctane fuels,” *Fuel Process. Technol.*, vol. 130, pp. 275–281, 2015.

[37] S. Tanaka, F. Ayala, J. C. Keck, and J. B. Heywood, “Two-stage ignition in HCCI combustion and HCCI control by fuels and additives,” *Combust. Flame*, vol. 132, no. 1–2, pp. 219–239, 2003.

[38] A. Uyumaz, “An experimental investigation into combustion and performance characteristics of an HCCI gasoline engine fueled with n-heptane, isopropanol and n-butanol fuel blends at different inlet air temperatures,” *Energy Convers. Manag.*, vol. 98, pp. 199–207, 2015.

[39] C. H. Zhang, J. R. Pan, J. J. Tong, and J. Li, “Effects of intake temperature and excessive air coefficient on combustion characteristics and emissions of HCCI combustion,” *Procedia Environ. Sci.*, vol. 11, no. PART C, pp. 1119–1127, 2011.

[40] C.-H. Zhang, L. Xue, and J. Wang, “Experimental study of the influence of λ and intake temperature on combustion characteristics in an HCCI engine fueled with n-heptane,” *J. Energy Inst.*, vol. 87, no. 2, pp. 175–182, 2014.

[41] M. Mohamed Ibrahim and a. Ramesh, “Investigations on the effects of intake temperature and charge dilution in a hydrogen fueled HCCI engine,” *Int. J. Hydrogen Energy*, vol. 39, no. 26, pp. 14097–14108, 2014.

[42] N. Dronniou and J. Dec, “Investigating the Development of Thermal Stratification from the Near-Wall Regions to the Bulk-Gas in an HCCI Engine with Planar Imaging Thermometry,” *SAE Int. J. Engines*, vol. 5, no. 3, pp. 1046–1074, 2012.

[43] J. E. Dec and W. Hwang, “Characterizing the Development of Thermal Stratification in an HCCI Engine Using Planar-Imaging Thermometry,” *SAE Int. J. Engines*, vol. 2, pp. 421–438, 2009.

[44] J. E. Dec, W. Hwang, and M. Sjöberg, “An Investigation of Thermal Stratification in HCCI Engines Using Chemiluminescence Imaging,” *SAE Tech. Pap. 2006-01-1518*, 2006.

[45] G. Haraldsson, P. Tunestål, and B. Johansson, “HCCI Closed-Loop Combustion Control Using Fast Thermal Management,” *Ratio*, 2004.

[46] G. T. Kalghatgi, *Fuel/Engine Interactions*. 2014.

[47] V. H. Rapp, W. J. Cannella, J.-Y. Chen, and R. W. Dibble, “Predicting Fuel Performance for Future HCCI Engines,” *Combust. Sci. Technol.*, vol. 185, no. 5, pp. 735–748, 2013.

[48] L. Starck, B. Lecointe, L. Forti, and N. Jeuland, “Impact of fuel characteristics on HCCI combustion: Performances and emissions,” *Fuel*, vol. 89, no. 10, pp. 3069–3077, 2010.

[49] X. C. Lü, W. Chen, and Z. Huang, “A fundamental study on the control of the HCCI combustion and emissions by fuel design concept combined with controllable EGR. Part 1. the basic characteristics of HCCI combustion,” *Fuel*, vol. 84, no. 9, pp. 1074–1083, 2005.

[50] S. M. Aceves, J. R. Smith, C. K. Westbrook, and W. J. Pitz, “Compression Ratio Effect on Methane HCCI Combustion,” *J. Eng. Gas Turbines Power*, vol. 121, no. 3, p. 569, 1999.

[51] B.-Q. He, J. Yuan, M.-B. Liu, and H. Zhao, “Combustion and emission characteristics of a n-butanol HCCI engine,” *Fuel*, vol. 115, pp. 758–764, Jan. 2014.

[52] R. K. Maurya and A. K. Agarwal, “Experimental investigations of performance, combustion and emission characteristics of ethanol and methanol fueled HCCI engine,” *Fuel Process. Technol.*, vol. 126, pp. 30–48, 2014.

[53] F. Contino, F. Foucher, C. Mounaïm-Rousselle, and H. Jeanmart, “Combustion characteristics of tricomponent fuel blends of ethyl acetate, ethyl propionate, and ethyl butyrate in homogeneous charge compression ignition (HCCI),” *Energy and Fuels*, vol. 25, no. 4, pp. 1497–1503, 2011.

[54] F. Contino, F. Foucher, C. Mounaïm-Rousselle, and H. Jeanmart, “Experimental characterization of ethyl acetate, ethyl propionate, and ethyl butanoate in a homogeneous charge compression ignition engine,” *Energy and Fuels*, vol. 25, no. 3, pp. 998–1003, 2011.

[55] C. Pera and V. Knop, “Methodology to define gasoline surrogates dedicated to auto-ignition in engines,” *Fuel*, vol. 96, pp. 59–69, 2012.

[56] V. Knop, C. Pera, and F. Duffour, “Validation of a ternary gasoline surrogate in a CAI engine,” *Combust. Flame*, vol. 160, no. 10, pp. 2067–2082, 2013.

[57] N. Morgan, A. Smallbone, A. Bhave, M. Kraft, R. Cracknell, and G. Kalghatgi, “Mapping surrogate gasoline compositions into RON/MON space,” *Combust. Flame*, vol. 157, no. 6, pp. 1122–1131, 2010.

[58] P. Saisirirat, C. Togbé, S. Chanchaona, F. Foucher, C. Mounaim-Rousselle, and P. Dagaut, “Auto-ignition and combustion characteristics in HCCI and JSR using 1-butanol/n-heptane and ethanol/n-heptane blends,” *Proc. Combust. Inst.*, vol. 33, no. 2, pp. 3007–3014, 2011.

[59] Y. C. Hou, X. C. Lu, L. L. Zu, L. Bin Ji, and Z. Huang, “Effect of high-octane oxygenated fuels on n-heptane-fueled HCCI combustion,” *Energy and Fuels*, vol. 20, no. 4, pp. 1425–1433, 2006.

[60] H. Guo, V. Hosseini, W. S. Neill, W. L. Chippior, and C. E. Dumitrescu, “An experimental study on the effect of hydrogen enrichment on diesel fueled HCCI combustion,” *Int. J. Hydrogen Energy*, vol. 36, no. 21, pp. 13820–13830, 2011.

[61] T. Shudo and H. Yamada, “Hydrogen as an ignition-controlling agent for HCCI combustion engine by suppressing the low-temperature oxidation,” *Int. J. Hydrogen Energy*, vol. 32, no. 14, pp. 3066–3072, 2007.

[62] J. C. G. Andrae, “Semidetailed Kinetic Model for Gasoline Surrogate Fuel Interactions with the Ignition Enhancer 2-Ethylhexyl Nitrate,” *Energy & Fuels*, p. 150519130945000, 2015.

[63] N. K. Miller Jothi, G. Nagarajan, and S. Renganarayanan, “Experimental studies on homogeneous charge CI engine fueled with LPG using DEE as an ignition enhancer,” *Renew. Energy*, vol. 32, no. 9, pp. 1581–1593, 2007.

[64] C. Kavuri, S. L. Kokjohn, D. T. Klos, and D. Hou, “Blending the benefits of reactivity controlled compression ignition and gasoline compression ignition combustion using an adaptive fuel injection system,” 2015.

[65] N. Jeuland and X. Montagne, “New HCCI/CAI combustion process development: Methodology for determination of relevant fuel parameters,” *Oil Gas Sci. Technol.*, vol. 61, no. 1, pp. 85–94, 2006.

[66] G. T. Kalghatgi, “Developments in internal combustion engines and implications for combustion science and future transport fuels,” *Proc. Combust. Inst.*, 2014.

[67] G. T. Kalghatgi, “The outlook for fuels for internal combustion engines,” *Int. J. Engine Res.*, vol. 15, no. 4, pp. 383–398, 2014.

[68] D. Bradley and R. a. Head, “Engine autoignition: The relationship between octane numbers and autoignition delay times,” *Combust. Flame*, vol. 147, no. 3, pp. 171–184, 2006.

[69] G. Shibata and T. Urushihara, “Auto-Ignition Charactersitics of Hydrocarbons and Development of HCCI Fuel Index,” *SAE Tech. Pap.*, 2007.

[70] I. Truedsson, “Development of a new test method for evaluating HCCI fuel performance,” *SAE Tech. Pap.*, 2014.

[71] C. Wilhelmsson, P. Tunest, and B. Johansson, “Operation strategy of a Dual Fuel HCCI Engine with VGT,” *Library (Lond).*, pp. 356–364, 2007.

[72] T. Johansson, B. Johansson, P. Tunestål, and H. Aulin, “Turbocharging to extend HCCI Operating Range in a Multi Cylinder Engine-Benefits and Limitations,” *World Automot. Congr.*, 2010.

[73] J. Hyvönen, G. Haraldsson, and B. Johansson, “Supercharging HCCI to Extend the Operating Range in a Multi-Cylinder VCR-HCCI Engine,” *Sae*, 2003.

[74] V. Hosseini and M. D. Checkel, “Intake Pressure Effects on HCCI Combustion in a CFR Engine,” *Proc. Combust. institute, Can. Sect.*, no. 2004, pp. 1–6, 2007.

[75] M. Christensen, B. Johansson, P. Amneus, and F. Mauss, “Supercharged homogeneous charge compression ignition,” *SAE Trans.*, vol. 107, no. 724, pp. 1129–1144, 1998.

[76] H. Liu, M. Yao, B. Zhang, and Z. Zheng, “Effects of inlet pressure and octane numbers on combustion and emissions of a homogeneous charge compression ignition (HCCI) engine,” *Energy and Fuels*, vol. 22, no. 4, pp. 2207–2215, 2008.

[77] E. J. Silke, W. J. Pitz, C. K. Westbrook, M. Sjöberg, and J. E. Dec, “Understanding the Chemical Effects of Increased Boost Pressure under HCCI Conditions,” *SAE Int. J. Fuels Lubr.*, vol. 1, no. 1, pp. 12–25, 2008.

[78] T. Aroonsrisopon, D. Foster, T. Morikawa, and M. Lida, “Comparison of HCCI Operating Ranges for Combinations of Intake Temperature , Engine Speed and Fuel Composition,” *SAE Tech. Pap.*, no. 2002–01–1924, 2002.

[79] R. Ebrahimi and B. Desmet, “An experimental investigation on engine speed and cyclic dispersion in an HCCI engine,” *Fuel*, vol. 89, no. 8, pp. 2149–2156, 2010.

[80] M. Christensen and B. Johansson, “The Effect of Combustion Chamber Geometry on HCCI Operation,” *Sae Tech. Pap. Ser.*, vol. 2002, no. 724, 2002.

[81] A. Vressner, A. Hultqvist, and B. Johansson, “Study on combustion chamber geometry effects in an HCCI engine using high-speed cycle-resolved chemiluminescence imaging,” *SAE Pap.*, 2007.

[82] S. M. Aceves, D. L. Flowers, F. Espinosa-Loza, J. Martinez-Frias, R. W. Dibble, M. Christensen, B. Johansson, and R. P. Hessel, “Piston-liner crevice geometry effect on HCCI combustion by multi-zone analysis,” *SAE Tech. Pap.*, 2002.

[83] A. B. Dempsey, N. R. Walker, E. Gingrich, and R. D. Reitz, “Comparison of Low Temperature Combustion Strategies for Advanced Compression Ignition Engines with a Focus on Controllability,” *Combust. Sci. Technol.*, vol. 186, no. 2, pp. 210–241, 2014.

[84] J. Benajes, J. V. Pastor, A. Garcia, and J. Monsalve-Serrano, “An experimental investigation on the influence of piston bowl geometry on RCCI performance and emissions in a heavy-duty engine,” *Energy Convers. Manag.*, vol. 103, pp. 1019–1030, 2015.

[85] J. Benajes, A. García, J. M. Pastor, and J. Monsalve-Serrano, “Effects of piston bowl geometry on Reactivity Controlled Compression Ignition heat transfer and combustion losses at different engine loads,” *Energy*, vol. 98, pp. 64–77, 2016.

[86] S. Gan, H. K. Ng, and K. M. Pang, “Homogeneous Charge Compression Ignition (HCCI) combustion: Implementation and effects on pollutants in direct injection diesel engines,” *Appl. Energy*, vol. 88, no. 3, pp. 559–567, 2011.

[87] John Kendall, “MCE-5 VCRi engine offers high output in small package,” *Automotive Engineering*, 2009.

[88] A. Shaik, N. S. V. Moorthi, and R. Rudramoorthy, “Variable compression ratio engine: A future power plant for automobiles - an overview,” *Proc. Inst. Mech. Eng. Part D J. Automob. Eng.*, vol. 221, pp. 1159–1168, 2007.

[89] M. Christensen, A. Hultqvist, and B. Johansson, “Demonstrating the Multi Fuel Capability of a Homogeneous Charge Compression Ignition Engine with Variable Compression Ratio,” *SAE Tech. Pap.*, pp. SAE 1999–01–3679, 1999.

[90] J. Hyvönen, G. Haraldsson, and B. Johansson, “Operating range in a Multi Cylinder HCCI engine using Variable Compression Ratio,” *SAE Tech. Pap. 2003-01-1829*, 2003.

[91] J.-O. Olsson, P. Tunestål, B. Johansson, S. Fiveland, R. Agama, M. Willi, and D. Assanis, “Compression Ratio Influence on Maximum Load of a Natural Gas Fueled HCCI Engine,” *Society*, vol. 111, no. 724, pp. 442–458, 2002.

[92] M.-B. Liu, B.-Q. He, and H. Zhao, “Effect of air dilution and effective compression ratio on the combustion characteristics of a HCCI (homogeneous charge compression ignition) engine fuelled with n-butanol,” *Energy*, vol. 85, pp. 296–303, 2015.

[93] P. Strandh, J. Bengtsson, R. Johansson, P. Tunestål, and B. Johansson, “Variable Valve Actuation for Timing Control of a Homogeneous Charge Compression Ignition Engine,” *SAE Tech. Pap.*, vol. 2005, no. 724, 2005.

[94] K. Yeom, J. Jang, and C. Bae, “Homogeneous charge compression ignition of LPG and gasoline using variable valve timing in an engine,” *Fuel*, vol. 86, no. 4, pp. 494–503, 2007.

[95] N. Milovanovic, R. Chen, and J. Turner, “Influence of the variable valve timing strategy on the control of a homogeneous charge compression (HCCI) engine,” 2004.

[96] M. Fathi, R. K. Saray, and M. D. Checkel, “The influence of Exhaust Gas Recirculation (EGR) on combustion and emissions of n-heptane/natural gas fueled Homogeneous Charge Compression Ignition (HCCI) engines,” *Appl. Energy*, vol. 88, no. 12, pp. 4719–4724, 2011.

[97] A. M. Andwari, A. Abdul Aziz, M. F. Muhamad Said, and Z. Abdul Latiff, “An experimental study on the influence of EGR rate and fuel octane number on the combustion characteristics of a CAI two-stroke cycle engine,” *Appl. Therm. Eng.*, vol. 71, no. 1, pp. 248–258, 2014.

[98] D. Jung and N. Iida, “Closed-loop control of HCCI combustion for DME using external EGR and rebreathed EGR to reduce pressure-rise rate with combustion-phasing retard,” *Appl. Energy*, vol. 138, pp. 315–330, 2015.

[99] L. Shi, Y. Cui, K. Deng, H. Peng, and Y. Chen, “Study of low emission homogeneous charge compression ignition (HCCI) engine using combined internal and external exhaust gas recirculation (EGR),” *Energy*, vol. 31, no. 14, pp. 2329–2340, 2006.

[100] A. M. Andwari, A. A. Aziz, M. F. M. Said, and Z. A. Latiff, “Experimental investigation of the influence of internal and external EGR on the combustion characteristics of a wcontrolled auto-ignition two-stroke cycle engine,” *Appl. Energy*, vol. 134, pp. 1–10, Dec. 2014.

[101] M. Sjöberg and J. E. Dec, “Influence of EGR Quality and Unmixedness on the High-Load Limits of HCCI Engines,” *SAE Int. J. Engines*, vol. 2, no. 1, pp. 492–510, 2009.

[102] M. Andre, B. Walter, G. Bruneaux, F. Foucher, and C. Mounaim-Rousselle, “Exhaust gas recirculation stratification to control diesel homogeneous charge compression ignition combustion,” *Int. J. Engine Res.*, vol. 13, no. 5, pp. 429–447, 2012.

[103] S. M. Aceves, D. Flowers, J. R. Smith, and R. Dibble, “HCCI Engine Control by Thermal Management,” 2000.

[104] M. Sjöberg, J. Dec, and W. Hwang, “Thermodynamic and chemical effects of EGR and its constituents on HCCI autoignition,” 2007.

[105] M. Sjöberg and J. E. Dec, “Effects of EGR and its constituents on HCCI autoignition of ethanol,” *Proc. Combust. Inst.*, vol. 33, no. 2, pp. 3031–3038, 2011.

[106] M. Christensen and B. Johansson, “Homogeneous Charge Compression Ignition with Water Injection,” *SAE Tech. Pap.*, 1999.

[107] E. W. Kaiser, M. M. Maricq, N. Xu, and J. Yang, “Detailed Hydrocarbon Species and Particulate Emissions from a HCCI Engine as a Function of Air-Fuel Ratio,” *SAE Int.*, vol. 2005–01–37, no. 724, pp. 1–11, 2005.

[108] H. Machrafi, S. Cavadias, and P. Guibert, “An experimental and numerical investigation on the influence of external gas recirculation on the HCCI autoignition process in an engine: Thermal, diluting, and chemical effects,” *Combust. Flame*, vol. 155, no. 3, pp. 476–489, 2008.

[109] S. Sato, Y. Yamasaki, H. Kawamura, and N. Iida, “Research on the Influence of Hydrogen and Carbon Monoxide on Methane HCCI Combustion,” *JSME Int. J.*, vol. 48, no. 4, pp. 725–734, 2005.

[110] M. Sjöberg and J. E. Dec, “An investigation into lowest acceptable combustion temperatures for hydrocarbon fuels in HCCI engines,” *Proc. Combust. Inst.*, vol. 30 II, pp. 2719–2726, 2005.

[111] M. H. Morsy, “Ignition control of methane fueled homogeneous charge compression ignition engines using additives,” *Fuel*, vol. 86, no. 4, pp. 533–540, 2007.

[112] M. Sjöberg and J. E. Dec, “Influence of Fuel Autoignition Reactivity on the High-Load Limits of HCCI Engines,” *SAE Int. J. Engines*, vol. 1, no. 1, pp. 39–58, 2008.

[113] A. Schönborn, P. Hellier, A. E. Aliev, and N. Ladommatos, “Ignition control of homogeneous-charge compression ignition (HCCI) combustion through adaptation of the fuel molecular structure by reaction with ozone,” *Fuel*, vol. 89, no. 11, pp. 3178–3184, 2010.

[114] A. Schönborn, P. Hellier, N. Ladommatos, C. P. Hulteberg, G. Carlström, P. Sayad, J. Klingmann, and A. A. Konnov, “1-Hexene Autoignition Control By Prior Reaction With Ozone,” *Fuel Process. Technol.*, vol. 145, pp. 90–95, 2016.

[115] A. Schönborn, “A ‘smart’ fuel of photochemically-controlled reactivity,” *Fuel*, 2015.

[116] V. I. Golovitchev and J. Chomiak, “Evaluation of Ignition Improvers for Methane Autoignition,” *Combust. Sci. Technol.*, vol. 135, no. 1–6, pp. 31–47, 1998.

[117] J. C. G. Andrae, “Kinetic modeling of the influence of NO on the combustion phasing of gasoline surrogate fuels in an HCCI engine,” *Energy and Fuels*, vol. 27, no. 11, pp. 7098–7107, 2013.

[118] G. Moréac, P. Dagaut, J. F. Roesler, and M. Cathonnet, “Nitric oxide interactions with hydrocarbon oxidation in a jet-stirred reactor at 10 atm,” *Combust. Flame*, vol. 145, no. 3, pp. 512–520, 2006.

[119] G. Dayma, K. H. Ali, and P. Dagaut, “Experimental and detailed kinetic modeling study of the high pressure oxidation of methanol sensitized by nitric oxide and nitrogen dioxide,” *Proc. Combust. Inst.*, vol. 31 I, no. 2, pp. 411–418, 2007.

[120] J. M. Anderlohr, R. Bounaceur, a. Pires Da Cruz, and F. Battin-Leclerc, “Modeling of autoignition and NO sensitization for the oxidation of IC engine surrogate fuels,” *Combust. Flame*, vol. 156, no. 2, pp. 505–521, 2009.

[121] A. Dubreuil, F. Foucher, C. Mounaïm-Rousselle, G. Dayma, and P. Dagaut, “HCCI combustion: Effect of NO in EGR,” *Proc. Combust. Inst.*, vol. 31 II, no. 1540, pp. 2879–2886, 2007.

[122] H. Machrafi, P. Guibert, and S. Cavadias, “HCCI Engine Modeling and Experimental Investigations – Part 2: The Composition of a NO-PRF Interaction Mechanism and the Influence of NO in EGR on Auto-Ignition,” *Combust. Sci. Technol.*, vol. 180, no. 7, pp. 1245–1262, 2008.

[123] F. Contino, F. Foucher, P. Dagaut, T. Lucchini, G. D’Errico, and C. Mounaïm-Rousselle, “Experimental and numerical analysis of nitric oxide effect on the ignition of iso-octane in a single cylinder HCCI engine,” *Combust. Flame*, vol. 160, no. 8, pp. 1476–1483, 2013.

[124] K. Kawasaki, S. Kubo, K. Yamane, and C. Kondo, “The Effect of the Induction of Nitrogen Oxides on Natural Gas HCCI Combustion,” *SAE Int. J. Fuels Lubr.*, vol. 7, no. 3, pp. 2014–01–2697, 2014.

[125] P. Risberg, D. Johansson, J. Andrae, G. Kalghatgi, P. Björnbom, and H.-E. Angström, “The influence of NO on the combustion phasing in an HCCI engine,” *SAE Tech. Pap. 2006-01-0416*, 2006.

[126] P. Ricklin, A. Kazakov, F. Dryer, S. Kong, and R. Reitz, “The effects of NOx addition on the

auto ignition behavior of natural gas under HCCI conditions," *SAE Tech. Pap.*, no. 724, pp. 2002–01–1746, 2002.

[127] S. Gersen, a. V. Mokhov, J. H. Darmeveil, H. B. Levinsky, and P. Glarborg, "Ignition-promoting effect of NO2 on methane, ethane and methane/ethane mixtures in a rapid compression machine," *Proc. Combust. Inst.*, vol. 33, no. 1, pp. 433–440, 2011.

[128] F. Deng, F. Yang, P. Zhang, Y. Pan, Y. Zhang, and Z. Huang, "An ignition delay time and chemical kinetic study of methane and nitrous oxide mixtures at high temperatures," *Energy & Fuels*, p. acs.energyfuels.5b02581, 2016.

[129] O. Mathieu, J. M. Pemelton, G. Bourque, and E. L. Petersen, "Shock-induced ignition of methane sensitized by NO2 and N2O," *Combust. Flame*, vol. 162, no. 8, pp. 3053–3070, 2015.

[130] R. Mével and J. E. Shepherd, "Ignition delay-time behind reflected shock waves of small hydrocarbons–nitrous oxide(–oxygen) mixtures," *Shock Waves*, vol. 25, no. 3, pp. 217–229, 2015.

[131] T. Ombrello, S. H. Won, Y. Ju, and S. Williams, "Flame propagation enhancement by plasma excitation of oxygen. Part I: Effects of O3," *Combust. Flame*, vol. 157, no. 10, pp. 1906–1915, 2010.

[132] F. Halter, P. Higelin, and P. Dagaut, "Experimental and Detailed Kinetic Modeling Study of the Effect of Ozone on the Combustion of Methane," *Energy & Fuels*, vol. 25, no. 7, pp. 2909–2916, 2011.

[133] X. Liang, Z. Wang, W. Weng, Z. Zhou, Z. Huang, J. Zhou, and K. Cen, "Study of ozone-enhanced combustion in H2/CO/N2/air premixed flames by laminar burning velocity measurements and kinetic modeling," *Int. J. Hydrogen Energy*, vol. 38, no. 2, pp. 1177–1188, 2013.

[134] Z. H. Wang, L. Yang, B. Li, Z. S. Li, Z. W. Sun, M. Aldén, K. F. Cen, and a. a. Konnov, "Investigation of combustion enhancement by ozone additive in CH4/air flames using direct laminar burning velocity measurements and kinetic simulations," *Combust. Flame*, vol. 159, no. 1, pp. 120–129, 2012.

[135] A. Ehn, J. J. Zhu, P. Petersson, Z. S. Li, M. Aldén, C. Fureby, T. Hurtig, N. Zettervall, A. Larsson, and J. Larfeldt, "Plasma assisted combustion: Effects of O3 on large scale turbulent combustion studied with laser diagnostics and Large Eddy Simulations," *Proc. Combust. Inst.*, 2014.

[136] X. Gao, Y. Zhang, S. Adusumilli, J. Seitzman, and W. Sun, “The Effect of Ozone Addition on Flame Propagation,” no. January, pp. 1–27, 2015.

[137] M. Pinchak, T. Ombrello, C. Carter, E. Gutmark, and V. Katta, “The effects of hydrodynamic stretch on the flame propagation enhancement of ethylene by addition of ozone,” *Phil. Trans. R. Soc. A*, vol. 373, no. November, p. 20140339, 2015.

[138] V. Caprio, a. Insola, and P. G. Lignola, “Ozone Activated Low Temperature Combustion of Propane in a C.S.T.R.,” *Combust. Sci. Technol.*, vol. 35, no. 5–6, pp. 215–224, 1983.

[139] T. Tachibana, K. Hirata, H. Nishida, and H. Osada, “Effect of ozone on combustion of compression ignition engines,” *Combust. Flame*, vol. 85, no. 3–4, pp. 515–519, 1991.

[140] C. Ragone, C. Depcik, E. Peltier, and M. Mangus, “The Influence of Ozone on Combustion in a Single-Cylinder Diesel Engine,” *SAE 2015-01-0787*, 2015.

[141] J. B. Heywood, *Internal Combustion Engine Fundamentals*. 1988.

[142] M. F. J. Brunt, H. Rai, and A. L. Emtage, “The Calculation of Heat Release Energy from Engine Cylinder Pressure Data,” *SAE Tech. Pap. 981052*, no. 724, 1998.

[143] R. Kumar Maurya, D. D. Pal, and A. Kumar Agarwal, “Digital signal processing of cylinder pressure data for combustion diagnostics of HCCI engine,” *Mech. Syst. Signal Process.*, vol. 36, no. 1, pp. 95–109, 2013.

[144] R. K. Maurya and A. K. Agarwal, “Investigations on the effect of measurement errors on estimated combustion and performance parameters in HCCI combustion engine,” *Measurement*, vol. 46, no. 1, pp. 80–88, 2012.

[145] M. Tazerout, O. Le Corre, and P. Stouffs, “Compression Ratio and TDC calibrations using Temperature - Entropy Diagram,” *SAE Tech. Pap.*, no. Figure 2, pp. SAE 1999–01–3509, 1999.

[146] M. Tazerout, O. Le Corre, and S. Rousseau, “Tdc Determination in Ic Engines Based on the Thermodynamic Analysis of the Temperature-Entropy Diagram,” *SAE Tech. Pap.*, no. 724, pp. 1999–01–1489, 1999.

[147] A. Burcat, “Extended Third Millenium Thermodynamic Database for Combustion and Air-Pollution Use with updates from Active Thermochemical Tables,” 2015.

[148] H. S. Soyhan, H. Yasar, H. Walmsley, B. Head, G. T. Kalghatgi, and C. Sorusbay, “Evaluation of heat transfer correlations for HCCI engine modeling,” *Appl. Therm. Eng.*, vol. 29, no. 2–3, pp. 541–549, 2009.

[149] M. Sjöberg and J. E. Dec, “An Investigation of the Relationship Between Measured Intake Temperature, BDC Temperature, and Combustion Phasing for Premixed and DI HCCI Engines,” *SAE Tech. Pap. 2004-01-1900*, vol. 113, no. 4, pp. 1271–1286, 2004.

[150] E. Pipitone and A. Beccari, “Determination of TDC in internal combustion engines by a newly developed thermodynamic approach,” *Appl. Therm. Eng.*, vol. 30, no. 14–15, pp. 1914–1926, 2010.

[151] H. J. Yun and W. Mirsky, “Schlieren-Streak Measurements of Instantaneous Exhaust Gas Velocities from a Spark-Ignition Engine,” *SAE Int.*, p. 16, 1974.

[152] A. Broatch, C. Guardiola, B. Pla, and P. Bares, “A direct transform for determining the trapped mass on an internal combustion engine based on the in-cylinder pressure resonance phenomenon,” *Mech. Syst. Signal Process.*, vol. 62–63, pp. 480–489, 2015.

[153] P. Giansetti, G. Colin, P. Higelin, and Y. Chamaillard, “Residual gas fraction measurement and computation,” *Int. J. Engine Res.*, vol. 8, no. 4, pp. 347–364, 2007.

[154] A. E. Lutz, R. J. Kee, and J. A. Miller, “Senkin: a fortran program for predicting homogeneous gas phase chemical kinetics with sensitivity analysis,” *Sandia Natl. Lab. Rep.*, 1988.

[155] H. Wang, X. You, A. V. Joshi, S. G. Davis, A. Laskin, F. Egolfopoulos, and C. K. Law, “High-Temperature Combustion Reaction Model of H2/CO/C1-C4 Compounds.”

[156] S. M. Sarathy, S. Vranckx, K. Yasunaga, M. Mehl, P. Oßwald, W. K. Metcalfe, C. K. Westbrook, W. J. Pitz, K. Kohse-Höinghaus, R. X. Fernandes, and H. J. Curran, “A comprehensive chemical kinetic combustion model for the four butanol isomers,” *Combust. Flame*, vol. 159, no. 6, pp. 2028–2055, 2012.

[157] S. M. Sarathy, P. Oßwald, N. Hansen, and K. Kohse-Höinghaus, “Alcohol combustion chemistry,” *Prog. Energy Combust. Sci.*, vol. 44, pp. 40–102, 2014.

[158] P. Dagaut and G. Dayma, “The high-pressure reduction of nitric oxide by a natural gas blend,” *Combust. Flame*, vol. 143, no. 1–2, pp. 135–137, 2005.

[159] B. Eliasson, M. Hirth, and U. Kogelschatz, “Ozone synthesis from oxygen in dielectric barrier discharges,” *J. Phys. D. Appl. Phys.*, vol. 20, no. 11, pp. 1421–1437, 2000.

[160] Y.-M. Sung and T. Sakoda, “Optimum conditions for ozone formation in a micro dielectric barrier discharge,” *Surf. Coatings Technol.*, vol. 197, no. 2–3, pp. 148–153, 2005.

[161] J. Kitayama and M. Kuzumoto, “Analysis of ozone generation from air in silent discharge,” *J. Phys. D. Appl. Phys.*, vol. 32, no. 23, pp. 3032–3040, 1999.

[162] Bosch - 8th Edition, *Automotive handbook*. 2011.

[163] T. J. Manning and J. Hedden, “Gas Mixtures and Ozone Production in an Electrical Discharge,” *Ozone Sci. Eng.*, vol. 23, no. 2, pp. 95–103, 2001.

[164] U. Kogelschatz, B. Eliasson, W. Egli, P. I. V France, and E. Abb, “Dielectric-Barrier Discharges. Principle and Applications,” *J. Phys. IV Fr. 7 Colloq. C4, supplément au J. Phys. III*, vol. 7, no. 1 997, pp. C4–47/C4–66, 1997.

[165] U. Kogelschatz, B. Eliasson, and M. Hirth, “Ozone generation from oxygen and air: discharge physics and reaction mechanisms,” *Ozone Sci. Eng.*, vol. 10, pp. 367–378, 1988.

[166] W. J. M. Samaranayake, Y. Miyahara, T. Namihira, S. Katsuki, R. Hackam, and H. Akiyama, “Ozone production using pulsed dielectric barrier discharge inoxygen,” *IEEE Trans. Dielectr. Electr. Insul.*, vol. 7, no. 6, 2000.

[167] P. Martinez and D. K. Brandvold, “Laboratory and field measurements of NO(x) produced from corona discharge,” *Atmos. Environ.*, vol. 30, no. 24, pp. 4177–4182, 1996.

[168] S. Pekárek and J. Rosenkranz, “Ozone and Nitrogen Oxides Generation in Gas Flow Enhanced Hollow Needle to Plate Discharge In Air,” *Ozone Sci. Eng.*, vol. 24, no. 3, pp. 221–226, 2002.

[169] V. I. Gibalov, V. G. Samoilovitch, and M. Wronski, “Electrosynthesis of nitrogen oxides and ozone in ozonizer,” *Proc. 7th Intl. Symposium on Plasma Chemistry*. pp. 401–406, 1985.

[170] R. D. Hill, I. Rahmin, and R. G. Rinker, “Experimental Study of the Production of NO, N20, and O3 in a Simulated Atmospheric Corona,” *Ind. Eng. Chem. Res.*, vol. 27, no. 7, pp. 1264–1269, 1988.

[171] B. Wang, Z. Wang, S. Shuai, H. Yang, and J. Wang, “Combustion and emission characteristics of Multiple Premixed Compression Ignition (MPCI) fuelled with naphtha and gasoline in wide load range,” *Energy Convers. Manag.*, vol. 88, pp. 79–87, 2014.

[172] F. Yang, C. Yao, J. Wang, and M. Ouyang, “Load expansion of a dieseline compression ignition engine with multi-mode combustion,” *Fuel*, vol. 171, pp. 5–17, 2016.

[173] D. R. Am Water Works Res, F., Langlais, B., Reckhow, D. A., & Brink, *Ozone in Water Treatment: Application and Engineering*. 1991.

[174] W. J. Masschelein, “Ozone Generation: Use of Air, Oxygen or Air Simpsonized with Oxygen,” *Ozone Sci. Eng.*, vol. 20, no. 3, pp. 191–203, 1998.

[175] J. A. Eng, “Characterization of Pressure Waves in HCCI Combustion Reprinted From : Homogeneous Charge Compression Ignition Engines,” *Society*, no. 724, 2002.

[176] J. Dernotte, J. Dec, and C. Ji, “Investigation of the Sources of Combustion Noise in HCCI Engines,” *SAE Int. J. Engines*, vol. 7, no. 2, 2014.

[177] S. Kook, C. Bae, P. C. Miles, D. Choi, and L. M. Pickett, “The Influence of Charge Dilution and Injection Timing on Low-Temperature Diesel Combustion and Emissions,” *SAE Trans.*, vol. 114, no. 4, pp. 1575–1595, 2005.

[178] P. Miles, “Sources and mitigation of CO and UHC emissions in low-temperature diesel combustion regimes : Insights obtained via homogeneous reactor modeling,” *13th Diesel Engine-Efficiency Emiss. Res. Conf.*, 2007.

[179] D. Willy, D. Alain, B. Xavier, and L. E. a Poitiers, “PIV Measurements of Internal Aerodynamic of Diesel Combustion Chamber,” no. 724, 2003.

[180] H. Liu, P. Zhang, Z. Li, J. Luo, Z. Zheng, and M. Yao, “Effects of temperature inhomogeneities on the HCCI combustion in an optical engine,” *Appl. Therm. Eng.*, vol. 31, no. 14–15, pp. 2549–2555, 2011.

[181] P. Miles, W. Colban, I. Ekoto, D. Kim, R. Reitz, M. Bergin, S. W. Park, and Y. Ra, “Light-Duty Advanced Diesel Combustion Research,” *US DOE EERE*, 2008.

[182] M. C. Sellnau, F. a Matekunas, P. a Battiston, C. Chang, and D. R. Lancaster, “Cylinder-Pressure-Based Engine Control Using Pressure-Ratio-Management and Low-Cost Non-Intrusive Cylinder Pressure Sensors,” *Sae*, no. 724, 2000.

[183] D. Schiefer, “Advantages of Diesel Engine Control Using In-Cylinder Pressure Information for Closed Loop Control,” vol. 2003, no. 724, 2012.

[184] S. Candel and N. Docquier, “Combustion control and sensors a review.pdf,” vol. 28, 2002.

[185] Z. Zhang, L. Li, and R. Dibble, “HCCI Cycle-by-Cycle Combustion Phase Control Based on Ion Current Technology in GDI Engine,” *Automot. Concept Model. Optim. Veh. NVH Perform.*, vol. 201, pp. 365–376, 2013.

[186] R. H. Butt, Y. Chen, J. H. Mack, S. Saxena, R. W. Dibble, and J.-Y. Chen, “Improving ion current of sparkplug ion sensors in HCCI combustion using sodium, potassium, and cesium acetates: Experimental and numerical modeling,” *Proc. Combust. Inst.*, no. 0, pp. 1–9, 2014.

[187] J.-C. Guibet, *Carburants et Moteurs: Technologies, Energie et Environnement*. 1997.

[188] ASTM International, “Standard Test Method for Research Octane Number of Spark-Ignition Engine Fuel,” 2008.

[189] ASTM International, “Standard Test Method for Motor Octane Number of Spark-Ignition Engine Fuel,” 2008.

[190] M. Ilbas, A. P. Crayford, I. Yilmaz, P. J. Bowen, and N. Syred, “Laminar-burning velocities of hydrogen-air and hydrogen-methane-air mixtures: An experimental study,” *Int. J. Hydrogen Energy*, vol. 31, no. 12, pp. 1768–1779, 2006.

[191] M. Christensen and B. Johansson, “Influence of mixture quality on homogenous charge compression ignition,” *SAE Trans.*, vol. 107, no. 724, pp. 948–960, 1998.

[192] S. Verhelst and T. Wallner, “Hydrogen-fueled internal combustion engines,” *Prog. Energy Combust. Sci.*, vol. 35, no. 6, pp. 490–527, 2009.

[193] I. D. Bedoya, S. Saxena, F. J. Cadavid, R. W. Dibble, and M. Wissink, “Experimental study of biogas combustion in an HCCI engine for power generation with high indicated efficiency and ultra-low NOx emissions,” *Energy Convers. Manag.*, vol. 53, no. 1, pp. 154–162, 2012.

[194] S. Swami Nathan, J. M. Mallikarjuna, and A. Ramesh, “An experimental study of the biogas-diesel HCCI mode of engine operation,” *Energy Convers. Manag.*, vol. 51, no. 7, pp. 1347–1353, 2010.

[195] A. K. Agarwal, “Biofuels (alcohols and biodiesel) applications as fuels for internal combustion engines,” *Prog. Energy Combust. Sci.*, vol. 33, no. 3, pp. 233–271, 2007.

Jean-Baptiste MASURIER

Etude expérimentale du contrôle de la combustion HCCI par l'utilisation d'espèces chimiques minoritaires oxydantes

Résumé :

Dans le but de réduire la consommation en carburant, les émissions de CO_2 et les polluants tout en maintenant le haut rendement des moteurs, de nouveaux modes de combustions ont été étudiés et sont d'excellents candidats pour remplacer les moteurs conventionnels. En particulier, le mode HCCI a montré une excellente aptitude pour répondre à ces objectifs. Néanmoins, en dépit de ses avantages, de nombreux challenges sont à surmonter avant de permettre le développement de tels moteurs. Parmi eux, obtenir un contrôle efficace de la totalité de ce processus de combustion sur un large domaine d'utilisation demeure le principal défi. Ces travaux de thèse s'intéressent à l'utilisation des espèces chimiques oxydantes comme un moyen robuste de contrôle de la combustion HCCI. En raison de ces fortes propriétés oxydantes, l'ozone a été la principale molécule étudié. De plus, son intérêt est renforcé par le fait que l'ozone peut être produit au sein d'un véhicule au moyen de petits générateurs, mais cela peut aussi produire des oxydes d'azote. Ces recherches ont été effectuées au moyen d'un banc moteur monocylindre HCCI et couplées avec des simulations de cinétique chimique. Les deux principaux objectifs ont été : (1) Evaluer le potentiel d'utilisation d'un générateur d'ozone pour contrôler la combustion HCCI. L'impact de plusieurs espèces chimiques oxydantes, ozone and NO_x, a été étudié sur la combustion de l'isooctane. De plus, un contrôle dynamique a été mis en place avec succès. (2) Comparer l'influence de l'ozone sur la combustion de l'isooctane et de carburants alternatifs. Des carburants à forte teneur en méthane et des alcools ont été étudiés en raison de leur forte résistance à l'autoinflammation et de leur structure chimique.

Mots clés : HCCI, Espèces chimiques oxydantes, Carburant, Contrôle de la combustion

Experimental study on the control of the HCCI combustion through the use of minor oxidizing chemical species

Summary :

To reduce the fuel consumption, CO_2 emissions and pollutant emissions while keep improving thermal efficiency of engines, alternative combustion modes are being investigated as good candidates to replace spark-ignited and diesel engines. In particular, Homogeneous Charge Compression Ignition (HCCI) engines have proven their potential to meet these requirements. However, despite of these advantages, several challenges remain to be addressed prior to the widespread implementation of HCCI engines. Among them, the control of the overall combustion process in such an engine over the full operating range is still considered as the main challenge to overcome. The present work introduces the use of oxidizing chemical species seeded in the intake system as a robust control technique for HCCI combustion process. In particular, ozone was examined due to its strong oxidizing characteristics. Moreover, ozone can be easily produced on-board a real vehicle from the intake oxygen thanks to small ozone generators, but can also lead to the production of NO_x. Investigations were carried out using a single-cylinder HCCI engine and kinetics computation analysis. The two main objectives of this work are: (1) Evaluate the potential of using ozone generator to control the HCCI combustion. Along these lines, the interaction between NO_x and ozone was investigated for isooctane as fuel and a real time control of the HCCI combustion was implemented and successfully tested. (2) Compare the influence of ozone on the combustion of isooctane and alternative fuels. Methane-based fuels (methane/propane and methane/hydrogen mixtures) and alcohols (methanol, ethanol, *n*-butanol) were selected due to their higher resistance to autoignition and their different chemical structure.

Keywords : HCCI, Oxidizing chemical species, Fuel, Control of the combustion

Laboratoire PRISME
8 Rue Léonard de Vinci 45071 Orléans

ICARE – CNRS INSIS
1 C Avenue de la Recherche Scientifique
45072 Orléans